



University  
of Glasgow

Lukashchuk, Vera (2010) *The roles of ND10 proteins ATRX and hDaxx in the regulation of herpesvirus infection*. PhD thesis.

<http://theses.gla.ac.uk/1919/>

Copyright and moral rights for this thesis are retained by the author

A copy can be downloaded for personal non-commercial research or study, without prior permission or charge

This thesis cannot be reproduced or quoted extensively from without first obtaining permission in writing from the Author

The content must not be changed in any way or sold commercially in any format or medium without the formal permission of the Author

When referring to this work, full bibliographic details including the author, title, awarding institution and date of the thesis must be given.

**The Roles of ND10 Proteins ATRX and hDaxx  
in the Regulation of Herpesvirus Infection**

**Vera Lukashchuk**

A thesis presented for the degree of Doctor of Philosophy in the  
Faculty of Biomedical and Life Sciences at the University of Glasgow

MRC Virology Unit  
Church Street  
Glasgow  
G11 5JR

2010

## Abstract

Protection against viruses is provided by the host innate, adaptive and cellular intrinsic immunities. Cellular intrinsic immunity, or intrinsic defence, against herpesviruses is in part enacted by components that constitute nuclear substructures known as ND10. ND10 (also called PML nuclear bodies after its major organising component) are dynamic nuclear domains that contain various cellular proteins, including PML itself, Sp100, hDaxx and ATRX. In the early stages of infection, herpesvirus genomes and sites of immediate early transcription become associated with ND10 and their components. Representative herpesviruses such as an alphaherpesvirus HSV-1 and a betaherpesvirus HCMV encode for strong transcriptional activators, namely the Immediate Early protein ICP0 and the tegument protein pp71, respectively. These proteins are known to counteract cellular intrinsic defence mechanisms.

In the context of HSV-1 and HCMV infections, the major ND10 component PML has been identified as an important constituent of cellular intrinsic defence. In addition, a number of research studies have demonstrated that Sp100 and hDaxx contribute to these processes during infection with HSV-1 and HCMV, respectively. The general hypothesis of the present study implies that cellular chromatin-associated factors within ND10 may act to repress viral gene expression. The two representative ND10 components present a particular interest for the current investigation based on the facts that: (i) hDaxx is a transcriptional co-repressor; (ii) ATRX is a chromatin-remodelling enzyme; and (iii) ATRX and hDaxx interact with each other to form a chromatin-remodelling complex with repressive properties. The purpose of the present study was therefore to investigate the roles of these two proteins in HSV-1 and HCMV infection. By using virus mutants incapable of efficient stimulation of Immediate Early gene expression (ICP0-null HSV-1 and pp71-null HCMV) it was possible to analyse the contribution of ATRX and hDaxx to the repression mechanism that occurs in the absence of these viral transactivators. An RNA interference approach was utilised for generating cell lines depleted of ATRX or hDaxx in order to assess their roles in viral infectivity. In addition, cell lines reconstituted with wt hDaxx, and ATRX-interaction or SUMO-interaction deficient hDaxx mutants were constructed in order to study the contribution of these functional elements to the role of hDaxx in the repression of ICP0-null mutant HSV-1.

The key findings presented in the current study can be summarised as follows:

- (1) ATRX contributes to the intrinsic resistance against HCMV infection, and this mechanism is strongly counteracted by viral pp71;
- (2) A chromatin-remodelling complex formed between ATRX and hDaxx contributes to the efficient repression of ICP0-null HSV-1 genomes, thereby constituting a part of anti-HSV-1 intrinsic cellular defence. ICP0 counteracts this process, and the possible mechanisms of ICP0 action are proposed.

These data provide the first evidence for the role of ATRX in viral infection and in addition demonstrate a role for hDaxx in the regulation of HSV-1 infection. The strong indication that ATRX and hDaxx act as a complex opens a possibility of chromatin-dependent repression of ICP0-null HSV-1 genomes. Whether ATRX and hDaxx contribute to the repression of pp71-null HCMV genomes as a complex is yet to be established. In summary, the conclusion of the studies presented in this thesis suggests regulatory roles of ND10-localised chromatin remodelling proteins ATRX and hDaxx in cellular anti-herpesvirus intrinsic resistance mechanisms.

## Acknowledgements

First of all and most importantly, I would like to thank my supervisor Prof. Roger Everett for providing enormous help and guidance during the three years of my PhD project; for choosing a productive project for me and always being encouraging and motivating.

I am very thankful to Prof. Duncan McGeoch for giving me an opportunity to join the MRC Virology Unit and Dr. Andrew Davison for being my advisor. I would also like to acknowledge the MRC Virology Unit administrative staff for being efficient and helpful dealing with various non-science issues; MRC Virology Unit technical support staff for their assistance, especially Claire Addison and Aidan Dolan for sequencing services; as well as people who provided reagents and services including Richard Gibbons for antibodies (MRC Haematology Unit, Oxford) and Tom Gilbey for the FACS services (Beatson Institute for Cancer Research, Glasgow).

I thank Prof. Chris Preston for the enjoyable and productive collaboration on the HCMV project, for provision of the recombinant viruses that have been used for a substantial part of the present work and for helpful discussions throughout; and the rest of C. Preston team especially Steven McFarlane for our collaborative work.

I cannot thank enough all my labmates of the R. Everett group who I have been so lucky to work with during these years, who have always been kind, helpful and supportive, and have made the work atmosphere extremely friendly and comfortable: Chris Boutell (for his grown-up life advice and for the singing in the morning), Kyle Grant (for his sense of humour and afternoon breaks), Emilia Vanni (for that camping trip), Nora Rauch, Anne Orr, Jill Murray, Louise Grant, Mandy Glass and Amanda Sykes. My special thanks go to my very good friends Carlos Parada, whose optimism has always been an inspiration, and Delphine Cuchet, who together with her fiancé Filipe have not let me stay homeless during my awkward living situation and who have constantly charged me with positivity.

I am very grateful to all my friends in Glasgow (Adrian, Angeline and Kim) and all fellow PhD students (especially Allan, Chris, Dan and Patricia) who have been extremely supportive and caring, a lot of fun to hang out with outside of work and who have always made sure I stay sane under the occasional stresses of work and life. Also I thank all my close friends around the UK and the rest of the world, who have always sent me their blessings and expressed their care, despite being miles away, including Irina (for faithfully staying my best friend), Anna, Josef and Vicky.

Finally, I would like to thank my Mum and Dad, who have been an endless source of motivation and support; my Grandma for being caring and encouraging; and my dearest sister Natasha whose determination and strength have always inspired me to achieve my goals.

# Table of Contents

<b>List of Figures</b> .....	<b>12</b>
<b>List of Tables</b> .....	<b>14</b>
<b>List of Abbreviations</b> .....	<b>15</b>
<b>1 Introduction</b> .....	<b>20</b>
<b>1.1 Family <i>Herpesviridae</i></b> .....	<b>20</b>
1.1.1 Overview of the family and key features.....	20
1.1.2 Subfamilies .....	22
1.1.2.1 Alphaherpesvirinae .....	22
1.1.2.2 Betaherpesvirinae.....	22
1.1.2.3 Gammaherpesvirinae .....	22
<b>1.2 Pathogenesis of herpesvirus infections</b> .....	<b>23</b>
1.2.1 HSV infections .....	23
1.2.1.1 Genital herpes .....	23
1.2.1.2 HSV infection of the central nervous system.....	24
1.2.1.3 Herpes simplex keratitis.....	24
1.2.2 HCMV infections .....	24
1.2.2.1 Congenital HCMV infections .....	25
1.2.2.2 HCMV infections of immunocompromised and immunosuppressed hosts.....	25
1.2.2.3 Treatment .....	25
1.2.3 Other herpesvirus infections.....	26
1.2.3.1 Varicella Zoster Virus.....	26
1.2.3.2 Kaposi's sarcoma-associated herpesvirus.....	26
1.2.3.3 Epstein-Barr virus .....	27
<b>1.3 Comparative structure of HSV-1 and HCMV virions</b> .....	<b>27</b>
1.3.1 Double-stranded DNA core .....	27
1.3.2 Capsid .....	28
1.3.2.1 The HSV-1 Capsid.....	28
1.3.2.2 The HCMV Capsid .....	28
1.3.3 Tegument.....	29
1.3.3.1 HSV-1 tegument proteins .....	29
1.3.3.2 HCMV tegument proteins.....	30
1.3.4 Envelope .....	30
<b>1.4 The overview of the HSV-1 and HCMV life cycles</b> .....	<b>31</b>

1.4.1	The lytic infectious cycle.....	31
1.4.1.1	Viral entry into the host cell.....	31
1.4.1.2	Gene expression.....	32
1.4.1.3	Viral DNA synthesis.....	33
1.4.1.4	Capsid assembly and packaging of viral DNA.....	34
1.4.1.5	Maturation and egress.....	36
1.4.2	Latency.....	37
1.4.2.1	HSV-1 latency and models of quiescent infection.....	37
1.4.2.2	HCMV latency.....	38
<b>1.5</b>	<b>Viral genomes and ND10 during the initial stages of infection.....</b>	<b>40</b>
1.5.1	ND10 and their components.....	40
1.5.1.1	PML.....	41
1.5.1.2	Sp100.....	42
1.5.1.3	SUMO family proteins.....	42
1.5.1.4	ATRX and hDaxx.....	43
1.5.1.5	Other ND10-localised proteins.....	43
1.5.2	Association of viral DNA and sites of Immediate Early transcription with ND10.....	43
1.5.2.1	HSV-1 and HCMV DNA at ND10.....	43
1.5.2.2	Relationships of other viruses with ND10.....	44
<b>1.6</b>	<b>Immediate Early gene expression.....</b>	<b>45</b>
1.6.1	Regulation of HSV-1 Immediate Early gene expression.....	45
1.6.2	HSV-1 Immediate Early proteins.....	46
1.6.2.1	ICP4.....	46
1.6.2.2	ICP27.....	46
1.6.2.3	ICP22.....	47
1.6.2.4	ICP47.....	47
1.6.3	Immediate Early protein ICP0.....	47
1.6.3.1	Overview of the gene and protein structure.....	47
1.6.3.2	Transcriptional activation by ICP0.....	48
1.6.3.3	ICP0 and E3 ubiquitin ligase function.....	49
1.6.3.4	ICP0 and association with ND10.....	50
1.6.3.5	ICP0-null mutant phenotype.....	50
1.6.3.6	ICP0 in reactivation from latency.....	52
1.6.4	Regulation of HCMV Immediate Early gene expression.....	53
1.6.5	HCMV tegument protein pp71.....	54
1.6.5.1	Transcriptional activation by pp71.....	54
1.6.5.2	Interaction with the cellular ND10 protein hDaxx.....	54
1.6.5.3	Effects of pp71 on cell cycle proteins.....	55

1.6.6	Immediate Early proteins IE1 and IE2 .....	56
1.6.6.1	Structure of the major IE transcript .....	56
1.6.6.2	Disruption of ND10 by IE1 .....	56
<b>1.7</b>	<b>Chromatin control of herpesvirus infection .....</b>	<b>57</b>
1.7.1	Chromatin organisation and structure.....	58
1.7.1.1	The nucleosome: The structural unit of chromatin .....	58
1.7.1.2	Chromatin regulation by histone acetylation, deacetylation and methylation .....	58
1.7.1.3	Chromatin regulation by DNA methylation.....	60
1.7.1.4	Chromatin remodelling by SWI/SNF family enzymes .....	61
1.7.2	Chromatin organisation during herpesvirus infection .....	61
1.7.2.1	Chromatin during lytic infection.....	62
1.7.2.2	Chromatin during latent infection.....	63
<b>1.8</b>	<b>The chromatin-associated ND10 Components: ATRX and hDaxx .....</b>	<b>64</b>
1.8.1	ATRX .....	64
1.8.1.1	The gene and protein structure.....	64
1.8.1.2	ATR-X syndrome .....	65
1.8.1.3	ATRX functions in chromatin remodelling .....	66
1.8.2	hDaxx .....	67
1.8.2.1	Structure and functional domains .....	68
1.8.2.2	hDaxx in apoptosis.....	68
1.8.2.3	The role of hDaxx phosphorylation in its functions .....	69
1.8.2.4	hDaxx in transcriptional regulation .....	69
1.8.2.5	The ATRX/hDaxx complex.....	71
<b>1.9</b>	<b>Immunity to viral infection .....</b>	<b>71</b>
1.9.1	Innate and adaptive anti-viral immunity.....	72
1.9.1.1	The functions of anti-viral adaptive immune system.....	72
1.9.1.2	The functions of innate anti-viral immune system.....	73
1.9.2	Cellular anti-viral intrinsic immunity .....	73
1.9.2.1	Discovery of anti-retroviral intrinsic immunity: APOBEC and TRIM5 $\alpha$ .....	74
1.9.2.2	ND10 proteins as constituents of anti-herpesvirus intrinsic immunity.....	75
<b>1.10</b>	<b>Aims and objectives of the study .....</b>	<b>76</b>
<b>2</b>	<b>Materials and Methods.....</b>	<b>77</b>
<b>2.1</b>	<b>Materials.....</b>	<b>77</b>
2.1.1	Antibodies.....	77
2.1.2	Plasmids.....	79
2.1.3	Enzymes .....	79

2.1.4	Oligonucleotides.....	80
2.1.5	Chemicals and reagents .....	80
2.1.6	Solutions .....	82
2.1.7	Viruses.....	83
2.1.7.1	HSV-1 virus strains.....	83
2.1.7.2	HCMV virus strains .....	83
2.1.8	Cells.....	84
2.1.8.1	Mammalian cells and culture conditions .....	84
2.1.8.2	Bacterial cells and culture conditions .....	85
<b>2.2</b>	<b>Molecular biology methods .....</b>	<b>85</b>
2.2.1	Bacterial culture handling.....	85
2.2.1.1	Transformation of competent bacterial cells.....	85
2.2.1.2	Growing bacterial cultures for plasmid DNA preparation.....	85
2.2.2	Plasmid DNA extraction and analysis .....	86
2.2.2.1	Small scale (miniprep) plasmid DNA extraction by boiling method.....	86
2.2.2.2	Large scale (maxiprep) plasmid DNA extraction by CsCl banding method .....	86
2.2.2.3	Using commercial kits for plasmid DNA extraction and purification .....	87
2.2.2.4	Plasmid DNA analysis by restriction digest and agarose gel electrophoresis .....	88
2.2.2.5	Ligation of DNA fragments .....	88
2.2.2.6	Sequencing of the purified plasmid DNA.....	89
2.2.3	Recovery of pLKO.puro-shATRX clones .....	89
2.2.4	Specific cloning strategies .....	91
2.2.4.1	Polymerase chain reaction .....	91
2.2.4.2	General cloning strategy .....	92
2.2.4.3	Construction of pLNGY-hDaxx .....	93
2.2.4.4	Deletion of hDaxx ATRX-interacting domain PAH1.....	94
2.2.4.5	Deletion of hDaxx SUMO-interaction motif .....	97
2.2.4.6	Mutagenesis of hDaxx SUMO-interaction motif.....	97
<b>2.3</b>	<b>Cell culture methods .....</b>	<b>98</b>
2.3.1	General cell culture manipulations .....	98
2.3.1.1	Maintenance and passaging of the laboratory cell lines .....	98
2.3.1.2	Cell seeding.....	98
2.3.1.3	Freezing and thawing of the cell stocks.....	98
2.3.2	Confocal immunofluorescence microscopy .....	99
2.3.3	Lentiviral transduction of cell lines .....	99
2.3.3.1	Transfection using Lipofectamine .....	100
2.3.3.2	Transduction of cell lines with lentivirus.....	102
2.3.3.3	Fluorescence activated cell sorting .....	102

<b>2.4</b>	<b>Protein methods .....</b>	<b>103</b>
2.4.1	Detection of protein expression by western blot .....	103
2.4.1.1	SDS-polyacrylamide gel electrophoresis .....	103
2.4.1.2	Transfer of the proteins to nitrocellulose membrane .....	104
2.4.1.3	Immunodetection of the proteins .....	104
2.4.1.4	Stripping of the nitrocellulose membrane.....	105
2.4.2	Co-Immunoprecipitation .....	105
<b>2.5</b>	<b>Virology methods .....</b>	<b>106</b>
2.5.1	General virus handling and infection assays .....	106
2.5.1.1	Propagation and titration of the viral stocks .....	106
2.5.1.2	Standard approaches for viral infection assays .....	106
2.5.2	Viral experimental assays.....	107
2.5.2.1	Establishing HSV-1 plaque formation efficiency using blue plaque assays.....	107
2.5.2.2	Immunofluorescence analysis of developing HSV-1 plaques .....	107
2.5.2.3	Kinetics of HSV-1 protein expression .....	107
2.5.2.4	Assay of establishment of HSV-1 quiescence .....	108
2.5.2.5	Fluorescence recovery after photobleaching.....	108
2.5.2.6	Phosphorylation analysis of HSV-1 infected cell lysates .....	109
2.5.2.7	Analysis of HCMV replication efficiency .....	109
<b>3</b>	<b>Characterisation of ATRX and hDaxx in Cell Culture.....</b>	<b>110</b>
<b>3.1</b>	<b>Introduction.....</b>	<b>110</b>
<b>3.2</b>	<b>Results.....</b>	<b>111</b>
3.2.1	Characterisation of ND10 protein expression in various cell lines .....	111
3.2.1.1	Analysis of ND10 protein expression in human cell lines by western blot .....	111
3.2.1.2	Analysis of ATRX localisation by immunofluorescence .....	114
3.2.2	Generation of ATRX- and hDaxx-depleted cell lines by RNA interference.....	114
3.2.2.1	Characterisation of ATRX-depleted cell lines .....	116
3.2.2.2	Characterisation of hDaxx-depleted cell lines .....	120
3.2.3	Reconstitution of hDaxx expression in hDaxx-depleted cells .....	122
3.2.3.1	Re-introduction of wild-type hDaxx into hDaxx-depleted cells .....	122
3.2.3.2	Deletion of the hDaxx ATRX-interacting region and disruption of the ATR/hDaxx complex .....	126
3.2.3.3	Mutagenesis of hDaxx SUMO-interaction motif.....	130
<b>3.3</b>	<b>Conclusions and discussion .....</b>	<b>132</b>
<b>4</b>	<b>Regulation of HCMV Infection by ATRX .....</b>	<b>137</b>

<b>4.1</b>	<b>Introduction to cellular intrinsic defence against HCMV infection.....</b>	<b>137</b>
<b>4.2</b>	<b>Results.....</b>	<b>139</b>
4.2.1	HCMV tegument protein pp71 displaces ATRX from ND10.....	139
4.2.2	ATRX is not required for pp71 localisation to ND10.....	140
4.2.3	ATRX contributes to the repression of HCMV IE protein synthesis in the absence of pp71.....	142
4.2.4	ATRX depletion results in the increased IE gene expression per cell infected with pp71-null mutant HCMV.....	145
4.2.5	ATRX depletion supports increased replication of pp71-null mutant HCMV.....	148
<b>4.3</b>	<b>Conclusions and discussion.....</b>	<b>149</b>
<b>5</b>	<b>Regulation of HSV-1 Infection by ATRX and hDaxx.....</b>	<b>153</b>
<b>5.1</b>	<b>Introduction to cellular intrinsic defence against HSV-1 infection.....</b>	<b>153</b>
<b>5.2</b>	<b>Results.....</b>	<b>155</b>
5.2.1	Analysis of ATRX and hDaxx redistribution in HSV-1 infected cells.....	155
5.2.1.1	ATRX and hDaxx are recruited to the sites associated with incoming HSV-1 genomes.....	155
5.2.1.2	Analysis of hDaxx dynamics at the sites of ICP0-null HSV-1 genomes in comparison to normal ND10.....	158
5.2.1.3	ATRX recruitment to the sites associated with the incoming HSV-1 genomes is not dependent on PML.....	160
5.2.1.4	ATRX recruitment to viral genome foci requires its interaction with hDaxx.....	162
5.2.2	The role of ATRX/hDaxx complex in the repression of HSV-1 infection in the absence of ICP0.....	167
5.2.2.1	Depletion of ATRX supports increased efficiency of ICP0-null mutant HSV-1 infection.....	167
5.2.2.2	hDaxx contributes to the repression of ICP0-null mutant HSV-1 infection.....	170
5.2.2.3	The ATRX interaction region of hDaxx is required for fully efficient repression of ICP0-null mutant HSV-1 infection and gene expression.....	172
5.2.3	The role of the ATRX/hDaxx complex in the establishment of HSV-1 quiescence.....	174
5.2.4	The role of hDaxx SUMO-interaction motif in regulating ICP0-null mutant HSV-1 infection.....	176
5.2.5	Analysis of ATRX and hDaxx modification during HSV-1 infection.....	179
5.2.5.1	ATRX is not degraded during wt HSV-1 infection.....	179
5.2.5.2	The ATRX/hDaxx complex is neither disrupted during HSV-1 infection nor interacts with ICP0.....	180
5.2.5.3	hDaxx phosphorylation levels are increased during wild-type HSV-1 infection.....	181

<b>5.3</b>	<b>Conclusions and discussion .....</b>	<b>184</b>
5.3.1	Fully efficient repression of the mutant HSV-1 genomes requires the ATRX/hDaxx complex .....	184
5.3.2	Phosphorylation of hDaxx as an ICP0-mediated response to antiviral cellular intrinsic defence .....	186
5.3.3	SUMO-dependent targeting of hDaxx to the sites of the viral genomes .....	188
<b>6</b>	<b>Summary, Discussion and Future Prospects .....</b>	<b>190</b>
<b>6.1</b>	<b>Summary of the data .....</b>	<b>190</b>
<b>6.2</b>	<b>Evidence for ATRX and hDaxx as the components of a multisubunit repressor complex during viral infection.....</b>	<b>191</b>
<b>6.3</b>	<b>The mechanisms of repression by ATRX/hDaxx complex during HCMV and HSV-1 infection.....</b>	<b>193</b>
6.3.1	Evidence that the pathways of ATRX/hDaxx-mediated repression of HSV-1 and HCMV infection are distinct .....	195
6.3.2	Regulation of the chromatin state of HSV-1 and HCMV genomes: the role of histone deacetylases .....	197
<b>6.4</b>	<b>Future directions in anti-viral cellular intrinsic immunity .....</b>	<b>200</b>
	<b>Reference List.....</b>	<b>203</b>

## List of Figures

Figure 1.1 Architecture of a typical herpesvirus infectious virion particle.....	21
Figure 1.2 Organisation of the HSV-1 and HCMV genomes .....	28
Figure 1.3 Overview of the herpesvirus lytic infectious cycle.....	35
Figure 1.4 A schematic diagram showing ICP0 protein structure .....	48
Figure 1.5 Overview of the regulation of HCMV Immediate Early transcription.....	53
Figure 1.6 Basic organisation of a nucleosome .....	59
Figure 1.7 The ATRX protein sequence .....	66
Figure 1.8 The hDaxx protein sequence .....	69
Figure 2.1 Lentiviral vector pLKO1.puro .....	90
Figure 2.2 pLKOneo.gD.EYFP (pLNGY).....	93
Figure 2.3 Construction of pLNGY-hDaxx .....	95
Figure 2.4 pLNGY-hDaxx construct.....	96
Figure 2.5 PCR-mediated gene splicing mutagenesis.....	96
Figure 2.6 Posttranslational processing by RNA interference .....	100
Figure 2.7 Short hairpin RNA in experimental RNAi-mediated gene silencing .....	101
Figure 3.1 Analysis of endogenous expression of ND10 proteins in cultured cell lines ...	112
Figure 3.2 ATRX localisation in different cell lines.....	115
Figure 3.3 Efficiency of ATRX depletion in human fibroblasts.....	116
Figure 3.4 Levels of ATRX depletion in cell lines .....	117
Figure 3.5 The effects of depleting ATRX on the localisation of ND10 proteins in human fibroblasts.....	118
Figure 3.6 The effects of depleting ATRX on the localisation of ND10 proteins in HepaRG cells .....	119
Figure 3.7 Wide-field view of ATRX and hDaxx localisation in ATRX-depleted HepaRG cells .....	120
Figure 3.8 hDaxx depletion in human fibroblasts.....	121
Figure 3.9 ATRX is dispersed in hDaxx-depleted HepaRG cells.....	121
Figure 3.10 Western blot analysis of hDaxx expression in cell lines expressing re-introduced EYFP-hDaxx.....	123
Figure 3.11 Re-introduced hDaxx targets ATRX back to ND10.....	125
Figure 3.12 Deletion of the ATRX interaction domain of hDaxx .....	127
Figure 3.13 The requirement of hDaxx ATRX-interaction domain for ATRX targeting to ND10.....	129
Figure 3.14 hDaxx SUMO-interaction motif is required for hDaxx localisation to ND10	131

Figure 4.1 ATRX depletion does not affect pp71 localisation.....	141
Figure 4.2 ATRX depletion increases Immediate Early gene expression in cells infected with pp71-null mutant HCMV .....	144
Figure 4.3 ATRX depletion increases IE protein synthesis of the individual cells infected with pp71-null mutant HCMV .....	147
Figure 4.4 ATRX depletion increases replication of pp71-null mutant HCMV.....	147
Figure 5.1 ATRX and hDaxx are recruited to the sites of incoming HSV-1 genomes in HepaRG cells .....	157
Figure 5.2 Dynamics of EYFP-hDaxx foci at ND10 of the mock-infected cells and sites associated with ICP0-null mutant HSV-1 genomes.....	159
Figure 5.3 PML is not required for ATRX recruitment to HSV-1 genome foci at the early stages of infection .....	161
Figure 5.4 ATRX is not recruited to the sites associated with ICP0-null mutant HSV-1 genomes in hDaxx-depleted HepaRG cells.....	163
Figure 5.5 EYFP-hDaxx targets ATRX back into foci associated with incoming viral genomes during ICP0-null mutant HSV-1 infection.....	165
Figure 5.6 Interaction between hDaxx and ATRX is required for ATRX recruitment to incoming viral genomes at the edge of ICP0-null mutant HSV-1 plaque .....	166
Figure 5.7 The effects of ATRX depletion on the infection with wt and ICP0-null mutant HSV-1 .....	169
Figure 5.8 hDaxx contributes to the efficient repression of ICP0-null mutant HSV-1 .....	171
Figure 5.9 The ATRX interaction region of hDaxx is required for fully efficient repression of ICP0-null mutant HSV-1 gene expression and plaque formation .....	173
Figure 5.10 Interaction between ATRX and hDaxx is required for the efficient establishment of quiescent infections in cultured cells .....	175
Figure 5.11 hDaxx SUMO-interaction motif is required for hDaxx and ATRX recruitment to the sites associated with the incoming ICP0-null mutant HSV-1 genomes.....	177
Figure 5.12 The SUMO-interaction motif of hDaxx is required for fully efficient repression of ICP0-null mutant HSV-1 infection.....	178
Figure 5.13 Analysis of ATRX expression during infection with HSV-1.....	179
Figure 5.14 ICP0 neither interacts with nor disrupts the ATRX/hDaxx complex .....	181
Figure 5.15 Phosphorylation of hDaxx during wild-type HSV-1 infection.....	183
Figure 6.1 Models of HCMV pp71 and HSV-1 ICP0 counteracting functions on ATRX/hDaxx complex during the initial stages of lytic infection .....	194

## List of Tables

Table 2.1 Primary antibodies used in the study .....	77
Table 2.2 Secondary antibodies used in the study .....	78
Table 2.3 Plasmids .....	79
Table 2.4 Oligonucleotides used in cloning procedures and sequencing.....	80
Table 2.5 Primer pairs used in pLNGY-hDaxx vector construction.....	92
Table 2.6 Lentivirus-transduced stable cell lines generated during the study .....	103
Table 3.1 Summary of localisation of PML, hDaxx and ATRX in transduced HepaRG cell lines .....	133
Table 4.1 IE protein expression in ATRX-depleted cells .....	146

## List of Abbreviations

### A-B

aa	amino acid
ADD	ATRX-DNMT3-DNMT3L
AIDS	acquired immunodeficiency syndrome
AmpR	ampicillin resistance gene
APC	antigen presenting cell
APL	acute promyelocytic leukaemia
APOBEC	apolipoprotein B mRNA-editing enzyme catalytic polypeptide
ATP	adenosine triphosphate
ATRX	alpha-thalassaemia mental retardation X-linked
BCR	B cell receptor
BHK	baby hamster kidney
BL	Burkitt's lymphoma
BP	binding protein

### C-D

cAMP	cyclin adenosine-monophosphate
CBP	CRE-binding protein
CD	cell differentiation
cDNA	complementary DNA
C/EBP $\beta$	CAAT/enhance-binding protein $\beta$
ChIP	chromatin immunoprecipitation
CoREST	co-repressor for repressor element-1-silencing transcription factor
CpG	cytosine-phospho-guanine
cPPT	polypurine tract
CRE	cyclic adenosine-monophosphate response element
CREB	cyclic adenosine-monophosphate response element binding
Daxx	death domain associated protein
DMEM	Dulbecco's modified Eagle's Medium
DMSO	dimethyl sulphoxide
DNA	deoxyribonucleic acid
DNMT	DNA methyltransferase
dNTP	deoxynucleotide triphosphate
DTT	dithiothreitol

**E-F**

<i>E. coli</i>	<i>Escherichia coli</i>
EBV	Epstein-Barr virus
EDTA	ethylene glycol-bis-(2-aminoethyl)-N,N,N', N'-tetraacetic acid
EGFP	enhanced green fluorescent protein
EGTA	ethylene glycol-bis-(2-aminoethyl)-N,N,N', N'-tetraacetic acid
EYFP	enhanced yellow fluorescent protein
FACS	fluorescence activated cell sorting
FBS	foetal bovine serum
FITC	fluorescein isothiocyanate
FRAP	fluorescence recovery after photobleaching

**G-H**

GFP	green fluorescent protein
H (3 or 4)	core histone 3 or 4
h	hour
HAT	histone acetyltransferase
HCF	host cell factor
HCMV	human cytomegalovirus
HDAC	histone deacetylase
HF	human fibroblasts
HF	high fidelity (in PCR reactions)
HFFF	human foetal foreskin fibroblasts
HHV	human herpesvirus
HIPK	homeodomain interacting protein kinase
HIV	human immunodeficiency virus
HP1	heterochromatin protein 1
hPGK	human phosphoglycerate kinase
hpi	hours post infection
HRP	horseradish peroxidase
HSK	herpes simplex keratitis
HSV	herpes simplex virus
HZ	herpes zoster

**I-J**

ICP	infected cell protein
IE	immediate early
IF	immunofluorescence
IFN	interferon
IgG	immunoglobulin
IP	immunoprecipitation
IR <sub>L</sub>	inverted repeat long
IR <sub>S</sub>	inverted repeat short
ISG	interferon stimulated gene
JNK	Jun-N-terminal kinase
<b>K-L</b>	
kbp	kilo base pairs
kDa	kilo-Dalton
KS	Kaposi's sarcoma
KSHV	Kaposi's sarcoma associated herpesvirus
LANA	latency associated nuclear antigen
LAT	latency associated transcript
LB	Luria-Bertani
LTR	long terminal repeats
<b>M-N</b>	
μl	microlitre
M	Molar
mM	millimolar
mm	millimetre
MCP	major capsid protein
MeCP	methyl-CpG-binding protein
MHC	major histocompatibility
MIEP	major immediate early promoter
mg	milligram
min	minute
miRNA	micro ribonucleic acid
ml	millilitre
MNase	micrococcal nuclease
MOI	multiplicity of infection

mRNA	messenger ribonucleic acid
ND	nuclear domain
NeoR	neomycin resistance gene
ng	nanogram
NF- $\kappa$ B	nuclear factor kappa B
NK	natural killer
nm	nanometre
<b>O-P</b>	
ORF	open reading frame
PAGE	polyacrylamide gel electrophoresis
PAH	paired amphipathic helices
PBS	phosphate buffered saline
PCR	polymerase chain reaction
PHD	plant-homeodomain
PI	propidium iodide
PML	promyelocytic leukaemia protein
pp	phosphoprotein
PuroR	puromycin resistance
<b>R-S</b>	
REST	repressor element-1-silencing transcription factor
RGB	resolving gel buffer
RING	really interesting new gene
RISC	RNA-induced silencing complex
RNA	ribonucleic acid
RNAi	RNA interference
rpm	revolutions per minute
RRE	rev response element
RSV	Rous sarcoma virus
<i>S. cerevisiae</i>	<i>Saccharomyces cerevisiae</i>
SDS	sodium dodecyl sulphate
sec	second
SENP	sentrin (SUMO) specific protease
SGB	stacking gel buffer
shRNA	short hairpin RNA

SIM	small ubiquitin modifier-interaction motif
sin	self-inactivating
siRNA	small interfering RNA
SNF	sucrose non-fermenting
SUMO	small ubiquitin-like modifier
SWI	mating type switch
<b>T-U</b>	
TG	trigeminal ganglia
<i>tk</i>	thymidine kinase
TRIM	tripartite motif
TR <sub>L</sub>	terminal repeat long
TR <sub>S</sub>	terminal repeat short
<i>ts</i>	temperature sensitive
TSA	trichostatin A
U <sub>L</sub>	unique long
U <sub>S</sub>	unique short
USP	ubiquitin specific protease
UV	ultraviolet
<b>V-X</b>	
VHS	virion-induced host shut-off protein
Vif	virion infectivity factor
VP	virion protein
VSV	vesicular stomatitis virus
VZV	varicella-zoster virus
WB	western blotting
WME	William's medium E
wt	wild-type
X-gal	5-bromo-4-chloro-3-indolyl-β-D-galactopyranoside

# 1 Introduction

Viruses have evolved to overcome various host anti-viral defences in order to enable productive infection. The current thesis represents an in-depth investigation into two large double-stranded DNA viruses, herpes simplex virus type 1 (HSV-1) and human cytomegalovirus (HCMV), with regard to their ability to overcome intrinsic intracellular anti-viral defence mechanisms. Both HSV-1 and HCMV are members of the family *Herpesviridae* and are widely spread in nature. The aims of the following Chapter are to provide a detailed background to the life cycles of HSV-1 and HCMV, with a particular focus on their immediate-early gene expression. For more details on a specific subject of herpesvirus biology, not covered in the present Chapter, the reader is referred to the reviews by Roizman et al (2007), Pellet and Roizman (2007) and Mocarski et al (2007) in “Fields Virology”, and relevant chapters of “Human Herpesviruses: Biology, Therapy and Immunoprophylaxis” (2007), cited throughout.

The various cellular mechanisms developed by the host organism to regulate and prevent the spread of viral infection include anti-viral immunity (innate, adaptive and intrinsic) and epigenetic mechanisms. A part of intrinsic defences against herpesviruses in humans is provided by the nuclear substructures ND10. Since many nuclear proteins involved in the regulation of chromatin state reside at ND10, this Chapter presents a detailed account on their functions in the viral life cycle.

## 1.1 Family *Herpesviridae*

### 1.1.1 Overview of the family and key features

The mammalian, avian and reptile representatives of the herpesviruses constitute the family *Herpesviridae* of the order *Herpesvirales*. The other two families of the order are *Alloherpesviridae* (fish and frog viruses) and *Malacoherpesviridae* (oyster virus) (Davison et al, 2009). Subfamilies distinguished within the *Herpesviridae* family are *Alpha-*, *Beta-*, and *Gammaherpesvirinae*. Members of these subfamilies include eight human herpesviruses: herpes simplex virus type 1 (HSV-1), a common cause of cold sores; HSV-2, the causative agent of genital herpes; human cytomegalovirus (HCMV); varicella-zoster virus (VZV), causing chicken pox; Epstein-Barr virus (EBV), human herpesvirus 6 and 7 (HHV6 and HHV7); and HHV-8, associated with Kaposi’s sarcoma (hence, another name, Kaposi’s sarcoma-associated herpesvirus; KSHV) and Castleman’s disease.

The major biological properties characteristic of all herpesviruses have been previously summarised in a following way (reviewed in Pellet and Roizman, 2007):

- All herpesviruses specify a selection of enzymes involved in nucleic acid metabolism, DNA synthesis and processing of proteins.
- The synthesis of viral DNA, assembly of capsids and DNA packaging into the capsid occur in the nucleus.
- Production of viral progeny during lytic infection is associated with the destruction of the infected cell.
- Herpesvirus genomes are able to persist in the natural hosts in a latent state in the form of closed circular molecules called episomes within the infected cell.

The structural characteristics of the virus particles define the members of *Herpesviridae*. A typical herpesvirus virion is approximately 120 to 260 nm in size and consists of the four major structural elements: a core, a capsid, a layer of tegument, enclosed within the envelope (Figure 1.1). The double-stranded DNA ranges from 124 to 230 kb in size, is linear within the virion, but circularizes into an episome immediately upon its release into the infected cell nucleus. The icosahedral capsid is approximately 125 nm in diameter and consists of capsid proteins. The proteinaceous tegument surrounds the capsid. Within the viral envelope viral glycoproteins are embedded with the spikes protruding away from the surface. During a productive HSV infection, coordinated gene expression is switched between immediate early (IE;  $\alpha$ ), early ( $\beta$ ) and late ( $\gamma$ ) genes. The key IE genes of HSV-1 and HCMV, which are of particular relevance to the present study, will be discussed in later sections of this Chapter.

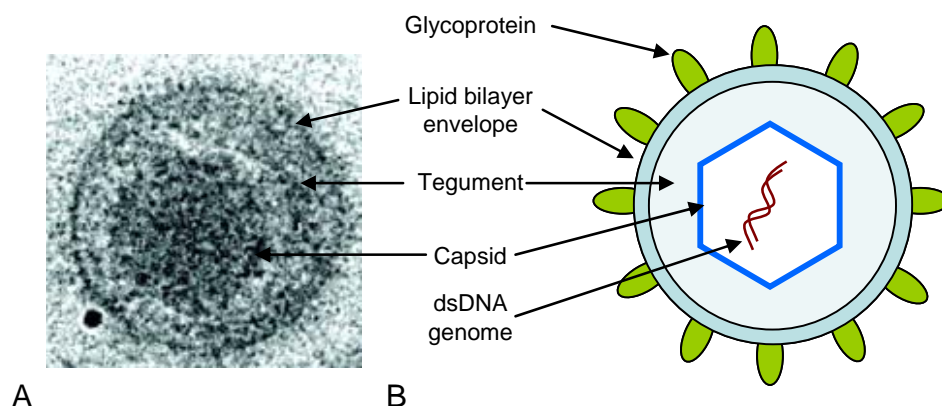


**Figure 1.1 Architecture of a typical herpesvirus infectious virion particle**

Key structural features are represented by tomographic re-construction of an HSV-1 virion (A; Grunewald et al, 2003) and a schematic diagram (B; adapted from Liu and Zhou, 2007).

### **1.1.2 Subfamilies**

Within the family *Herpesviridae*, three subfamilies are recognised. Their characteristics are briefly discussed below (Pellet and Roizman, 2007). Particular attention will be given further to the representatives of the  $\alpha$ - and  $\beta$ -subfamilies of herpesviruses, HSV-1 and human cytomegalovirus HCMV, respectively.

#### ***1.1.2.1 Alphaherpesvirinae***

The members of this subfamily are characterised by their variable host range, relatively short reproductive cycle, rapid spread in culture, efficient destruction of infected cells, and capacity to establish latent infections primarily in sensory ganglia. This subfamily contains the genera Simplexvirus (HSV-1), Varicellovirus (VZV), Mardivirus (GaHV-2), and Iltovirus (GaHV-1). The former two genera have mammalian hosts, and the latter two have avian hosts. Rapid spread of HSV-1 in common laboratory epithelial or fibroblastic cell lines make HSV-1 convenient to study in standard laboratory settings.

#### ***1.1.2.2 Betaherpesvirinae***

Betaherpesviruses differ from alphaherpesviruses by their restricted host range. The reproductive cycle is long, and the infection progresses slowly in culture, and particularly in primary cell lines. The sites of latency establishment are secretory glands, lymphoreticular cells, kidneys, and other tissues. The subfamily is further subdivided into genera of Cytomegalovirus (HCMV), Muromegalovirus (MCMV), Roseolovirus (HHV-6), and Proboscivirus (EIHV-1).

#### ***1.1.2.3 Gammaherpesvirinae***

The members of Gammaherpesviruses are usually specific for either T- or B-lymphocytes. *In vitro* all members replicate in lymphoblastoid cells, and some also cause lytic infections in some types of epithelial and fibroblastic cells. This subfamily contains four genera: *Lymphocryptovirus*, *Rhadinovirus*, *Macavirus* and *Percavirus* (Davison et al, 2009). Human representatives are EBV and HHV-8 (or Kaposi's sarcoma-associated virus; KSHV). *In vitro* EBV efficiently infects primary human B lymphocytes, which results in nonpermissive conditions for EBV replication and transformation of B cells into long-term lymphoblastoid cell lines. The cell culture system for KSHV is primary effusion lymphocytes (proliferating B-cells from end-stage AIDS patients), which harbour latent KSHV genomes and only 1-5% show lytic replication (for reviews see Kieff and Rickinson, 2007; Ganem, 2007).

## **1.2 Pathogenesis of herpesvirus infections**

Despite most human herpesvirus infections being asymptomatic, or symptoms being generally mild in immunocompetent individuals, life-threatening infections may occur in immunocompromised individuals or people with suppressed immunity, and especially neonates. Treatment of herpesvirus infections is largely based on nucleoside analogues, which target viral DNA polymerase during the process of replication. The clinical manifestations of these infections will be summarised in this part of the Chapter.

### **1.2.1 HSV infections**

Primary or recurrent HSV-1 or HSV-2 infections can be symptomless. Prevalence of HSV-1 infection is substantially higher than that of HSV-2 but the figures vary largely between geographic regions and amongst different age groups. Thus, in the US the population of HSV-1 seropositive individuals reaches 80%, and similar values were observed amongst European populations. HSV-2 seroprevalence rises from about 20-30% at the age of 15-29 years and up to 35-60% by the age of 60 in the US. Substantially lower figures were obtained for most of the European populations: between 3% in post-adolescent population rising to 25% in 40-year olds in the UK, and as low as 2-6% in Spain (Smith & Robinson, 2002; Whitley & Roizman, 2001).

#### ***1.2.1.1 Genital herpes***

Genital herpes can result from both HSV-1 and HSV-2 infections, however it is HSV-2 that is mostly responsible for recurrent genital herpes (accounting for 85-90% of outbreaks). Genital herpes infections are acquired *via* a sexual route. Primary and recurrent infections are associated with appearance of sores, result in physical discomfort and bear a psychosocial impact; however in most people symptoms remain unnoticed and unrecognized. Due to this, asymptomatic shedding of HSV-2 infections represents the most common cause of the increasing rate of HSV-2 transmission. Treatment involves oral administration of acyclovir at the time of the appearance of lesions. Suppressive therapy using valaciclovir during asymptomatic shedding is known to reduce transmission significantly (Leone, 2005).

### ***1.2.1.2 HSV infection of the central nervous system***

Although rare, severe HSV-related disorders of the central nervous system can result from acquisition of HSV infections *via* a congenital route causing neonatal herpes. Later in life these infections may result in life-threatening encephalitis or the more benign aseptic meningitis. In immunocompetent adults, over 90% of herpesviral encephalitis cases result from HSV-1 infection and a remainder from HSV-2. The clinical manifestation of herpes simplex encephalitis is acute focal, necrotizing encephalitis with inflammation and swelling of the brain tissue. Recurrent aseptic meningitis is caused mostly by HSV-2, and is associated with repeated episodes of fever, severe headache and meningismus. Treatment of both herpes simplex encephalitis and aseptic meningitis involves intravenous administration of acyclovir (Gilden et al, 2007; Tyler, 2004).

### ***1.2.1.3 Herpes simplex keratitis***

Following HSV-1 infection of the eye, herpes simplex keratitis (HSK) may develop. HSK can represent either primary disease, resulting upon the infection of a subject with no previous exposure; initial ocular disease of the host previously exposed to HSV-1; recurrent HSK or superinfection with another HSV-1 strain. Notably, infection with HSV-1 *via* the ocular route by scarification of the ocular surface is very common in experimental approaches studying HSV-1 in mouse models. In these models, infection results in subsequent establishment of latency in the cornea, iris and trigeminal ganglia (TG). The clinical manifestations of the ocular disease include lid and conjunctival disease, which may result in detrimental effects on vision. Recurrent infection is the principal cause of blindness, therefore development of suitable treatment strategies to prevent reactivation of the virus is of key importance. Acyclovir therapy so far proves to be efficient in the prevention strategy (reviewed in Kaye & Choudhary, 2006)

## **1.2.2 HCMV infections**

Most primary HCMV infections are asymptomatic, and the virus becomes latent within months after infecting an immunocompetent individual. Seroprevalence figures vary between 35-95% in different populations, although most infected individuals may lack clinical manifestations (Malm & Engman, 2007). Since the virus can infect leukocytes, endothelial cells, connective tissue cells and epithelial cells, HCMV infection can be acquired through blood transfusion, sexual and perinatal routes, or by transplantation. HCMV has a potential to transform human tissues, since high viral titres can be detected in

a number of cancer biopsies. HCMV-associated malignancies are due to the ability of HCMV to inhibit the function of p53 tumour suppressor (reviewed in Doniger et al, 1999).

### ***1.2.2.1 Congenital HCMV infections***

Congenital infections of the newborns present a significant concern. These infections can result from CMV infections during pregnancy, which although asymptomatic can be manifested in premature delivery (Pereira et al, 2007). About 0.5 to 2.5% of all newborns are infected at birth, and HCMV has therefore become the most common cause of viral birth defects in congenitally infected babies. About 10-15% of neonates with congenital CMV show infection-related symptoms. Cytomegalic inclusion disease is a representative consequence of such infections, and is characterised by the involvement of multiple organs, in particular reticuloendothelial and central nervous systems, potentially involving ocular and auditory damage. Further symptoms include jaundice, hepatosplenomegaly, microcephaly, seizures, hypotonia and lethargy. Such congenital infections may cause a variety of subsequent disabilities, including mental retardation and learning disabilities, hearing impairment and visual deficit (Malm & Engman, 2007).

### ***1.2.2.2 HCMV infections of immunocompromised and immunosuppressed hosts***

HCMV infections are most commonly symptomatic and present significant management concerns amongst immunocompromised hosts. HCMV-related disorders of human immunodeficiency virus (HIV)-infected adults can be life-threatening. The most common disorder in HCMV-infected acquired immunodeficiency syndrome (AIDS) patients is retinitis, accounting for 85% of cases (Steininger, 2007). In addition, HCMV infection comprises an important complication in organ transplantation, and is known to have been associated with significant morbidity and mortality of post-transplant individuals. Over 75% of solid transplantation patients are newly infected or reactivate latent CMV. CMV disease can then be manifested by fever, hepatitis, pneumonitis, gastroenteritis and retinitis, but is usually treatable using standard anti-CMV drugs discussed below (Fishman et al, 2007).

### ***1.2.2.3 Treatment***

No anti-HCMV vaccine exists, but therapies for HCMV disease are based on the development of anti-viral drugs. These have become essential in prophylactic treatment of transplant patients (Fishman et al, 2007). Five compounds have been approved for the

treatment of established HCMV infections: ganciclovir, its oral prodrug valganciclovir, foscarnet, cidofovir (polymerase inhibitors) and fomivirsen (an oligonucleotide that acts as a translation inhibitor and targets the HCMV IE gene locus). High dose acyclovir or valaciclovir have also been used as prophylactic agents against HCMV, since these drugs are not sufficient for the use in treatment of active HCMV disease (Malm & Engman, 2007).

### **1.2.3 Other herpesvirus infections**

#### ***1.2.3.1 Varicella Zoster Virus***

VZV is another member of *Alphaherpesvirinae* subfamily and very widely spread among the human population. It causes chickenpox and establishes latency in cranial nerve, dorsal root and autonomic nervous system ganglia. Herpes zoster (HZ; or shingles) results from reactivation of the virus, decades after the establishment of latency and is a consequence of declining VZV-specific host immunity. The symptoms of HZ are associated with painful rash, which appears anywhere in the body upon reactivation. Antiviral therapy of these symptoms is based on valaciclovir or famciclovir rather than acyclovir. If the virus spreads to blood vessels of the brain after herpes zoster, VZV can cause vasculopathy, particularly in immunocompromised patients. This can be treated using intravenous acyclovir therapy (Gilden et al, 2007).

#### ***1.2.3.2 Kaposi's sarcoma-associated herpesvirus***

KSHV is a gammaherpervirus which establishes latency in lymphoid tissues. KSHV is detected in Kaposi's sarcomas (KS), the most common tumour of AIDS patients. The disease is associated with the appearance of its proliferating so-called spindle cells which are thought to be of endothelial lineage. KS lesions also contain infiltrating monocytes, T cells and plasma cells. Within the tumour, KSHV targets spindle cells, most of which become latently infected, however 1%-2% of the infected cells express lytic markers. Latently infected spindle cells are positive for KSHV latency-associated transcript LANA, which is known to possess a number of tumourigenic properties (such as inhibition of tumour suppressor p53 and induction of NF- $\kappa$ B). There are a number of models that address how the lytically infected cells contribute to tumour progression but the mechanism remains incompletely understood. Treatment of KS in advanced AIDS patients relies on addition of parenteral ganciclovir, a drug that blocks lytic but not latent KSHV infection, which results in a prompt and dramatic decline in the incidence of new KS tumours (reviewed in Ganem, 2007).

### **1.2.3.3 Epstein-Barr virus**

EBV is another human member of gammaherpesviruses. It infects B and T lymphocytes of more than 90% of the general population. Primary infection can produce infectious mononucleosis. The cell transforming potential of EBV is associated with development of several carcinomas amongst which are nasopharyngeal carcinoma, Hodgkin's disease and Burkitt's lymphoma (BL). BL tumour cells are characterised by the presence of EBV episomes and expression of only one EBV protein, EBV nuclear antigen 1 (EBNA-1), which functions in maintaining episomal DNA replication in latently infected cells. The characteristic of BL cells is chromosomal translocation resulting in the abnormal regulation of the *c-myc* oncogene (Cohen, 2000).

## **1.3 Comparative structure of HSV-1 and HCMV virions**

The architecture of both HSV-1 and HCMV virions is consistent with the schematic diagram presented on Figure 1.1. The size of the average HSV-1 particle is approximately 186 nm in diameter whereas that of HCMV is somewhat larger and ranges in size between 200-300 nm in diameter. The main structural features of the two viruses are described further.

### **1.3.1 Double-stranded DNA core**

The tightly packaged double-stranded DNA genomes of herpesviruses constitute the core of the mature infectious viral particles. These genomes replicate by circularization, followed by a 'rolling circle' mode (see Section 1.4.1.3) to produce linear concatemers which are cleaved into unit-length genomes during the process of packaging. The general structure of HSV-1 and HCMV genomes is represented in Figure 1.2 (reproduced from (McGeoch et al, 1988)). Both are of similar arrangement, and are characterised by the presence of the unique long ( $U_L$ ) and unique short ( $U_S$ ) regions flanked by terminal and inverted repeat sequences ( $TR_L$  and  $IR_L$ ;  $TR_S$  and  $IR_S$ , respectively). During DNA replication, segment inversion occurs resulting in equimolar amounts of genomes containing the two orientations of  $U_S$  and  $U_L$  regions within the viral population. Terminal *a* and internal *a'* (inverted of *a*) sequences consist of direct repeat (DR) elements that are highly conserved, but may vary in numbers. They provide a signal for packaging *via* two conserved elements *pac-1* and *pac-2* (Roizman et al, 2007; Davison, 2007). The size of the HSV-1 genome is approximately 152 kbp, and it comprises around 75 open reading frames

(ORFs) (McGeoch et al, 1988). HCMV genome is about 50% larger and is 235 kbp in size. It encodes for approximately 165 proteins (Dolan et al, 2004).



**Figure 1.2 Organisation of the HSV-1 and HCMV genomes**

### 1.3.2 Capsid

The typical capsid of the herpesvirus virion is a T=16 icosahedron and composed of 12 pentons forming the vertices, 150 hexons forming the faces and edges, and 320 triplexes interconnecting the pentons and hexons. Three different types of capsids are designated as A, B and C-capsids, of which only the latter contains viral DNA (Liu and Zhou, 2007).

#### 1.3.2.1 The HSV-1 Capsid

Four viral proteins constitute the outer shell of the HSV-1 capsid: the major capsid protein (MCP) VP5 (UL19), VP26 (UL35), VP23 (UL18), VP19C (UL38). An additional constituent of the HSV-1 capsid VP24 functions as the protease that processes the internal capsid scaffold during DNA encapsidation (reviewed in Roizman et al, 2007). Pentons and hexons are composed of five and six copies of VP5, respectively. The six copies of VP26 form a ring on top of the VP5 subunits on each hexon. Triplexes are made up of one VP19C molecule and two VP23 molecules that link adjacent capsomeres (Schrag et al, 1989; Zhou et al, 2000). A portal for viral DNA packaging is formed by the UL6 gene product (Chang et al, 2007; Newcomb et al, 2001).

#### 1.3.2.2 The HCMV Capsid

The HCMV capsid is similarly organised, and the five proteins that constitute its capsid are: the MCP encoded by the UL86 gene; triplexes composed of two subunits – the minor capsid protein together with the minor capsid protein binding protein; the smallest capsid protein (SCP, encoded by UL48A gene) at the MCP tips; and a portal protein (PORT, the UL104 gene product) as a specialized vertex in DNA encapsidation (Butcher et al, 1998).

### 1.3.3 Tegument

The tegument of a herpesvirus virion is defined as the space between the inner surface of the envelope and the outer surface of the capsid in a mature particle. Some tegument proteins are associated with capsid. The tegument compartments of HSV-1 and HCMV particles are largely unstructured (reviewed in Roizman et al, 2007; Kalejta, 2008b).

#### *1.3.3.1 HSV-1 tegument proteins*

Amongst HSV-1 tegument proteins the most studied ones include virion transactivator protein VP16 and virion-induced host shut-off (VHS) protein, which are described in more detail in the next paragraphs. Other tegument constituents include VP22, VP1/2, VP11/12 and VP13/14. VP22 encoded by the gene UL49 has a proposed role in cell to cell spread, since mutant plaques appear much smaller in size than wt plaques and viral titres of UL49-mutants are lower (Duffy et al, 2006). VP1/2 (UL36 gene product) is essential for viral replication and plays a role in capsid transport and viral DNA release at the nuclear pore during viral entry. IE-gene encoded proteins ICP0 and ICP4 and the Early protein thymidine kinase (*tk*) are also found within HSV-1 tegument but present a significant interest from the aspect of their expression as the products of their respective classes of genes (reviewed in Kelly et al, 2009).

VP16 is an important protein to consider because of its transactivating functions. It is a 490-amino acid protein, encoded by a late gene UL48, with an acidic C-terminal transcriptional activation domain. In lytic infection, around 500-1000 VP16 molecules within the HSV-1 tegument are delivered to the host cell, and the VP16-induced complex is assembled (reviewed in Wysocka & Herr, 2003). VP16 associates with cellular proteins Host Cell Factor (HCF) and Oct-1, which bind specific sequences of the regulatory elements of IE promoters to induce activation of IE gene transcription. Analysis of VP16 mutant viruses has identified the domains necessary for IE transcription, as well as for virion assembly. These mutants are defective in plaque formation, and cells infected at low multiplicities of infection (MOI) have a high tendency to harbour HSV-1 genomes in a quiescent state (Ace et al, 1988; Ace et al, 1989). Recruitment of cellular chromatin remodelling proteins such of SWI/SNF family enzymes and histone acetyltransferases (see Section 1.7.1) to VP16-induced complexes (Herrera & Triezenberg, 2004; Memedula & Belmont, 2003) strongly correlates with the high transcriptional activity from the IE gene promoters very early during the infection.

The virion induced host shut-off protein (VHS) is encoded by the UL41 gene and is phosphorylated in infected cells (Smibert et al, 1992). VHS contributes to the global decline of host mRNA levels (shut-off) by acting as RNase or a subunit of RNase complex (Elgadi et al, 1999; Everly et al, 2002). In addition, VHS-induced host cell mRNA destabilization promotes loss of the major histocompatibility complex (MHC) class I from the cell surface, thereby rendering the infected cells resistant to lysis by cytotoxic (CD8+) T lymphocytes (see Section 1.9). This mechanism suggests the role of VHS in immune evasion (reviewed in Smiley, 2004).

### ***1.3.3.2 HCMV tegument proteins***

Most HCMV tegument proteins are phosphorylated, however the purpose of this phosphorylation for their function has not been defined. The functions of various tegument proteins have been extensively reviewed elsewhere (Kalejta, 2008a; Kalejta, 2008b). These include activation of gene expression, immune evasion, and stages of viral entry, assembly and egress during the lytic phase of infection. For example, HCMV UL47 and UL48 proteins that associate with viral capsid can interact with microtubule motor proteins in order to facilitate the delivery of capsids to the nuclear pore complex. Pp65 (encoded by the UL83 gene) is a major constituent of HCMV particles and is delivered to the nucleus of the infected cells at the initial stages of lytic infection, however it is completely dispensable for replication in cultured fibroblasts. This protein is the dominant target antigen of cytotoxic T lymphocytes. Pp65 and pp71 are neighbouring genes and are expressed from an overlapping mRNA transcript of approximately 4 kb (Ruger et al, 1987). Pp71 is a very potent transcriptional activator of IE gene expression, and pp71-null mutant HCMV replicates in culture very poorly (reviewed in Kalejta, 2008b). A specific section dedicated to pp71 and its role in transcriptional activation is presented later (Section 1.6.5), because of its direct relevance to the subject of the present thesis.

### **1.3.4 Envelope**

Approximately 11 different viral glycoproteins are embedded into the lipid bilayer of the viral envelope. The HSV-1 virion envelope glycoproteins are gB (VP7 and VP8.5; encoded by the UL27 gene), gC (VP8; UL44), gD (VP17 and VP18; US6), gE (VP12.3 and VP12.6; US8), gG (US4), gH (UL22), gI (US7), gL (UL1), and gM (UL11) (Roizman et al., 2007). Envelope glycoproteins of HCMV include homologues of those found within HSV-1 envelope, and similarly, mediate roles in attachment and entry into the host cell (reviewed in Davison and Bhella, 2007; Mocarski, 2007).

## 1.4 The overview of the HSV-1 and HCMV life cycles

Herpesviruses life cycles are characterised by the ability to switch between lytic (associated with the release of viral progeny) and latent modes of infection. The precise mechanisms underlying this switch remain largely unclear. The sequences of events occurring during the establishment of lytic herpesvirus infections are very much alike. These are addressed below with the focus on HSV-1 and HCMV.

### 1.4.1 The lytic infectious cycle

The members of *Alphaherpesvirinae* and *Betaherpesvirinae* have similar pathways of the initiation of lytic cycle infection due to their abilities to infect mucosal membranes. For the purposes of this Chapter, specific molecular mechanisms occurring during each stage of the lytic life cycle of HSV-1 and HCMV will not be covered. These can be found in the reviews by Roizman et al (2007) and Mocarski et al (2007), as well as those cited throughout the next paragraphs. The schematic diagram on Figure 1.3 (p.35) represents the overview of the lytic infectious cycle.

#### 1.4.1.1 Viral entry into the host cell

The process of entry into the host cells involves a series of defined steps prior to the release of viral DNA into the nucleus: (i) binding to specific cell surface receptors; (ii) fusion of the envelope with the cellular membrane followed by a release of nucleocapsids into the cytoplasm; (iii) nucleocapsid association with cytoskeletal elements and translocation to the nuclear membrane, where release of viral DNA finally occurs. Initial attachment involves interaction between viral glycoproteins and heparan sulphate molecules on the host cell membrane. In HSV-1 the initial binding of the viral particle involves the interaction of glycoproteins gC and gB with host cell surface heparan sulphate and between gD and host cell entry receptors nectins and herpesvirus entry mediator HVEM. The process of fusion is facilitated by the heterodimer formed between gH and gL (reviewed in Spear et al, 2000). In HCMV the process of viral cell fusion also requires the functions of gH/gM heterodimer. In addition to heparan sulphate molecules, host cell  $\beta$ 2-microglobulin and annexin II participate in HCMV entry (reviewed in Campadelli-Fiume and Menotti, 2007; Mocarski, 2007).

Trafficking of the infectious virion particles relies on the interactions between viral tegument proteins and the components of the cell cytoskeleton. Thus, it has been proposed

that the microtubule motor dynein is involved in the intra-cellular trafficking of HSV-1 capsids (Dohner et al, 2002). The HSV-1 capsid protein VP26 and the largest tegument protein pUL36 have been shown to be required for this process (Douglas et al, 2004; Shanda & Wilson, 2008). The interactions between HCMV proteins and host-cell intracellular trafficking machinery are less understood, but microtubules are also thought to be responsible for this process in HCMV infection. The largest tegument protein encoded by UL48 may be required for the process of viral replication by analogy with HSV-1 UL36 functions, in controlling uncoating and release of viral DNA at nuclear pores. Once the viral capsid has reached the nuclear membrane, viral DNA is released through the nuclear pore. In HSV-1 the protein that is likely to play a role in this process is VP1/2 whereas in HCMV the functional homologue of this protein is thought to be the large tegument protein pUL48 and its binding partner pUL47 (Mocarski et al, 2007).

#### ***1.4.1.2 Gene expression***

Herpesvirus gene expression occurs in a temporally regulated cascade, utilizing pre-existing viral and cellular proteins for activation of IE gene expression. Thus, the genes are classified according to their timing of expression as Immediate Early (IE; or  $\alpha$ ), Early ( $\beta$ ; also called Delayed Early for CMV) or Late ( $\gamma$ ) genes. IE gene products are essential for efficient transcriptional activation (see Section 1.6). Early genes encode enzymes that are involved in nucleotide metabolism and DNA replication (for example, HSV-1 *tk* and HCMV viral protein kinase VPK, which function as nucleoside kinase), as well as a number of glycoproteins. Late genes are principally responsible for the expression of structural proteins that make up the virion. While IE gene expression does not require *de novo* protein synthesis and is activated by viral and host cell transcriptional factors, Early and Late gene regulation is highly dependent on the synthesis of IE gene products (Honess & Roizman, 1974). The aspects of IE gene regulation and the functions of IE proteins will be addressed in more detail later (see Section 1.6).

During infection with either HSV-1 or HCMV, the viral genome circularises into an episome upon entry into the nucleus (McVoy & Adler, 1994; Strang & Stow, 2005). These episomal DNA structures become associated with components of nuclear domains termed ND10. In wt HSV-1 and HCMV infections, ND10 are disrupted prior to the initiation of DNA replication by viral tegument and IE proteins (see Sections 1.5.2, 1.6.3 and 1.6.5). With the expression of Early gene products, DNA synthesis begins. At this early stage of

viral infection, so-called replication compartments are formed within the nucleus of an infected cell (Wilkinson & Weller, 2003).

### ***1.4.1.3 Viral DNA synthesis***

#### ***HSV DNA replication***

HSV-1 DNA contains three sites that act as origins of replication. The seven essential HSV-1 genes that are required and sufficient for genome replication are the three subunits of DNA helicase-primase complex UL5, UL8, and UL52; the origin-binding protein UL9; the DNA binding protein ICP8, the product of UL29; DNA polymerase encoded by UL30; and the processivity factor UL42. Firstly, pUL9 binds the replication origin on the episomal DNA in a sequence-specific manner. Then ICP8 interacts with the C terminus of UL9 protein, inducing its DNA-dependent ATPase and DNA helicase activities. This is followed by a three-subunit DNA helicase-primase complex interaction with ICP8, which promotes DNA unwinding for the access of DNA polymerase. Viral DNA polymerase encoded by the UL30 gene also expresses a 3' → 5' exonuclease activity, which is required for deoxynucleotide polymerization and provides a proof-reading function. An additional protein, the processivity factor UL42, acts to enhance the activity of viral DNA polymerase. Replication proceeds in a rolling-circle model and generates linear DNA concatemers (Lehman & Boehmer, 1999).

#### ***HCMV DNA replication***

There are six HCMV proteins that are essential for its DNA synthesis. In common with HSV-1 and other herpesviruses, these include the UL54-encoded polymerase catalytic subunit associated with the UL44 gene product polymerase processivity factor in a polymerase complex; the UL57 encoded single-strand DNA binding protein; and the three-subunit complex of helicase-primase consisting of gene products of UL105, UL70 and UL102. The proteins known as origin binding proteins are IE2 and UL84. These proteins are thought to form complexes that stimulate transcription across the HCMV origin of replication *oriLyt*. The replication model supports the rolling-circle mechanism as for HSV-1. Additional proteins with auxiliary roles in viral DNA synthesis are UL36-38 gene products, which are thought to maintain a more favourable cellular environment for DNA replication in HCMV infected cells. DNA synthesis allows activation of Late gene expression, resulting in the production of proteins required for assembly and egress of the viral particles (Anders et al, 2007).

#### ***1.4.1.4 Capsid assembly and packaging of viral DNA***

Apart from infectious virions, non-infectious viral particles and dense bodies are found in the culture media of the cells that are lytically infected with HSV-1 or HCMV (Figure 1.3). The ratio of these particles to mature infectious virions can sometimes reach 20:1, which implies that they are produced in great excess (Liu and Zhou, 2007). Proteins that are required for nucleocapsid formation are MCP, triplex proteins (pUL18 and pUL38 of HSV-1), and a maturational protease (pUL26 of HSV-1). Additional proteins, the small capsid protein at the hexon tips and the portal protein are non-essential in alphaherpesviruses for capsid formation but are essential in beta- and gammaherpesviruses (Mettenleiter et al, 2009); Mocarski et al, 2007).

Encapsidation of viral DNA is a process conserved between HSV-1 and HCMV and involves cleavage of viral progeny DNA concatemers into unit length monomers (Roizman et al., 2007). The process of cleavage of the concatemeric DNA is conserved and requires the heterotrimeric (HSV) or heterodimeric (HCMV) protein named terminase. HSV-1 terminase is composed of proteins pUL15 (putative ATPase subunit), pUL28 and pUL33 (Mettenleiter et al, 2009). In HCMV the terminase consists of ATPase subunit pUL89 (TER1) and a capsid recognition subunit pUL56 (TER2). The functions of the terminase complex include the regulation of the threading of a particular genome length of DNA into the capsid, scanning for a *pac* site and determining the position of DNA cleavage to produce genomic ends. The conserved *pac* elements located within the *a* sequences (Figure 1.2) of the HSV and HCMV genomes therefore trigger the packaging and cleavage processes (Mocarski et al, 2007).

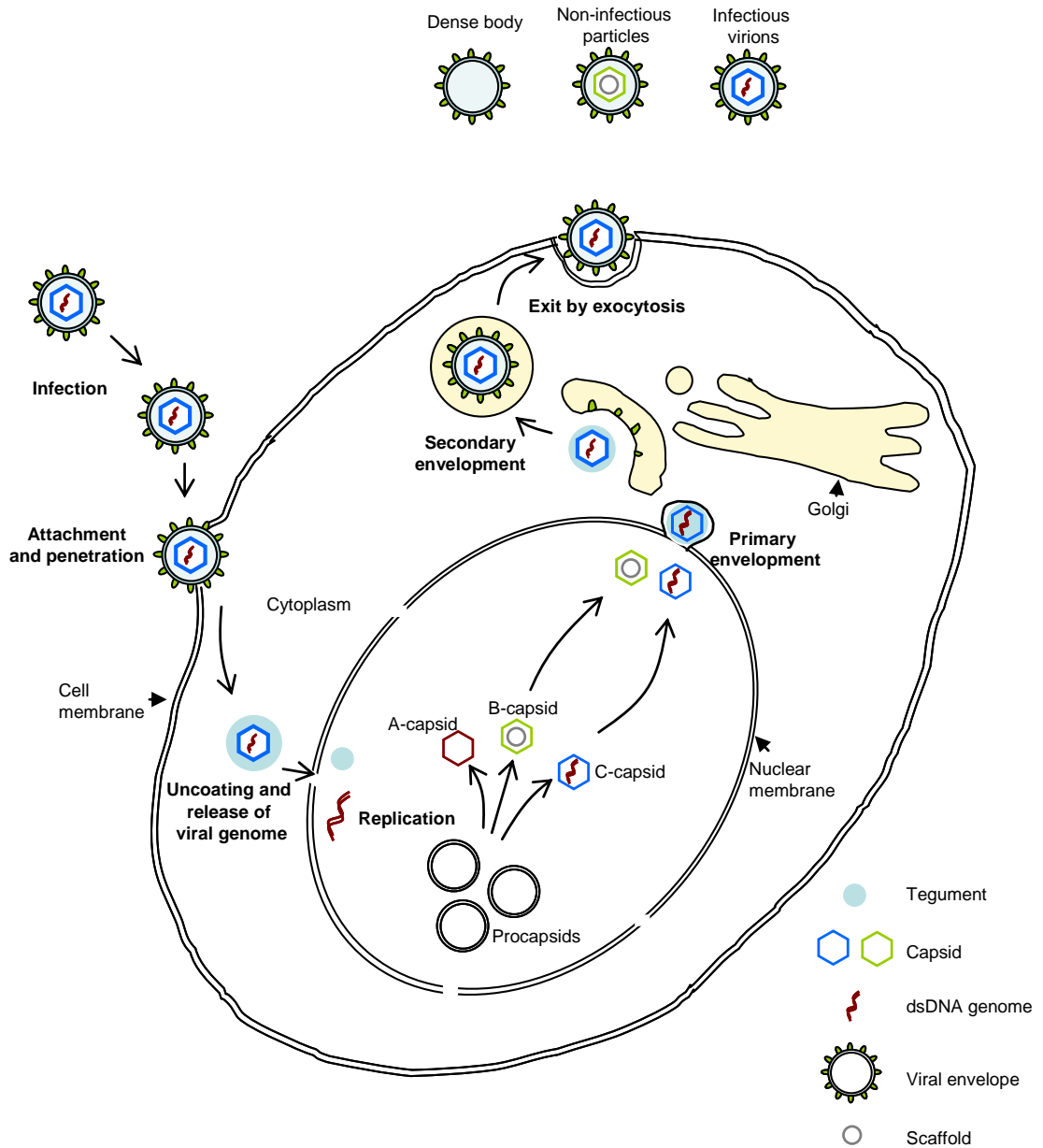


**Figure 1.3 Overview of the herpesvirus lytic infectious cycle**

The infectious virion infects the cell by either endocytosis or fusion with the cell membrane, which results in release of the nucleocapsid and some tegument proteins into the cytoplasm. The nucleocapsid is transported across the cytoplasm, and the viral DNA is injected into the nucleus through the nuclear pore. DNA replication and assembly of virions take place in the nucleus. Procapsids mature into the C-capsids (infectious). A-capsids are abortive which result from failure to encapsidate DNA. Both B- and C- capsid can acquire some tegument proteins at the nuclear membrane. Scaffold protein of the infectious capsids is released prior to DNA encapsidation. Cytoplasmic capsids are enveloped and released by exocytosis. The model presented on this diagram, which applies to HCMV lytic infection, is consistent with the envelopment-deenvelopment model of virion assembly. During HSV-1 replication, apart from the infectious viral particles, empty L-particles can also be produced (adapted from Liu and Zhou, 2007 and Mettenleiter et al, 2009).

#### ***1.4.1.5 Maturation and egress***

The models of capsid maturation are somewhat controversial. The dominant model states that tegument proteins function together with non-structural proteins to control a complex two-stage envelopment and egress process that initiates at the nucleus and results in the virion release by exocytosis at the plasma membrane. This model is referred to as the envelopment-deenvelopment model in some reviews (Mettenleiter et al, 2009); Figure 1.3). Alternative models propose different scenarios. One of them suggests a single envelopment event at the nuclear membrane and subsequent vesicular transport of the enveloped particle to the plasma membrane. The other model proposes enlargement of the nuclear pore to a size which readily allows the egress of the unenveloped capsids into the cytoplasm (reviewed in Roizman et al, 2007).

According to the first and currently mostly accepted model, in both HSV-1 and HCMV the primary envelopment starts at the inner nuclear membrane followed by the de-envelopment process at the outer nuclear membrane, releasing the capsid into the cytoplasm. Secondary envelopment occurs at the endosomal membranes, which produce vesicles carrying the fully mature virions to the cell surface *via* the cellular exocytosis. The virus-cell interactions required for the process of maturation and egress of mature virions are thought to be different from those involved in viral entry and are less well understood. The two conserved herpesvirus proteins (in HSV-1 referred to as UL31 and UL34 gene products) participate in the early steps of the budding process at the nuclear membrane. For the nucleocapsids to gain access to the inner nuclear membrane, which is obstructed by the nuclear lamins, cellular kinases are recruited by the pUL31/pUL34 complex. At this stage, viral kinases (e.g. pUL97 in HCMV and pUS3 of HSV-1) can also induce phosphorylation of nuclear lamins in order to gain access for interaction between nuclear capsids and the inner nuclear membrane. Since the final envelopment occurs in the cytoplasm, viral tegument includes a small amount of cellular proteins, particularly actin as well as small RNA molecules. Exocytosis follows the final envelopment stage, where the mature virion is carried inside a vesicle to the cell surface for release. The release of the virus particle is thought to follow cellular vesicular trafficking pathways. Released infectious viral particles can infect adjacent cells by cell-to-cell spread or be carried into the sites of latency establishment (reviewed in Mettenleiter, 2002; Mettenleiter et al, 2009; Mocarski, 2007).

## 1.4.2 Latency

A prominent characteristic of all herpesviruses, that confers their evolutionary success, is their ability to persist in the host in a latent state. Herpesvirus latency is generally characterised by production of a very small number of transcripts and a gene expression profile distinct from that of lytic cycle. Despite extensive research, the mechanisms that operate during latency establishment and reactivation remain incompletely understood. Some evidence regarding these mechanisms in HSV-1 and HCMV latent infection is therefore discussed in the next paragraphs.

### *1.4.2.1 HSV-1 latency and models of quiescent infection*

Following lytic infection in epithelial tissues, HSV-1 enters sensory nerve fibres within the stratified epithelium, and then travels by retrograde axonal transport along the microtubules to the cell body of the neurons in order to establish a lifelong latent infection of these neurons in the sensory ganglia. Neurons are the primary site of HSV-1 latency establishment. In mouse models active viral replication is initially supported during the first three to four days of infection during the acute phase, but no infectious viral progeny is detected later on, indicating efficient establishment of latency in neurons (Cook et al, 1974; Speck & Simmons, 1991; Stevens & Cook, 1971). Intermittent reactivation of the virus occurs spontaneously and results in axonal anterograde microtubule-associated transport of the virus, where the virus crosses back into the epithelia, usually in the area of the initial infection, replicates and is shed into oral secretions (Cunningham et al, 2006). In latently infected cells the viral genome is thought to exist in an episomal conformation. This conformation is also associated with lytic infection when the viral DNA first encounters nuclear environment; however the transcriptional programme of latent genomes differs substantially. Hence, there are a number of markers that are known to associate with latent HSV-1 genomes.

Firstly, latency is characterised by the lack of detectable lytic gene expression, which is thought to be due to the failure of IE transcription. Inability to initiate IE transcription has been linked to the lack of the tegument IE transactivator VP16 in neurons. Additional factors such as neuronal-specific expression of distinct Oct and HCF proteins, unable to associate with VP16 for efficient IE transcriptional stimulation, can also account for suppressed IE gene expression during latency (reviewed in Preston, 2000). In tissue culture it is possible to establish a model of latent-like infection, referred to as quiescent infection, by introducing mutations into the domain of VP16 required for interaction with Oct-1 and

HCF resulting in the disruption of activation of IE gene expression (Ace et al, 1989). This approach has been extended by introducing additional mutations into ICP0 and ICP4 coding regions that disrupt their abilities to stimulate gene expression, rendering the mutant virus susceptible to cell repression mechanisms even at high MOIs and resulting in quiescently infected cell cultures (Preston & Nicholl, 1997; Preston & Nicholl, 2005). These models have become useful in identifying cellular and viral factors required for reactivation, such as the requirement for ICP0 (see Section 1.6.3.6).

Secondly, latent genomes commonly express latency associated transcripts (LATs) in the infected neurons. LATs are processed RNA products of the primary LAT gene transcript of approximately 8.5 kb, of which the most abundant is the 2.0 kb transcript derived from an intron, and one of lesser abundance of approximately 1.5 kb (Wagner & Bloom, 1997). Analysis of the genetic composition of the major LAT intron implicates ICP0 as the target for inhibition of its expression by antisense targeting (Farrell et al, 1991), and hence correlates with suppressed IE gene expression in such cells. However, evidence in favour of this model remains inconclusive.

Another hallmark of the HSV-1 latent genome is its association with the presence of markers of facultative heterochromatin (repressed chromatin) (reviewed in Knipe & Cliffe, 2008), which implicates cellular epigenetic mechanisms in viral genome repression. This aspect of latency regulation will be discussed further (Section 1.7.2). In addition, recent evidence has suggested a role for LAT-encoded microRNAs (miRNAs), that inhibit expression of the HSV-1 neurovirulence factor ICP34.5, ICP0 and ICP4 (Tang et al, 2008; Tang et al, 2009; Umbach et al, 2008), suggesting an additional mechanism for maintenance of latency at the level of inhibition of lytic gene expression.

#### ***1.4.2.2 HCMV latency***

During natural primary infection of the human host, HCMV first infects epithelial cells of the rhinopharynx or genital tract depending on the route of transmission, or the vascular endothelial cells if acquired during blood transfusion. Leukocytes are then recruited to the sites of infection, take up the virus and viral products, and initiate the spread through the blood stream to various tissues including salivary glands, kidneys, liver and mammary glands. The virus then establishes and maintains latency in the bone marrow, but the precise mechanisms underlying the process of latency establishment are yet to be identified. *In vivo* latency may be established in various cell types, including endothelial cells,

monocyte-derived macrophages, smooth muscle cells, epithelial cells, fibroblasts, T-lymphocytes, granulocytes, stromal cells, neuronal cells and hepatocytes. Critical sites of latency establishment *in vivo* are considered to be certain cell types of the myeloid lineage such as CD34+ hematopoietic progenitors within the bone marrow, however reactivation in these cells is observed during *in vitro* infection (reviewed in Jarvis and Nelson, 2007; Revello & Gerna, 2010; Sinclair & Sissons, 2006). The latent load of HCMV in healthy seropositive individuals constitutes approximately 1 genome-positive cell per 10,000 peripheral blood mononuclear cells and mainly in the leukocyte fraction of peripheral blood, where the genome exists as episomes between two and ten copies. Experimental models of latency have largely relied on the use of CD34+ cells, haematopoietic cell precursors of monocytes (reviewed in Reeves & Sinclair, 2008).

The properties of the gene expression programme during latency in HCMV infected cells are similar to HSV-1 in that lytic transcription is efficiently repressed and the viral genome is assembled into a repressed chromatin structure. Maintenance of latency within myeloid cells is associated with a repressed chromatin structure assembled on the MIEP (Murphy et al, 2002; Reeves et al, 2005). Consistent with these observations, in HCMV latently infected cells the major IE proteins IE1 and IE2 (see Section 1.6.6) are not expressed (Taylor-Wiedeman et al, 1994). Infected cells express a number of cytomegalovirus latency transcripts. These include UL111a (a viral homologue of interleukin 10), UL138 and LUNA (Revello & Gerna, 2010). Of particular interest here is latency transcript LUNA which is partially antisense to genes UL81 and UL82 (Bego et al, 2005). Synthesis of the UL82 gene product pp71, required for efficient stimulation of IE gene expression (Baldick et al, 1997; Bresnahan et al, 2000; Bresnahan & Shenk, 2000); see Section 1.6.5), is therefore inhibited, and this provides a clue to the mechanism of latency control at the level of repression of lytic transcription. Additional regulators of the establishment and maintenance of latency are suggested to be the gene product of UL138 gene (Goodrum et al, 2007) and a number of miRNAs that can target viral genes required in the lytic cycle of replication (Stern-Ginossar et al, 2009).

Reactivation of HCMV from latency does not require viral transactivators and therefore may be dependent on certain cellular stimuli. Thus, cellular stress is thought to take part in this process *via* recruiting cytokines and other pro-inflammatory factors to the sites of reactivation. At the level of molecular changes, reactivation is associated with stress-induced changes of histone modifications around the MIEP making it permissive for activation of IE transcription (Reeves & Sinclair, 2008).

## **1.5 Viral genomes and ND10 during the initial stages of infection**

A characteristic of many DNA viruses is the association of their genomes with distinct nuclear dot-like substructures known as ND10, followed by their subsequent disruption (reviewed in Everett, 2001; Everett, 2006; Maul, 1998). In the case of HSV-1 and HCMV this disruption is caused by viral regulatory proteins: HSV-1 ICP0, and HCMV pp71 and IE1. The presence of intact ND10 however is not required for initiation of lytic gene expression in herpesviruses since removal of the major protein component promyelocytic leukaemia (PML) protein permits more efficient replication of HSV-1 and HCMV in the absence of their transcriptional activators (ICP0 and IE1, respectively) (Everett et al, 2006; Tavalai et al, 2006). Since the discovery of this phenomenon, extensive investigations have been undertaken in order to investigate the relationships between viral DNA, the viral regulatory proteins and the individual components of ND10.

### **1.5.1 ND10 and their components**

The nucleus is a highly organised cellular organelle, bounded by a nuclear envelope. A number of subnuclear compartments are distinguished, amongst which are the nucleolus, which is the site of ribosomal RNA (rRNA) synthesis, rRNA processing and assembly of ribosomal subunits, dynamic Cajal bodies comprising pre-mRNA splicing factors and ND10 (Nuclear Domain 10; also widely referred to as PML nuclear bodies) (reviewed in Spector, 2001). ND10 have been identified as distinct multiprotein domains present in a small number (around 10 per cell in human fibroblasts) within the nuclei of different cell types (Ascoli & Maul, 1991; Maul & Everett, 1994). Despite initially being detected using autoimmune sera from patients with biliary cirrhosis (directed against, amongst other proteins, the Sp100 antigen, see later; (Ascoli & Maul, 1991), the most prominent and the major organising component of ND10 was later demonstrated to be PML (for promyelocytic leukaemia; (Daniel et al, 1993). Amongst the different ND10 components present with each single domain are proteins involved in apoptosis, DNA damage and repair, transcriptional repression/activation and protein modification. These proteins co-exist in a dynamic protein-protein interaction relationship (reviewed in Negorev & Maul, 2001). Specific attention to proteins particularly relevant to the present study is given below.

### ***1.5.1.1 PML***

PML is so named because of its implication in the pathogenesis of acute promyelocytic leukaemia (APL). Cells from APL patients are characterised by a gene fusion between PML and retinoic acid receptor  $\alpha$  (RAR $\alpha$ ) loci as a result of a specific chromosomal translocation t(15;17). PML has been linked to roles in tumour suppression, apoptosis, transcriptional regulation and senescence (reviewed in Everett & Chelbi-Alix, 2007; Salomoni & Pandolfi, 2002; Zhong et al, 2000b). PML-null mice have an impaired activation of caspase-dependent signalling, demonstrating PML roles in caspase-dependent apoptosis. Other apoptotic pathways, including that of interferon (IFN)-dependent have also been implicated in PML function. Importantly, PML expression can be upregulated by interferon (IFN) (Chelbi-Alix et al, 1995; Heuser et al, 1998), classifying it as an IFN-response gene (ISG, for IFN-stimulated gene). More than 100 identified proteins encoded by ISGs have roles in IFN-mediated signalling, including anti-tumour and anti-viral responses. These pathways are consistent with the roles of PML in these processes (reviewed in Regad & Chelbi-Alix, 2001).

The *PML* gene is alternatively spliced from an ORF of 9 exons to yield six major nuclear isoforms and one cytoplasmic isoform. Nuclear PML isoforms share the first exons 1-6 and differ in length and sequence across their C-terminal regions. They are expressed differentially, but all localise to ND10 (Condemine et al, 2006). However, when expressed separately none of the individual isoforms can fully reconstitute normal ND10 structures (Cuchet et al, 2010, in preparation). The important structural feature of all PML isoforms is the presence of the domain composed of a RING-finger, two B-boxes and a coiled coil domain (named RBCC motif) that is conserved amongst a large family of Tripartite Motif (TRIM) proteins (reviewed in Everett & Chelbi-Alix, 2007). TRIM proteins have a variety of cellular functions involved in signalling pathways and in anti-viral intrinsic immune responses (reviewed in Nisole et al, 2005).

PML is posttranslationally modified by members of the small ubiquitin modifier (SUMO)-protein family (Sternsdorf et al, 1997). This modification is important for the regulation of its functions, protein-protein interactions and transcriptional repression. Strong evidence regarding the roles of SUMO-modified PML in cellular anti-viral defence has been demonstrated by several studies (Everett & Maul, 1994; Everett et al, 2008; Everett et al, 2006; Kyratsous & Silverstein, 2009; Tavalai et al, 2006).

### ***1.5.1.2 Sp100***

Sp100 was the first marker of ND10 to be identified as the antigen recognised by sera extracted from patients with primary biliary cirrhosis (Ascoli & Maul, 1991; Fusconi et al, 1991). The Sp100 gene is alternatively spliced to yield four isoforms. Two isoforms of less than 500 aa in length and the two higher molecular weight isoforms have been identified (Guldner et al, 1999). The major Sp100 isoform is 488 aa in length is also post-translationally modified by SUMO-1. The longest isoform referred to as Sp100-HMG (for high mobility group) contains a conserved HMG domain involved in DNA binding (Sternsdorf et al, 1997). Discovery of its interaction with HP1 proteins has provided a further insight into a dynamic link between ND10 and the chromatin compartment of the nucleus (Seeler et al, 1998).

### ***1.5.1.3 SUMO family proteins***

SUMO (for small-ubiquitin modifier) is a class of small protein molecules, which provide post-translational modification of various proteins by covalent linkage to lysine residues in their specific consensus modification sites. Consensus sites are defined as  $\Psi$ KXE where  $\Psi$  is a large hydrophobic amino acid (isoleucine, leucine or valine), K is the lysine residue that is modified; X is any residue and E is a glutamic acid (Rodriguez et al, 2001). SUMO family proteins in vertebrates are encoded by three genes SUMO-1, -2 and -3. Modification of proteins by SUMO-molecules involves a three-step SUMO-conjugation pathway. In brief, the pathway starts with a SUMO-activating enzyme E1, which activates the SUMO C-terminus in an ATP-dependent manner and then transfers activated SUMO to a SUMO-conjugating enzyme E2, called Ubc9. SUMO is then transferred from Ubc9 to the substrate in a process, often enhanced by a SUMO E3 ligase, to form a covalent isopeptide linkage to the lysine side chain in the consensus sequence. SUMO-modification of different proteins can determine their fate and functions. Thus, it is becoming increasingly recognised that SUMO-modification of transcription factors attracts binding of transcriptional co-factors *via* a specific interaction between SUMO and SUMO-interaction motifs (SIMs) of these proteins (reviewed in Hay, 2005; Johnson, 2004). Consensus SIM sequences are defined as V/I-X-V/I-V/I, and are present in nearly all proteins involved in SUMO-related processes (Song et al, 2004). Both major ND10 components PML and Sp100 are modified by SUMO-1 (Sternsdorf et al, 1997). SUMO-modification of PML is responsible for sequestering several proteins to ND10, including CBP and hDaxx (LaMorte et al, 1998; Lin et al, 2006; Zhong et al, 2000a). Recent evidence has also demonstrated that modification of PML by SUMO-2 can result in

degradation of PML by E3 ubiquitin ligase RNF4 under certain conditions (Tatham et al, 2008). These reports represent the importance of SUMO-modification for proper functioning and organisation of ND10 proteins.

#### ***1.5.1.4 ATRX and hDaxx***

The two ND10-localised proteins named ATRX and hDaxx interact to form a chromatin-remodelling complex that is found localised to ND10 and heterochromatin. Despite the fact that no specific target genes of the complex have yet been identified, evidence invokes hDaxx as the targeting component and ATRX as the chromatin-remodelling component (Ishov et al, 2004; Tang et al, 2004; Xue et al, 2003). Due to the direct relevance of these two proteins to the present investigation their structures and cellular roles will be discussed in more detail in Section 1.8.

#### ***1.5.1.5 Other ND10-localised proteins***

Various additional ND10-associated proteins have been also characterised. Amongst them is NDP55, which has been used as an ND10 marker for a number of studies in normal and infected cells (Bell et al, 2000; Doucas et al, 1996; Ishov et al, 1999). Other proteins that stably localise to ND10 include BLM (Bloom's syndrome protein; (Bischof et al, 2001), which is a helicase involved in DNA recombination and repair. Some proteins are thought to be present at ND10 at certain stages of the cell cycle (e.g. HP1), accumulate in response to proteasome inhibition (e.g. p53), or when overexpressed (reviewed in Negorev & Maul, 2001).

### **1.5.2 Association of viral DNA and sites of Immediate Early transcription with ND10**

#### ***1.5.2.1 HSV-1 and HCMV DNA at ND10***

One of the earliest indications that herpesvirus genomes may be associated with ND10 came from the observations that ND10 are disrupted during HSV-1 infection due to the function of HSV-1 IE protein ICP0 to cause removal of the major ND10 constituent from ND10 (Everett & Maul, 1994; Maul et al, 1993). Indeed, HSV-1 parental genomes were found juxtaposed to ND10 foci, indicating that ND10 can mark sites of initiation of DNA replication (Maul et al, 1996). Analysis of the HCMV infection has revealed that a similar scenario applies to HCMV infected cells, characterised by the co-localisation with PML of

the major IE protein (IE1) very early after the onset of infection, followed by subsequent disruption of these structures (Ahn et al, 1998; Ahn & Hayward, 1997; Ahn & Hayward, 2000; Kelly et al, 1995; Koriath et al, 1996). In addition, the HCMV tegument protein pp71, which is delivered to the nucleus with the incoming genomes, associates with ND10 by interacting with hDaxx (Cantrell & Bresnahan, 2005; Ishov et al, 2002). Thus, similarly for both HSV-1 and HCMV, one of the earliest outcomes of infection in the host cell nucleus is the disintegration of ND10 structures. This phenomenon correlates with HSV-1 and HCMV functions to abolish SUMO-modification of PML and Sp100 (Everett et al, 1998a; Lee et al, 2004; Muller & Dejean, 1999; Parkinson & Everett, 2000). This issue is also addressed in Chapters 4 and 5.

A unique phenomenon, so far reported only for HSV-1, is the asymmetric re-distribution of ND10 proteins into novel ND10-like foci associated with the incoming viral genomes in cells at the edge of developing plaques (Everett & Murray, 2005). This event has not yet been reported for HCMV infected cells, which may indicate differences in the dynamics of initiation of lytic gene expression and in the rapidity of the cellular intrinsic response, hence it may also be more difficult to observe in HCMV plaques. In HCMV infection, as the viral genomes are released into the cell nucleus, IE gene products induce the formation of so-called Immediate Early transcript environment. This is characterised by the presence of HCMV major IE transcripts, the viral proteins IE1 and IE2, and the host cell SC35 domains, which are the sites of spliceosome factor SC35 localisation. It has been established that HCMV DNA associates first with ND10 at the sites where ND10 are found juxtaposed to SC35 domains. Nascent IE transcripts and proteins localise to SC35 domains where HCMV IE transcription continues (Ishov et al, 1997).

### ***1.5.2.2 Relationships of other viruses with ND10***

In addition to the current viruses of study HSV-1 and HCMV, the genomes of other herpes and DNA viruses have been implicated in associating with ND10. In VZV infected cells, for example, PML re-distributes upon the expression of its ICP0 homologue ORF61p. Although PML is not degraded, knock-down of PML expression in cells results in a substantial increase of VZV replication (Kyratsous & Silverstein, 2009). During the infection with the gammaherpesvirus EBV, ND10 are disrupted by the actions of EBV IE gene product BZLF1 (Adamson & Kenney, 2001). This process occurs sequentially, such that Sp100, hDaxx and NDP55 (another ND10 marker protein) are dispersed first followed by a delayed dispersal of PML. Unlike in HSV-1 and HCMV, however, complete

disintegration of ND10 was not observed until the initiation of Early gene expression (Bell et al, 2000). Adenoviral protein E4ORF3 is also capable of ND10 disruption (Carvalho et al, 1995). Similarly, in the case of adenovirus, redistribution of Sp100 and NDP55 is seen first, before any effect on PML (Doucas et al, 1996). These data indicate that complete disintegration of ND10 is not a pre-requisite for initiation of gene expression in some of these viruses, where association with ND10 is observed. In addition, PML has been demonstrated to act as a restriction factor in vesicular stomatitis virus (VSV) and influenza virus infections (Chelbi-Alix et al, 1998), which is indicative of ND10 functions targeted against RNA viruses.

Association between viral DNA and ND10 have sparked substantial interest in their roles as domains with anti-viral properties in an attempt to explain the mechanism, reasons and consequences of this association. A separate section (1.9.2) of this Chapter and Chapters 4 and 5 (4.1 and 5.1 respectively) are specifically dedicated to the discussion of these aspects.

## **1.6 Immediate Early gene expression**

Transcription of viral genes initiates following the release of viral DNA into the cell nucleus. As mentioned earlier in the Chapter (Section 1.4.1.2) Immediate Early genes are the first genes to be transcribed. The products of the IE genes play essential roles in the regulation of Early and Late genes, and hence viral particle formation and replication. The processes associated with the regulation of IE gene expression have therefore received extensive attention in herpesvirus research.

### **1.6.1 Regulation of HSV-1 Immediate Early gene expression**

Since IE genes do not require *de novo* protein synthesis for expression, their regulation must involve activation of IE promoters by pre-existing factors. In HSV-1 such control is provided by the complex formed between viral tegument factor VP16, and host cell proteins Oct-1 and HCF (reviewed in Weir, 2001). The mechanism of regulation by VP16-Oct-1-HCF complex is not entirely understood. Existing data suggests that HCF assists nuclear import of VP16, since VP16 itself does not contain a nuclear localisation signal (La Boissiere et al, 1999). It is also thought that HCF bound to VP16 induces a conformational change allowing binding of Oct-1, and therefore serves as auxiliary protein for the activation of transcription by VP16 and Oct-1 (Flint & Shenk, 1997). Mutational

analysis of VP16 has revealed that specific mutations in VP16 that abolish interactions with Oct-1 and HCF lead to severe impairment of the ability of VP16 to stimulate IE gene expression and leads to establishment of quiescent genomes in cell culture (Ace et al, 1989; Greaves & O'Hare, 1990). The DNA binding by Oct-1/VP16 is sequence specific and targets TAATGARAT sequences within the IE promoters. The hallmark of the Oct-1/VP16 specific binding to TAATGARAT sequence involves the POU domain of Oct-1 and the VP16 N terminus. The C terminus of VP16 possesses an acidic activation domain, which confers its ability to stimulate transcription and is proposed to bind to transcription initiation factors (Flint & Shenk, 1997). VP16-Oct-1-HCF binding to consensus sequences on HSV-1 IE promoters triggers the cascade of IE gene expression.

## **1.6.2 HSV-1 Immediate Early proteins**

Of the five IE proteins, two (ICP4 and ICP27) are essential for viral replication, while ICP22 and ICP0 play critical roles in the regulation of HSV gene expression, and the fifth member ICP47 is a virulence factor (Weir, 2001; Whitley et al, 1998). ICP0 is an IE protein of a particular relevance to the present investigation and is a promiscuous activator of the expression of all the classes of viral genes, which will be discussed in more detail later due to its direct relevance to the present investigation (see Section 1.6.3).

### ***1.6.2.1 ICP4***

ICP4 is the product of the gene RS1, which encodes a phosphoprotein of about 175 kDa. The protein has been shown to be essential for the transcriptional activation of the Early and Late classes of viral genes, using ICP4 temperature sensitive mutant *tsK* (Watson & Clements, 1980). Activation of transcription is allowed by the ability of ICP4 to bind directly to the specific sequences on IE, Early and Late promoter sites (Kuddus & DeLuca, 2007; Sampath & DeLuca, 2008), as well as to associate with the proteins of the host transcription machinery such as TFIID and TATA-binding proteins (Smith et al, 1993). ICP4 has also been found to repress VP16-mediated activation of IE promoters in certain assays (Gu et al, 1995).

### ***1.6.2.2 ICP27***

ICP27 is another essential protein in viral replication, and is 63 kDa in size. Functions assigned to ICP27 include inhibition of pre-mRNA splicing, and regulation of viral nucleocytoplasmic RNA transport during Early and Late gene expression. Therefore its principal roles are through post-transcriptional mechanisms (reviewed in Smith et al, 2005).

Thus, ICP27 contributes to the regulation of Late gene expression by facilitating the export of late RNAs (Soliman et al, 1997). Inhibition of host mRNA splicing by ICP27 has been shown to contribute to viral-induced host cell shutoff resulting in the block of cellular protein expression (Hardwicke & Sandri-Goldin, 1994).

#### ***1.6.2.3 ICP22***

ICP22, although non-essential for viral replication in many cell types, is required for the normal transcriptional programme and has a role in gene expression by negatively regulating the expression of IE genes thus avoiding their over-production. It is phosphorylated by viral kinase UL13, which is proposed to contribute to ICP22-mediated modification of the cellular RNA polymerase II (Long et al, 1999; Rice et al, 1995).

#### ***1.6.2.4 ICP47***

The fifth member of IE gene products, ICP47, contributes to the mechanism of neurovirulence of HSV-1 by inhibiting presentation of peptides derived from viral antigens on the cell surface, hence blocking T cell responses. Therefore ICP47 constitutes a component of immune evasion mechanism of HSV-1 (Goldsmith et al, 1998).

### **1.6.3 Immediate Early protein ICP0**

ICP0 is one of the most studied HSV-1 proteins, and despite being a non-essential gene for replication in cell culture, it induces dramatic effects on the cell during the infection. Because of its central role in determining the fate of the virus, i.e. whether the infection would proceed as lytic or latent, ICP0 has received a lot of attention from various research groups.

#### ***1.6.3.1 Overview of the gene and protein structure***

ICP0 protein is encoded by the IE-1 (or  $\alpha 0$ ) gene within the TR<sub>L</sub>/IR<sub>L</sub> region of the genome, meaning that the gene is present in two copies. The primary transcript contains introns and therefore the IE-1 transcript is one of the few of HSV-1 that undergo splicing. The ICP0 polypeptide is composed of 775 aa (in strain 17 *syn+*), and has a predicted molecular weight of 80 kDa (Perry et al, 1986). Since on polyacrylamide gels it migrates as a band corresponding to the size of approximately 110 kDa, in earlier work it has also been widely referred to as Vmw110. Although a small amount of the protein is carried within the

tegument of the virion and is capsid-associated (Yao & Courtney, 1992), the functions of the protein are conferred by the newly synthesised protein.

ICP0 functions have been extensively studied *via* mutational analysis of the protein, and at least five functional domains required for its full transcriptional activation potential have been identified (Everett, 1987; Everett, 1988). These domains have now been mapped and defined as the following (Figure 1.4): (a) RING finger domain that confers its E3 ligase activity; (b) a nuclear localisation signal; (c) a USP7-interaction domain; (d) a region required for localisation to ND10; (e) multimerization domain (reviewed in Everett, 2006).

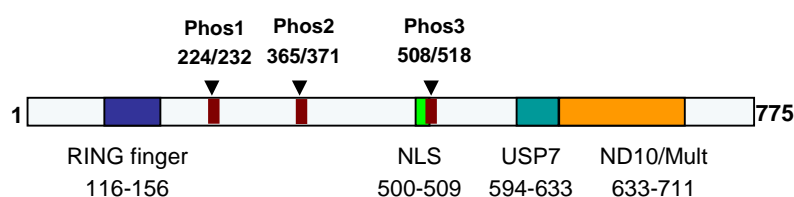


**Figure 1.4 A schematic diagram showing ICP0 protein structure**

The key structural domains and phosphorylation sites are indicated (adapted from Everett, 2006).

### ***1.6.3.2 Transcriptional activation by ICP0***

One of the earliest indications that ICP0 is essential for HSV-1 full transcriptional activation potential was the discovery that ICP0 activates rabbit  $\beta$ -globin promoter and enhances transcription activity of ICP4 to a considerable extent in co-transfection assays (Everett, 1984). Subsequent studies of various ICP0 mutants have concluded that the transcriptional activation activity of ICP0 for viral promoters is associated primarily with the N-terminal half of the polypeptide (Cai & Schaffer, 1989; Everett, 1987; Everett, 1988; Perry et al, 1986). A specific deletion of the 2 kb region within this region has yielded an ICP0-null HSV-1 strain *dl1403* unable to express functional ICP0 (Stow & Stow, 1986). Despite being a promiscuous activator of gene expression, ICP0 does not directly interact with viral DNA (Everett et al, 1993a). This discovery was somewhat unexpected since ICP0 was originally thought to contain a zinc finger motif, classes of which are known to be involved in DNA binding. Instead, this motif has been identified as RING finger domain with E3 ubiquitin ligase activity (Barlow et al, 1994; Boutell et al, 2002; Everett et al, 1993a). The RING domain and its enzymatic activity are essential for ICP0 functions as a transcriptional regulator. Therefore this domain is discussed in more detail below.

### ***1.6.3.3 ICP0 and E3 ubiquitin ligase function***

The ability of ICP0 to degrade cellular proteins has been exclusively assigned to the presence of the N-terminal RING finger motif, which is involved in its E3 ubiquitin ligase activity (Boutell et al, 2002). Various RING finger-containing proteins with E3 activity have also been implicated in diverse cellular functions and processes, such as cell cycle, signalling, transcription, DNA repair and apoptosis (Joazeiro & Weissman, 2000), which may indicate the potential range of ICP0 cellular functions during the infection that are yet to be identified.

In brief, the pathway of proteasomal ubiquitin-dependent degradation is the step-wise process of addition of ubiquitin molecule to the substrates, and consists of three very well defined steps:

- (1) Activation of monomeric ubiquitin in ATP-dependent reaction involving the formation of a high energy covalent thiolester bond between the C-terminal carboxy group of ubiquitin and the active site cysteine residue in the E1 activating enzyme;
- (2) Transfer of the ubiquitin to another thiolester bond with the active site cysteine of an E2 ubiquitin conjugating enzyme;
- (3) E3 ubiquitin ligase mediated transfer of the ubiquitin to form an isopeptide bond with the lysine side chains in the target molecule;

Addition of more than 4 ubiquitin monomers in a polyubiquitin chain to a substrates results in the substrate recognition by the 26S proteasome and degradation. The polyubiquitin chains are then removed and ubiquitin monomers are re-generated by ubiquitin-specific proteases (USP) (Hershko & Ciechanover, 1998).

The functionality of the RING-finger domain of ICP0 is crucial for its functions, since ICP0 RING-finger mutants are unable to complement ICP0-deletion mutants in plaque assays (Everett et al, 2009). Based on several reports, the RING finger has been shown to be required for ICP0-mediated transcriptional activation function and efficient viral replication (Everett et al, 1995) and to confer ICP0 functions in degrading PML and Sp100, (Chelbi-Alix et al, 1998; Everett et al, 1998a; Parkinson & Everett, 2000), centromeric proteins CENP-A, -B and -C (Everett et al, 1999a; Everett et al, 1999b; Lomonte & Morency, 2007; Lomonte et al, 2001) and proteins involved in DNA damage response (Lilley et al, 2009). Identification of the role of RING finger motifs associated with E3 ubiquitin ligase activities therefore led to the hypothesis that ICP0 may function through the cellular ubiquitin proteasome pathway during infection (Everett et al, 1998b). This prediction has proven to be correct following observations that the degradation of the

above mentioned proteins during HSV-1 infection occurs in a proteasome-dependent manner, since the use of ICP0 $\Delta$ RING mutant virus or the addition of the inhibitor MG132 (synthetic proteasome inhibitor) blocks this activity (Boutell et al, 2003; Boutell et al, 2002). In addition, the RING finger function of ICP0 has also been shown to be required for ICP0 incorporation into the virion (Delboy et al, 2010).

The E3 ligase function of ICP0 suggests that ICP0 is capable of inducing its own degradation, and therefore in order to avoid it there must be a mechanism by which ICP0 stabilises itself. This property has been assigned to the ability of ICP0 to interact with USP7 (also termed HAUSP in some reports for herpes-associated USP). The strong interaction has been confirmed by *in vitro* assays as well as in infected cells, and is suggested to play a key role in stabilization of ICP0 (Boutell et al, 2003; Canning et al, 2004). In cells infected with ICP0 USP7-interaction deficient mutant virus, notable decreases in plaque formation efficiencies and the abilities to efficiently degrade PML and Sp100 have been reported (Canning et al, 2004; Everett et al, 1999c), probably because the mutant ICP0 is unstable and accumulates to lower levels.

#### ***1.6.3.4 ICP0 and association with ND10***

As soon as ICP0 becomes detected in the nuclei of the infected cells, it localises to ND10 (Maul et al, 1993). This association is transient and is followed by rapid disintegration of ND10 due to PML being degraded by the E3 ligase activity of ICP0 (Boutell et al, 2003; Chelbi-Alix & de The, 1999; Everett et al, 1998a; Parkinson & Everett, 2000). Localisation of ICP0 to ND10 does not require its RING-finger domain (Everett & Maul, 1994; Everett et al, 2009; Maul & Everett, 1994). Therefore, based on the analyses of RING-finger mutants, it appears that the localisation of ICP0 to ND10 is not a pre-requisite for the efficient replication of the virus but is highly dependent on its RING finger function (see above).

#### ***1.6.3.5 ICP0-null mutant phenotype***

In order to study the ICP0 function, various ICP0-mutants of HSV-1 have been generated and extensively characterised (Cai & Schaffer, 1989; Chen & Silverstein, 1992; Everett, 1988; Everett et al, 2004; Sacks & Schaffer, 1987; Stow & Stow, 1986). The ICP0-null mutant *d11403*, containing a 2 kb deletion in both copies of the gene within terminal and internal repeats (Stow & Stow, 1986), has been used extensively for the present investigation (Chapter 5). Interpreting the phenotype of an ICP0-null mutant HSV-1 is not

very straightforward, and a number of its features have to be considered when using in experimentation.

The first is the multiplicity-dependent phenotype of ICP0-null mutant HSV-1. Strain *dl1403* has an approximately 1000-fold defect in plaque formation efficiency in human fibroblasts, and the viral genomes are sequestered in a quiescent state (Stow & Stow, 1989; Stow & Stow, 1986). However, in the osteosarcoma cell line U2OS, *dl1403* is as efficient in replication as a wt HSV-1, suggesting that U2OS cells either encode for an activity that substitutes for ICP0, or that they lack a cellular mechanism of repression, which is counteracted by HSV-1 ICP0 (Yao & Schaffer, 1995). In other cell lines such as Vero and HeLa the differences in the infection efficiencies of ICP0-null and wt HSV-1 are relatively minor, however these become more pronounced as lower multiplicities of ICP0-null mutant virus are used (Chen & Silverstein, 1992; Everett et al, 2004). As MOI of ICP0-null mutant virus increases, however, a certain threshold is reached allowing the virus to replicate in restrictive cell lines as efficiently as wt HSV-1. For *dl1403* infections this threshold MOI ranges between 5 and 10 in fibroblasts depending on the viral stock. This observation has become a key in the subsequent attempts to characterise ICP0-null mutants (Everett et al, 2004).

Linking with the multiplicity-dependence of ICP0-null HSV-1, the second distinguished property of this mutant strain is the probability of establishing lytic infection, or what is often referred to as the ‘probability phenotype’ (Everett, 2000). Unlike for the wt HSV-1 virus, in ICP0-null mutant infections the relationship between the number of plaques obtained from a given number of viral particles applied to a cell monolayer is not linear. This ratio is referred to as the particle to plaque forming unit (PFU) ratio. Whereas in wt infections this ratio is around 20-50, depending on the viral stock and the cell line, for ICP0-null mutant strains it is highly variable depending on the cell type. Thus, HFFF human fibroblasts are restrictive to ICP0-null virus, and it takes up to 1000 times the number of ICP0-null particles to produce approximately the same number of PFU as in a wild-type virus infection. This defect however is not observed in U2OS cells (Everett et al, 2004; Yao & Schaffer, 1995), which is the reason why they are widely used for titration of wt and ICP0-null mutant stocks. Supplying ICP0 to *dl1403*-infected restrictive cell lines, using an ICP0-inducible system, fully complements ICP0-null mutant *dl1403* (Everett et al, 2009). Thus, the ‘probability phenotype’ of ICP0-null mutant HSV-1 is considered to be a measure of probability that a cell receiving a potentially infectious virus particle will commit to lytic infection (reviewed in Everett, 2000). It still however remains unclear why

upon infection with ICP0-null virus certain cells have a higher probability of establishing quiescent infection and some cells manage to initiate lytic replication, hence resulting in plaque formation virtually as efficient as that of the wt virus.

#### ***1.6.3.6 ICP0 in reactivation from latency***

The data regarding the requirement of ICP0 during reactivation from latency is somewhat controversial. Reactivation of ICP0-null mutant or deletion strains from the infected mouse neurons is considerably less efficient than that of wt virus (Halford & Schaffer, 2001; Thompson & Sawtell, 2006). On the other hand, supplying ICP0 to the cultured infected TG mouse neurons in which quiescent genomes have been established, using viruses deficient for IE gene expression (Samaniego et al, 1998), results in active replication of viral genomes, suggesting the requirement for ICP0 in reactivation (Terry-Allison et al, 2007). Other studies have confirmed this conclusion using other quiescently infected restrictive cell lines of neuronal and fibroblast origin. The efficiency of reactivation is dependent on ICP0 RING finger activity (Wilcox et al, 1997).

Although ICP0 transcripts were detected in latently infected mouse neurons extracted from different neuronal sites of latency (Maillet et al, 2006; Thompson & Sawtell, 2006), the mechanism of ICP0 action in this process has not been identified. Induction of hypothermic stress in the latently infected mouse neurons activates splicing of ICP0 transcripts, which implicates ICP0 function in the efficient reactivation from latency. On the other hand however, it became clear that ICP0 was not required for initiation of reactivation (at least in terms of detection of viral antigens), hence implicating stress as an important factor (Thompson & Sawtell, 2006). Consistent evidence from a number of studies suggests that although ICP0 may increase the titres of reactivated virus, it is not absolutely necessary for reactivation under the conditions of stress (Bringhurst & Schaffer, 2006). Accordingly, the use of quiescent infection models in cell culture has also identified different stress factors which are sufficient for reactivation of the quiescent HSV-1 genomes (Preston & Nicholl, 2008). It may therefore be concluded that despite the strong evidence supporting the role of ICP0 in reactivation from latency, the different models of study may affect the extent to which ICP0 is required for this process. Hence, the precise function of ICP0 during the process of reactivation from latency still remains to be established.

### 1.6.4 Regulation of HCMV Immediate Early gene expression

Regulation of IE gene expression in HCMV relies on the strong promoter/enhancer element named the major immediate early promoter (MIEP; see Figure 1.5 for the basic outline of the regulation). MIEP serves as a binding site for various cellular transcription factors, for which sequence specific binding elements have been identified. Nuclear factor kappa-B (NF- $\kappa$ B) and cAMP response element binding (CREB)/activating transcription factor 1, for instance, are amongst the cellular transcription factors required for the activation of MIEP, and the binding sites for these proteins are conserved in the MIEPs of CMVs of other species (reviewed in Stinski & Isomura, 2008). As discussed in more detail in the following section, viral tegument protein pp71 (Liu & Stinski, 1992) and major IE proteins (Cherrington et al, 1991; Cherrington & Mocarski, 1989; Hermiston et al, 1990) play central roles in the MIEP-regulated transcription.

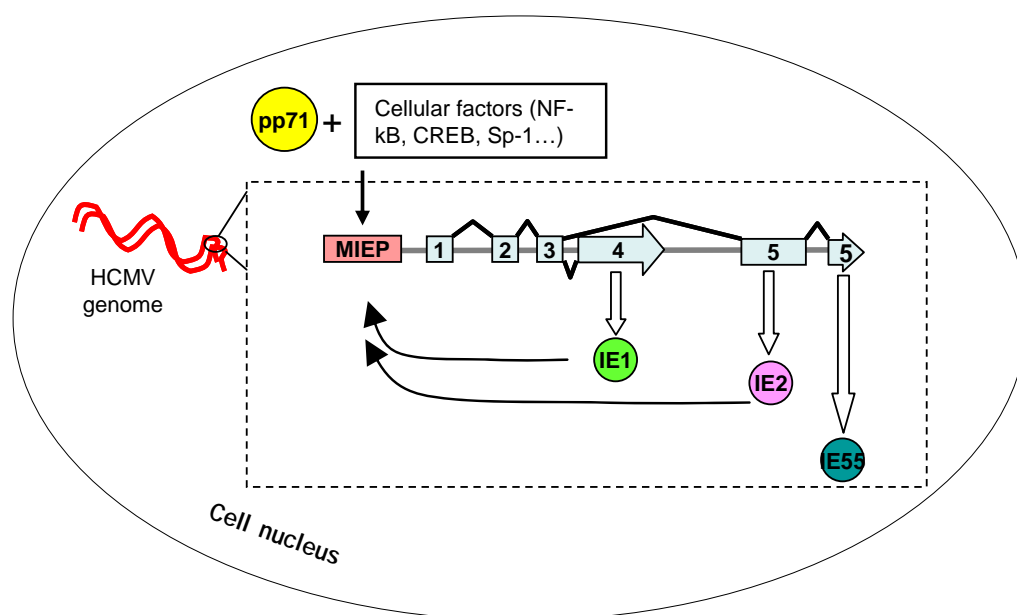


**Figure 1.5 Overview of the regulation of HCMV Immediate Early transcription**

The key elements required for activation of IE transcription are shown. HCMV tegument protein pp71 is required for efficient stimulation of IE transcription through its ability to counteract hDaxx mediated repression (see below). IE1 and IE2 result from alternative splicing of the major IE transcript. Once expressed, IE proteins IE1 and IE2 induce expression from MIEP positively and negatively, respectively.

## **1.6.5 HCMV tegument protein pp71**

Pp71 is the product of the gene UL82 that codes for a 71 kDa phosphoprotein. The protein is an abundant component of viral tegument and is expressed with Early-Late kinetics. It is delivered to the nucleus of the infected cell during the initial stages of infection. In latently infected cells, however, pp71 remains in the cytoplasm (reviewed in Kalejta, 2008b).

### ***1.6.5.1 Transcriptional activation by pp71***

One of the early reports on the function of pp71 in increasing the infectivity of HCMV was based on transfection-based assays of co-transfected HCMV DNA and plasmids encoding for different tegument proteins. A dramatic increase of around 200-fold in DNA replication was detected in cells transfected with pp71-expressing plasmid, compared to control or any other tegument-protein expressing plasmid (Baldick et al, 1997). Construction of an UL82 deletion mutant of HCMV (ADSubUL82) further confirmed the high requirement for pp71 for the activation of productive infection by HCMV. According to these studies, inability to express pp71 results in failure to initiate productive infection in restrictive cell lines. Therefore, pp71-null mutant virus can be efficiently propagated on complementing cells, such as life-extended fibroblasts expressing a catalytic subunit of telomerase and the UL82 gene (Bresnahan et al, 2000; Bresnahan & Shenk, 2000). In addition, pp71 is able to induce expression from HSV-1 promoters and partially substitute for the lack of ICP0 (Homer et al, 1999; Marshall et al, 2002).

### ***1.6.5.2 Interaction with the cellular ND10 protein hDaxx***

A particularly intriguing property of pp71 that has been extensively studied and presents significant relevance to the current line of investigation is its ability to associate with the cellular transcriptional repressor hDaxx (Section 1.8.2). This interaction will also be addressed in more detail in the introductory part to Chapter 4 (Section 4.1). In infected cells pp71 localises to ND10, where it interacts with hDaxx and induces its degradation (Cantrell & Bresnahan, 2005; Hofmann et al, 2002; Hwang & Kalejta, 2007; Ishov et al, 2002; Saffert & Kalejta, 2006). Interaction between hDaxx and pp71 was initially detected by two independent groups, one using transient overexpression methods and yeast-two-hybrid screens (Hofmann et al, 2002), and the other using HCMV-infected cells (Cantrell & Bresnahan, 2005). The pp71-interaction domain of hDaxx, however, is still an issue of controversy. Hofmann *et al* work delineated the two regions of pp71-interaction within hDaxx, the first of which (aa 439-501) has yielded positive interactions in both yeast-two-

hybrid and CoIP assays, while the second of weaker strength was only revealed in CoIP assays of transfected cell lysates and mapped a larger region between aa 43 and 371 (Hofmann et al, 2002). Yet another group did not detect an interaction between the C-terminal part of hDaxx and pp71, and mapped the pp71-interacting region of hDaxx to aa 142-290 (Ishov et al, 2002), indicating that this may be the region responsible for the N-terminal interaction detected by Hofmann et al (2002). The domains of pp71 required for hDaxx binding have been mapped to two short aa stretches between pp71 aa 206-213 and 324-331 (Hofmann et al, 2002). Mutant viruses with lesions in these regions are unable to efficiently stimulate viral gene expression, an effect observed at low MOIs (Cantrell & Bresnahan, 2005). These findings have triggered further research into the functional significance of the pp71-hDaxx interaction for the progression of infection.

Depletion of hDaxx *via* RNA interference improves replication efficiency of wt virus (Tavalai et al, 2008; Woodhall et al, 2006). Conversely, hDaxx overexpression or hDaxx stabilization by treatment with lactacystin of the cells results in repression of HCMV infectivity (Saffert & Kalejta, 2006; Woodhall et al, 2006). These data correlate with the requirement of pp71-hDaxx interaction for the efficient initiation of IE gene expression. Interestingly, depletion of hDaxx supports an even further increase in IE gene expression and replication of pp71-null mutant HCMV, as noted by several groups (Preston & Nicholl, 2006; Saffert & Kalejta, 2006; Saffert & Kalejta, 2007; Tavalai et al, 2008). Pp71-mediated proteasomal degradation of hDaxx during wt HCMV infection may explain the increased efficiency of pp71-null mutant virus in the absence of hDaxx (Hwang & Kalejta, 2007; Saffert & Kalejta, 2006). These reports have identified hDaxx as a potent mediator of cellular anti-viral response to HCMV.

#### ***1.6.5.3 Effects of pp71 on cell cycle proteins***

In addition to the effects on hDaxx, pp71 is able to induce proteasome-dependent ubiquitin-independent degradation of Rb family tumour suppressors, which are involved in the cell cycle arrest at G1, by directly binding to them (Kalejta et al, 2003; Kalejta & Shenk, 2003). This function of pp71 is proposed to be related to the ability of HCMV to induce the G1 to S phase transition during the cell cycle. However, the ability of pp71 to degrade Rb family proteins does not affect infectivity of the virus (Cantrell & Bresnahan, 2005; Kalejta et al, 2003; Kalejta & Shenk, 2003), suggesting other viral components may be responsible for these functions. Indeed, it has been demonstrated that IE1 can bind and phosphorylate Rb family proteins (Poma et al, 1996), while IE2 drives quiescent G0 cells into the cell cycle (Castillo & Kowalik, 2002).

## **1.6.6 Immediate Early proteins IE1 and IE2**

### ***1.6.6.1 Structure of the major IE transcript***

Activation of the MIEP by pp71 and cellular factors results in the initiation of transcription from the two adjacent genes, namely UL123/122. The first to be transcribed is the product of UL123, 1.95 kb mRNA in size and contains exons 1 through to 4 (Figure 1.5) which codes for the IE1 protein (also referred to as IE72 according to its molecular weight). Gene UL122 yields two transcripts as a result of alternative splicing. The first one is 2.25 kb in size and is composed of the first 3 exons shared with IE1 and an additional exon 5, as a result of alternative splicing from UL123/122 gene. The 2.25 kb mRNA encodes a 579 aa (82–86 kDa) nuclear protein, IE2 (also known as IE86). The second transcript of the UL122 gene, of 1.7 kb, encodes a 425 aa (55 kDa) protein, less well characterised in literature, known as IE55. IE55 is identical to IE86 except for a 154 aa deletion between residues aa 365 and 519 resulting from a splicing event within exon 5. As a result of alternative splicing, the three IE products share the same first N-terminal 85 aa of the sequence. IE1 and IE2 have received the most attention in research due to their key functions in HCMV lytic infection and their properties in the interaction with ND10 proteins and induction of the cell cycle (reviewed in Castillo & Kowalik, 2002).

### ***1.6.6.2 Disruption of ND10 by IE1***

One of the earliest indications of ND10 disruption by HCMV has come from Kelly et al (1995) demonstrating complete dispersal of PML foci in cells infected with wt HCMV, which was observed in a high proportion of cells at the early hours post infection. This disruption requires the initiation of IE gene expression since UV-inactivated virus fails to perform this function (Kelly et al, 1995). With the initiation of IE1 production, other ND10 proteins such as Sp100 and NDP52 also become dispersed (Korioth et al, 1996). IE2 is found juxtaposed to ND10 with the start of infection, consistent with the development of what has been termed the IE transcript environment (Ishov et al, 1997). The role in disruption of ND10, however, has been assigned to IE1, rather than IE2, based on transient transfection methods (Ahn & Hayward, 1997; Korioth et al, 1996) and studying IE1-deletion HCMV mutants (Ahn et al, 1998). Attempts to map the domain of IE1 responsible for ND10 disruption have concluded that most of the protein sequence is required for efficient ND10 disruption, except for the C-terminal acidic domain (aa 347-491) (Ahn et al, 1998; Wilkinson et al, 1998). The regions that are considered particularly important for this function, although not sufficient, were mapped to exons 2 and 3, which encode the putative leucine zipper and zinc-finger domains (Wilkinson et al, 1998). The function of

the IE1 acidic domain, on the other hand, is associated with binding to the transcriptional activator STAT2, a protein involved in IFN-signalling. Disruption of this interaction has been shown to be detrimental to virus growth (Huh et al, 2008). IE1-mediated disruption of ND10 correlates with the efficient initiation of viral replication. This has been concluded from analogous approaches to those used to study the role of hDaxx in the repression of HCMV genomes. Thus, targeted knock-down of PML and the use of IE1-deficient mutant virus have identified PML as a component of cellular anti-viral defence (Tavalai et al, 2006). These issues will be addressed further in the Section “Intrinsic Immunity” and in Chapter 4 (4.1).

The mechanism utilised by IE1 to disrupt ND10, although still not entirely clear, involves interaction with PML, as discovered using yeast-two-hybrid screens. The PML-interaction region of IE1 has been mapped aa 1-346 (Ahn et al, 1998). Unlike HSV-1 ICP0, IE1 does not cause degradation of PML, although it is capable of abrogating SUMO-modification of both PML and Sp100 (Lee et al, 2004; Muller & Dejean, 1999). These studies therefore suggest related pathways for inhibiting cell-mediated anti-viral response by the two different herpesvirus IE proteins, ICP0 and IE1, and implicate SUMO modification as an important factor in this process.

## **1.7 Chromatin control of herpesvirus infection**

In addition to the control of herpesvirus infection by ND10 components, as discussed above, chromatin-associated mechanisms of regulation of viral infection have also received significant attention in research. It is generally considered that the cellular response to the intrusion of foreign DNA into the cell nucleus would involve the assembly of repressed chromatin structure. Hence, numerous studies have been conducted aimed to investigate the roles of chromatin modifications and the changes in chromatin dynamics during viral lytic and latent infection and reactivation from latency. Because of the dynamic nature of nuclear subcompartments, there is a constant exchange between ND10 proteins and chromatin. The chromatin-associated proteins that localise to ND10 are therefore of particular interest for the study of herpesvirus infection. Therefore, the following part of this Chapter is of special relevance to the present line of investigation. Before going into the discussion on the current understanding of the role chromatin state and the function of chromatin-associated proteins in viral infection, a few paragraphs must address the basic characteristics of chromatin organisation and regulation within the cell.

## 1.7.1 Chromatin organisation and structure

### *1.7.1.1 The nucleosome: The structural unit of chromatin*

Chromatin constitutes a sub-nuclear compartment. So-called chromosome territories are occupied by individual chromosomes and they include transcriptionally inactive condensed heterochromatin or less condensed transcriptionally active euchromatin (Lamond & Sleeman, 2003). The structural subunit of chromatin is the nucleosome. A single nucleosome consists of four types of histone molecules – H2A, H2B, H3 and H4, represented as dimers within each nucleosome, with approximately two turns of DNA wrapped around the octameric core (Figure 1.6). Nucleosomes are spaced at intervals of about 200 base pairs in higher eukaryotes along chromosomal DNA. In addition to the core histones, linker histones H1 are associated with the exterior of nucleosomes and are important for stabilization of the highly condensed state of chromatin fibres (Hayes & Hansen, 2001). The amino termini of the core histones protrude outside the nucleosomal core and are post-translationally modified by acetylation, methylation and phosphorylation. Thus, active transcription is generally associated with a higher load of acetylated histones, whereas the histones of heterochromatin are mostly methylated and hypoacetylated (Figure 1.6). Exceptions include methylated H3K4 (lysine residue 4 of histone H3), which is a marker of active transcription, and acetylated H3K12, a marker of transcriptional silencing (Grant, 2001).

### *1.7.1.2 Chromatin regulation by histone acetylation, deacetylation and methylation*

Histone acetylation or methylation at  $\epsilon$ -amino groups of lysine side chains determines the status of transcriptional activity. The most abundant and conserved sites targeted for acetylation/deacetylation are the lysine residues of histones H3 (K9, -14, 18 and 23) and H4 (H4K5, -8, -12 and 16). Acetylated H3K9 is a common marker for determining active transcription. In contrast, methylation of histone H3 residues K9 and K27 and of histone H4K20 is associated with repressed chromatin. In humans, histone methyltransferase (HMT) activity can be provided by the enzyme SUV39H1, which targets H3K9 for methylation (reviewed in Grant, 2001; Grunstein, 1997). Methylated H3K9 then attracts binding of heterochromatin protein 1 (HP1), serving as another marker for heterochromatin formation (Bannister et al, 2001). The processes of histone modification are dynamic and implicate many nuclear factors, the list of which has been rapidly expanding. The enzyme families of histone deacetylases and histone acetyltransferases, directly involved in modification of histone tails, are briefly described in the next paragraphs.

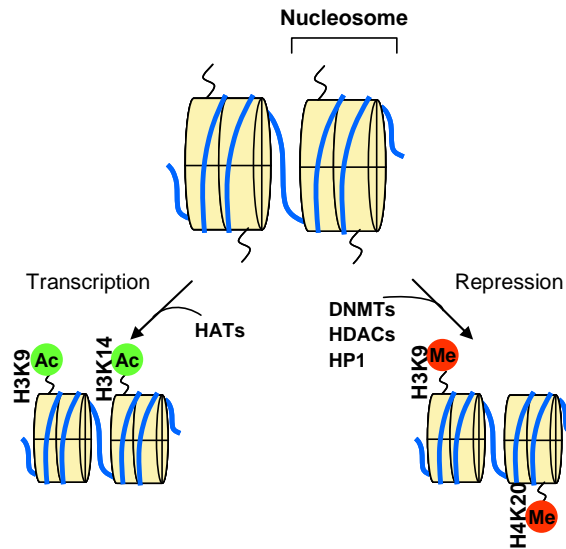


**Figure 1.6 Basic organisation of a nucleosome**

Core histones with free N-terminal ends are shown in yellow. DNA wrapped around the nucleosome is shown in blue. Post-translational modifications of core histones are marked as Ac (acetylated; green) and Me (methylated; red), indicative of active or repressed transcription.

### Histone Deacetylases

The mode of histone deacetylase (HDAC) action, as the name implies, involves removal of acetyl group from the lysine of the acetylated histone protein, thereby restoring the positive charge and allowing the condensation of nucleosomes. The HDAC family is large and comprised of two major classes according to their structural characteristics. Twelve HDACs have been identified so far and all share a homologous catalytic domain. Members of Class I HDACs, HDAC1 and -2 are highly similar with sequence identity of approximately 85%. Cellular proteins interact with HDACs and form repressive complexes on heterochromatin (reviewed in de Ruijter et al, 2003; Marks et al, 2000). Various protein-protein interactions are involved in regulating HDAC function by binding directly to HDACs and recruiting co-repressor complexes (Sengupta & Seto, 2004). Interaction between ND10 protein hDaxx and HDACs (Hollenbach et al, 2002; Lin et al, 2006) is particularly intriguing in the context of the present investigation, hence will be addressed in relevant sections of this thesis. To study the properties of HDAC function in cell culture, HDAC inhibitors such as trichostatin A (TSA) and other compounds are used. These act by targeting enzymatic activity of HDACs thereby relieving repression. Such methods for HDAC inhibition have become widely used for determining the nature (HDAC-dependent or not) of transcriptional repression (Marks et al, 2000).

### Histone Acetyltransferases

Histone acetyltransferases (HATs) are the enzymes that, in reverse to HDAC action, transfer the acetyl group to the  $\epsilon$ -amino group of the internal lysine residue of a histone tail in a reaction that can be reversed by HDACs. Two representatives of HATs are p300 and CBP (CREB-binding protein), often referred to as p300/CBP due to their high similarities. They target histones H3 and H4 for acetylation, and to a lesser extent H2A and H2B (Kuo & Allis, 1998).

### Histone Methyltransferases

One of the representative and best characterised HMTs is SUV39H1. It can interact with HP1, and presumably recruit it to methylated H3K9 residues, thereby contributing to the formation of heterochromatin (reviewed in Shinkai, 2007).

#### ***1.7.1.3 Chromatin regulation by DNA methylation***

Methylation of DNA in addition to histone deacetylation and recruitment of transcriptional repressors, provides another important pathway of transcriptional repression. The process of DNA methylation involves the addition of a methyl group to nucleotide bases, most commonly cytosine. Cytosine methylation is catalysed by DNA methyltransferases (DNMTs). In mammalian cells cytosine methylation occurs almost exclusively at cytosines residing 5' to guanine nucleotides. The short stretches of DNA comprising repeated occurrences of these C-G sequences are referred to as CpG (cytosine-phospho-guanine) islands, where CpG sequences are clustered within 0.5 to 4 kb lengths of DNA (Siedlecki & Zielenkiewicz, 2006). Methylated CpG islands present binding sites for methyl-CpG-binding proteins (MeCPs). Of these the most studied is MeCP2, which binds CpG sites and causes transcriptional repression by recruiting transcriptional repressor complexes, some of which include HDACs (Nan et al, 1998). MeCP2 can in turn interact with additional co-factors and complexes that promote assembly of repressed chromatin structures.

One of the more recently proposed hypotheses states that cytosine methylation within the DNA is linked to histone methylation of the adjacent nucleosome. Since methylation of H3K9 serves as a docking site for heterochromatin protein HP1 (Bannister et al, 2001) and DNMTs (Fuks et al, 2003), HP1 may activate the methyltransferase activity of DNMTs and reinforce gene repression (reviewed in Brenner & Fuks, 2007).

#### ***1.7.1.4 Chromatin remodelling by SWI/SNF family enzymes***

An additional level of transcriptional regulation by modifying chromatin structure is provided *via* the action of SWI/SNF ATPase/helicase chromatin remodelling enzymes. The SWI/SNF genes were initially identified in yeast *Saccharomyces cerevisiae* as activators of the *HO* and *SUC2* genes; SWI stands for mating type SWItch and SNF for Sucrose Non-Fermenting. Mutations in both of these genes result in reductions in growth rate. SWI/SNF complexes cause ATP-dependent disruption of histone-DNA interactions within the nucleosome *in vitro*, possibly by sliding histone octamers to other sites on the same DNA molecule. This process is thought to expose transcription sites allowing transcriptional factors to bind and activate gene expression. It is also believed that interaction of SWI/SNF complex subunits with acetylated histones may contribute to activation of certain gene targets (reviewed in Muchardt & Yaniv, 1999; Sudarsanam & Winston, 2000). Apart from helicase-related properties in transcriptional activation, repressive functions have also been described for ATP-dependent nucleosome remodelling complexes. The existence of complexes that contain, in addition to nucleosome remodelling activity, histone deacetylase activities have been reported (e.g. NuRD complex; Xue et al, 1998).

Evidently, the different pathways of chromatin regulation do not occur independently of one another but are dynamic with exchange of transcriptional repressors and activators. The different mechanisms of chromatin regulation cannot be described exhaustively here, therefore only those relevant to the further discussion have been addressed in this section.

#### **1.7.2 Chromatin organisation during herpesvirus infection**

It has been discovered some time ago that viral DNA is associated with the markers indicative of active or repressed gene transcription depending on the stage of the life cycle. A powerful technique that is widely used for analysing the chromatin structure of viral genomes is chromatin immunoprecipitation (ChIP) that relies on co-immune precipitation of the histone complexes associated with viral DNA, and then PCR amplification of selected viral sequences. The current understanding of the chromatin control of viral infection is summarised below. These aspects have also been recently reviewed (Knipe & Cliffe, 2008; Kutluay & Triezenberg, 2009b; Lu & Triezenberg, 2009; Sinclair, 2008).

### ***1.7.2.1 Chromatin during lytic infection***

One of the earliest pieces of evidence demonstrating that HSV-1 DNA in lytic cells is not extensively associated with nucleosomes came from micrococcal nuclease (MNase) digestion of the DNA extracted from the infected cells (Leinbach & Summers, 1980). These data suggest that viral DNA is probably not assembled into a regular chromatin-like structure. In contrast to HSV-1, MNase digesting approach used in HCMV infected cells has demonstrated that viral DNA during productive HCMV infection is mostly nucleosomal, and at later stages of infection the nucleosome load becomes restricted towards specific genomic regions (Nitzsche et al, 2008). Therefore, the mechanisms of HSV-1 and HCMV gene repression during the lytic stage of infection seem to differ significantly.

In HCMV infected cells repression that occurs around the MIEP is HDAC-dependent. A high load of histones associated with the MIEP undergoes dynamic acetylation and methylation modifications, subject to temporal changes (reviewed in Sinclair, 2008). Thus, overexpression of HDAC3 results in substantial decrease in the infectivity by HCMV in permissive culture, and conversely, TSA treatment of HCMV-infected non-permissive cells increases the efficiency of infection (Murphy et al, 2002). In addition, HCMV MIEP also associates with HP1 in latent infection models (Murphy et al, 2002), which further confirms heterochromatin structure of latent HCMV genomes.

The evidence concerning the role of HDACs in lytic phase of HSV-1 infection, however, is conflicting (reviewed in Kutluay & Triezenberg, 2009b). While some reports have suggested that inhibition of HDAC activities by TSA treatment can complement for lack of ICP0 in ICP0-null HSV-1 infected cells (Poon et al, 2006; Poon et al, 2003), similar studies by other groups did not confirm these observations (Everett et al, 2008). Moreover, analysis of ICP0 functions specifically required for efficient plaque formation has also indicated that ICP0-HDAC interaction (Lomonte et al, 2004) was not required for efficient gene expression and plaque formation (Everett et al, 2009), and that ICP0 does not have a TSA-like effect on the levels of histone acetylation (Lomonte et al, 2004). In support of heterochromatin-independent repression of the lytically HSV-1 infected cells, a study by Herrera and Triezenberg has demonstrated the relatively low histone occupancy on IE gene promoters. Interestingly, the same study has demonstrated the association of IE promoters with CBP/p300, a protein involved in histone acetyltransferase activities (see above). Using VP16-activation domain deficient mutant, it was determined that VP16 recruits not only HATs but members of SWI/SNF complex to IE promoters, ensuring active

transcription during the lytic infection (Herrera & Triezenberg, 2004). It is intriguing that upon infection with a VP16-activation domain mutant, a significant increase in core histone occupancy on IE promoters is observed (Kutluay & Triezenberg, 2009a). This suggests VP16 counteracts the formation of repressed chromatin structure during lytic infection.

#### ***1.7.2.2 Chromatin during latent infection***

In contrast to lytic infection, there are more similarities in the mechanism of chromatin control of latently HSV-1 and HCMV infected cells and during reactivation, and it most certainly involves assembly of latent viral DNA into a heterochromatin structure. Indeed, earlier work has shown that latent HSV-1 genomes are associated with nucleosomes (Deshmane & Fraser, 1989). Moreover, nucleosomal HSV-1 DNA has also been detected in a cell culture model of quiescent infection using IE-gene expression deficient virus (Ferenczy & DeLuca, 2009). Specific regions of nucleosome formation that include IE and Early gene promoters become enriched with repressed histone markers, notably methylated H3K9, in mouse trigeminal neurons (Wang et al, 2005). Systems that have used cell culture models of quiescent infections for analysis of chromatin control have produced evidence that the ICP0 promoter in these cells is associated with tri-methylated H3K9, whereas HSV-2 superinfection results in de-repression and acetylation of ICP0 and gC (Early gene) promoters (Coleman et al, 2008).

On the other hand, actively transcribed LAT HSV-1 promoters are heavily acetylated in latently infected cells (Kubat et al, 2004a; Kubat et al, 2004b). It is interesting however that decreased transcription levels of LAT are not associated with decreased acetylated histone levels on the 5' region of the LAT promoter (Kubat et al, 2004a). Although methylation plays an important role in maintaining repressed chromatin structures, evidence suggests that there are no methylated DNA markers present on latent HSV-1 genomes (Kubat et al, 2004b).

The role for HDACs in HSV-1 in the maintenance of repressed chromatin structure has been an issue of extensive investigation, particularly in view of the controversy for lytically-infected cells. There is, however, more firm data regarding HDAC function on quiescent or latent genomes. Thus, TSA treatment of latently HSV-1 infected neuronal cultures results in derepression of gene expression (Terry-Allison et al, 2007). However, TSA mediated de-repression of quiescent HSV-1 genomes does not occur in fibroblasts

(Preston & Nicholl, 2005; Terry-Allison et al, 2007). Repression by HDACs during models of HCMV latency in non-permissive cell lines is thought to involve the hDaxx co-repressor activities since removal of hDaxx by RNA interference (RNAi) relieves the silencing of IE transcription in these cells, in the same manner as treatment with TSA (Saffert & Kalejta, 2007). According to other studies that used ChIP analyses, hDaxx depletion results in a de-repressed chromatin structure around HCMV promoters (Woodhall et al, 2006). In addition to HDAC activity, it has been shown that in monocytes extracted from healthy HCMV-positive carriers, but not in differentiated dendritic cells, repressed chromatin marker HP1 associates with the MIEP. In contrast, reactivation of HCMV following differentiation of monocytes into dendritic cells is associated with the enrichment of acetylated H4, indicative of active transcription (Reeves et al, 2005).

## **1.8 The chromatin-associated ND10 Components: ATRX and hDaxx**

As discussed above, active or repressed chromatin is subject to the regulation by additional cellular factors commonly referred to as transcriptional regulators, co-repressors or co-activators. The various proteins that are found localised to ND10 include several such factors. The candidate subjects of the present investigation into the role of ND10 proteins in herpesvirus infection are ATRX and hDaxx, as both have roles in chromatin remodelling and transcriptional regulation. These aspects of their functions in the cell are discussed below.

### **1.8.1 ATRX**

#### ***1.8.1.1 The gene and protein structure***

When first discovered, the human ATRX gene was localised to the Xq13.3 region, telomerically flanking locus DXS56 of the human X chromosome, and by sequence analyses shown to contain domains homologous to helicase-like proteins of SWI/SNF family such as *Saccharomyces cerevisiae* RAD54 and SNF2. The human counterpart of RAD54, hRAD54 is highly homologous to the C-terminal portion of ATRX, hence its structural and functional characteristics may also provide clues for ATRX function. Hence, ATRX since then has been referred to as a member of the family of SWI/SNF chromatin modifying complexes and sub-family of SNF2 helicases. The ATRX gene is mutated in  $\alpha$ -thalassaemia mental retardation X-linked (ATR-X) syndrome, a condition that is perhaps

caused by aberrant regulation of ATRX target genes (Gibbons et al, 1995; Picketts et al, 1996; Stayton et al, 1994). ATRX-null mice do not survive past embryogenesis, suggesting roles in the regulation of development and differentiation (Berube et al, 2005).

The large ATRX gene is composed of about 11,000 nucleotides, of which the cDNA sequence of the major ATRX isoform is approximately 7,500 nucleotides in size. The major isoform of the ATRX protein is composed of 2288 amino acids and has a predicted molecular weight of 280 kDa (Gibbons et al, 1995; Picketts et al, 1996). When analysed on a polyacrylamide gel using an antibody recognising a short N-terminal peptide sequence of the protein, two bands of 280 kDa and 180 kDa can be detected. This pattern of migration has led to identification of an additional truncated isoform (ATRXt), which is predicted to arise from alternative splicing (Garrick et al, 2004). N-terminal structural characteristics of ATRX include its well characterised PHD-like zinc finger domain. The typical architecture of a PHD finger domain is represented as C4HC3 (four cysteines – one histidine – three cysteines) that coordinate two zinc atoms in a cross-brace manner. The unique feature of ATRX PHD finger domain is that all coordinating atoms are cysteine residues (Bienz, 2006). This organisation is also shared by specific DNMTs – namely DNMT3A, -3B and -3L, which are involved in DNA methylation (as mentioned above). Therefore, the domain has been named as the ADD domain (Figure 1.7) and is involved in core histone recognition (Argentaro et al, 2007; Ooi et al, 2007; Otani et al, 2009).

#### ***1.8.1.2 ATR-X syndrome***

Mutations of *ATRX* gene that result in the development of ATR-X syndrome are mapped to various regions of the protein, mostly the PHD finger domain and some to the SNF2 homology region. Since the PHD finger is likely to be involved in DNA binding, it is thought that mutations in this region cause disruptions in ATRX-mediated chromatin remodelling functions. Clinical manifestations of the disease include psychomotor abnormalities, facial dysmorphisms, urogenital abnormalities and severe mental retardation and learning difficulties (Gibbons, 2006; Gibbons et al, 1997). Patient mutations within the SNF2 region disrupt localisation of ATRX to ND10 and are proposed to be involved in aberrant regulation of gene expression (Berube et al, 2008).

## ATRX protein structure

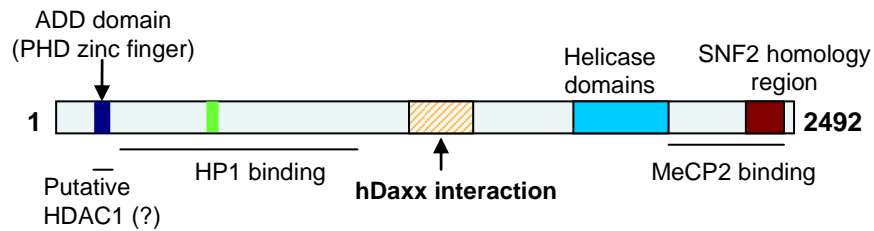


**Figure 1.7 The ATRX protein sequence**

Key structural features showing: SNF2 homology region and helicase domains (Garrick et al, 2004; Tang et al, 2004); hDaxx interacting domain (aa 1189-1326; Tang et al, 2004); ADD domain (Argentaro et al, 2007); HP1 binding region (Le Douarin et al, 1996) and PxVxL sequence (green; aa 561-595) (Lechner et al, 2005).

### 1.8.1.3 ATRX functions in chromatin remodelling

The highest homology of ATRX to the SNF2 subfamily of chromatin remodelling enzymes is within its C terminus. This part of the polypeptide is homologous to *S. cerevisiae* RAD54, a protein that functions in nucleosome repositioning within homologous DNA target sites and therefore has been demonstrated to be involved in DNA recombination (Alexeev et al, 2003). Accordingly, ATRX has been demonstrated to remodel DNA by nucleosome repositioning using *in vitro* assays (Xue et al, 2003). However, a substantial portion of the N-terminal part of the protein contains a domain involved in HP1 binding (Picketts et al, 1998) and a PHD zinc finger motif (Gibbons et al, 1997), which suggest functions in DNA binding and chromatin repression. Hence, a number of ATRX protein interactions has been determined, in support of its role in transcriptional repression.

Firstly, the proposed interaction between HP1 and a mouse ATRX homologue HP1-BP38 has been identified using a yeast two hybrid screen (Le Douarin et al, 1996). It appeared that this protein was around 83% identical across the majority of the N terminus of ATRX (Picketts et al, 1998). Interestingly, HP1 and ATRX co-localise at condensed chromatin during mitosis (Berube et al, 2000), which suggests the functional significance of this interaction. In other studies, interaction between the chromoshadow domain of HP1 $\alpha$  and a common HP1 binding motif of ATRX termed PxVxL has been confirmed using GST pull-down assays (Lechner et al, 2005), providing so far the most convincing evidence of this interaction. ATRX may therefore serve as co-repressor by interacting with HP1. This possibility is addressed in Chapter 6.

A second piece of evidence in favour of ATRX repressive functions is its association with MeCP2. Both proteins co-localise at distinct foci within the nuclei of mouse brain cells, as a result of interaction between ATRX C-terminal helicase domains and MeCP2. Loss of MeCP2 or expression of aberrant MeCP2 containing mutations that are characteristic of patients with mental retardation syndrome lead to a dispersed ATRX distribution pattern. It therefore follows that DNA regulation by the MeCP2/ATRX complex is required for proper development (Nan et al, 2007).

Thirdly, structural features within the ADD domain of ATRX shared with DNMTs suggest a role for ATRX in DNA methylation and thus a function as a transcriptional repressor. For example, DNMT3a and DNMT3L has been shown to interact with the core histone H3 *via* their ADD domains (Argentaro et al, 2007; Fuks et al, 2003; Otani et al, 2009). DNMT3L binds non-methylated histone H3 but this interaction is abolished by H3K4 methylation (Ooi et al, 2007). This may suggest a similar mechanism for ATRX interaction with histones. Interestingly, novel evidence demonstrates the interaction between ATRX and a histone variant H3.3 *via* H3.3 lysine 4. This association is proposed to regulate telomere replication (Wong et al, 2010).

Additional ATRX roles in chromatin regulation include functions in normal chromosome segregation during mitosis (Ritchie et al, 2008) and an HDAC-dependent activity at centromeric heterochromatin during meiosis (De La Fuente et al, 2004), supporting the requirement of ATRX in cell division.

### **1.8.2 hDaxx**

The role of the protein hDaxx as an ND10 protein with repressive functions during HCMV infection has been discussed (Section 1.6.5.2). HDaxx is the second protein that is being researched in the present study, therefore its general functional characteristics and cellular roles are described further.

### ***1.8.2.1 Structure and functional domains***

Daxx is ubiquitously expressed throughout different tissues (Yang et al, 1997). Mouse (m) and human Daxx (hDaxx) aa sequences share 69% identity. The hDaxx protein includes 740 aa with a molecular weight of 81.3 kDa, and it is predominantly a nuclear protein that can be localised to ND10, heterochromatin and the nucleolus (reviewed in Chen et al, 2009). Cloning of the mDaxx gene has identified 7 exons. Targeted disruption of the gene in mice leads to embryonic lethality associated with extensive apoptosis (Michaelson et al, 1999). At the structural domain level hDaxx is poorly characterised. Amongst the known conserved domains are the two paired amphipathic helices domains (PAH1 and -2), which are present in other proteins involved in co-repressor functions. Acid-rich and serine-proline-threonine rich domains are also shown (Figure 1.8; adapted from (Yeung et al, 2008). Regions of interaction with relevant proteins that are discussed here are mapped within Figure 1.8 based on the available evidence from the cited reports.

### ***1.8.2.2 hDaxx in apoptosis***

There is some inconsistency in reports regarding pro-apoptotic and anti-apoptotic roles attributed to hDaxx (reviewed in Salomoni & Khelifi, 2006). Daxx was originally identified as a protein that interacts with a cell death receptor Fas in both *in vitro* and *in vivo* assays. This interaction activates the Jun-N-terminal kinase (JNK), which results in downstream events leading to apoptosis (Yang et al, 1997). This pathway also involves an hDaxx adaptor function *via* association with apoptosis signal-regulating kinase 1 which has a central role in JNK activation (Chang et al, 1998).

On the other hand, anti-apoptotic roles of hDaxx have also been proposed. One group observed increased apoptosis incidence in cells devoid of hDaxx expression, using *Daxx*<sup>-/-</sup> mouse embryo models and using an RNAi approach for targeted knock-down of Daxx expression (Michaelson et al, 1999; Michaelson & Leder, 2003). Another study has reported elevated apoptosis incidence in transformed APL cells treated with HDAC inhibitors. This coincided with downregulation of hDaxx. The authors therefore suggested a function of hDaxx in protecting APL cells from apoptosis in an HDAC-dependent manner (Amin et al, 2001). According to these studies, Daxx may function as both anti-apoptotic and pro-apoptotic factor, depending on the cellular environment.

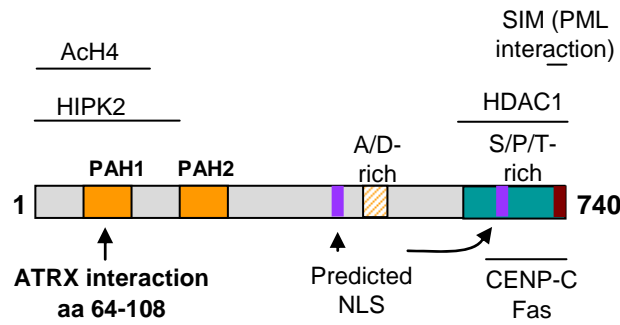


**Figure 1.8 The hDaxx protein sequence**

Key structural features showing the characterised protein interaction regions with HDAC1 and acetylated histone H4 (Hollenbach et al, 2002), ATRX (Tang et al, 2004), HIPK2 (Hofmann et al, 2003) and other proteins, as indicated. Predicted nuclear localisation signal (NLS), acidic A/D-rich and S/P/T-rich domains, and paired amphipathic helices (PAH1 and PAH2) are also indicated (Yeung et al, 2008).

### ***1.8.2.3 The role of hDaxx phosphorylation in its functions***

Phosphorylation of hDaxx is known to regulate its interaction with protein binding partners and nuclear localisation. Thus, CRM1 (chromosomal region maintenance 1) interacts with hDaxx when hDaxx is phosphorylated at residue S667 to promote its nuclear export under conditions of glucose deprivation (Song & Lee, 2004). Recent evidence also suggests that phosphorylation at S178 attracts binding of the enzyme prolyl isomerase Pin1, which is overexpressed in tumours. This interaction induces degradation of hDaxx, and is proposed to inhibit induction of apoptosis by hDaxx (Ryo et al, 2007). Importantly, phosphorylation at S669 of mouse Daxx by direct interaction with homeodomain-interacting protein kinase (HIPK) 1 induces displacement of hDaxx from ND10. In cells overexpressing HIPK1, notable de-repression in transcriptional activities as determined by luciferase assays was observed (Ecsedy et al, 2003). In human cells, hDaxx phosphorylation can be induced by HIPK2 expression. Co-expression of both proteins induced the JNK signalling pathway, proposing a role of HIPK2 in hDaxx-mediated JNK activation during apoptosis (Hofmann et al, 2003). Hence, hDaxx phosphorylation can efficiently modulate hDaxx activities.

### ***1.8.2.4 hDaxx in transcriptional regulation***

One of the earliest pieces of evidence for the transcriptional repression function of hDaxx was demonstrated by (Torii et al, 1999) using luciferase reporter assays. Following this observation the repressor functions of hDaxx have been subject to extensive research. Mutational analysis of hDaxx suggests that multiple domains are required for fully

efficient repression. Notably, hDaxx mutants lacking both PAH domains or the C-terminal S/P/T region had the lowest ability to repress transcription amongst the different mutants tested in the assay (Hollenbach et al, 2002). Interaction of hDaxx with chromatin-associated proteins such as HDACs, core histones, HP1 $\alpha$  and centromeric protein CENP-C suggest a mechanism for its possible regulation of gene repression (Hollenbach et al, 2002; Ishov et al, 2004; Li et al, 2000; Pluta et al, 1998).

The ability of hDaxx to interact with HDAC1 has been mapped to its C-terminal part that spans the S/P/T motif. Due to the high homology between HDACs of class I it is proposed that hDaxx can interact with all three members (HDAC 1, -2, and -3). The HDAC/hDaxx interaction is essential for hDaxx properties as a transcriptional repressor and suggests the two proteins function as a complex that represses transcription from its target genes (Li et al, 2000). Consistent with these observations, additional interaction between class II HDACs and hDaxx has been demonstrated (Hollenbach et al, 2002).

An important observation that identified a consensus SUMO-interaction motif within the last 8 amino acids has become an indication of SUMO-mediated transcriptional repression by hDaxx (Ryu et al, 2000). SUMO-specific protease SENP1 releases hDaxx from ND10 (Ryu et al, 2000), indicating the importance of hDaxx interaction with SUMO-modified substrates for its sequestration at ND10. Interactions between SUMO-modified co-repressors and hDaxx have been shown to be important for hDaxx-mediated transcriptional repression (reviewed in Shih et al, 2007). These targets include PML, the glucocorticoid receptor, Smad4 and CBP (Holmstrom et al, 2008; Ishov et al, 1999; Kuo et al, 2005; Lin et al, 2004; Lin et al, 2006; Meinecke et al, 2007; Zhong et al, 2000a). HDaxx itself has been reported to be post-translationally modified by SUMO (Jang et al, 2002), which may indicate that hDaxx itself is targeted to SIMs of other proteins, although the precise roles of this modification in modulation of its transcriptional activities are yet to be established.

Other transcriptional targets of hDaxx include CAAT/enhancer-binding protein  $\beta$  (C/EBP $\beta$ ), involved in differentiation of APL cells (Wethkamp & Klempnauer, 2009) and c-met factor, required for cell growth and differentiation (Morozov et al, 2008). According to the first study, hDaxx binds to the transcriptional activator C/EBP $\beta$  and induces repressed transcription (Wethkamp & Klempnauer, 2009). The latter study was the first one to show a different mode of hDaxx-mediated repression, in which hDaxx physically associated with the c-met DNA promoter (Morozov et al, 2008). Taken together,

these studies describe the importance of hDaxx-dependent transcriptional regulation in cell differentiation, tumour suppression and the cell cycle.

#### ***1.8.2.5 The ATRX/hDaxx complex***

A particularly intriguing interaction is that between ATRX and hDaxx. Several studies have detected an interaction between transiently expressed or endogenous proteins (Ishov et al, 2004; Tang et al, 2004; Xue et al, 2003) and have suggested functions of this complex in chromatin repression. The ATRX-interaction region of hDaxx has been mapped to the PAH1 domain (Tang et al, 2004), which is conserved amongst other proteins involved in chromatin regulation. *In vitro* studies of ATRX chromatin-remodelling activities have created some controversy regarding the chromatin repressor functions of the complex. Whereas one study suggests that hDaxx interferes with ATRX repressive functions by sequestering it at ND10 (Tang et al, 2004), the other suggests that hDaxx is not required for ATRX actions in nucleosome displacement assays (Xue et al, 2003). Protein interaction partners of ATRX and hDaxx (discussed above), however, strongly suggest the potential involvement of the complex in heterochromatin formation. Besides, since ATRX-hDaxx and ATRX-MeCP2 (Nan et al, 2007) interactions occur *via* distinct regions of ATRX, it is possible that ATRX serves as an adaptor that recruits co-repressor hDaxx to the sites of repressed gene transcription (discussed in Chapter 6). In addition to these pieces of evidence, there is an indication the ATRX PHD domain may be involved in HDAC interaction (Zhang et al, 1998). Since hDaxx and HDACs also interact (Hollenbach et al, 2002; Lin et al, 2006), it is possible that chromatin regulation by ATRX and hDaxx involves their incorporation as the subunits of a large chromatin repressor complex.

## **1.9 Immunity to viral infection**

Chromatin assembly around viral genomes and ND10-mediated regulation of viral gene expression, as discussed in previous sections of this Chapter, are all linked to anti-viral intrinsic cellular responses. These phenomena have formed the basis of the concept of anti-viral intrinsic immunity, which is central to the present investigation. Prior to discussing anti-viral intrinsic immunity, the different pathways of host defences against viral infection must be considered. Anti-viral immunity can act on several levels: innate immunity provided by pre-existing phagocytic cells and natural killer (NK) cells; adaptive immunity provided by B and T lymphocytes; and intrinsic provided by the pre-existing intracellular

components. Viruses have co-evolved mechanisms of counteracting and evading immune responses of the host on all these levels, therefore understanding of the mechanisms which are utilised by viruses to overcome host responses may become crucial in vaccine and therapy development. Below the basic features of the anti-viral immune systems are described.

## **1.9.1 Innate and adaptive anti-viral immunity**

### ***1.9.1.1 The functions of anti-viral adaptive immune system***

The adaptive immune system relies on the action of T lymphocytes and B lymphocytes. B cells produce antibodies directed against the invading pathogens. They recognise antigens *via* B cell receptors (BCRs), which are expressed on their surface and termed immunoglobulins (IgGs), or antibodies. While memory B cells recognise viral antigens and present them on the surface in association with MHC class II molecules, plasma B cells produce IgGs in secretory form. Antibodies specific to the infecting virion particles can then neutralise them by preventing interaction with host cells or disrupting the viral envelope, and therefore inhibit entry into the cell. In addition, many phagocytic cells express specific receptors for the constant IgG chain, which are recognised by antibodies bound with their variable site of the protein to the antigen. This recognition results in the destruction of the pathogen by a phagocytic cell.

T lymphocytes recognise the infected cells and either destroy those (CD8<sup>+</sup> T cells) or assist B cells in antibody production (CD4<sup>+</sup> T cells). T cells express T cell receptors that recognise antigens expressed by the infected cells. Within virus-infected cells viral proteins are subjected to proteolysis through the proteasome pathway, and the resulting peptide remnants are trafficked through the cell eventually to be presented on the cells surface in complex with MHC molecules. CD8<sup>+</sup> T cells recognise antigens presented in a complex with MHC class I surface molecules, while CD4<sup>+</sup> T cells recognise antigens presented by MHC class II molecules. Importantly, interactions between CD4<sup>+</sup> T cells and B cells are recognised as a crucial step in the anti-viral immune response, since the B cells act as antigen presenting cells in this case. Memory B cells internalise viral antigen *via* surface bound antibodies and present the processed peptides in association with MHC class II molecules. Interaction with CD4<sup>+</sup> T cells triggers their differentiation into antibody secreting plasma cells. Lack of functional B cells results in more aggressive viral spread (reviewed in Whitton et al, 2004). For example, in HSV-1 infected mice, antibodies

produced by B cells play important roles in suppression of lesions formed after primary infection by HSV-1 (Deshpande et al, 2000).

### ***1.9.1.2 The functions of innate anti-viral immune system***

Components of the innate immune systems include phagocytic cells that are capable of binding microorganisms, then internalising and destroying them. These cells act as the first line of defence against infection with various microbes. Natural killer (NK) cells, however, have been identified as one of the key components in a rapid anti-viral response (reviewed in Biron et al, 1999). In herpesviruses infections, the NK cell response is associated with cytotoxicity and IFN- $\gamma$  production. IFN- $\gamma$  produced by the activated NK cells mediate potent anti-viral activity *via* different pathways within the first hours to a few days during infection, whilst B and T cell responses may take over a week to develop. Cytotoxicity of NK cells is dependent on activation of IFN- $\alpha/\beta$  responses, which are produced by virally infected cells. NK cell depletion in mice renders them substantially more susceptible to HSV-1 infection, affecting production of efficient adaptive immune response by CD8<sup>+</sup> T cells (Nandakumar et al, 2008).

Clearly, components of innate and adaptive immune system present are in constant interaction. Thus, phagocytes can act as antigen presenting cells and therefore induce development of T cell memory. Interferons produced by a subset of T cells can activate NK cells to elicit destruction of the infected cells. Co-evolution of viruses with the host cells in many cases impedes an efficient antiviral response. It is therefore necessary to understand what subcellular and molecular processes are responsible for development of viral countermeasure activities during the infection. This aspect is described further.

### **1.9.2 Cellular anti-viral intrinsic immunity**

The concept of cellular intrinsic defence or immunity has emerged recently, due to expanding research into the cellular proteins involved in inhibition of various stages of viral replication on the subcellular and subnuclear levels. The term is applied to the collective set of activities that are potent inhibitors of viral gene expression (Bieniasz, 2004). This definition encompasses the functions of various nuclear, cytoplasmic and transmembrane proteins that fall outside the conventional constituents of host adaptive and innate immunity systems. Since provided by the pre-existing components of the cell, intrinsic immunity can also be considered as a part of innate anti-viral immunity.

### ***1.9.2.1 Discovery of anti-retroviral intrinsic immunity: APOBEC and TRIM5 $\alpha$***

Unlike adaptive and innate immune systems of mammals that require *in vivo* study systems, intrinsic immunity can be studied in cell culture. Hence, using cell-based approaches the factors that restrict replication by retroviruses have been identified. Of the most intriguing proteins shown to restrict HIV replication are APOBEC3G and TRIM5 $\alpha$  (reviewed in Huthoff & Towers, 2008; Nisole et al, 2005; Sokolskaja et al, 2006).

APOBEC (apolipoprotein B mRNA-editing enzyme catalytic polypeptide) proteins constitute a family of cytidine deaminases that act on single stranded DNA or mRNA molecules. APOBEC3G specifically deaminates single stranded DNA of the minus strand of nascent viral DNA. It is thought that APOBEC3G interferes with reverse transcription in HIV-infected cells, although the precise mechanism has not been determined. APOBEC3G has been identified as a repressive factor that renders cells non-permissive to a mutant HIV-1 infection that does not express HIV virion infectivity factor Vif. Hence Vif serves as a strong countermeasure to APOBEC-mediated cellular intrinsic resistance mechanism (Huthoff & Towers, 2008).

Certain TRIM (tripartite motif) protein family members have been clearly demonstrated to restrict infection by HIV-1. Their structural characteristics include a RING domain within the RBCC motif, which is shared with that of TRIM19 also known as PML. TRIM5 $\alpha$  is the largest isoform of the TRIM5 gene, and it contains a SPRY domain that possesses viral restriction specificity (reviewed in Nisole et al, 2005). TRIM5 $\alpha$  is a cytoplasmic protein that has been shown to contribute to an HIV infectivity block using an RNAi approach, since TRIM5 $\alpha$  deficient cells are more susceptible to infection (Stremlau et al, 2004). The mechanism of TRIM5 $\alpha$  action, although yet unidentified, is proposed to involve SPRY-mediated recognition of the incoming viral particles and the enzymatic activity of the RBCC box, thereby inhibiting viral infectivity. Ubiquitin ligase activity provided by the RING domain of TRIM5 proteins has provided clues to the mode of TRIM5 $\alpha$ -mediated viral restriction (reviewed in Huthoff & Towers, 2008; Sokolskaja et al, 2006). The precise mechanism of TRIM5 $\alpha$  action still remains to be clarified. Hence, further research will potentially focus on anti-viral properties of all TRIM family members.

### ***1.9.2.2 ND10 proteins as constituents of anti-herpesvirus intrinsic immunity***

With the identification of hDaxx as a potent regulator of repression of the HCMV MIEP (see Section 1.6.5.2), the term intrinsic immunity has been increasingly applied to ND10 protein mediated cellular defences against herpesviruses (Saffert & Kalejta, 2007; reviewed in Tavalai et al, 2008). The observations by different groups that upon the infection released herpesvirus genomes become associated with ND10, followed by the ND10 disruption by viral regulatory proteins, have provided the evidence for anti-viral functions of certain ND10 components (as discussed earlier in Section 1.5.2). Indeed, the following sets of evidence support this hypothesis: (a) HSV-1 ICP0-mediated degradation of PML and Sp100 is functionally significant for efficient productive infection, since ICP0-null mutant HSV-1 replicates more efficiently in the absence of either or both PML and Sp100 (Everett et al, 2008; Everett et al, 2006); (b) HCMV IE-deficient mutant replicates more efficiently in PML-dependent cells, which correlates with IE1-mediated abrogation of SUMO-modification of PML and Sp100 (Lee et al, 2004; Muller & Dejean, 1999; Tavalai et al, 2006; Tavalai et al, 2008); (c) HCMV pp71 is capable of inducing proteasomal degradation of hDaxx, which in turn restricts initiation of IE gene expression and hence blocks viral replication in pp71-null mutant infections (Hwang & Kalejta, 2007; Preston & Nicholl, 2006; Saffert & Kalejta, 2006; Saffert & Kalejta, 2007; Woodhall et al, 2006).

Interestingly, certain parallels can be drawn regarding the functions of PML and TRIM5 $\alpha$  in anti-viral immunity, hence supporting the need for investigation and identification of novel TRIM family members that may be involved in restricting viral replication. For example, adenoviral regulatory protein E4ORF3 has also been shown to reorganise ND10 structures (Carvalho et al, 1995; Doucas et al, 1996) *via* an interaction with PML, as well as to interact with another TRIM family member, TIF1 $\alpha$  motif (Yondola & Hearing, 2007). Similarly, both PML- and hDaxx-depletion were able to improve the infectivity of a mutant adenovirus deficient in E4ORF4 expression (Ullman & Hearing, 2008). These observations provide support for the hypothesis that one function of ND10 is in anti-viral defence, particularly in the case of DNA viruses. Further research into the potential candidate components within ND10 is required in order to establish the mechanisms of viral genome repression and the ways adopted by viruses to counteract them.

## 1.10 Aims and objectives of the study

The earliest events of host anti-viral defences are exhibited on a subcellular level thereby providing intrinsic anti-viral immunity. Repression of gene expression by pre-existing cellular proteins hence restricts viral replication, cell-to-cell spread and release of viral progeny into the host internal systems. Cellular intrinsic anti-viral immunity is a recently-emerged concept, although extensive research is being conducted in an attempt to elucidate the cellular mechanisms responsible for this process.

The study presented here was stimulated by the following key existing concepts regarding the relationships between herpesviruses and functions of ND10 components:

- (1) ND10 are recognised as nuclear domains that include certain proteins with cellular intrinsic anti-viral properties;
- (2) In addition to ND10, regulation of herpesvirus on chromatin level has provided potent repression mechanisms, especially during establishment of latency and reactivation by the two herpesviruses HSV-1 and HCMV;
- (3) The two chromatin associated factors ATRX and hDaxx constitute a complex that localises to ND10 and is proposed to function in chromatin repression pathways.

Based on these existing data, investigation into the potential roles of ATRX and hDaxx in the context of HSV-1 and HCMV was of great interest. The primary purpose of the present study therefore is to identify the roles of ATRX and hDaxx in the regulation of HCMV and HSV-1 infection. The presentation of the results is divided into three principal parts, which were aimed to: (a) Characterise ATRX and hDaxx in cell lines used for the present study, as well as the construction of the various recombinant cell lines utilised as tools in further investigations (Chapter 3); (b) Investigate the role of ATRX in the regulation of HCMV infection (Chapter 4); and (c) Determine the roles of ATRX/hDaxx complex in regulating HSV-1 infection, and identify potential mechanisms how ICPO counteracts the action of this complex. The observations presented in the current study demonstrate evidence for the existence of a chromatin-associated complex that contributes to intrinsic cellular defence against HSV-1 and HCMV infections. Whether this occurs *via* direct chromatin-remodelling of viral genomes is currently unclear.

## 2 Materials and Methods

### 2.1 Materials

#### 2.1.1 Antibodies

Primary and secondary antibodies used throughout the study and the purpose of their use are listed in Tables 2.1 and 2.2, respectively, below.

**Table 2.1 Primary antibodies used in the study**

<i>Antibody</i>	<i>Type</i>	<i>Target</i>	<i>Dilution in WB</i>	<i>Dilution in IF</i>	<i>Source</i>
AC-40	Mouse monoclonal	Actin	1:1000 – 1:2000	N/A	Sigma-Aldrich
H-300	Rabbit polyclonal	ATRX	N/A	1:200	Santa-Cruz sc-15408
39F	Mouse monoclonal	ATRX	1:20	1:20	Richard Gibbons, Oxford
D-19	Goat polyclonal	ATRX	N/A	1:100	Santa-Cruz sc-10078
r1866	Rabbit polyclonal	hDaxx	N/A	1:1000	(Pluta et al, 1998)
07-471		hDaxx	N/A	1:100	Upstate
D7810		hDaxx	1:1000	N/A	Sigma-Aldrich
Ab290	Rabbit polyclonal	EYFP	1:2500	N/A	Abcam
11060	Mouse monoclonal	ICP0	1:2000	1:1000	(Everett et al, 1993b)
R190	Rabbit polyclonal	ICP0	IP only	IP only	(Everett et al, 1998b)
58S	Mouse monoclonal	ICP4	1:1000	1:100	(Showalter et al, 1981)
E13	Mouse monoclonal	IE1 and IE2	1:2500	1:500	Serotec Laboratories
5E10	Mouse monoclonal	PML	1:20	1:20	(Stuurman et al, 1992)
r8	Rabbit polyclonal	PML	N/A	1:5000	(Boddy et al, 1996)
ab2595	Mouse monoclonal	pp65	1:1000	N/A	Abcam
SpGH	Rabbit polyclonal	Sp100	1:1000	1:1000	(Sternsdorf et al, 1995)
Z1F11	Mouse monoclonal	UL42	1:1000	N/A	(Schenk et al, 1988)
BL851	Rabbit polyclonal	USP7	1:1000	N/A	Bethyl Laboratories
R201	Rabbit polyclonal	USP7	IP only	IP only	(Everett et al, 1999c; Everett et al, 1997)

**Table 2.2 Secondary antibodies used in the study**

	<i>Antibody</i>	<i>Raised in</i>	<i>Dilution</i>	<i>Source</i>
Anti-mouse	FITC-conjugated IgG	Sheep	1:100	Sigma-Aldrich F3008
	Alexa Fluor 555 IgG	Donkey	1:5000	Invitrogen, Molecular probes A31570
	Cy3-conjugated IgG	Goat	1:2000	GE Healthcare PA43002
	Anti-mouse IgG Horseradish peroxidase conjugate	Sheep	1:1000	Sigma-Aldrich A4416
Anti-rabbit	Alexa Fluor 555 IgG	Donkey	1:5000	Invitrogen, Molecular probes A31572
	Alexa Fluor 647 IgG	Donkey	1:5000	Invitrogen, Molecular probes A21432
	Alexa Fluor 488 IgG	Goat	1:5000	Invitrogen, Molecular probes A11001
	Cy5-conjugated IgG	Goat	1:2000	GE Healthcare PA45004
	Cy3-conjugated IgG	Goat	1:2000	GE Healthcare PA43004
	Anti-rabbit IgG Horseradish peroxidase conjugate	Sheep	1:20000	Sigma-Aldrich A4914
Anti-goat	Alexa Fluor 555 IgG	Donkey	1:5000	Invitrogen, Molecular probes A21432

## 2.1.2 Plasmids

The plasmids used in the study that were obtained from commercial sources or elsewhere, and the purpose of their use are detailed below. Construction of all other plasmids generated during the current study is described in the Section 2.2.

**Table 2.3 Plasmids**

<i>Plasmid</i>	<i>Source</i>	<i>Purpose</i>
pEYFP-C1	Clontech	Vector backbone for gene insertion
pLKO1.puro	Sigma-Aldrich (Figure 2.1)	Lentiviral vector backbone for selected shRNA sequences
pLKO.shLuci	Constructed from pLKO.1puro (Everett et al, 2008)	Lentiviral vector used as shRNA control
pLKO.neo.gD.EYFP (pLNGY)	Constructed from pLKO1.puro (Everett et al, 2008)	Lentiviral vector backbone for gene insertions
pLKO.ShDaxx2	Constructed from pLKO1.puro using the siRNA sequence described in (Michaelson & Leder, 2003)	Lentiviral vector coding for shRNA targeting hDaxx <sup>1</sup>
pcDNA3.hDaxx	A gift from John Sinclair	hDaxx-coding vector
pCMV.DR.8.91	A gift from D. Trono ( <a href="http://tronolab.epfl.ch">http://tronolab.epfl.ch</a> )	Lentivirus helper vector
pVSV-G	BD biosciences	For expression of VSV envelope protein for pseudotyped lentivirus production

<sup>1</sup> shDaxx2 sequence: 5'-GGAGTTGGATCTCTCAGAA-3' (Michaelson & Leder, 2003)

## 2.1.3 Enzymes

Restriction endonucleases and their respective buffers were purchased from Roche apart from *Age* I and *Apa* I (New England Biolabs).

T4 DNA ligase and  $\lambda$ -phosphatase and their buffers were from New England Biolabs.

## 2.1.4 Oligonucleotides

Oligonucleotides used throughout the study were purchased from Sigma-Aldrich. All oligonucleotides were dissolved in water to a concentration of 100  $\mu$ M by adding as the volume specified for each primer by the manufacturer. Their sequences and purpose of use are detailed below:

**Table 2.4 Oligonucleotides used in cloning procedures and sequencing**

F, forward; R, reverse.

<i>Name</i>	<i>Sequence 5'-3'</i>	<i>Purpose of use</i>
E-Daxx Age F	AGCTTAACCGGTCGCCACCATGGTGAGC	Construction of pLNGY-hDaxx
Daxx Stop Eco R	GACCTGGAATTCCTAATCAGAGTCTGAGAG	
Daxx Xho F	CTCGAGCCATGGCCACCGCTAACAGC	
Daxx si-ve F	GAGTTAGATCTGAGCGAATTGGATGACCCA	Introduction of si-ve site within hDaxx sequence
Daxx si-ve R	CTGCAGGAAAAGGAGTTAGATCTGAGCGAA	
Daxx Apa F	GGATTCTGGTGAGGGCCCTAGTGGAATGGC	Construction of pLNGY-hDaxx
Daxx Apa R	GCCATTCCACTAGGGCCCTCACCAGAATCC	
Daxx dPAH1 F	TCTCTGAGCCTCATGGGGCCGCAAGCTCTATG TCTAC	Deletion of hDaxx ATRX-interaction domain
Daxx dPAH1 R	GGCCCCATGAGGCTCAGAGGAGCTAGG	
Daxx dSIM R	TCTCGAGGTCGAGAATTCCTACTCTTCTGGATCG CATTGTG	Deletion of hDaxx SUMO-interaction motif
Daxx MSIM R	CGAGGTCGAGAATTCCTAATCAGAGTCTGAGCC CGCGCCGATCTCTTCTGGATCGC	Mutation of hDaxx SUMO-interaction motif
Daxx1701 F	GTTACAGGAGCGACGTCACC	Sequencing of the hDaxx-expressing plasmids
Daxx2021 F	CCTCCAGAGCTGAGACAGATG	
Daxx201 F	GCTGTTCGAAGAGTTCCTTG	
Daxx Pst F	GACTCCGCATACCTGCAGGAGGCACGGTTG	
Daxx Pst R	CAACCGTGCCTCCTGCAGGTATGCGGAGTC	
LKO F	CGATACAAGGCTGTTAG	
LKO R	GCAAACCCAGGGCTGCCTTG	
SV40 E	GCTGCAATAAACAAGTT	Sequencing of pEYFP-C1 plasmids
GFP-C1	CCTGAGCAAAGACCCCAACG	

## 2.1.5 Chemicals and reagents

All reagents were purchased from Sigma-Aldrich unless specified in the list below or elsewhere in the text:

5-bromo-4-chloro-3-indolyl-b-D-galactoside (X-gal):	Melford Laboratories Ltd
30% (w/v) Acrylamide :	National Diagnostics
BenchTop 1 Kb DNA ladder:	Promega
Ammonium persulphate:	Bio-Rad Laboratories Ltd
Ampicillin:	Melford laboratories
Autoradiography Film:	UV Kodak X-Omat 18x24cm - Kodak
Caesium Chloride:	Melford Laboratories Ltd
Chloroform:	VWR International Ltd
Dialysis tubing:	Medicell International Ltd
Dulbecco's modified Eagle's medium:	Invitrogen
Ethanol:	Fisher Scientific UK Ltd
Ethylene diamine tetra acetic acid (EDTA):	VWR International Ltd
Foetal bovine serum gold:	PAA laboratories
Foetal calf (bovine) (FBS) serum:	Invitrogen
Giemsa stain:	VWR International Ltd
Glycerol:	VWR International Ltd
Glycine:	VWR International Ltd
Human serum:	MP Biomedicals
Hybond-ECL nitrocellulose membrane:	Amersham Biosciences
Isopropanol:	VWR International Ltd
L-glutamine:	Invitrogen
Methanol:	VWR International Ltd
NP40 substitute:	EuroClone
Penicillin/Streptomycin solution:	Invitrogen
Protease inhibitor cocktail tablets, EDTA-free:	Roche
Protein G/salmon sperm DNA:	Upstate (Millipore)
Protein Rainbow Marker:	GE Healthcare
Skimmed milk powder:	Marvel
Sodium chloride:	VWR International Ltd
Sodium dodecyl sulphate (SDS):	VWR International Ltd
Spectra multicolour broad range protein ladder:	Fermentas
Sucrose:	VWR International Ltd
Tris:	Roche
Williams modified Eagle's medium:	Invitrogen

## 2.1.6 Solutions

Immunoprecipitation (IP) lysis buffer:	50 mM HEPES pH 7.4, 150 mM NaCl, 0.1% (v/v) NP40, 5% (v/v) glycerol, 1 mM EDTA, 1 mM EGTA, 2 mM DTT; 1 tablet of protease inhibitors dissolved in 1 ml of water, 400 $\mu$ l per 10 ml of buffer used
Luria-Bertani (LB) broth:	10 g NaCl, 10 g Bactopeptone, 5 g yeast extract in 1 L water, pH 7.5
Phosphate buffered saline (PBS):	170 mM NaCl, 3.4 mM KCl, 10 mM Na <sub>2</sub> HPO <sub>4</sub> , 1.8 mM KH <sub>2</sub> PO <sub>4</sub> , pH 7.2
Protein gel running buffer:	0.05 M Tris, 0.05 M glycine, 0.1% SDS
Resolving gel buffer (RGB):	1.5 M Tris-HCl, 0.4% SDS, pH 8.8
SDS-PAGE loading buffer:	50 mM Tris-HCl, pH 6.8, 2.24% SDS (w/v), 11.1% (v/v) glycerol, 666.6 mM $\beta$ -mercaptoethanol
STET:	8% (w/v) sucrose, 5% (v/v) Triton-X 100, 50 mM EDTA pH 8.0, 50 mM Tris-HCl pH 8.0
Stacking gel buffer (SGB):	0.5 M Tris-HCl, 0.4% SDS, pH 6.8
Stripping buffer:	2% SDS, 62.5 mM Tris-HCl, 100 mM $\beta$ -mercaptoethanol, pH 6.7
1 $\times$ TAE:	40 mM Tris, 1 mM EDTA, 5 mM sodium acetate, glacial acetic acid to pH 7.6
Tris-EDTA (TE):	10 mM Tris-HCl, pH 8.0, 1 mM EDTA
Transfer buffer (TOWBIN):	20% methanol, 25 mM Tris, 192 mM glycine pH 8.3
Versene:	0.6 mM EDTA in PBS, 0.02% phenol red
X-gal solution:	5 mM potassium ferrocyanide, 5 mM potassium ferricyanide, 2 mM magnesium chloride, 0.01% NP 40, in PBS; X-gal in DMSO (40 mg/ml) added to a final concentration of 2.4 mM

YTB medium: 8 g bacto-tryptone, 5 g yeast extract, 2.5 g NaCl to 1 L water, pH 5.0

## 2.1.7 Viruses

### 2.1.7.1 HSV-1 virus strains

All HSV-1 strains were propagated in BHK cells, using Glasgow-modified Eagle's medium, and titrated on U2OS cells by Anne Orr (MRC Virology Unit).

Wild-type HSV-1 strain was 17 *syn*<sup>+</sup> (also known as Glasgow strain; 17+ for short) and was previously described (Brown et al, 1973). The full sequence of this strain is described in McGeoch et al (1988). ICP0-null *ddl1403* HSV-1 strain was the derivative of the wild-type strain 17+ (Stow & Stow, 1986). Strains *in1863* (wild-type recombinant) and its ICP0-null *ddl1403*/CMV*lacZ* counterpart were produced and kindly provided by Prof. Chris Preston (MRC Virology Unit). These strains contained an insertion of *Escherichia coli* gene *lacZ* coding for  $\beta$ -galactosidase within the *tk* locus.

HSV-1 temperature-sensitive (*ts*) strain, *tsK*, and the mutant derivative strain *in1374* were kindly provided by Chris Preston. Strain *tsK* has a lesion in ICP4 gene and was previously characterised (Marsden et al, 1976; Preston, 1979). Strain *in1374* is a derivative of *tsK* virus, and in addition to a temperature-sensitive lesion in ICP4, also contains a deletion of the ICP0 gene, a mutation within the tegument protein VP16 that inactivates its ability to stimulate IE gene expression and an insertion of HCMV-IE promoter drive *LacZ* gene within UL43 (Preston & Nicholl, 2005). The HSV-1 mutant *in1316* has mutations that inactivate the transcriptional activities of VP16, ICP0, and ICP4 and an insertion encoding EYFP-tagged pp71, controlled by HCMV MIEP, at the *tk* locus (Marshall et al, 2002). Strain *in1360* was a derivative of the above, containing untagged pp71 (Preston and Nicholl, 2005).

### 2.1.7.2 HCMV virus strains

The wild-type HCMV strain used was AD169. HCMV mutant strain ADSubUL82 has a deletion within the UL82 gene than encodes pp71, and was kindly provided by Thomas Shenk (Princeton University). UV-irradiated strain AD169UV was provided by Chris Preston and its preparation is described elsewhere (Lukashchuk et al, 2008).

## 2.1.8 Cells

### 2.1.8.1 Mammalian cells and culture conditions

The cells used throughout this study and the purpose of their use are detailed below (in the order of relevance). Cells were maintained either in DMEM or WME media (as specified). DMEM was supplemented with 10% FBS for all cell manipulations unless specified otherwise. WME medium was supplemented with 10% FBS Gold (PAA Laboratories Ltd.), 2 mM L-glutamine, 5 µg/ml insulin and 0.5 µM hydrocortisone (referred to as complete WME medium). All cell growth media were supplemented with 100 units/ml penicillin and 100 µg/ml streptomycin. Cells transduced with lentiviral stocks were maintained in additional antibiotic selection media, generally 0.5 µg/ml puromycin and/or 0.5 mg/ml G418/neomycin as specified for each individual cell line in Table 2.6.

HepaRG: Human hepatoma cell line with properties closely related to primary human hepatocytes (Gripon et al, 2002) was maintained in complete WME medium. HepaRG were the major experimental cell line used.

HF cells: A primary human fibroblast (HF) cell line isolated from human foreskin tissue, obtained from the Department of Urology, University of Erlangen, and grown in DMEM. HF cells were the second major experimental cell line.

HEK-293T cells: Human embryonic kidney cells transformed with adenovirus 5 DNA and SV40 Large T antigen. The cells were obtained from BD Biosciences and maintained in DMEM. The cells were used for the generation of lentiviral stocks expressing shRNA molecules or a protein of interest throughout the study.

HEp-2 cells: Human epithelial cell line, originally established from human laryngeal carcinoma; obtained from the MRC Virology Unit cytology department, and maintained in DMEM. The cells were used in a small proportion of experimental manipulations.

ws-HeLa cells: Epithelial cell line, originally established from human cervical carcinoma cells. Obtained from the MRC Virology Unit cytology department and grown in DMEM. The cells were used in a small proportion of experimental manipulations.

U2OS: Human osteosarcoma cell line, obtained from the MRC Virology Unit cytology department and grown in DMEM. The cells were used for virus titration and other experiments.

### ***2.1.8.2 Bacterial cells and culture conditions***

The *E. coli* strain DH5 $\alpha$  chemically-competent cells (Invitrogen) were used in cloning procedures and plasmid DNA purification. DH5 $\alpha$  were grown in LB-broth or plated out on LB agar plates. LB media was supplied with appropriate antibiotics for transformed bacterial cells.

## **2.2 Molecular biology methods**

### **2.2.1 Bacterial culture handling**

#### ***2.2.1.1 Transformation of competent bacterial cells***

For transforming chemically competent DH5 $\alpha$  bacterial cells, 50 $\mu$ l aliquots were thawed on ice and mixed gently with appropriate quantity of plasmid DNA. For re-transforming plasmid DNA, 5-10 ng of DNA mix was used. For transforming ligation mix (see Section 2.2.2.5), depending on the number of fragments, 3-5  $\mu$ l of ethanol-precipitated plasmid DNA was used. The mixture was incubated on ice for 30 min, transferred to a 37 °C water bath for 1 min heat shock, placed back on ice for 2 min and mixed with 1 ml of YTB broth pre-warmed to 37 °C. Bacterial cells were allowed to recover at 37 °C for an 1 hour with horizontal shaking, centrifuged in the microfuge at 5,000 rpm for 2 min, resuspended in 200  $\mu$ l of YTB broth and plated out on pre-warmed agar plates, supplied with appropriate antibiotic (ampicillin or kanamycin as specified). Plates were incubated at the 37 °C incubator overnight, or generally for a period of less than 24 hours, and colonies were picked the following day for inoculating small scale cultures for plasmid miniprep analysis.

#### ***2.2.1.2 Growing bacterial cultures for plasmid DNA preparation***

In order to grow up cultures for small scale DNA preparation (minipreps), an individual colony from an LB agar plate was inoculated into 3 ml LB-broth supplied with appropriate antibiotic, and cultures were incubated with horizontal shaking at 37 °C overnight.

For large scale DNA preparation (maxipreps), bacterial cultures were set up in a larger volume of LB media. A starter culture was first set up by inoculating 10 ml of LB-broth with a single bacterial colony, grown over approximately 6-8 hours, and then mixed with 350 ml LB-broth supplied with antibiotics. The large maxiprep culture was then propagated at 37 °C overnight with horizontal shaking.

## **2.2.2 Plasmid DNA extraction and analysis**

### ***2.2.2.1 Small scale (miniprep) plasmid DNA extraction by boiling method***

Bacterial cultures grown overnight in 3 ml LB-broth were transferred to 1.5 ml Eppendorf tubes and centrifuged in the microfuge at 13,000 rpm for 1 min. Bacterial pellets were resuspended in 200 µl STET buffer, mixed with 5 µl of lysozyme/STET solution (10 mg/ml) and boiled for 50 sec in the boiling water bath. Lysed bacterial cells were then centrifuged at 13,000 rpm for 20 min to spin down cell debris. The supernatant was transferred to a fresh Eppendorf tube, and the final volume was adjusted to 160 µl with additional STET as required. Supernatants were mixed with 135 µl of isopropanol and centrifuged in the microfuge at 13,000 rpm for 2 min. The supernatant was discarded and the DNA pellet was washed in 70% ethanol by a short 13,000 rpm spin. The pellets were dried at room temperature and resuspended in 30 µl of distilled water. This method for plasmid DNA preparation produces impure DNA which can only be used for general analysis by restriction digest and agarose gel electrophoresis (as described in section 2.2.2.4).

### ***2.2.2.2 Large scale (maxiprep) plasmid DNA extraction by CsCl banding method***

Bacteria from the large overnight cultures were centrifuged in GSA tubes (400 ml) using the Sorvall GSA rotor in the Beckman GPR free-standing centrifuge at 5 k for 10 min at 4°C. Pellets were resuspended in 20 ml of STET and transferred to 50 ml beakers. The suspension was mixed with 2.5 ml of lysozyme/STET solution (10 mg/ml) and incubated for 1 min at room temperature before bringing to the boil over the Bunsen burner and finally boiling for 50 sec in the boiling water bath. Lysed bacterial cells were transferred to 50 ml SS34 tubes and centrifuged using the Sorvall SS34 rotor in the Beckman GPR centrifuge at 18,000 rpm for 45 min. Supernatant was then mixed with 0.9 volumes of isopropanol in 50 ml Falcon tubes and centrifuged at 3,000 rpm for 5 min at 4 °C to pellet DNA. The resulting dense DNA pellet was dissolved by adding 5 ml of 1×TE and incubating at 37 °C with horizontal shaking. When the pellet was completely dissolved, the obtained DNA solution was made up to a total volume of 6.3 ml with 1×TE and mixed with 7 g CsCl and 200 µl EtBr. The mixture was incubated on ice for 20-30 min, centrifuged at 3,000 rpm in a benchtop centrifuge (Sorvall RT7) for 10 min at 4 °C in order to pellet insoluble debris and carefully transferred into 65V13 tubes for CsCl banding. CsCl banding was performed by an overnight spin at 45,000 rpm for 16 hours in the Beckman L7-65 ultracentrifuge at 15 °C using the 65 V13 high speed rotor. After the centrifugation the two bands were separated, of which the lower band corresponded to

plasmid DNA while the upper was chromosomal and linear DNA. The upper chromosomal layer was carefully removed using a needle and a 2 ml syringe; the lower band was then isolated and transferred into a 15 ml Falcon tube. In order to remove CsCl, dialysis against 800 ml of 1×TE for 2 hours at room temperature with light stirring was performed. The dialysed plasmid was transferred into a 10 ml Sarstedt tube and treated with 100 µg/ml RNase by incubation at 65 °C for 1 hour. The solution was cooled then mixed with 100 µg/ml proteinase K and 0.1% (w/v) SDS, and incubated at 37 °C for 1 hour. To extract the DNA, the solution was mixed with one volume of pre-saturated phenol and centrifuged at 3,000 rpm for 10 min at 4 °C. The aqueous top layer was mixed with an equal volume of chloroform in a fresh Sarstedt tube, centrifuged at 3,000 rpm for 10 min at 4 °C (benchtop Sorvall RT7 centrifuge) in order to separate the upper aqueous layer. This was transferred to another fresh Sarstedt tube, mixed with 1/20 volume of 5 M sodium chloride and 2.5 volumes of 100% ethanol and incubated at -20 °C overnight to precipitate the plasmid DNA. To pellet the DNA, the tubes were centrifuged at 3,000 rpm for 10 min at 4 °C, the pellet was dissolved in 400 µl of distilled water and transferred to a 1.5ml Eppendorf tube for an additional round of ethanol precipitation on a small scale. The solution was mixed with 20 µl (1/20 volumes) of 5 M sodium chloride and 1 ml (2.5 volumes) ethanol, incubated on dry ice for 20 min and centrifuged at 13,000 rpm in the microfuge (OLE DICH microcentrifuge; Camlab) for 10 min. The resulting DNA pellet was washed with 80% ethanol by 5 min centrifugation at 13,000 rpm, air-dried at room temperature and finally dissolved in 0.1 - 0.3 ml 1×TE depending on the size of the final pellet. DNA concentrations of the maxipreps were determined using an Eppendorf BioPhotometer. The purified plasmid DNA was stored at 4 °C.

### ***2.2.2.3 Using commercial kits for plasmid DNA extraction and purification***

Due to impurities contained within DNA solution obtained by a boiling miniprep method (described in section 2.2.2.1), QIAquick® PCR purification kit (QIAGEN) were used to clean up selected miniprep DNAs following the manufacturer's instructions. The clean DNA miniprep was then used for sequencing reactions.

For an alternative method of large scale plasmid DNA extraction, NucleoBond® Xtra Maxi Plus kit (Macherey-Nagel) was used according to manufacturer's instructions, using the maxiprep protocol.

#### ***2.2.2.4 Plasmid DNA analysis by restriction digest and agarose gel electrophoresis***

For a standard restriction digest reaction, the total volume of each reaction was made up to 20  $\mu$ l with distilled water. Each reaction contained 10 units (or 1  $\mu$ l) of restriction enzyme and 2  $\mu$ l of its appropriate 10 x restriction buffer. If digesting PCR reactions, they were first purified using QIAquick® PCR purification kit, and the total volume of the purified reaction (30  $\mu$ l of the column-eluted fragment) was used to set up a restriction digest reaction with 10 units of the restriction enzyme and 1 x restriction buffer. Reactions were incubated for 2 hours at 37 °C.

For restriction analysis or fragment purification, 1% (w/v) agarose gels were prepared in 1xTAE buffer. Restriction digest reactions were mixed with 6xDNA loading dye (Promega) and DNA fragments produced by restriction enzyme digestions were separated by agarose gel electrophoresis at 100 volts. The gel was then stained in ethidium bromide/1xTAE solution (approximately 1  $\mu$ g/ml) for 15 min on a shaker and rinsed with water. The DNA was visualised with short wave UV on a U.V. Products Inc transilluminator. For fragment preparation, 5-10  $\mu$ g plasmid DNA was digested, and following electrophoresis the DNA bands were visualised under long wave UV and appropriate fragments were excised. In order to extract fragment DNA from a gel slice, QIAquick® gel extraction kit (QIAGEN) was used according to manufacturer's instructions. Fragments were eluted in 30  $\mu$ l of QIAGEN Elution Buffer.

#### ***2.2.2.5 Ligation of DNA fragments***

Prior to setting up a ligation reaction, DNA fragments were purified from agarose gels as described above. If using PCR fragments, they were digested and purified using the QIAquick® PCR purification kit. For a standard ligation reaction, 5  $\mu$ l of each QIAGEN column-eluted DNA fragment was mixed with 4  $\mu$ l of T4 DNA ligase buffer and 1  $\mu$ l T4 DNA ligase in a total reaction volume of 20  $\mu$ l. Reactions were incubated at room temperature overnight. The following day each ligation mix was made up to a total volume of 200  $\mu$ l with 1xTE, and DNA was precipitated using 1/20 vol of 5 M NaCl and 2.5 vol 100% ethanol as described for the final steps of the CsCl banding method (see section 2.2.2.2). The invisible DNA pellet was resuspended in 10  $\mu$ l distilled water. Depending on the number of fragments used per ligation reaction, 2-5  $\mu$ l of resulting DNA solution was used for transforming competent bacterial cells as described in section 2.2.1.1.

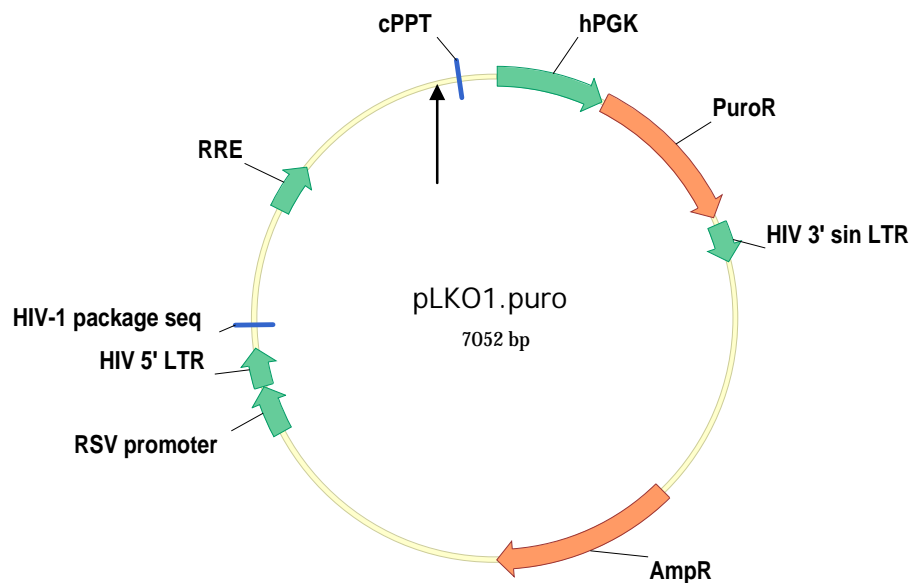
#### ***2.2.2.6 Sequencing of the purified plasmid DNA***

Prior to sequencing, correct construction of the recombinant plasmid was confirmed by appropriate restriction digests and selected miniprep DNA was purified using a QIAGEN column and following the PCR purification protocol. Sequencing was performed to ensure that no random mutagenesis has occurred throughout bacterial cloning procedures. Sequencing reactions were submitted to Claire Addison and Aidan Dolan (MRC Virology Unit) as reactions of 6 µl total volume containing 3 nmoles primer and 50-70 ng DNA. In brief, DNA/primer solutions were mixed with 0.5 µl Big Dyes (ABI version 3.1), 1.75 µl ABI Dilution Buffer and 1.75 µl of distilled water. The sequencing mixes were then subject to PCR cycling (PCR systems 9700) and ethanol-precipitated (work done by C. Addison and A. Dolan). The pellets of the sequencing reactions were submitted to the Glasgow University sequence service. Ready sequences were analysed using VectorNTI software.

#### **2.2.3 Recovery of pLKO.puro-shATRX clones**

Plasmid DNA expressing shRNA molecules targeting endogenous cellular ATRX were part of MISSION shRNA library (Sigma-Aldrich) and were based on the construct pLKO1.puro (Figure 2.1, A). These plasmids were sourced commercially and provided as glycerol stocks of transformed bacteria. This vector contained the essential elements for lentiviral production, including 5' and 3' LTRs, HIV-1 packaging sequence, a gene for ampicillin resistance (AmpR) for selective growth of the transformed bacterial colonies, a coding sequence for puromycin resistance for mammalian cell selection. The bacterial stock expressing pLKO-shATRX90 was delivered as transformed bacterial cells, which were plated out on agar plates supplied with 100 µg/ml ampicillin. The following day colonies were inoculated into LB-broth for small-scale plasmid DNA preparation using the boiling method. Minipreps were screened by restriction digest, sequenced and respective miniprep cultures were grown for large-scale DNA preparations. Plasmid DNA was extracted by the CsCl banding method as described in Section 2.2.2.2. The target sequence of ShATRX90 within the ATRX gene is 5'-CGACAGAACTAACCCCTGTAA-3' and is schematically represented on Figure 2.1, B.

A



B



**Figure 2.1 Lentiviral vector pLKO1.puro**

A: Map showing the features of the lentiviral vector. Abbreviations of the features: RRE - rev response element, hPGK promoter - human phosphoglycerate kinase promoter, cPPT - polypurine tract, LTR - long terminal repeats, sin – self-inactivating, RSV promoter - Rous sarcoma virus promoter. The vector also bears a gene for puromycin resistance (PuroR) for mammalian cell selection and ampicillin resistance (AmpR) for selective growth of transformed bacterial colonies. The site of shRNA sequence insertion is indicated by an arrow. B: The ATRX open reading frame demonstrating the position of the target site shATR90. The ATRX cDNA is marked by a grey arrow.

## 2.2.4 Specific cloning strategies

Specific approaches for cloning the hDaxx native sequence into a pLKO-based vector and hDaxx mutagenesis were designed. The resulting constructs were used for generating cell lines that were utilized for a significant part of the studies described in Chapters 3 and 5.

### 2.2.4.1 Polymerase chain reaction

The following polymerase chain reaction (PCR) conditions were used throughout the procedures, according to the Phusion<sup>®</sup> High-Fidelity (HF) PCR manual (Finnzymes), with minor alterations as indicated in the text:

#### PCR reaction

5× HF PCR buffer	10 µl
Primer 1	0.5 µM
Primer 2	0.5 µM
Aliquoted dNTP mix	0.1 mM
Template DNA	50 ng
dH <sub>2</sub> O	to 49 µl
Phusion <sup>®</sup> HF DNA polymerase (2 units/µl)	2 units (1 µl)

#### Cycling conditions

Initial denaturation cycle	98 °C	30s	
Denaturation	98 °C	10s	} × 30 cycles
Primer annealing	60-65 °C	20s	
Extension	72 °C	≥30s	
Final extension	72 °C	5 min	
Hold	4 °C	∞	

Extension time was allowed as at least 30 sec per 1 kb of DNA fragment, hence for fragments larger than 1 kb it was increased accordingly as specified. Primer pairs used for the strategies described in the current section are listed in the table below. Each primer pair introduces a restriction site that is unique for each particular fragment amplified in a PCR.

**Table 2.5 Primer pairs used in pLNGY-hDaxx vector construction**

	<i>Primer pair</i>	<i>Restriction sites</i>	<i>Size of the amplified fragment</i>	<i>Purpose</i>
1	Daxx Xho F Daxx si-ve R	<i>Xho</i> I <i>Bgl</i> II	650 bp	hDaxx cloning into pLNGY
2	Daxx si-ve F Daxx Apa R	<i>Bgl</i> II <i>Apa</i> I	625 bp	
3	Daxx Apa F Daxx Eco stop R	<i>Apa</i> I <i>EcoR</i> I	969 bp	
4	E-Daxx Age F Daxx dPAH R	<i>Age</i> I -	890 bp	Deletion of ATRX-interaction region
5	Daxx dPAH F Daxx Eco stop R	- <i>EcoR</i> I	1,900 bp	
6	E-Daxx Age F Daxx dSIM R	<i>Age</i> I <i>EcoR</i> I	~2.9 kb	Deletion of SUMO-interaction motif
7	E-Daxx Age F Daxx MSIM R	<i>Age</i> I <i>EcoR</i> I	~3,000 kb	Mutagenesis of SUMO-interaction motif

#### **2.2.4.2 General cloning strategy**

The cloning strategies utilized in construction of the plasmids throughout this section consisted of all or in part of the main principal steps:

1. PCR using conditions specified above with minor alterations.
2. Gel electrophoresis of 5 µl of the PCR product was using 1% agarose gel to confirm the correct size of the product.
3. Purification of the remaining reaction using QIAquick® PCR purification system; eluted in 30 µl of the Elution Buffer (QIAGEN), unless detailed below otherwise.
4. Restriction digest of the purified PCR fragment (if specified).
5. Purification of the restriction digest reaction using QIAGEN PCR purification system.
6. Ligation of the resulting fragment containing sticky ends with other fragments.
7. Ethanol precipitation of the ligation reaction and transformation of competent bacterial cells.
8. Small-scale DNA extraction (by boiling method, section 2.2.2.1), analytical restriction digestion for screening for correct insertion of the fragments, and sequencing.
9. Large-scale DNA extraction using transformed bacterial cells from successful DNA minipreps.

### 2.2.4.3 Construction of pLNGY-hDaxx

The vector backbone for cloning hDaxx sequence was pLKO.neo.gD.EYFP (pLNGY for short; Figure 2.2). The vector contained in addition to the elements required for lentivirus production, a coding sequence for neomycin resistance (G418/neoR), an HSV-1 glycoprotein D gene (gD) promoter and the EYFP coding region. Plasmid pcDNA3.hDaxx expressing native hDaxx (GenBank accession code NM\_001350) was kindly provided by John Sinclair (Cambridge).

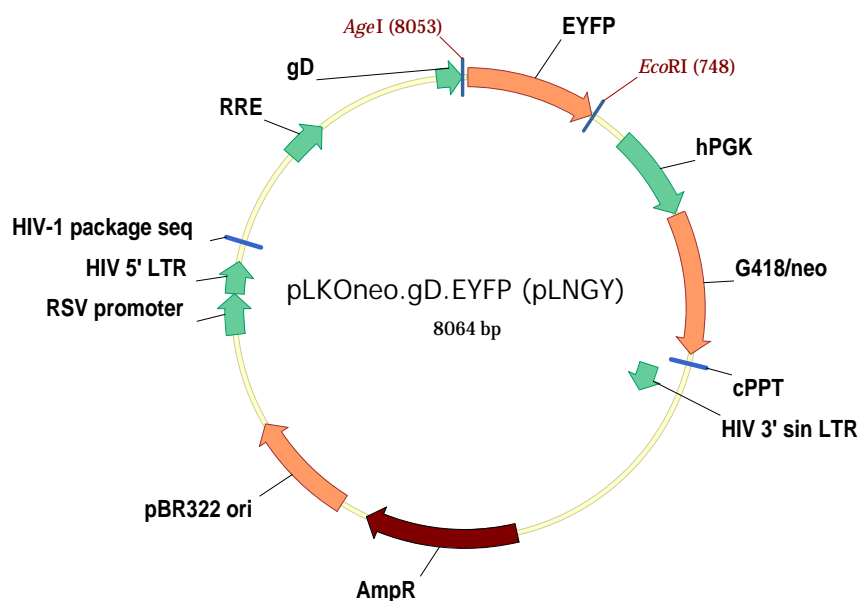


**Figure 2.2 pLKOneo.gD.EYFP (pLNGY)**

Backbone lentiviral vector containing neomycin resistance gene for mammalian selection (G418/neo), the weak gD promoter and EYFP for N-terminally tagging the insert gene. For all other marked features refer to Figure 2.1 A.

The strategy for cloning of hDaxx sequence in pLNGY is depicted in Figure 2.3. In order to generate the construct pLNGY-hDaxx, firstly, three hDaxx fragments were amplified in separate PCR reactions using pcDNA3.hDaxx plasmid as a template DNA, primer pairs 1-3 and following the reaction conditions as described above, with the fragment extension time 30 sec and primer annealing temperature 60 °C. The forward and reverse primers Daxx si- (siRNA negative) introduced a silent mutation into shDaxx2 target site, in addition to a *Bgl* II restriction site. Each purified PCR fragment was digested with respective restriction enzymes (Table 2.5, restriction enzymes for primer pairs 1-3; Figure 2.3) and ligated into the pEYFP-C1 plasmid backbone (digested with *Xho* I and *EcoR* I) in order to generate the intermediate clone pEYFP-C1.hDaxx. The plasmid was transformed

into *E. coli* cells and plated out on agar plates supplied with kanamycin (25 µg/ml). Individual colonies were grown for small-scale plasmid DNA extraction, extracted plasmid DNA preps were screened for correct insertion of the fragments by restriction digests and successful minipreps were sequenced. DNA clones containing the correct plasmid pEYFP-C1.hDaxx were digested with *Age* I (5') and *EcoR* I (3') and the fragment corresponding to EYFP-hDaxx coding region of approximately 3 kb was isolated by gel extraction. In the meantime, pLNGY vector was digested with *Age* I and *EcoR* I to yield the fragment corresponding to pLKOneo.gD. The fragments were ligated together, transformed into competent bacterial cells the following day and plated onto agar supplemented with ampicillin (150 µg/ml). The obtained colonies were first grown for small-scale DNA extraction, and DNA minipreps were further processed as described in the general strategy above. Plasmid pLNGY-hDaxx (Figure 2.4) was extracted by the CsCl banding method as described in section 2.2.2.2, and the sequence of the entire hDaxx open reading frame was authenticated.

#### **2.2.4.4 Deletion of hDaxx ATRX-interacting domain PAH1**

For deletion of hDaxx ATRX-interaction domain PAH1, mutagenesis by the gene splicing approach described in (Heckman & Pease, 2007) was performed. In summary, the technique involved two rounds of PCR, where round 1 generated overlapping fragments comprising the nucleotides upstream and downstream of the region to be deleted, and round 2 produced the full length product that lacked the region to be deleted (Figure 2.5).

For the first round PCR reactions, plasmid pLNGY-hDaxx was used as the template DNA. In round 1 PCR, primer pairs 4 and 5 (Table 2.5) were used to generate overlapping hDaxx DNA fragments. Two reactions were set up with primer pairs 4 and 5 (corresponding to primers a+b and c+d in Figure 2.5, respectively) and subjected to 30 PCR cycles, using product extension temperature of 1 min. For the second round of PCR, 1 µl of each product obtained from the reactions of round 1 were mixed into one PCR reaction containing all the essential PCR components as detailed in PCR conditions above, apart from the primers. The reaction was initially subjected to 5 PCR cycles using a product extension time of 1 min 30 sec. This step allows denaturation of the two products from the first round of PCR and re-annealing of the strand containing overlapping fragments, which are complementary to each other. Next, primers E-Daxx Age F and Daxx Eco stop R were added to the reaction, and the reaction was finally subjected to the remaining 25 cycles of PCR, which amplified the whole fragment EYFP-hDaxx.ΔPAH. The product was then treated as

described above in the general cloning strategy (section 2.2.4.2) and DNA maxipreps were prepared according to CsCl banding method.

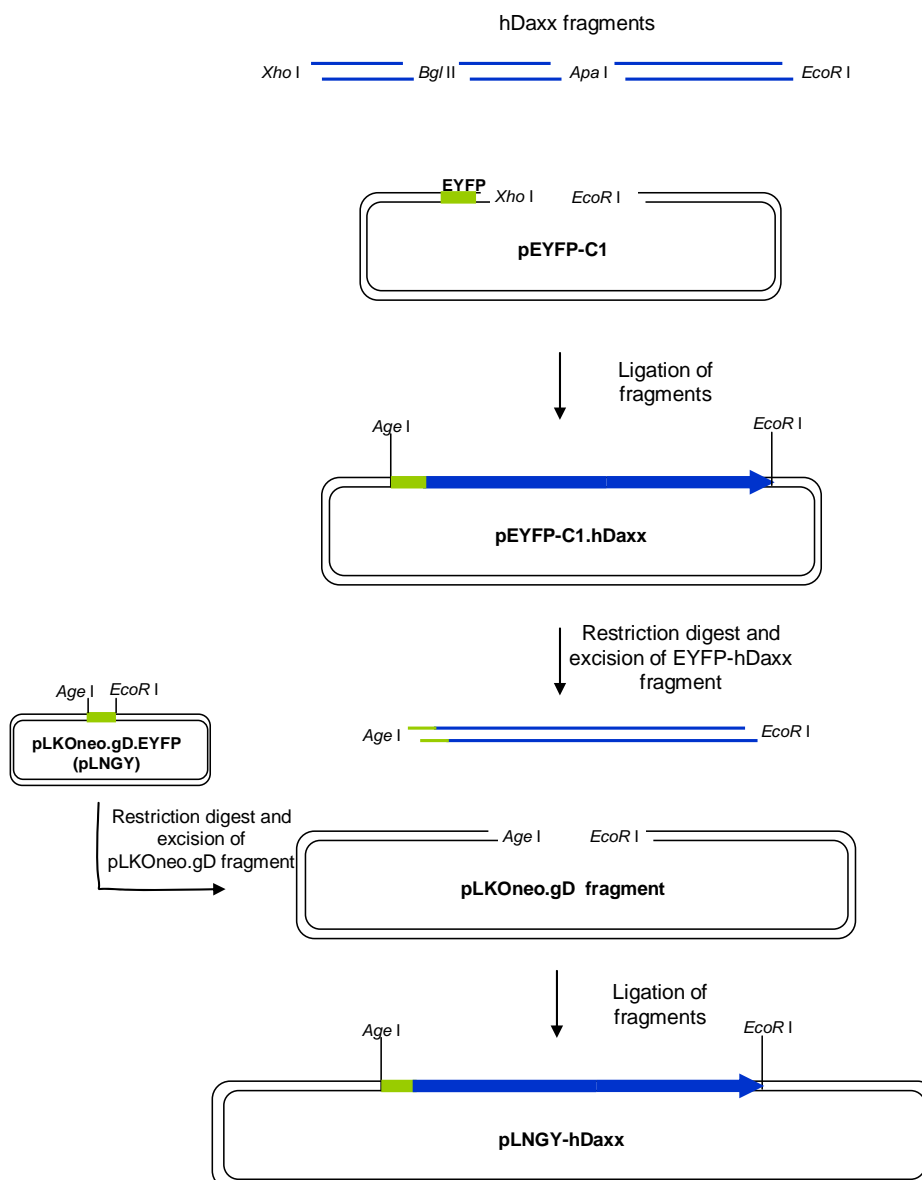


### Figure 2.3 Construction of pLNGY-hDaxx

hDaxx fragments amplified *via* three different PCR reactions (see text) and pEYFP-C1 intermediate vector were digested with the indicated restriction enzymes. Four fragments have been ligated together and transformed into bacteria. Purified plasmid pEYFP-C1.hDaxx and vector pLKOneo.gD.EYFP (pLNGY) were digested with *Age* I and *EcoR* I and fragments corresponding to EYFP-hDaxx and pLKOneo.gD, respectively were excised from agarose gel. Final pLNGY-hDaxx construct was produced by ligation of the two fragments and amplification of the resulting DNA *via* bacterial transformation.

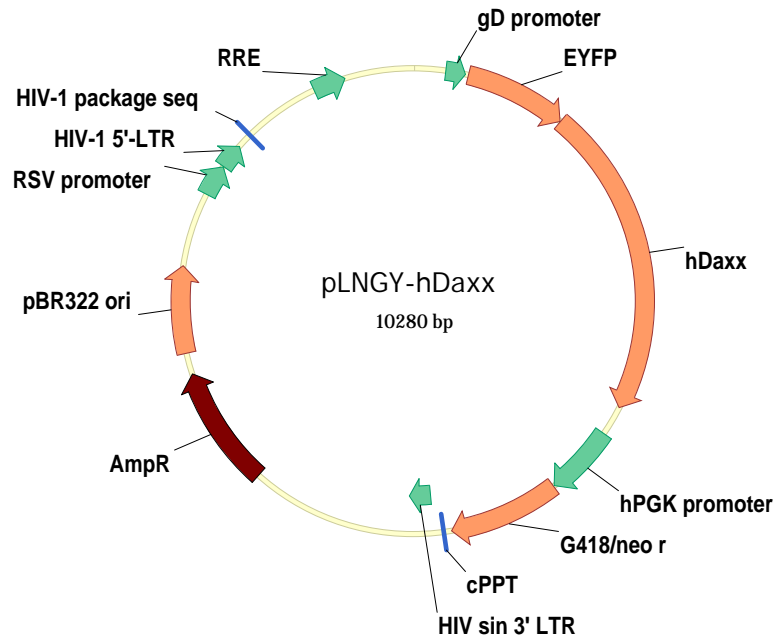


**Figure 2.4 pLNGY-hDaxx construct**

Schematic representation of wild-type hDaxx insert within pLNGY lentiviral vector.

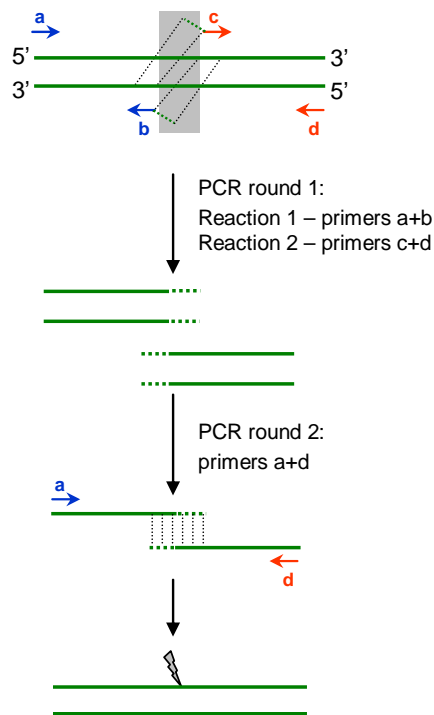


**Figure 2.5 PCR-mediated gene splicing mutagenesis**

The region to be deleted is marked with a shaded box. During the first round of PCR, the overlapping fragments are generated, where the overlapping regions are complementary to downstream and upstream regions to be deleted. During the second round of PCR, denaturation step produces single strands, so that the overlapping regions, complementary to each other, anneal and extend using dNTPs in the following steps of the reaction. The point of resulting deletion of the final PCR product is indicated (adapted from Heckman and Pease, 2007).

#### 2.2.4.5 Deletion of hDaxx SUMO-interaction motif

For the SUMO-interaction motif (SIM) deletion, primer pair 6 (Table 2.5) was used to amplify the whole EYFP-hDaxx fragment and introduce a deletion of the last 8 amino acids in one PCR step. For PCR, template DNA was pLNGY-hDaxx. Reaction and cycling conditions for mutagenesis were the same as described above, product extension time was 1 min 30 sec and annealing temperature was 65 °C. The obtained EYFP-hDaxx.ΔSIM fragment was purified, treated with restriction enzymes *Age* I and *EcoR* I and cloned into pLKOneo.gD vector as described in the previous section. After screening and analysing the small-scale DNA preps, DNA maxipreps were produced by CsCl method.

#### 2.2.4.6 Mutagenesis of hDaxx SUMO-interaction motif

In order to mutate the hDaxx SIM, the essential residues for SUMO binding were mutated using PCR-based site-directed mutagenesis protocol. For the PCR, pLNGY-hDaxx was the template and cycling conditions were as above, with the product extension time 1 min 30 sec and primer annealing temperature 65 °C. Primer pair 7 was used in the reaction (Table 2.5). The primer Daxx MSIM R used in the reaction introduced mutations coding for three amino-acids which replaced sequence I-V-L of the SIM to G-A-G (as indicated below).

```

              733 734 735 736 737 738 739 740
              D P E E I I V L S D S D
GC GAT CCA GAA GAG ATC ATC GIG CIC TCA GAC TCT GAT TAG GAATTCTCGACCTCG

              G A G
GC GAT CCA GAA GAG ATC GGC GCG GGC TCA GAC TCT GAT TAG GAATTCTCGACCTCG
```

Purified PCR product was digested with *Age* I and *EcoR* I, and the further steps were followed as described in Section 2.2.4.2.

## **2.3 Cell culture methods**

### **2.3.1 General cell culture manipulations**

#### ***2.3.1.1 Maintenance and passaging of the laboratory cell lines***

All cell lines were maintained in their respective growth media as specified in the Section 2.1.8.1. Additional antibiotic selection for lentivirus-transduced cell lines was used as detailed further in the Section 2.3.3.2 and Table 2.6. All cell lines were maintained in the incubator at the temperature 37 °C and 5% CO<sub>2</sub> and passaged on a regular basis. All media and versene solutions were pre-warmed to 37 °C prior to passaging. To passage the cells, media was removed, cells were washed once with versene solution and incubated with trypsin/versene solution for 2-5 min to trypsinise the cells from the surface of the tissue culture flask. Trypsinised cells were then resuspended in media and transferred to a new flask. Depending on the cell type and the confluency of the cells required, cell lines were split at a range of ratios between 1/3 to 1/10.

#### ***2.3.1.2 Cell seeding***

For experiments and assays, equal numbers of cells as specified for each experiment were seeded into appropriate tissue culture dishes. Cells were counted using the improved Neubauer haemocytometer chamber and determined as cells/ml. Generally, cell density of  $1 \times 10^5$  cells per well or 13 mm glass coverslip of the 24-well plate was used throughout the experiments, unless specified otherwise. For other tissue culture dishes, cells were seeded at the density specified individually for each experiment.

#### ***2.3.1.3 Freezing and thawing of the cell stocks***

For storage, cell suspension was centrifuged at 1,500 rpm for 5 minutes (Sorvall RT7) and cell pellet was resuspended in cell freezing mix containing appropriate media without selective antibiotic, additional 20% foetal bovine serum and 10% (v/v) DMSO. 1 ml of the resuspended cell pellet was transferred to 1.5 ml cryo-vials. The vials were wrapped in several layers of tissue paper, transferred to -70 °C for overnight storage and then transferred to the liquid nitrogen freezer.

For recovery from frozen, cells were thawed at 37 °C and put into media warmed to 37 °C containing appropriate antibiotic selection if required. Cells were allowed to attach to the tissue culture flask surface for a few hours before changing the medium, in order wash off residual DMSO.

### **2.3.2 Confocal immunofluorescence microscopy**

Confocal immunofluorescence microscopy is a method used widely throughout this study for analysis of protein localisation within normal or infected cells. Cells seeded onto 13 mm glass coverslips were fixed with 0.5 ml formaldehyde fix solution [5% (v/v) formaldehyde solution, 2% (w/v) sucrose, in PBS] by incubation at room temperature for 10 min. After removing the fix solution and washing the coverslips twice in PBS, 0.5 ml of permeabilisation solution [10% (w/v) sucrose, 0.5% (v/v) NP40, in PBS] was added and the cells were incubated at room temperature for 10 min. The cells were then washed three times in PBS supplemented with 1% FBS and probed with appropriate antibodies, as indicated for each individual experiment.

Generally, incubation times were 1 hour with primary antibodies and 1 hour with secondary antibodies, diluted appropriately in PBS/1% FBS (see Table 2.1), with 3 or 4 washes in PBS/1% FBS solution in between. Each coverslip was incubated with 25 µl of a diluted antibody by placing a coverslip onto the 25 µl drop with cell side facing down. After antibody staining, coverslips were finally rinsed in distilled water to remove PBS salts, air-dried at room temperature and mounted onto glass slides using a drop of about 10 µl Citifluor AF1 (antifade agent in PBS/glycerol). The coverslips were analysed immediately or stored at 4°C until further analysis.

Confocal microscopy analysis was carried out using a Zeiss LSM 510 confocal microscope with 488-, 543- and 633-nm laser lines, under image capture conditions that eliminated channel overlap. Samples were observed with a ×63 or ×40 NA 1.4 objective lens. The images were exported as files in a Tif format using the LSM Image Browser and edited using Adobe Photoshop.

### **2.3.3 Lentiviral transduction of cell lines**

Generation of lentiviruses and transduction of cell lines was used for either the production of cell lines with stable knock-down of protein expression by RNAi approach (Figures 2.6 and 2.7), or for re-constitution of the endogenous protein by introducing EYFP-fusion proteins. Depletion of endogenous protein expression was based on RNAi-mediated gene silencing (for reviews see McManus & Sharp, 2002; Meister & Tuschl, 2004). The overview of RNAi pathway is represented on Figure 2.6, demonstrating the key enzymatic complexes involved in the process. Utilization of short hairpin RNA (shRNA) molecules,

expressed by specially designed lentiviral plasmids, in this pathway is detailed in Figure 2.7.

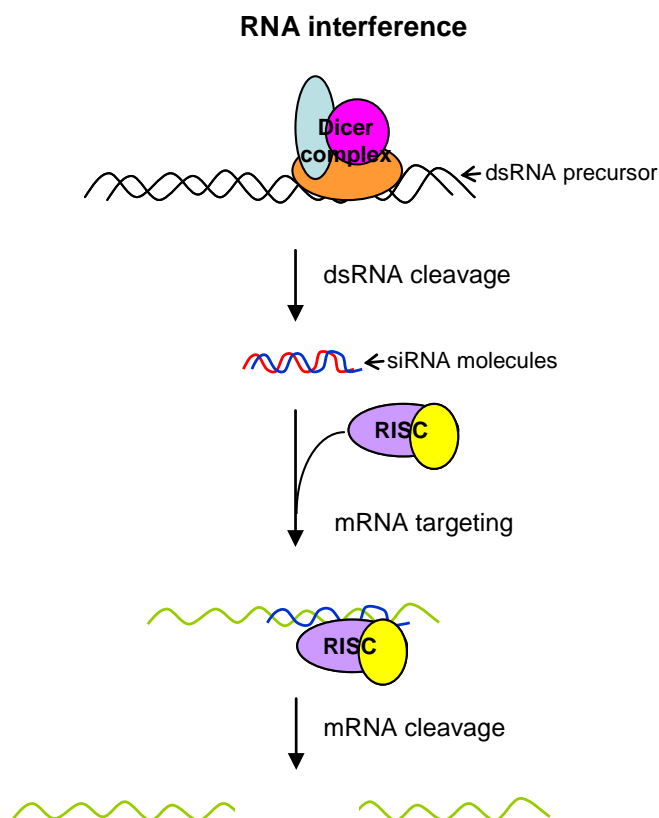


**Figure 2.6 Posttranscriptional processing by RNA interference**

Double stranded RNA (dsRNA) is recognised by the enzyme Dicer, which has a catalytic RNase III activity, and is cleaved into short double stranded RNA molecules, called small interfering RNA (siRNA) molecules. SiRNA molecules associate with the protein complexes to form the RNA-induced silencing complex (RISC). Mature RISC contains the antisense single stranded RNA molecules (blue) that target the complementary sense sequence of the mRNA molecule (green). This results in mRNA cleavage and hence gene silencing (adapted from McManus & Sharp, 2002).

### ***2.3.3.1 Transfection using Lipofectamine***

Transfection procedures utilized throughout the study were aimed at production of the lentiviral stocks only.

HEK-293T cells were seeded into a 60 mm tissue culture dish on the day preceding transfection procedure at a density of approximately  $1.5$  to  $1.7 \times 10^6$  cells per dish. For each transfection, 4  $\mu\text{g}$  of each plasmid DNA and DMEM without foetal bovine serum and penicillin/streptomycin antibiotic mix (referred to as serum-free DMEM), were used. The DNA mix for transfection contained the plasmid DNA of interest and two helper plasmids for production of lentiviral particles, pCMV.DR8.91 and pVSV-G. DNA was first mixed

with 250  $\mu$ l of serum-free DMEM and 8  $\mu$ l of PLUS reagent, and the mixture was incubated for 15 min at room temperature. 250  $\mu$ l of serum-free DMEM and 12  $\mu$ l of lipofectamine reagent were then added and the whole mixture was incubated at room temperature for a further 15 min. Meanwhile, media was removed from HK-293T cells and kept at 37 °C (referred to as conditioned media). Cells were washed with serum-free DMEM once and 1 ml of serum-free media was then added to the cells. Finally, the transfection mixture was added to the cells dropwise, and the plates were incubated for 3 hours at 37 °C, before overlaying with conditioned media. Cells were allowed to recover for additional 2-4 hours and media was changed to fresh DMEM. Lentiviral particles were then produced by the cells over the period of 72 hours, before harvesting supernatants.

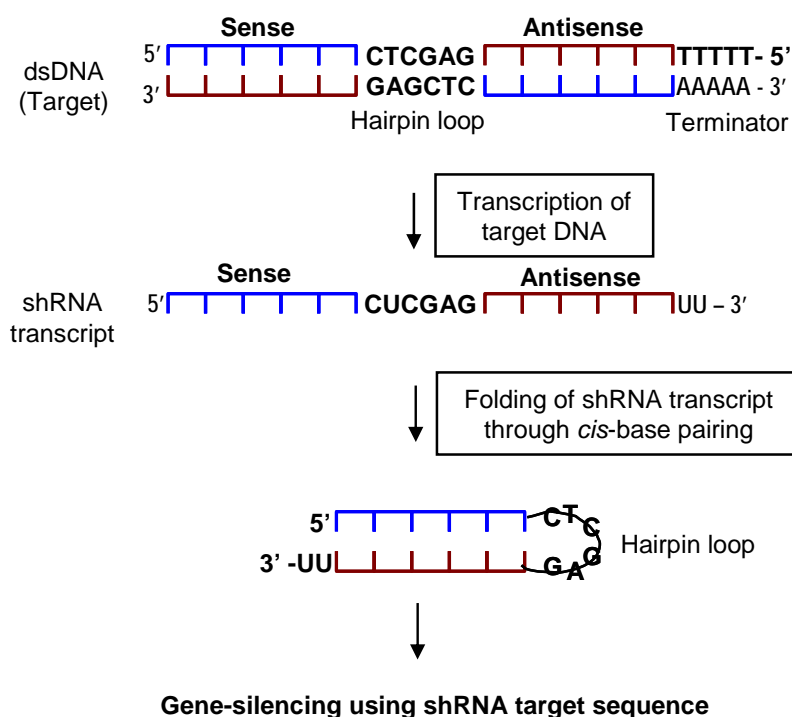


**Figure 2.7 Short hairpin RNA in experimental RNAi-mediated gene silencing**

DNA sequence is transcribed from a lentiviral vector to yield shRNA precursor molecules. Hairpin loop sequence allows folding through *cis*-base pairing to form an shRNA molecule that is recognised by Dicer which directs it for RISC assembly.

### ***2.3.3.2 Transduction of cell lines with lentivirus***

Cells to be transduced were seeded into 60 mm dishes at a density of  $0.5 \times 10^6$  the day before transduction with the lentiviral stocks. After 72 h post transfection, the supernatants from HEK-293T cells containing lentiviral particles were harvested and centrifuged (using benchtop centrifuge Sorvall RT7) at 1,500 rpm for 10 minutes to remove floating cell debris. The cleared supernatant was then filtered using 0.45  $\mu\text{m}$  filter. 1 ml of the supernatant was added to the cells to be transduced, together with 5  $\mu\text{g}$  of polybrene to aid adsorption of the virus. The lentivirus was allowed to adsorb during 1 hour by 37 °C incubation with gentle agitation every 5-10 minutes. After that, the procedure was repeated additional two times using fresh lentivirus and polybrene solution each time, and finally the cells were overlaid with fresh media supplemented 5  $\mu\text{g}/\text{ml}$  polybrene. Appropriate selection was applied the following day. Initial antibiotic selection was applied as 1  $\mu\text{g}/\text{ml}$  puromycin or 1 mg/ml G418/neomycin, depending on the plasmid, which was subsequently reduced to constant selection of 0.5  $\mu\text{g}/\text{ml}$  puromycin or 0.5 mg/ml neomycin. The resulting cell lines produced are detailed in the Table 2.6.

### ***2.3.3.3 Fluorescence activated cell sorting***

Enrichment of cells expressing EYFP fusion proteins after transduction with lentiviruses derived from plasmids of the pLNGY- series was achieved by fluorescence activated cell sorting (FACS). The service was kindly provided by Thomas Gilbey (Beatson Institute for Cancer Research, Glasgow).

For FACS analysis, negative control cells (HepaRG) and cells expressing EYFP-hDaxx fusion proteins (see Table 2.6) were harvested in normal growth media, centrifuged in 15 ml tubes at 1,500 rpm for 5 min and washed twice in 5 ml media containing 1% FBS and 200 units/ml penicillin, 200  $\mu\text{g}/\text{ml}$  streptomycin (2% penicillin/streptomycin solution). Cells were finally resuspended in 1 ml of media with 1% FBS and 2% penicillin/streptomycin and transferred to FACS tubes. Tubes were stored on ice for a short time before sorting EYFP-positive cells on a Becton Dickinson SORP FACSaria machine. After sorting, the total numbers of cells varied between 0.5 to  $1 \times 10^6$  cells. Cells were mixed with normal growth media (10% FBS) without antibiotic selection, centrifuged and finally transferred to a 35 mm or 60 mm tissue culture dish, depending on the number of cells. Concentration of penicillin/streptomycin solution was maintained at 2 % for additional 24 hours, before the media was changed to normal media supplied with antibiotic selection.

**Table 2.6 Lentivirus-transduced stable cell lines generated during the study**

<i>Name</i>	<i>Phenotype</i>	<i>Resistance</i>
HF-ShLuci	HF + pLKO.puro.ShLuci	Puromycin
HF-ShA90	HF + pLKO.puro.ShATRX90	Puromycin
HALL	HepaRG + pLKO.puro.ShLuci	Puromycin
HAA90	HepaRG + pLKO.puro.ShATRX90	Puromycin
HALD2	HepaRG + pLKO.puro.ShDaxx2	Puromycin
HL-E	HepaRG + pLKO.puro.ShLuci + pLNGY	Puromycin/neomycin
HL-ED	HepaRG + pLKO.puro.ShLuci + pLNGY-hDaxx	Puromycin/neomycin
HD-E	HepaRG + pLKO.puro.ShDaxx2 + pLNGY	Puromycin/neomycin
HD-ED	HepaRG + pLKO.puro.ShDaxx2 + pLNGY-hDaxx	Puromycin/neomycin
HD.ΔPAH	HepaRG + pLKO.puro.ShDaxx2 + pLNGY-hDaxxΔPAH1	Puromycin/neomycin
HD.ΔSIM	HepaRG + pLKO.puro.ShDaxx2 + pLNGY-hDaxxΔSIM	Puromycin/neomycin
HD.MSIM	HepaRG + pLKO.puro.ShDaxx2 + pLNGY-hDaxxMSIM	Puromycin/neomycin

## 2.4 Protein methods

### 2.4.1 Detection of protein expression by western blot

The following sections describe the methods for analysis of the protein expression that were utilized consistently throughout the study. Bio-Rad systems were used for resolving and transferring proteins onto a nitrocellulose membrane. The buffers used in the various steps are detailed in Section 2.1.6.

#### 2.4.1.1 SDS-polyacrylamide gel electrophoresis

In order to analyse expression of the proteins, protein samples were harvested in SDS-PAGE loading buffer and subjected to SDS-PAGE, based on the method described in

(Laemmli, 1970). Cells in the wells of 24-well plates ( $1 \times 10^5$  cells) were harvested in 70  $\mu$ l of SDS-PAGE loading buffer, boiled for 3 min, then 20  $\mu$ l of the sample was loaded onto polyacrylamide gels and the rest stored at  $-20$  °C. Generally samples were resolved on 7.5% polyacrylamide gels, although 6 % gels were also commonly used for resolving proteins of higher molecular weights or for better separation of high molecular weight bands. Gels fully submerged into running buffer (see Section 2.1.6) were run at a voltage ranging between 80-110 Volts.

#### ***2.4.1.2 Transfer of the proteins to nitrocellulose membrane***

Resolved proteins were transferred onto Hybond nitrocellulose membranes following a previously described method (Towbin et al, 1979), at a constant voltage either at 50 mAmp overnight at  $4$  °C or at 250 mAmp at a room temperature for 2.5 hours.

#### ***2.4.1.3 Immunodetection of the proteins***

All incubations and washes of the membranes were performed with constant agitation. All primary and secondary antibodies were diluted in the blocking buffer and stored at  $-20$  °C. Membranes were incubated with the blocking buffer (5% (w/v) Marvel milk powder, 1% (v/v) Tween 20 in PBS) by incubating for 1 hour at room temperature or overnight at  $4$  °C and incubated first with primary antibodies. Membranes were incubated at a room temperature for 2-2.5 hours with most of the antibodies used throughout the study, although certain antibodies (such as anti-Daxx D7810) were used overnight at  $4$ °C. Anti-HCMV IE1 antibody was always used at  $4$  °C overnight. After incubation with a primary antibody, the membrane was washed three times with PBS/1% (v/v) Tween 20, with each wash lasting at least 10 min. Next, the appropriate anti-rabbit or anti-mouse horseradish peroxidase-conjugated secondary antibody was added for a 1 hour incubation at room temperature. Membranes were then washed with PBS/1% (v/v) Tween 20 three times. The protein bands were then visualised by staining the membrane with enhanced chemiluminescence system (Perkin-Elmer Life Sciences) according to the manufacturer's manual and exposing the membrane to Kodak X-Omat film for the appropriate length of time, depending on the efficiency of the antibody binding.

#### ***2.4.1.4 Stripping of the nitrocellulose membrane***

In order to re-probe the membrane, it was incubated in stripping buffer (see section 2.1.6) at 55 °C for 30-40 min with occasional agitation. The membrane was then washed, blocked and re-probed as described above. For re-probing of the membrane, it was only stripped once.

#### **2.4.2 Co-Immunoprecipitation**

Co-immunoprecipitation (CoIP) was used for detection of interactions between either endogenous or re-introduced proteins. Cell monolayers were seeded into 100 mm tissue culture dishes at  $4.5 \times 10^6$  cells per dish, unless specified otherwise. The cells were harvested in 3 ml of immunoprecipitation (IP) lysis buffer (50 mM HEPES pH 7.4, 150 mM NaCl, 0.1% NP40, 5% glycerol, 1 mM EDTA, 1 mM EGTA, 2 mM DTT) supplemented with protease inhibitors using the rubber plunger from a 2 ml syringe. Cells were incubated on ice for 15 min prior to lysing by bath sonication (2 cycles of 1 min each, at 4°C) using Branson digital sonifier. Cell debris were removed by centrifugation at 25,000 rpm for 30 min at 4°C, and the lysates were pre-cleared by incubating with Protein G beads supplemented with salmon sperm DNA (Millipore) for 30 min at 4°C, with continuous mixing. After centrifugation at 13,000 rpm for 10 min at 4 °C to remove the beads and non-specifically bound proteins, immunoprecipitation was carried out by incubating the lysates for 2 hours at 4 °C with 1 µg of rabbit antibodies per 750 µl lysate, using no antibody control or irrelevant pre-immune rabbit serum control as indicated per each experiment, utilizing continuous mixing. Immune complexes were then captured by incubation with Protein G beads for 90 min at 4°C, with continuous mixing. The beads were washed 3 times with 1 ml IP lysis buffer and once with 200 µl IP buffer before resuspending in 30 µl SDS-PAGE loading buffer. Samples were boiled for 5 min to dissociate complexes from the beads, centrifuged to pellet the beads and processed for western blotting by resolving on a 6% polyacrylamide gel as described above.

## **2.5 Virology methods**

### **2.5.1 General virus handling and infection assays**

#### *2.5.1.1 Propagation and titration of the viral stocks*

All HSV-1 viral stocks were provided by Anne Orr (MRC Virology Unit). Virus was propagated on BHK cells and harvested as cell-released or cell-associated virus stocks. Viral stocks were titrated on U2OS cells because of their property to complement ICP0-null mutant HSV-1 (Yao & Schaffer, 1995). For HSV-1 titration, cells were stained for the appearance of the plaques with Giemsa stain 48 hours post infection.

All HCMV stocks were propagated and provided by Chris Preston. HCMV strains were titrated on human fibroblasts cell line HFFF2. Propagation of ADSubUL82 was previously described (Bresnahan & Shenk, 2000).

#### *2.5.1.2 Standard approaches for viral infection assays*

The following method for infection of the cells seeded into appropriate tissue culture dishes was used throughout the experiments, unless otherwise specified for particular HCMV infection assays.

In order to infect the cells seeded into appropriate volume, firstly the required amount of virus to be used was determined according to the required multiplicity of infection (MOI), based on the number of cells seeded into the dish on the day prior to infection procedures. MOI is specified for each individual experiment. Media was removed from the cells so that a small amount of media was left to form a meniscus in the dish when tilted. This was conditioned media and was stored at 37 °C until further use. Appropriate amount of virus was added onto the cells to fully cover the cell monolayer, virus was allowed to adsorb at 37 °C for 1 hour with gentle agitation every 5-7 min. After 1 hour of virus adsorption, the cells were overlaid with conditioned media with or without 1% human serum, as detailed.

## **2.5.2 Viral experimental assays**

### ***2.5.2.1 Establishing HSV-1 plaque formation efficiency using blue plaque assays***

Cells in 24-well plates were infected with sequential three-fold dilutions of the wt and ICP0 null mutant viruses containing a CMV*lacZ* insertion cassette. Starting dilutions for the stocks of *in1863* and *dl1403/CMVlacZ* were  $10^{-4}$  and  $10^{-2}$ , respectively, with the stocks having been diluted to titres of approximately  $1 \times 10^9$  pfu/ml as determined on U2OS cells. After adsorption of the virus (as described above) and overlay with conditioned media supplied with 1% human serum in order to neutralise cell released virus, plaque formation by cell-to-cell spread was allowed to proceed over approximately 24-26 hour period. The cells were washed once in PBS and fixed in 1% (v/v) glutaraldehyde in PBS solution by incubating at room temperature for 20-30 min. Meanwhile, X-gal solution was prepared (see Section 2.1.6) and warmed to 37 °C. Fixed cells were washed twice in PBS. Prior to adding the solution onto cells, it was filtered, then 0.5 ml of the solution was added onto cells and the plates were incubated at 37 °C for at least 1 hour to allow  $\beta$ -galactosidase staining to develop. The plates were then washed and dried.

Analysis of the plaque formation efficiency included determining the plaque numbers in the control cell line first (such as normal HepaRG or HALL cells) and calculating the relative number of plaques obtained with the same dilution of virus in the other cell lines tested. The averages were determined based on the different sets of dilutions and generally on three to four independent experiments (as specified).

### ***2.5.2.2 Immunofluorescence analysis of developing HSV-1 plaques***

Cells seeded onto coverslips were infected with either 17+ or *dl1403* at the indicated MOIs. Virus was adsorbed as described and overlaid with conditioned media containing 1% human serum, in order to neutralise cell-released virus and to only allow cell-to-cell spread. After plaques were allowed to develop over 18-24 hour period (or overnight), cells were processed for immunofluorescence as described in section 2.3.2. Cells infected at the edge of a developing plaque were analysed for distribution of ND10 components and the viral transcription regulator ICP4, which binds to viral genomes (Pizer et al, 1991).

### ***2.5.2.3 Kinetics of HSV-1 protein expression***

For kinetics of viral protein expression, standard infection assays utilized HSV-1 strains 17+ and *dl1403*. Cells seeded into the wells of the 24-well plate were infected with the

virus at an appropriate MOI, as specified for each individual experiment. Virus was allowed to adsorb as described in section 2.5.1.2, and infected cells were overlaid with conditioned media. Samples were harvested at the indicated time points after adsorption of the virus (referred to as hours post infection) in SDS-PAGE loading buffer. Samples were either processed for Western blot analysis as described in section 2.4.1 or stored at -20 °C.

#### ***2.5.2.4 Assay of establishment of HSV-1 quiescence***

In order to analyse the efficiency of the establishment of HSV-1 quiescence, virus *in1374* was used. Cells, seeded into 24-well plates, were infected with *in1374* at an MOI of 5, virus was allowed to adsorb at 37 °C and overlaid with conditioned media. For determining the maximum potential of reactivation, cells were also co-infected with *tsK* virus at MOI 1. The cells were then transferred to a non-permissive temperature of 38.5 °C, and infection was allowed to proceed for approximately 16-18 hours (or overnight). The following day cells were stained for  $\beta$ -galactosidase expression with X-gal solution as described for blue plaque assays in section 2.5.2.1. Efficiency of establishment of quiescence was determined as the number of cells, expressing the marker gene  $\beta$ -galactosidase, which appeared blue following X-gal staining.

#### ***2.5.2.5 Fluorescence recovery after photobleaching***

Fluorescence recovery after photobleaching (FRAP) analysis was performed on HD-ED cells, expressing EYFP-hDaxx fusion protein. In order to set up cells for FRAP analysis, cells were seeded at a density  $5 \times 10^5$  cells per dish into 35 mm dishes with a hole in the bottom and a coverslip fixed to cover the hole. The following day cells were infected with *d11403* at MOI 1.2 and overlaid with conditioned media containing 1% human serum. Cells were washed once with DMEM, free of phenol red (Invitrogen) and kept in phenol red free DMEM for the length of the experiment. Dishes were placed into the live cell chamber of a Zeiss LSM 510META confocal microscope, with environmental control to provide an atmosphere adjusted to 37°C and 5% CO<sub>2</sub>. Mock infected and cells demonstrating clear redistribution of EYFP-hDaxx to foci associated with HSV-1 genomes were selected for analysis. ND10 foci (generally 3 per cell) were photobleached using 15 re-iterations of the 514 nm laser set at 100%. The region of interest was then scanned 20 times at 1.5 sec intervals to determine the speed of recovery. Control areas were unbleached ND10 dot and unbleached area within the nuclei. Data was calculated as percentages of fluorescence recovery using Excel. Data was averaged from two

independent experiments, each analysing between 20 and 25 ND10 foci from mock infected cells or those associated with incoming *dl1403* genomes.

#### ***2.5.2.6 Phosphorylation analysis of HSV-1 infected cell lysates***

Cells seeded into 24-well plates were infected the following day with 17+ and *dl1403* at MOI 5 and 10. Cells were harvested in 70  $\mu$ l IP lysis buffer, without EDTA, at the indicated time points post infection. Lysates were incubated on ice for 15 min and lysed by bath sonication as described above. Reactions were set up using  $\lambda$ -phosphatase (New England Biolabs) according to the manufacturer's instructions. For 20  $\mu$ l of cell lysate, 400 units of  $\lambda$ -phosphatase was used. Reactions were supplemented with 1 $\times$  phosphatase buffer, 2 mM MnCl<sub>2</sub> and made up to the total volume of 30  $\mu$ l with IP buffer. After incubation treatment for 1 hour at 30 °C, samples were mixed with 20  $\mu$ l of SDS-PAGE loading buffer, boiled for 5 min and processed for western blot analysis as described above. 25  $\mu$ l of the reaction was loaded onto a gel and the remaining aliquots stored at -20°C.

#### ***2.5.2.7 Analysis of HCMV replication efficiency***

HF cells on 13 mm glass coverslips were infected with AD169 or ADSubUL82 as follows. 100  $\mu$ l of the virus dilution was added directly onto a coverslip placed onto a lid of the 24-well plate, with cell side facing upwards, and virus was adsorbed at 37 °C without shaking. Coverslips were then transferred into a well of a 24-well plate filled with 1 ml of medium. The infection was allowed to proceed for up to 11 days. Because of the EGFP cassette inserted in place of deleted UL82 gene in mutant virus ADSubUL82, the plaques could be visualised by green fluorescence using the 488 nm laser. Supernatants of the cell released virus were harvested and their titres determined by Chris Preston on HFFF2 human fibroblast cells, by infecting the coverslips and processing them for immunofluorescence (as described above). Titres were determined as IE1-positive units using anti-IE1 antibody staining.

## **3 Characterisation of ATRX and hDaxx in Cell Culture**

### **3.1 Introduction**

In the main introduction to this thesis (Chapter 1) the topic of anti-viral activities of ND10 proteins has been discussed. To summarise the key points, during herpesvirus infection, viral transcriptional activators such as HCMV tegument protein pp71 and HSV-1 IE protein ICP0 localise to ND10 very early after infection which, in the case of ICP0, results in disintegration of these structures (Everett & Maul, 1994; Everett & Zafiropoulos, 2004; Ishov et al, 2002; Marshall et al, 2002; Maul et al, 1993). In the absence of these viral transactivators, replication of both HSV-1 and HCMV is considerably less efficient in restrictive cell lines (Bresnahan & Shenk, 2000; Everett et al, 2004).

The general hypothesis that drives the work of this thesis states that ND10 proteins contribute to the immediate anti-viral intrinsic cell defence responses, which take place as soon as the viral genomes are released into the cell nucleus. Experimental investigation of this hypothesis using restrictive cell lines by several research groups, referenced above, noted that ICP0 and pp71 counteract these mechanisms. Based on the available data so far, it follows that ND10 protein factors collectively contribute, either separately or as a part of a complex, to the repression mechanism that occurs in the absence of the viral transcriptional activators. In support of this statement, PML has been identified as the component of cellular intrinsic resistance to both HCMV and HSV-1 (Everett et al, 2006; Tavalai et al, 2006). In addition, Sp100 and hDaxx have been also found to contribute to intrinsic resistance against HSV-1 and HCMV infection, respectively, by independent groups (Cantrell & Bresnahan, 2006; Everett et al, 2008; Kyratsous & Silverstein, 2009; Preston & Nicholl, 2006; Saffert & Kalejta, 2006; Tavalai et al, 2008). These findings have instigated further investigation into ND10-localised regulators of viral infection. The considerable evidence of the role of chromatin in the regulation of viral infection has stimulated a further interest into investigating chromatin-associated proteins that localise to ND10, such as ATRX and hDaxx.

Transcriptional repressor hDaxx binds several transcriptional regulators, thereby influencing transcription of its target genes (Chang et al, 2005; Hollenbach et al, 2002; Holmstrom et al, 2008; Ishov et al, 1999; Ryo et al, 2007), and in some reports has been shown to directly repress gene promoters (Morozov et al, 2008). One of the hDaxx-interacting partners is ATRX (Ishov et al, 2004; Tang et al, 2004; Xue et al, 2003). The

key characteristics of ATRX are that it includes motifs related to chromatin-remodelling enzymes of the SWI/SNF family of ATP-dependent helicases, that it localises to ND10 (Ishov et al, 2004; Tang et al, 2004), and that it interacts with chromatin-associated proteins MeCP2 and HP1 (Baumann et al, 2008; De La Fuente et al, 2004; Le Douarin et al, 1996; Lechner et al, 2005; Nan et al, 2007). Since ATRX and hDaxx constitute a complex with chromatin-remodelling activities, which are likely to be repressive (Tang et al, 2004; Xue et al, 2003), it was of interest to investigate whether the two proteins contribute to the cellular intrinsic defence mechanism against HSV-1 and HCMV infection.

The present chapter summarises the preliminary work conducted for the purpose of: (a) analysing ND10 components, with the focus on ATRX and hDaxx in different cell lines; (b) generating cell lines depleted of endogenous ATRX and hDaxx, as tools for studying the functions of the two proteins, and (c) re-constitution of wild-type or mutant hDaxx expression in hDaxx depleted cells in order to study its functions in HSV-1 infection in more detail. The cell lines characterised in this Chapter have been used throughout the investigation into the roles of ATRX and hDaxx in HSV-1 and HCMV infection, and the results are described in Chapters 4 and 5.

## **3.2 Results**

### **3.2.1 Characterisation of ND10 protein expression in various cell lines**

#### ***3.2.1.1 Analysis of ND10 protein expression in human cell lines by western blot***

Differences in the defect in plaque-forming efficiency of ICP0-null mutant HSV-1 range between 1000- to 500-fold in restrictive cell lines such as HFs and HepaRG, respectively, to around a 10-fold defect in transformed cell lines such as HeLa. Interestingly, there is no such replication defect in U2OS cells that are known to complement ICP0-null mutant HSV-1 by a mechanism that remains unidentified (Yao & Schaffer, 1995). It is possible that cell type differences in expression or function of ND10-related intrinsic resistance proteins may contribute to variations in replication efficiency of the mutant virus. In order to test this hypothesis, expression levels of a number of ND10 proteins in different cell lines were analysed and compared (Figure 3.1).

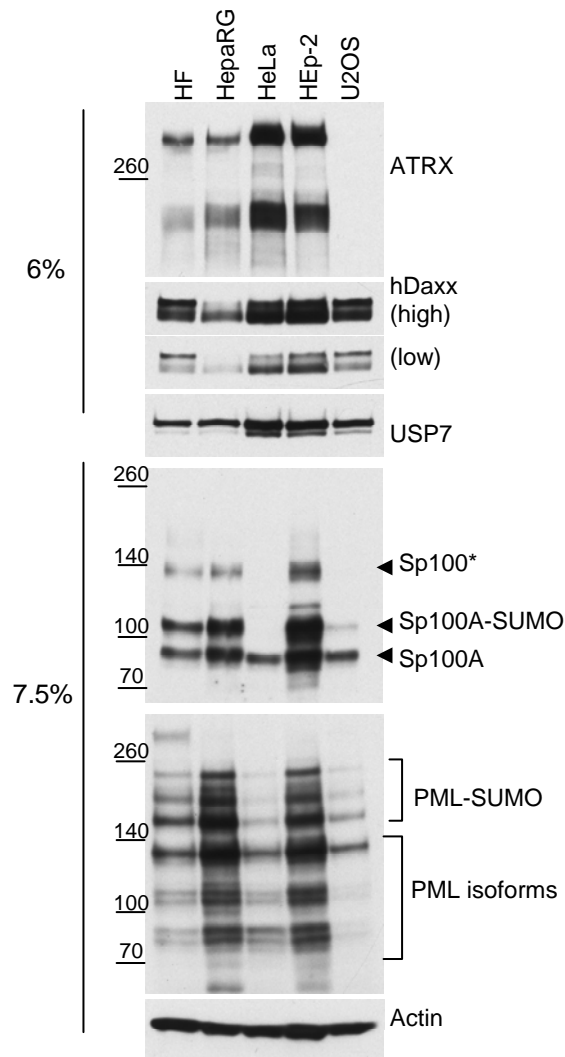


**Figure 3.1 Analysis of endogenous expression of ND10 proteins in cultured cell lines**

Samples of the indicated cells were harvested and whole cells extracts derived from approximately  $3 \times 10^4$  cells were loaded onto 7.5% or 6% polyacrylamide gels. The antibodies used for western blot detection were anti-PML 5E10, anti-ATRAX 39F, anti-Daxx D7810, anti-Sp100 SpGH, anti-actin AC-40, and anti-USP7 BL851. HDaxx blots designated as ‘high’ and ‘low’ represent different exposure times of the membrane to photographic film. USP7 and actin were used as loading controls for 6% and 7.5% gels, respectively. The differences in USP7 expression were reproducible.

Equal numbers of HF, HepaRG, HEP-2, HeLa and U2OS cells were seeded for a western blot analysis. The relative abundance of the analysed proteins was different amongst the five cell lines (Figure 3.1), although only minor variations in the cell extract amounts were seen according to the actin blot, which served as a loading control. Due to the differences in cell growth rates between the cell lines, the resulting numbers of cells harvested for analysis the day following seeding might be varying. These differences however were minor and could not account for differential protein expression in the cell lines analysed here.

As discussed in the introductory Chapter 1 (Section 1.8.2) hDaxx is a phosphoprotein, and its phosphorylation at particular sites can determine the fate of hDaxx in the cell (Ryo et al, 2007; Song & Lee, 2004). On a western blot, endogenous hDaxx appears as a double band corresponding to its phosphorylated forms (Figure 3.1). Expression of hDaxx was fairly uniform amongst this set of cells, with higher levels seen in highly transformed cell lines such as HeLa, Hep-2 and U2OS. This pattern of hDaxx migration is consistent with previous reports (Ecsedy et al, 2003). However, the detection of the phosphorylated band of hDaxx in HepaRG cells was not consistent throughout the experiments. This could be due to number of reasons, including cell-cycle dependent variation in phosphorylation levels (Ishov et al, 2004) and the efficiency of phospho-band detection by the available antibody. hDaxx phosphorylation levels, detected in other assays, were higher. Phosphatase treatment assays have confirmed that the slower-migrating hDaxx band was indeed due to phosphorylation (see Chapter 5).

ATRX was expressed in HF, HepaRG, HeLa and HEp-2 cells, although in the latter two cell lines it was expressed at similarly higher levels than in the former two cell lines. The appearance of the two bands corresponding to major ATRX isoforms of approximately 280 kDa and ATRXt (a truncated ATRX isoform) was consistent with previously published work (Berube et al, 2000; Garrick et al, 2004). Strikingly, ATRX was not expressed in U2OS cells. This, however, can by no means explain the efficient replication of ICP0-null mutant virus replication in U2OS cells, since ATRX is expressed normally in HEp-2 and 293T cells, in which the ICP0-null mutant defect is also relatively minor; (R.D. Everett group, unpublished observations). USP7 was normally used as a loading control for 6% polyacrylamide gels, however, its expression pattern was not uniform amongst the cell lines. Since this pattern was reproducible, this was not attributed to loading inaccuracies and suggested cell-type specific differences in USP7 expression as well.

Both Sp100 and PML were expressed in all of the cell lines tested, demonstrating the patterns of migration consistent with previous observations (Condemine et al, 2006; Sternsdorf et al, 1999) (Figure 3.1). Both proteins are apparently expressed at higher levels in HepaRG and HEp-2 cells, while PML is least well expressed in HeLa and U2OS cells. The reduced level of expression of PML in these cells appears to correlate with reduced expression and SUMO-modification of Sp100 (Figure 3.1). Interestingly, normal SUMO-modification of Sp100 is dependent on PML (Everett et al, 2008; Everett et al, 2006). These observations imply that cell-type specific differences in the expression of different

ND10 proteins may contribute to differences in permissiveness to viral infection amongst the different cell types.

### ***3.2.1.2 Analysis of ATRX localisation by immunofluorescence***

Whereas hDaxx is ubiquitously expressed throughout different tissues and is generally found at ND10 (Chen et al, 2009), ATRX protein is less studied although its ND10 residency has been clearly observed in previous studies (Ishov et al, 2004; Tang et al, 2004; Xue et al, 2003). As one of the starting points to investigating the role of ATRX in viral infection, its nuclear localisation has been compared amongst some of the commonly used laboratory cell lines (Figure 3.2). In HF, HEp-2 and HepaRG cells (Figure 3.2, panels A, B and C, respectively), as well as in a number of additional cell lines analysed (HeLa and 293T; data not shown) ATRX showed clear ND10 localisation by co-localising with PML. ATRX localisation to heterochromatic foci in mouse cells was previously reported (Ishov et al, 2004). Therefore, nuclear diffuse staining pattern that was observed here was likely to represent association of ATRX with chromatin. The intensity of nuclear diffuse ATRX staining was varied between the cell types and between the cells within the same cell monolayer to some extent, suggesting the cell cycle differences in ATRX chromatin localisation. Thus, visual scanning of stained coverslips revealed that in HepaRG cells ATRX nuclear staining was more diffuse than that in HFs. Consistent with the western blot analysis, no ATRX signal was observed in U2OS cells (Figure 3.2, panel D). These observations propose a conserved ATRX role amongst the analysed set of cell lines, and demonstrate that ATRX is not essential for cell survival in culture.

### **3.2.2 Generation of ATRX- and hDaxx-depleted cell lines by RNA interference**

A common way to analyse the role of a specific protein in viral infection, and an approach used by our and other groups, is to use RNAi to generate cell lines depleted of the protein of interest (Everett et al, 2008; Everett et al, 2006). Therefore, ATRX and hDaxx depleted cell lines have been constructed, where the levels of the individual proteins have been severely suppressed by stable expression of shRNA molecules targeting endogenously expressed ATRX or hDaxx. The following section describes the construction and analysis of the resulting cell lines.

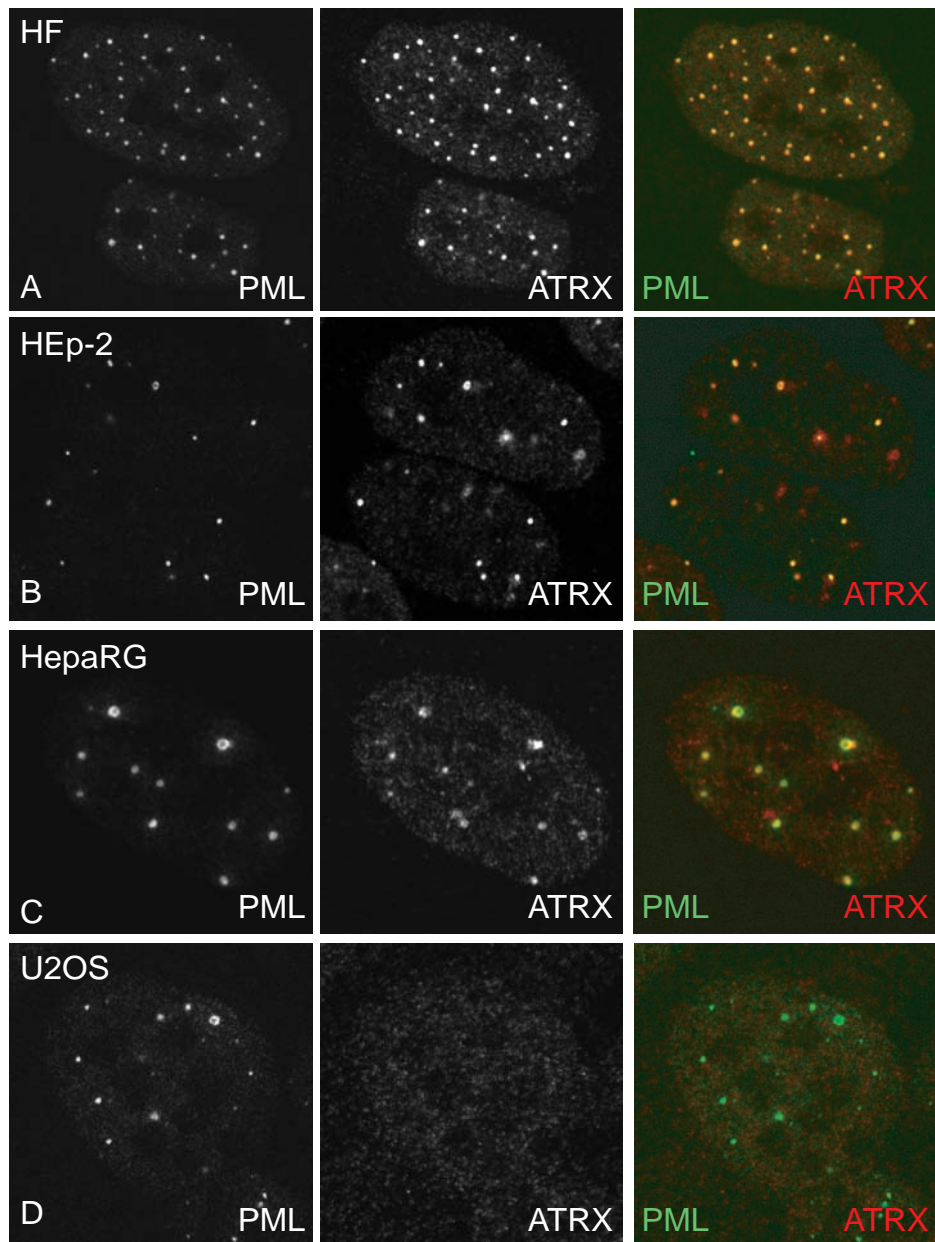


**Figure 3.2 ATRX localisation in different cell lines**

Cells on coverslips were fixed in formaldehyde solution and stained with anti-PML 5E10 and anti-ATR X H300 antibodies. Secondary antibodies were anti-mouse FITC-conjugated and anti-rabbit Cy3-conjugated (panels A, B and D) or anti-rabbit AlexaFluor-conjugated 555 (panel C).

### 3.2.2.1 Characterisation of ATRX-depleted cell lines

For ATRX depletion, primary HF and HepaRG were the cell lines of choice. In order to produce lentiviral stocks, HK-293T cells were transfected with plasmid pLKO-ShATR90 together with plasmids encoding for lentivirus components, as described in Chapter 2, Section 2.3.3. At 72 hours post transfection, the supernatants were harvested and used to transduce monolayers of HF or HepaRG cells. Cells were expanded after selecting with puromycin-containing media and maintained in this selection (see Chapter 2, Section 2.3.3.2). These cells were named HF-ShATR90 and HAA respectively. In order to determine the efficiency of ATRX protein knock-down in HFs,  $1 \times 10^5$  cells were seeded into a 24-well plate, transduced with the lentiviral stocks expressing shATR90, then wells were harvested for analysis by western blotting at increasing times after selection had been applied (Figure 3.3). ATRX expression levels were analysed in HF-ShATR90 cells in comparison to a control cell line (HF-ShGFP) that expresses an shRNA against EGFP. According to the data presented in Figure 3.3, successful ATRX depletion in HF-ShATR90 cells was observed from day 2 after applying lentiviral stocks, with subsequent reduction of ATRX to virtually undetectable levels by day 7. USP7 was used as a loading control, and as expected, its levels were slightly increased throughout the 7-day experiment.

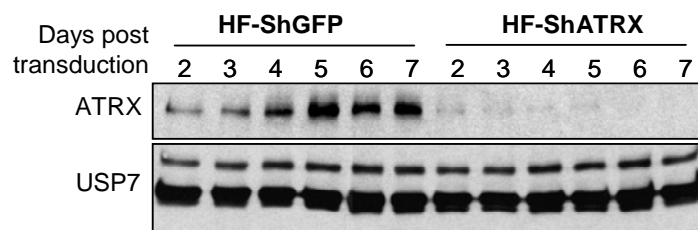


**Figure 3.3 Efficiency of ATRX depletion in human fibroblasts**

Cells were seeded into a 24-well plate at a density of  $1 \times 10^5$  cells per well and transduced with lentiviral stocks expressing either shGFP or shATR90 the following day. On day 1 post transduction, puromycin selection of  $2 \mu\text{g/ml}$  was added, which was reduced to  $1 \mu\text{g/ml}$  on day 2. Samples were harvested in SDS-PAGE loading buffer every 24 hours between days 2 and 7 post transduction. Samples were resolved on a 6% gel and membrane was probed with anti-ATR90 H300 antibody. USP7 (BL851) was a loading control.

The levels of ATRX depletion in HF-ShATRAX and HAA cells, produced on a larger scale, were confirmed by a western blot (Figure 3.4, A and B, respectively). Notably, stable ATRX knock-down was never achieved in either of the cell lines, because ATRX expression had a tendency to recover after a certain number of cell passes, and therefore ATRX depleted cells had to be re-generated on a regular basis.

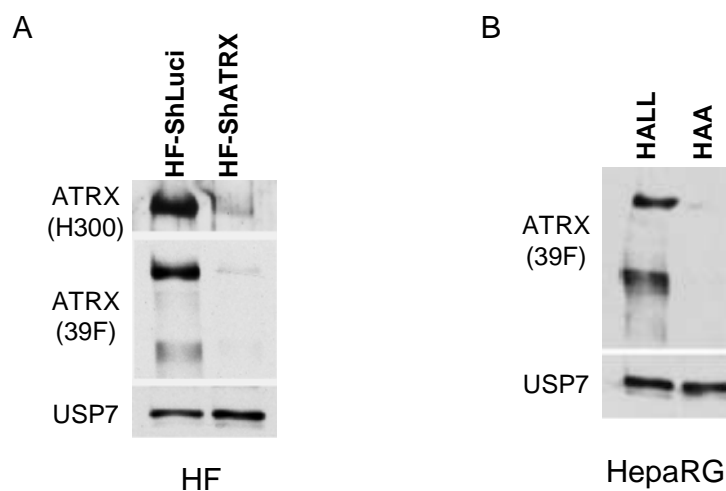


**Figure 3.4 Levels of ATRX depletion in cell lines**

HF (A) and HepaRG (B) were transduced with either ShLuci- or ShATRAX90-expressing lentiviral stocks. Knock-down of protein expression in the resulting cell lines was confirmed by western blot, (A) in HF-ShATRAX and (B) HAA cells. ATRX was detected with the indicated antibodies. USP7 was detected with BL851. Knock-down of major and truncated ATRX isoforms was achieved successfully in these cell lines.

Confocal immunofluorescence analysis of the ATRX-depleted cell lines was performed in order to confirm the efficiency of a knock-down and to analyse localisation of other ND10 proteins, such as the major ND10 component PML and the ATRX-interacting protein hDaxx. Figures 3.5 and 3.6 demonstrate that removal of ATRX from cells has not affected PML or hDaxx localisation significantly in either HF or HepaRG cells, respectively. However, depletion of ATRX in HepaRG cells (HAA) resulted in hDaxx being more nuclear diffuse in a higher proportion of cells than in control HALL cells (Figure 3.7), an effect not seen in HF-ShATRAX cells (data not shown). Overall, ATRX depletion did not result in significant effects on the localisation patterns of either hDaxx or PML.

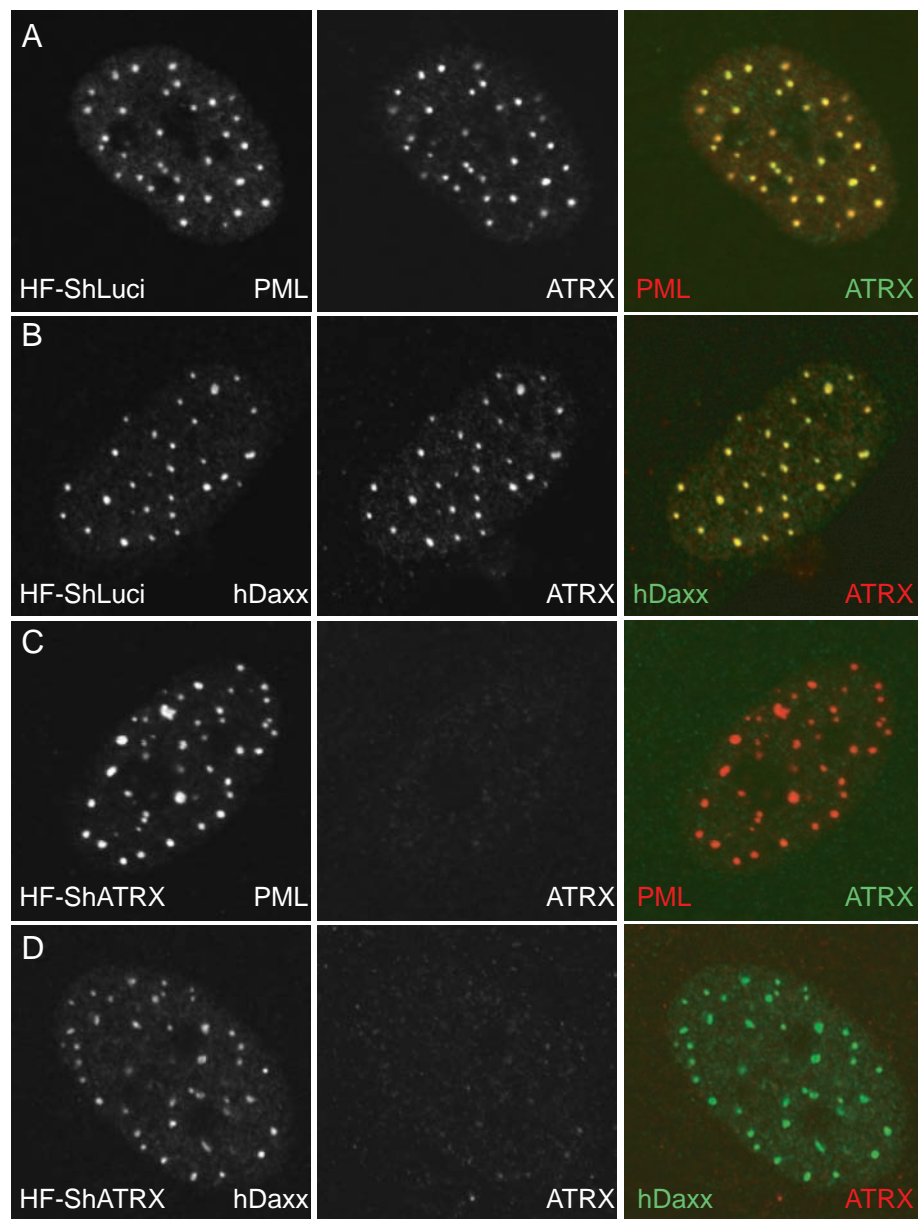


**Figure 3.5 The effects of depleting ATRX on the localization of ND10 proteins in human fibroblasts**

Control (HF-ShLuci) and ATRX-depleted (HF-ShATRX) cell cultures were analyzed by confocal immunofluorescence, using antibodies specific for PML (panels A and C - 5E10), ATRX (panels A and C - H300; panels B and D - 39F) or hDaxx (panels B and D - r1866). Secondary antibodies were anti-rabbit FITC-conjugated and anti-mouse Cy3-conjugated.

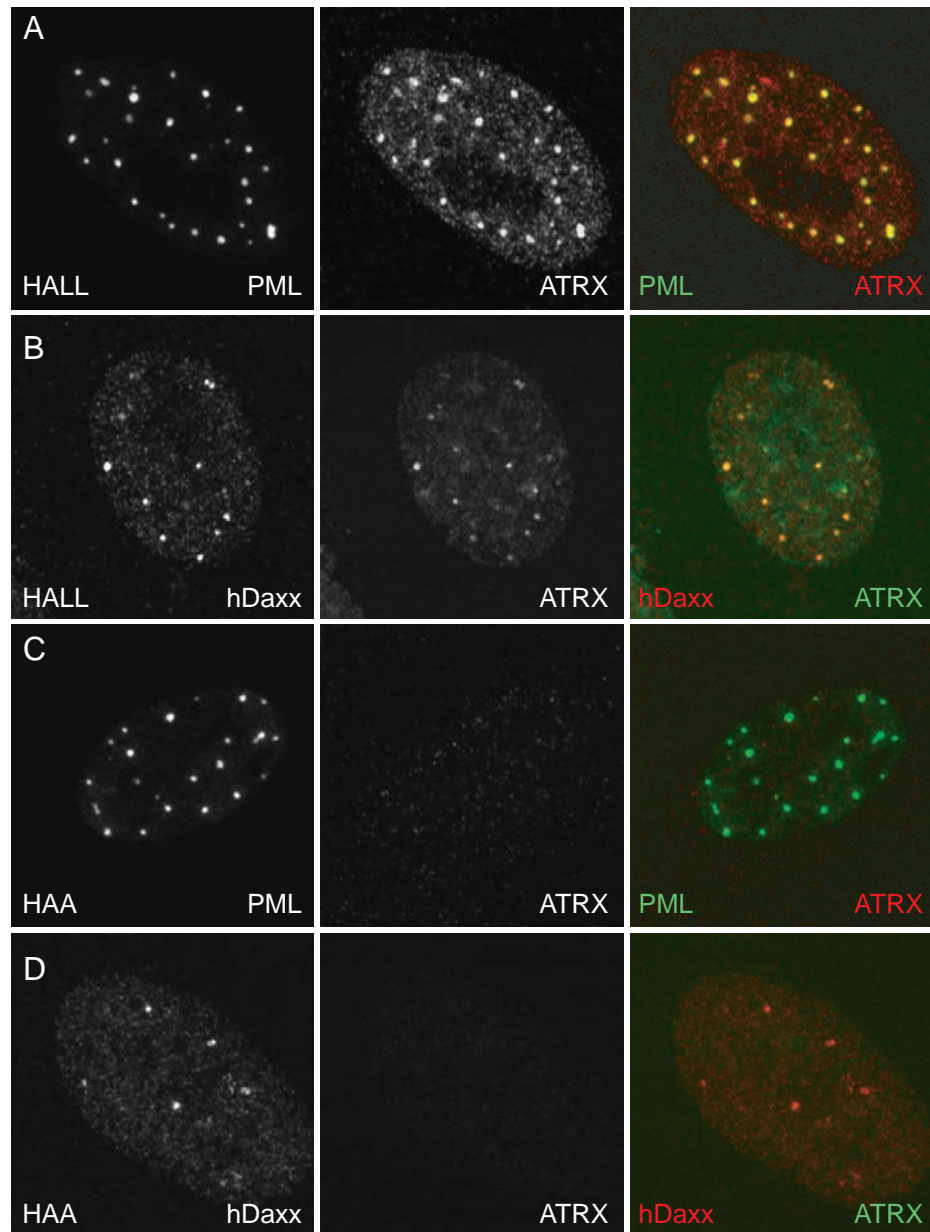


**Figure 3.6 The effects of depleting ATRX on the localisation of ND10 proteins in HepaRG cells** Control (HALL; panels A-B) and ATRX-depleted (HAA; panels C-D) cell cultures were analysed by confocal immunofluorescence, using antibodies specific for PML (panels A and C - 5E10), ATRX (panels A and C - H300; panels B and D - 39F) or hDaxx (panels B and D - 07-471). Secondary antibodies were anti-mouse FITC-conjugated and anti-rabbit AlexaFluor-conjugated 555.

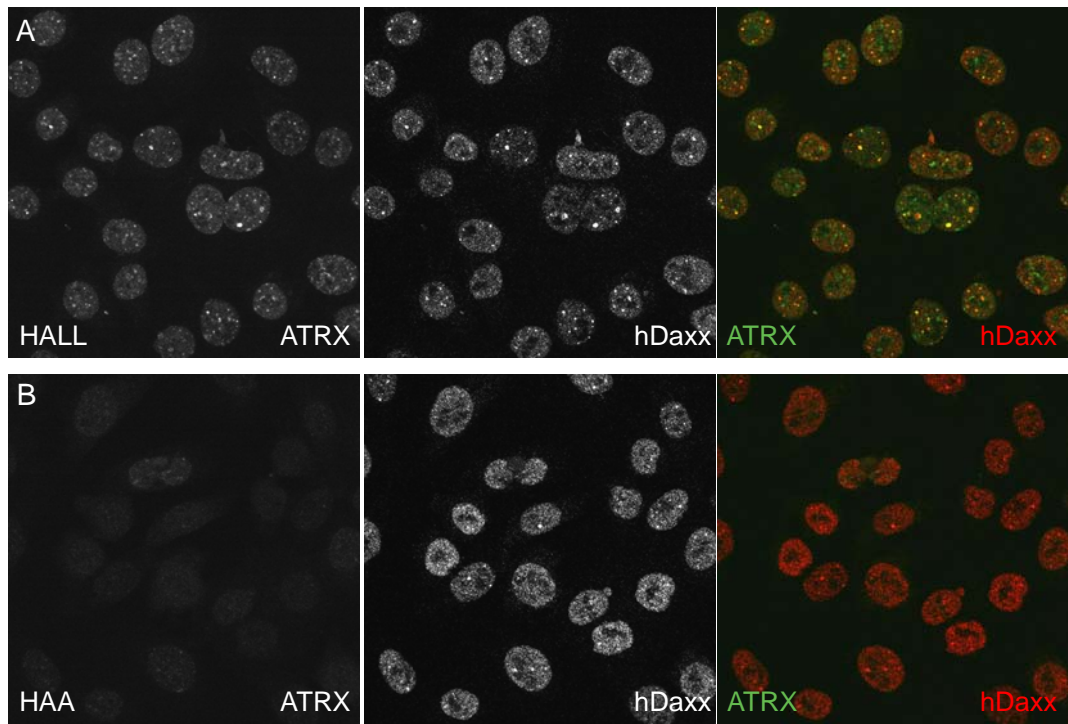


**Figure 3.7 Wide-field view of ATRX and hDaxx localisation in ATRX-depleted HepaRG cells**  
 HALL and HAA cells were seeded onto coverslips and processed for analysis by immunofluorescence. Fixed cells were probed with anti-ATRAX (39F) and anti-hDaxx (07-471) antibodies.

### 3.2.2.2 Characterisation of hDaxx-depleted cell lines

The approach for generating hDaxx-depleted cells was essentially the same as described above for ATRX-depleted cells. The following two figures summarise data obtained from immunofluorescence analysis of hDaxx-depleted HFs (Figure 3.8) and HepaRG cells (Figure 3.9). As evident from Figure 3.8 (HF-ShDaxx, panels C-D) and Figure 3.9 (HALD2, panel B), hDaxx depletion resulted in ATRX dispersal, whereas PML remained in punctate foci. This observation was consistent with previous reports (Ishov et al, 2004) and confirms the absolute requirement of wt hDaxx expression in ATRX targeting to ND10. Visual scan of the fixed cells using the confocal microscope revealed that the proportion of cells with undetectable levels of hDaxx was close to 100%, which indicated higher efficiency of depletion than of ATRX in ATRX-knock down cells (data not shown).

HF-ShDaxx cells were not used in further studies, therefore no further data with these cells will be presented. Figure 3.9 C shows levels of hDaxx knock-down in HALD2 determined by a western blot analysis. Stable knock-down of hDaxx in these cells was achieved to undetectable levels, as compared to endogenous hDaxx expression by naïve HepaRG and control HALL cells.

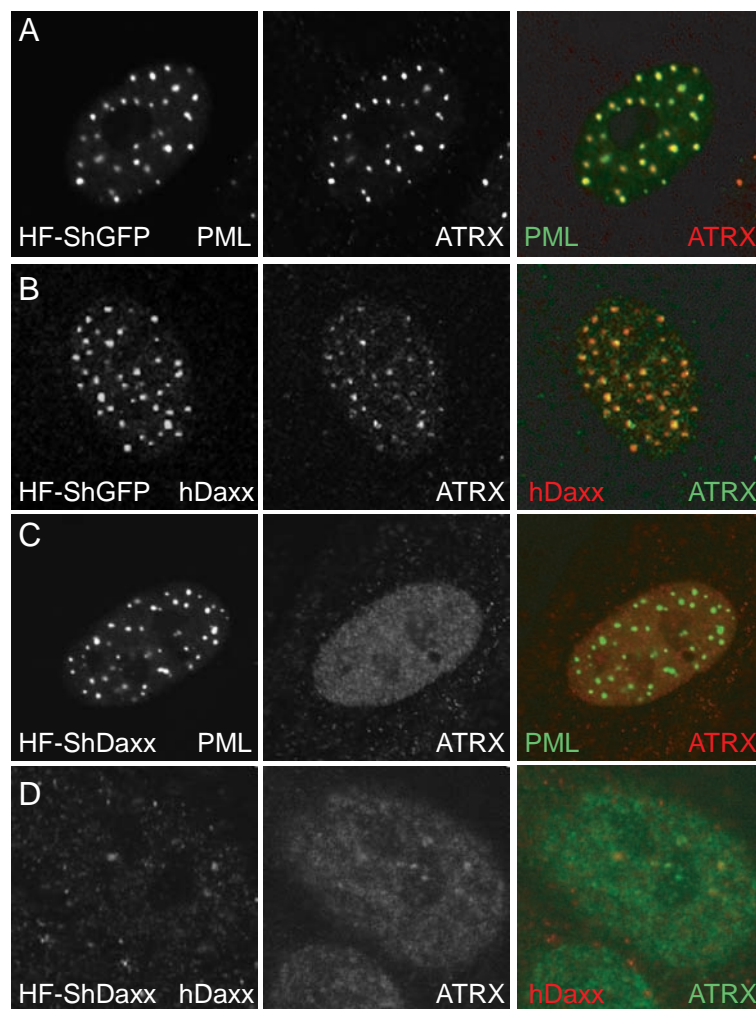


**Figure 3.8 hDaxx depletion in human fibroblasts**

HF-ShGFP and HF-ShDaxx cells were probed with anti-PML (5E10), anti-ATR<sub>X</sub> (panels A-B H300; panels C-D 39F) and anti-hDaxx (r1866) antibodies.

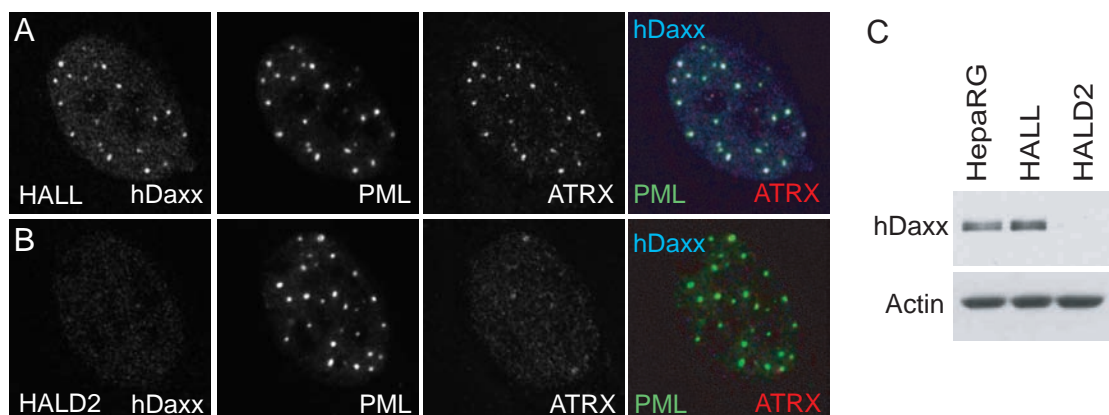


**Figure 3.9 ATR<sub>X</sub> is dispersed in hDaxx-depleted HepaRG cells**

A-B: Confocal immunofluorescence images demonstrating simultaneous detection by triple staining of hDaxx, ATR<sub>X</sub> and PML in HALL (A) and HALD2 (B) cells, using rabbit anti-Daxx (07-471), mouse anti-PML (5E10) and goat anti-ATR<sub>X</sub> (D19) antibodies. Secondary antibodies were anti-mouse FITC-conjugated, AlexaFluor-conjugated anti-rabbit 647 and anti-goat 555. C: Western blot analysis of hDaxx depletion in HepaRG cells. Cell extracts harvested from normal HepaRG, shLuci-expressing HALL and shDaxx-expressing HALD2 cells were resolved on a 7.5% polyacrylamide gel, and hDaxx expression was detected using D7810 antibody. Actin was a loading control.

### 3.2.3 Reconstitution of hDaxx expression in hDaxx-depleted cells

Given that hDaxx is required for ATRX targeting to ND10 but not *vice versa* (Figure 3.9), it is possible that hDaxx is required for ATRX functions at its target genes, and particularly at the viral genomes. Therefore, the interaction between ATRX and hDaxx was studied in more detail. Consistent with previously published reports that ATRX and hDaxx co-exist and function as a complex (Ishov et al, 2004; Tang et al, 2004; Xue et al, 2003), it was hypothesized that ATRX and hDaxx also may act as a complex on viral genomes. In order to investigate this issue, an approach for analysis of a specific protein function has been developed, whereby either the wild-type or mutant protein of interest is re-introduced back into depleted cells, using a lentiviral vector. Application of such an approach for studying hDaxx function is described below.

#### 3.2.3.1 Re-introduction of wild-type hDaxx into hDaxx-depleted cells

Construction of the pLNGY-hDaxx vector utilised for re-introduction of wt EYFP-hDaxx fusion protein back into hDaxx-depleted HepaRG cells is described in Chapter 2 (Section 2.2.4.3). In brief, hDaxx-depleted HepaRG cells HALD2 were transduced with lentiviral stocks derived from pLNGY-hDaxx. The resulting cell lines were maintained in media supplied with double antibiotic selection of 0.5 µg/ml puromycin and 0.5 mg/ml neomycin. The hDaxx cDNA within the pLNGY-hDaxx vector had been designed to contain silent mutations that conferred resistance to anti-hDaxx shRNA molecules expressed by the HALD2 cell line. The other key feature of this vector system is the use of a weak promoter (that of the HSV-1 glycoprotein gD gene) to avoid excessive expression of the reintroduced protein. The names of the various cell lines relevant to these experiments are presented in Table 2.6.

Control cell lines expressing EYFP only (using plasmid pLNGY) were also produced to account for any effects of EYFP expression in the subsequent assays. After expanding the HD-ED cell line along with the additional control cell lines (see Table 2.6) enrichment of EYFP-hDaxx positive cells was performed by FACS, allowing the isolation of cell populations in which close to 100% of the cells expressed the re-introduced proteins. The effect of re-introduction of EYFP-hDaxx fusion protein in these cell lines was confirmed by western blot and confocal immunofluorescence (Figures 3.10 and 3.11, respectively). Western blot analysis of the resulting cell lines using antibodies against hDaxx and EGFP indicated that the re-introduced hDaxx fusion protein was expressed at close to endogenous levels, with the EYFP-hDaxx band (approximately 140 kDa) corresponding to the size of

endogenous hDaxx plus the EYFP tag of approximately 25 kDa (Figure 3.10). Cell line HL-ED expressed both endogenous hDaxx and re-introduced EYFP-hDaxx, but was not used in any further experiments. Cell line HD-E (HepaRG cells expressing shDaxx2 and EYFP) was used here and in subsequent experiments as a control for the hDaxx knock-down phenotype.

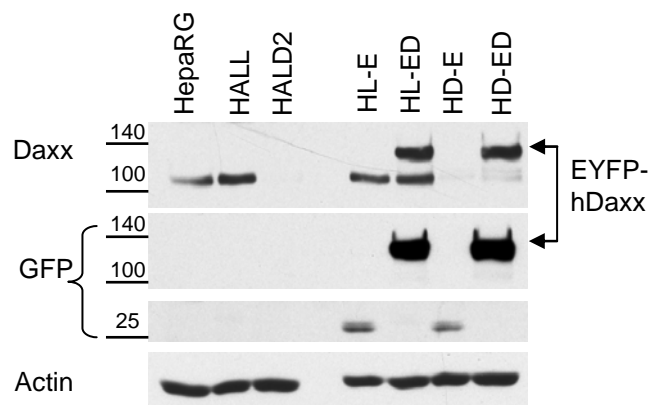


**Figure 3.10 Western blot analysis of hDaxx expression in cell lines expressing re-introduced EYFP-hDaxx**

Reintroduced fusion protein EYFP-hDaxx in HD-ED cells is indicated by arrow heads on the right. Antibodies used for detection of the proteins are indicated on the left: hDaxx and EYFP expression levels were detected by anti-hDaxx antibody (D7810) and anti-GFP antibody (ab290), respectively. The positions of relevant size markers are indicated.

Localisation of ND10 proteins in HD-ED cells was compared to that of naïve HepaRG and hDaxx-depleted EYFP-expressing HD-E cells, using essentially the same set of antibodies and image acquisition settings between the three cell lines to account for any background that may have resulted from the expression of EYFP tag (Figure 3.11). Panels A and D show representative images of naïve HepaRG cells, using the same set of antibodies. Analysis of HD-E cells revealed that the localisation patterns of PML and notably ATRX were consistent with those in HALD2 cells (Figure 3.9), indicating that EYFP expression alone did not affect these patterns (Figure 3.11, panels B and E). Analysis of HD-ED cells demonstrated that re-introduced wt EYFP-hDaxx co-localises with PML at ND10 (Figure 3.11, panel F). More importantly, the re-introduced EYFP-hDaxx relocates ATRX back into these structures (Figure 3.11, panel C), suggesting that the interaction between EYFP-hDaxx and ATRX was likely to occur in the same way as in non-transduced HepaRG cells between endogenous hDaxx and ATRX. Cells were also stained with anti-hDaxx antibody to confirm depletion of endogenous hDaxx and expression of the re-introduced fusion

protein (Figure 3.11, panel F). The intensity of EYFP-hDaxx fluorescence varied amongst the cells (Figure 3.11, panel G), and the intensity of ATRX staining in ND10 appeared to be proportional to that of the re-introduced EYFP-hDaxx. It is therefore likely that the functions of ATRX at ND10 may be regulated by the total amount of hDaxx expressed per cell.

---

**Figure 3.11 Re-introduced hDaxx targets ATRX back to ND10**

Immunofluorescence analysis of PML, ATRX and hDaxx distribution in HepaRG (panels A and D), hDaxx-depleted HD-E (panels B and E) and EYFP-hDaxx re-introduced HD-ED (panels C and F) cells. Cells on coverslips were co-stained for PML (r8) and ATRX (39F) (A-C) or PML (5E10) and hDaxx (07-471) (D-F). Secondary antibodies were anti-rabbit Cy5 (blue) and anti-mouse Alexa 555 (red). Panel G: Cells were stained with anti-ATRX antibody (H300) only and the distribution of EYFP-hDaxx positive cells and ATRX localisation was assessed by taking a wide-field image. Green fluorescence resulted from autofluorescence of the EYFP tag.

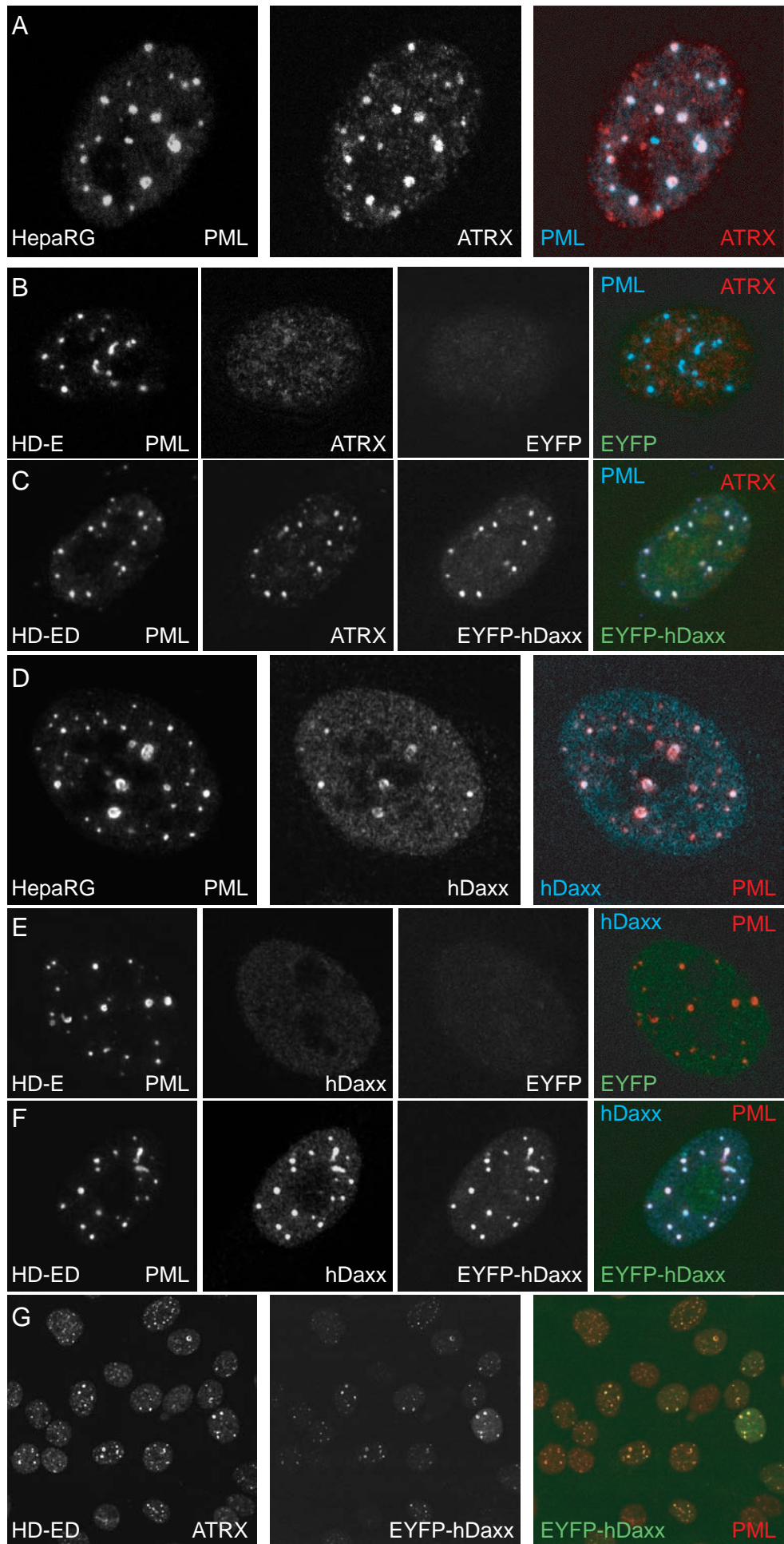


Figure 3.11 - Legend on the previous page.

### *3.2.3.2 Deletion of the hDaxx ATRX-interacting region and disruption of the ATRX/hDaxx complex*

Based on the system described in the previous section, it was convenient to introduce a deletion of ATRX-interacting domain PAH1 into hDaxx. The intention was to disrupt ATRX/hDaxx complex and analyse the consequence of this on HSV-1 infection (see Chapter 5). Hence, generation of the cell line expressing EYFP-hDaxx $\Delta$ PAH is described further.

Two PAH domains are adjacent to each other within the N-terminal portion of hDaxx, of which the first one is essential for interaction with ATRX (Tang et al, 2004); and Figure 3.12, A). PAH1 spans amino acids 66 to 108 of hDaxx protein sequence, a region encoded by 129 bp within the 5' region of the coding sequence. Using a PCR-mediated splicing mutagenesis approach, a region of 219 bp and a total of 73 amino acids that includes the PAH1 domain were deleted from the hDaxx coding sequence within the pLNGY-hDaxx lentiviral vector construct, as described in Chapter 2 (Section 2.2.4.4) and using the approach schematically represented in Figure 2.5. The resulting cell line, referred to as HD. $\Delta$ PAH, was produced using lentiviral transduction. The EYFP-hDaxx $\Delta$ PAH1 insert, which was cloned into a pLKO backbone vector, is illustrated on Figure 3.12 A, in comparison with the wt hDaxx and EYFP-hDaxx constructs. Having established the cell line after initial transduction with lentiviruses made from pLNGY-hDaxx $\Delta$ PAH, enrichment of EYFP-hDaxx. $\Delta$ PAH expressing cells was achieved by FACS, and the cell line was maintained in media supplemented with appropriate concentrations of puromycin and neomycin.

Expression of the EYFP-hDaxx $\Delta$ PAH in the resulting cell line was confirmed by western blotting (Figure 3.12, B), in comparison to non-transduced HepaRG, control HALL, hDaxx-depleted HD-E and wt hDaxx re-introduced HD-ED cells. Again, levels of EYFP-hDaxx $\Delta$ PAH were close to endogenous and similar to those obtained in cells with the re-introduced wt EYFP-hDaxx fusion protein. The band corresponding to EYFP-hDaxx $\Delta$ PAH migrated faster than that of EYFP-hDaxx, confirming the deletion of the fragment (73 amino acids) from the protein sequence.

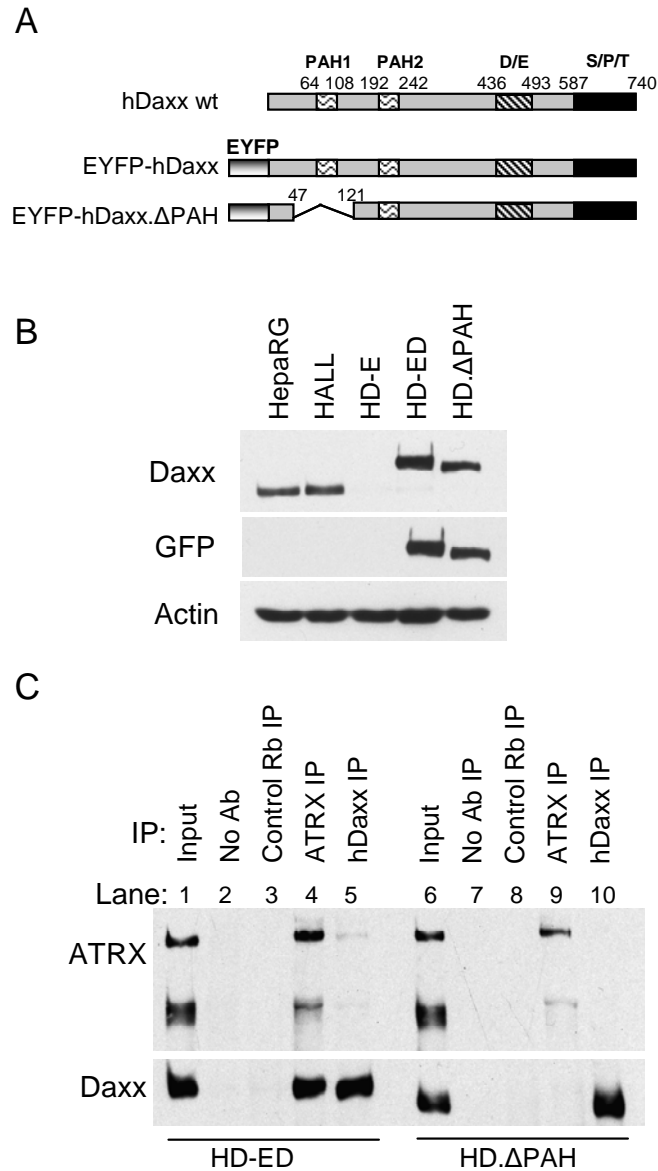


**Figure 3.12 Deletion of the ATRX interaction domain of hDaxx**

A: Schematic representation of wt hDaxx (adapted from (Yeung et al, 2008)), the EYFP-hDaxx construct and the EYFP-Daxx $\Delta$ PAH mutant, from which amino acids 48-120 spanning the ATRX interacting domain PAH1 were removed by PCR-based splicing mutagenesis. PAH, paired amphipatic helices; D/E, Asp/Glu-rich motif; S/P/T, Ser/Pro/Thr-rich domain. B: Western blot analysis of expression of hDaxx proteins in HepaRG, HALL, HD-E, HD-ED and HD. $\Delta$ PAH cells. The membrane was probed with the indicated antibodies. Samples were resolved on a 7.5% polyacrylamide gel. C: Immunoprecipitation analysis of ATRX and hDaxx interaction in HD-ED cells and HD. $\Delta$ PAH cells. Lanes 1 and 6 represent 2.5% input of the total extract sample incubated in each immunoprecipitation reaction. HD-ED and HD. $\Delta$ PAH cells extracts were immunoprecipitated with either anti-ATRX (antibody H300, lanes 4 and 9), anti-hDaxx (antibody 07-471, lanes 5 and 10), control rabbit serum 201 raised against USP7 (lanes 3 and 8) or no antibody (lanes 2 and 7). Samples were analysed on a 6% polyacrylamide gel and probed with anti-ATRX 39F and anti-hDaxx D7810 antibodies.

In order to confirm that the interaction between ATRX and hDaxx had indeed been eliminated, co-immunoprecipitation (CoIP) assays were performed in HD-ED and HD. $\Delta$ PAH cells (Figure 3.12, C). Prior to the experiment, the solubility of the two proteins was confirmed by testing the appropriate buffers in non-transduced HepaRG cells (data not shown). The buffer conditions were designed on the basis of previously published work (Tang et al, 2004), with some modifications. As evident from Figure 3.12 C, bands corresponding to both ATRX and hDaxx were detected in immune precipitates prepared from extracts of HD-ED cells using either anti-ATRX or anti-Daxx antibodies, respectively (Figure 3.12 C, lanes 4 and 5), confirming the interaction between the two proteins. The anti-Daxx antibody failed to work under present immunoprecipitation conditions as efficiently as the anti-ATRX antibody. The relatively low level intensity of the ATRX band in the anti-Daxx IP lane (Figure 3.12 C, lane 5) was consistent between independent experiments. The reciprocal co-immune precipitation was not observed when extracts from HD. $\Delta$ PAH were used, although both proteins were precipitated independently by their respective antibodies (Figure 3.12 C, lanes 9 and 10). This result was reproducible and indicates that the interaction between ATRX and hDaxx has been abolished in HD. $\Delta$ PAH cells. An anti-USP7 rabbit serum was used as an irrelevant antibody control in CoIP reactions (lanes 3 and 8). An interaction between hDaxx and USP7 reported previously (Tang et al, 2006) was not detected in these CoIP assays, possibly due to different cell lysis conditions.

Immunofluorescence analysis of HD. $\Delta$ PAH cells (Figure 3.13, panels A-C) revealed that the ATRX interaction domain of hDaxx is required for ATRX localisation to ND10 consistent with previous reports, in which deletions within the N-terminal portion of hDaxx were conducted (Ishov et al, 2004; Tang et al, 2004). In cells expressing the highest levels of hDaxx. $\Delta$ PAH, however, weak localisation of ATRX in ND10 was noted (compare panels A and B of Figure 3.13). This could occur due to residual interaction of ATRX *via* PAH2, which was proposed (Tang et al, 2004). The possibility of signal overlap was eliminated by carefully adjusting image capture settings prior to taking an image. Interestingly, EYFP-hDaxx $\Delta$ PAH was still co-localised with PML at ND10 (Figure 3.13 C), most likely due to its C-terminal SUMO-interaction domain responsible for its interaction with SUMO-modified PML (Ishov et al, 1999). These observations confirmed that the interaction between ATRX and hDaxx is not essential for the ability of hDaxx to localise to ND10, but it is required for ATRX targeting to ND10.

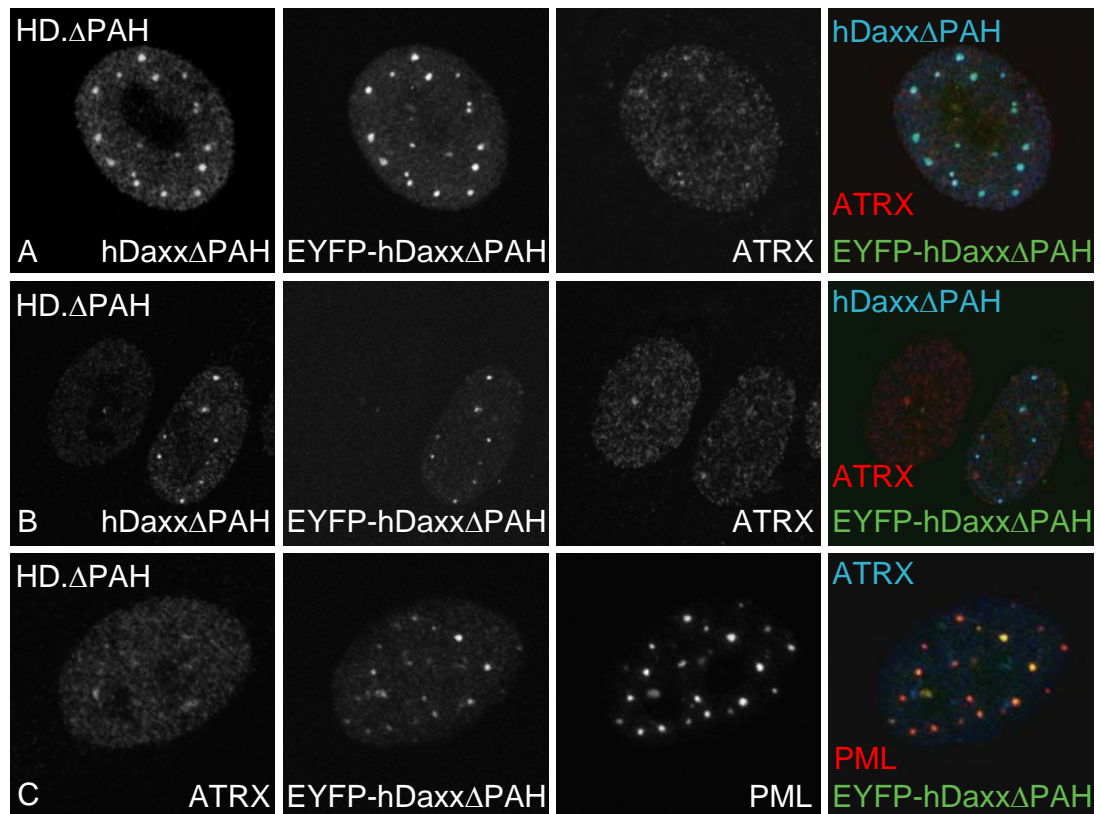


**Figure 3.13 The requirement of hDaxx ATRX-interaction domain for ATRX targeting to ND10**

Panels A-B: Cells fixed on coverslips were stained with anti-ATRX (39F) and anti-Daxx (07-471) antibodies. Representative cells with higher (A) and lower (B) EYFP-hDaxxΔPAH expression are shown. Panel C: Cells were stained with anti-ATRX (H300) and anti-PML (5E10) antibodies. Secondary antibodies were anti-mouse AlexaFluor-conjugated 555 and anti-rabbit Cy5 conjugated. EYFP signal resulted from autofluorescence. hDaxxΔPAH indicates re-introduced EYFP-hDaxxΔPAH detected with the anti-hDaxx antibody 07-471.

### 3.2.3.3 Mutagenesis of hDaxx SUMO-interaction motif

The ability of hDaxx to interact with the SUMO-modified proteins *via* its SUMO-interaction motif (SIM) is important for repressor activities on its target genes (Ishov et al, 1999; Lin et al, 2006; Shih et al, 2007). HDaxx interacts with PML also *via* its SIM, and this interaction is required for hDaxx localisation to ND10 (Ishov et al, 1999). In order to assess the requirement of hDaxx to interact with PML as well as with other SUMO-modified proteins during viral infection (see Chapter 5), the hDaxx SIM was mutated so that the amino-acid residues known to be conserved amongst other SIMs (Song et al, 2004) were changed (as described in Chapter 2, Section 2.2.4.6). PCR was performed in order to introduce mutations at several codons by site-directed mutagenesis, and the final pLNGY-hDaxxMSIM construct was produced using the same cloning procedures as for pLNGY-hDaxx. The cell lines transduced with lentiviral stocks expressing EYFP-hDaxxMSIM were sorted by FACS. The resulting cell line, referred to as HD.MSIM, was analysed by western blotting and immunofluorescence (Figure 3.14). As with the other hDaxx proteins, the EYFP-hDaxxMSIM fusion protein was expressed at close to endogenous levels, when compared to control HALL cells and HD-ED cells (Figure 3.14, A). Immunofluorescence images (Figure 3.14 panels B and C) demonstrate that EYFP-hDaxxMSIM does not co-localise with PML and remains dispersed within the nucleoplasm. Based on the previous data (Ishov et al, 1999), the interaction between PML and EYFP-hDaxxMSIM has been abolished in HD.MSIM cells, however this is based on previous findings and has not been confirmed by CoIP assays in the current study. Moreover, in these cells ATRX also fails to localise to ND10, although PML is distributed as in normal HepaRG cells, which therefore provides an additional support for the importance of hDaxx in targeting ATRX to ND10.

HDaxx knock-down cells were also reconstituted with a SIM deletion mutant of hDaxx (EYFP-hDaxx $\Delta$ SIM) to generate cell line HD. $\Delta$ SIM (see Table 2.6). Deletion of the entire hDaxx SIM (IIVLSDS motif) resulted in the same hDaxx localisation phenotype as that of EYFP-hDaxxMSIM, however the protein appeared to be unstable or toxic as the cells rapidly lost expression of the mutant protein (data not shown). In summary, the interaction between ATRX and hDaxx is not sufficient for localisation of the ATRX/hDaxx complex to ND10 but requires the ability of hDaxx to interact with SUMO.

A

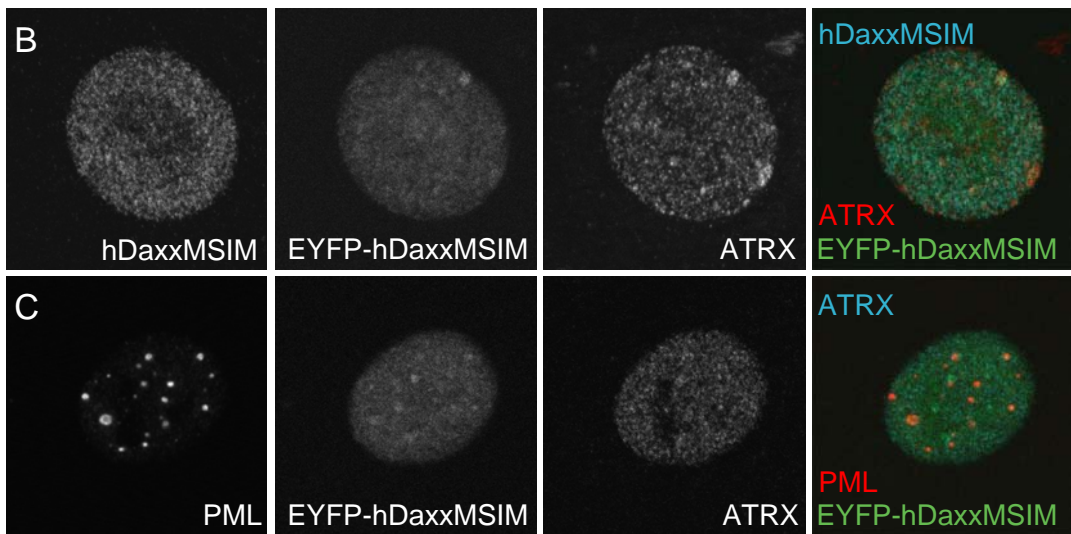
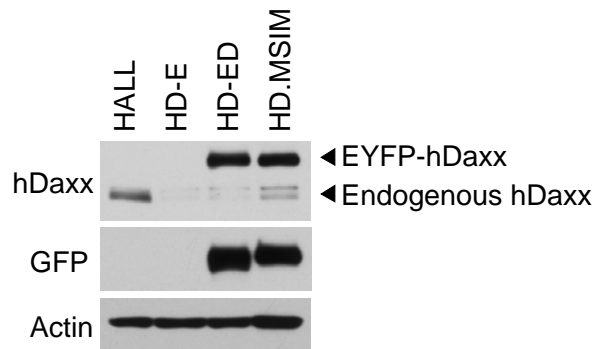


**Figure 3.14 hDaxx SUMO-interaction motif is required for hDaxx localisation to ND10**

A: Expression EYFP-hDaxxMSIM determined by western blot and compared to that of endogenous hDaxx in HALL cells, depleted hDaxx in HD-E and re-introduced wt EYFP-hDaxx in HD-ED cells. hDaxx and EYFP signal were detected using anti-Daxx D7810 and anti-GFP ab290 antibodies respectively. Actin (AC-40) was a loading control. B-C: HD.MSIM cells on coverslips were fixed for analysis by immunofluorescence and co-stained for ATRX and hDaxx (panel B) or ATRX and PML (panel C), using anti-PML 5E10, anti-ATRX H300 and anti-Daxx 07-471 antibodies. Secondary antibodies were anti-mouse AlexaFluor 555-conjugated and anti-rabbit Cy5-conjugated. EYFP signal resulted from autofluorescence. hDaxxMSIM indicates re-introduced EYFP-hDaxxMSIM detected with the anti-hDaxx antibody 07-471.

### 3.3 Conclusions and discussion

ATRX and hDaxx are nuclear proteins that interact to form a chromatin-remodelling complex that localises to ND10. ND10 localisation of ATRX is dependent on hDaxx (Ishov et al, 2004; Tang et al, 2004), whereas that of hDaxx itself requires its interaction with SUMO-modified PML *via* its SIM (Lin et al, 2006).

Whilst hDaxx is a ubiquitously expressed protein, ATRX appears to be expressed in many but not all cell types. Analysis of ATRX and hDaxx protein expression levels in different commonly used laboratory cell lines (Figure 3.1) has revealed that U2OS cells lack ATRX. It is possible that in transformed cells isolated from human tumours compensatory mutations may exist that overcome the loss of an important protein. Attempts to reconstitute ATRX in these cells by transfection have resulted in very low efficiency of ATRX reconstitution, but demonstrated that when expressed at low levels ATRX can localise to ND10 structures (data not shown). Further improvements of the transfection procedures have been abandoned due to the large size of the ATRX cDNA and the difficulty of its use in cloning procedures.

In the present Chapter, for the purposes of the further investigation, cell lines in which ATRX or hDaxx expression levels have been severely reduced by RNAi approach and in which wt and mutant hDaxx forms have been re-introduced, were described and characterised. Consistent with previously published work (Ishov et al, 2004; Tang et al, 2004), ATRX failed to localise to ND10 upon hDaxx depletion in cells of primary origin. ATRX itself, on the contrary, is not required for hDaxx localisation to ND10, suggesting that hDaxx serves as the ND10-targeting component within the ATRX/hDaxx complex. In addition further analysis of ATRX/hDaxx complex has been restricted to analysing the requirement of interaction between the two components of the complex in the localisation of either of the proteins to ND10. Thus, the region spanning the ATRX-interaction domain of hDaxx PAH1 (Tang et al, 2004) was deleted, and the mutant hDaxx was re-introduced. The use of a system that allows reconstitution of hDaxx-depleted cells with wt or mutant hDaxx proteins, expressed at close to endogenous levels has become the crucial step in the investigation of the roles of ATRX and hDaxx in HSV-1 infection. The key cell lines produced in this part of the study were ATRX- and hDaxx-depleted cell lines, using either HF or HepaRG cells, and HepaRG-based cell lines reconstituted with wt or mutant hDaxx.

The following conclusions regarding ATRX and hDaxx localisation within the cells can be drawn from the analysis of these cell lines: (a) ATRX is dispersed in the absence of hDaxx; (b) hDaxx is able to localise to ND10 in the absence of ATRX; (c) ND10 localisation of ATRX is restored upon reconstitution of hDaxx-depleted cells with EYFP-hDaxx; (d) interaction between ATRX and hDaxx *via* hDaxx PAH1 domain is necessary for ATRX localisation to ND10, and (e) interaction between hDaxx and SUMO-modified proteins is required for hDaxx localisation to ND10. These data are summarised in Table 3.1, where + or - signifies whether the protein is ND10 localised or not, respectively. No significant cytopathology or changes in morphology that could have been adverse for experimental procedures were noticed amongst all the produced cell lines. Interestingly, the hDaxx localisation pattern in ATRX-depleted HepaRG cells differed to a certain extent from that in ATRX-depleted HFs. Whereas in HFs hDaxx was localised to ND10 as in normal cells, in ATRX-depleted HepaRG cells hDaxx was more dispersed within a high proportion of the nuclei (as depicted on Figure 3.7). Since HepaRG cells go through the cell division process in cell culture faster than HFs, it is possible that these difference in hDaxx localisation may be related to cell cycle progression differences between the two cell lines, implying that a higher proportion of hDaxx may be associated with chromatin in ATRX-depleted HepaRG at a given time point.

**Table 3.1 Summary of localisation of PML, hDaxx and ATRX in transduced HepaRG cell lines**

<i>Cell line</i>	<i>ND10 localisation</i>		
	PML	ATRX	hDaxx
HALL	+	+	+
HAA	+	Depleted	+
HALD2 / HD-E	+	-	Depleted
HD-ED	+	+	+
HD. $\Delta$ PAH	+	-	+
HD.MSIM	+	-	-
HD. $\Delta$ SIM	+	-	-

Production of stable ATRX depleted cell lines using the methods described above for HFs and HepaRG cells was never fully achieved and the cells had to be regenerated on a regular basis, in order to perform reproducible assays, which are detailed in Chapters 4 and 5. A number of reasons could explain this. Firstly, ATRX plays a role in chromosomal cohesion

and segregation during mitosis (Ritchie et al, 2008), which suggests its role in mitosis and provide clues as to why ATRX depletion could have been detrimental to cell cycle progression. The authors however used ATRX-depleted HeLa cells, which exhibited substantial mitotic and growth defects. The use of the primary fibroblasts or hepatoma cell line [with the phenotype close to primary hepatocytes (Gripon et al, 2002)], which did not show such severe nuclear morphology in the absence of ATRX, may point out the differences between the use of primary cell lines and highly transformed ones. Secondly, in any cell population generated by shRNA technology there will be a proportion of cells in which depletion has occurred to lesser extent than in the majority, or not at all. Outgrowth of these cells so that they become the major component after serial passages requires only that they have a slight growth advantage over the highly depleted cells.

In contrast to the ATRX knock-down cell lines, those depleted of hDaxx expression demonstrated efficient and stable knock down of the protein levels, which allowed re-introduction of EYFP-tagged wt or mutant hDaxx proteins using the lentiviral vectors, in order to study the function of hDaxx in more detail. Therefore, an important issue to be addressed is how the introduction of the mutant hDaxx proteins may have affected transcriptional regulation of its targets. If the deletion of PAH1 domain in the above assays affected the hDaxx interaction with other proteins, it could have resulted in a reduced repressive potential of hDaxx as a negative transcriptional regulator. Analysis of the previously published work by Hollenbach et al. (2002), in which several hDaxx deletion mutants have been generated, revealed that this was unlikely to be the case. Indeed, based on their experimental data using transcription reporter assays, it was demonstrated that neither the deletion of PAH1 domain nor that of the first 132 aa of hDaxx significantly altered transcriptional repression by hDaxx (Hollenbach et al, 2002). Interestingly, this domain is also required for hDaxx interaction with acetylated core histone H4 (AcH4), complexed with HDAC II (Hollenbach et al, 2002), suggesting possible competitive interactions of hDaxx with its partners ATRX, AcH4 and HDACs. Another group has identified the first 400 amino acids of hDaxx as the region required for the interaction with kinase HIPK2 (Hofmann et al, 2003). HIPK2 interaction with hDaxx promotes its phosphorylation, which has a proposed role in the induction of apoptosis. Disruption of the HIPK2-hDaxx interaction decreased the total level of hDaxx phosphorylation (Hofmann et al, 2003). Based on the data shown on Figure 3.12, the effects of hDaxx PAH1 deletion on phosphorylation differences were not significant or difficult to discern on a western blot because of the faster migration of the protein due to the deletion of PAH1 domain.

HDaxx interacts with SUMO-1 *via* its C-terminal domain (Lalioi et al, 2002; Ryu et al, 2000), and the specific SUMO-interaction domain has been mapped to the last 8 amino acids of the protein sequence (Lin et al, 2006). The ability of hDaxx to interact with SUMO-modified substrates plays a role in transcriptional repression by a number of proteins, amongst which are PML, Smad4 (which is involved in tumour growth factor- $\beta$  signalling), and androgen and glucocorticoid receptors (Lin et al, 2004; Lin et al, 2006); (Ishov et al, 1999; Li et al, 2000). Figure 3.13 demonstrates that mutagenesis of the hDaxx SIM leads to its displacement from ND10, most likely due to inability to interact with PML (Ishov et al, 1999), thereby leading to ATRX dispersal. Other protein interactions of hDaxx that involve its C-terminal domain, such as those with a centromeric protein CENP-C (Pluta et al, 1998) and a protein involved in apoptosis activation Fas (Yang et al, 1997), could also have been disrupted. The downstream effects of disruption of these interactions will not be considered here. However, based on previous work identifying hDaxx as a negative transcriptional regulator it would be expected that depletion of hDaxx or mutagenesis of its SIM would lead to enhanced transcription of its target genes, as well as to alterations in apoptosis regulation and chromatin remodelling processes.

Within the three different cell lines generated in this part of the study, namely cell lines depleted of hDaxx, or expressing hDaxx $\Delta$ PAH1 or hDaxxMSIM, ATRX had a dispersed localisation pattern. Inability of ATRX to localise to ND10 can elicit a number of effects on gene expression. Studies of various ATRX mutants, particularly those that fail to localise to ND10, including the ones that are commonly seen in ATR-X syndrome, have suggested that SNF2 domain of ATRX may be involved in both chromatin remodelling and targeting of ATRX to ND10 (Berube et al, 2008). Based on this model, efficient association of ATRX with ND10 correlates with its chromatin remodelling functions. In addition, this evidence implicates C-terminal SNF2 domain of ATRX in its ND10 localisation, suggesting that the interaction with hDaxx is essential but not the only requirement for ATRX ND10 localisation. Hence, it has been proposed that when ATRX is dispersed in the nucleus it is likely to become incapable of its full chromatin remodelling potential (Berube et al, 2008). Therefore, dispersed ATRX localisation would be expected to result in the inefficient regulation of certain gene targets specific for the ATRX/hDaxx complex, which are yet to be identified. This issue needs to be taken into account when addressing chromatin repressive properties of the complex in the different cell lines utilized throughout the study.

As discussed in Chapter 1 and in Section 3.1 of the present Chapter, ND10 components constitute a part of cellular intrinsic defence mechanism against both HCMV and HSV-1. Generation of the above described cell lines in the present part of the study demonstrates a convenient approach for studying functions of other cellular proteins that may be involved in this mechanism and therefore is a useful tool in the studies of cell biology mechanisms. The use of the cell lines depleted of ATRX or hDaxx, as well as in which ATRX-hDaxx interaction had been disrupted, provides the basis of the investigation presented in the next two Chapters.

## 4 Regulation of HCMV Infection by ATRX

### 4.1 Introduction to cellular intrinsic defence against HCMV infection

In Chapter 1, cellular intrinsic defence against viral infection has been defined as a collective set of cellular activities that provides potent protection from viral infection, distinct from those provided by adaptive and innate host immunity systems (Bieniasz, 2004). In the current and subsequent chapters this definition is applied to the set of nuclear activities that act to inhibit HCMV and HSV-1 transcription, amongst which are functions performed by the components of ND10. In addition to the activities of ND10 proteins, histone modifications, being involved in the chromatin state of the viral genomes, are also considered to contribute to the efficiency of cellular anti-viral intrinsic immunity. The aspects of chromatin structure of HCMV genomes during lytic and latent infectious cycles have been addressed in Chapter 1 and previously reviewed (Sinclair, 2009). The following account will therefore summarize the data regarding specific ND10 proteins, namely PML and hDaxx, which have been shown to contribute to an anti-HCMV intrinsic defence mechanism by a number of different studies referenced below.

At the very early stages after the onset of HCMV infection and release of its genome together with tegument components into the cell nucleus, the Immediate Early transcript environment is formed. This is characterised by the presence of major IE transcripts and the spliceosome assembly factor SC35, which become associated with ND10 components as IE transcription initiates (Ishov et al, 1997). The two crucial events that are distinguished at this stage of the infection are (a) the association of HCMV tegument protein pp71 with ND10 component hDaxx and (b) the association of PML with HCMV genomes and the co-localisation of the major Immediate-Early protein IE1 (ie72) with PML. As the investigations into the effect of HCMV infection on ND10 have progressed, it was discovered that disruption of ND10 *via* PML re-distribution was a result of IE gene expression, and was therefore observed within the first hours of infection (Kelly et al, 1995). IE1 was found to initially co-localise with ND10 while IE2 (ie86) formed foci immediately adjacent to these structures, and subsequently the ND10 components became distributed diffusely throughout the nucleus (Ahn & Hayward, 1997; Koriath et al, 1996; Wilkinson et al, 1998). This disruption of ND10 is a result of the specific interaction between IE1 and the major ND10 component PML, followed by IE1-driven removal of PML from ND10 in the infected human fibroblasts (Ahn et al, 1998; Ahn & Hayward,

1997). The mechanism by which this occurs is thought to involve abolition of SUMO-modification in both PML and Sp100 by IE1, leading to disorganisation of these structures (Lee et al, 2004; Muller & Dejean, 1999). The effect of IE1 on Sp100 suggests the importance of Sp100 in the intrinsic cellular anti-HCMV response, by analogy with HSV-1 (Everett et al, 2008; Negorev et al, 2006; Negorev et al, 2009), however this hypothesis has not been extended in subsequent research. Interestingly, PML depletion results in greater efficiencies of infection of wild-type and, to an even greater extent, IE1-deficient HCMV (Tavalai et al, 2006; Tavalai et al, 2008), which demonstrates the functional significance of IE1-dependent PML displacement during the wt HCMV infection. These observations have suggested that IE1 counteracts the cellular response provided mainly by PML.

In addition to PML, hDaxx has also been shown to have a significant role in HCMV infection by a number of reports from independent research groups (Cantrell & Bresnahan, 2005; Cantrell & Bresnahan, 2006; Groves & Sinclair, 2007; Hofmann et al, 2002; Hwang & Kalejta, 2007; Ishov et al, 2002; Preston & Nicholl, 2006; Saffert & Kalejta, 2006; Saffert & Kalejta, 2007; Tavalai et al, 2008; Woodhall et al, 2006). The HCMV tegument protein pp71 can be detected at ND10 virtually immediately after its release into the cell nucleus, where it interacts with hDaxx and subsequently induces its degradation (Hofmann et al, 2002; Hwang & Kalejta, 2007; Ishov et al, 2002; Saffert & Kalejta, 2006). The interaction between pp71 and hDaxx is required for efficient initiation of IE transcription (Cantrell & Bresnahan, 2005; Ishov et al, 2002). Importantly, evidence supporting the functional role of hDaxx as a component of cellular intrinsic defence came from the observations by independent groups who demonstrated that depletion of hDaxx from cells relieves repression of HCMV infection to a significant extent, and to a higher extent for pp71-null mutant HCMV infection (Cantrell & Bresnahan, 2006; Preston & Nicholl, 2006; Saffert & Kalejta, 2006; Woodhall et al, 2006). In normal fibroblasts HCMV is unable to efficiently replicate in the absence of pp71 (Bresnahan et al, 2000). Further work has proposed the involvement of hDaxx in a similar pathway of repression in the cell culture model of quiescent HCMV infection (Saffert & Kalejta, 2007). Therefore, these studies have established that hDaxx-mediated intrinsic defence mechanism is antagonised by HCMV tegument protein pp71.

In the search of additional components that contribute to cellular intrinsic defence, the next part of the studies described in this thesis focuses on ATRX. Since ATRX localises to ND10 and interacts with hDaxx (Tang et al, 2004), it is a suitable and appealing candidate for investigation for a potential role in HCMV infection. Hence, the aim of the following

part of the study was to analyse whether ATRX, by analogy with hDaxx, contributes to the cellular intrinsic defence mechanism against HCMV infection. The next set of data will demonstrate how ATRX localisation is affected during HCMV infection and the effect of ATRX depletion on replication of pp71-null mutant virus. Due to this work being conducted in collaboration with Chris Preston and Steven McFarlane (MRC Virology Unit, Glasgow), a significant part of the results is not presented in this chapter since it was not performed by the author, and the reader is directed to the original manuscript (Lukashchuk et al, 2008).

## 4.2 Results

### 4.2.1 HCMV tegument protein pp71 displaces ATRX from ND10

The following section summarises the key findings obtained from the work conducted by Chris Preston and Steven McFarlane (Lukashchuk et al, 2008). HCMV tegument protein pp71 and viral genomes become associated with ND10 as soon as they are released into the cell nucleus (Hofmann et al, 2002; Ishov et al, 2002; Marshall et al, 2002; Preston & Nicholl, 2005). This localisation depends on pp71 interaction with hDaxx. In light of understanding the role of hDaxx-interacting partner ATRX in HCMV infection, the effect of pp71 on ATRX localisation has been investigated using a number of different assays, all based on confocal immunofluorescence microscopy.

Firstly, recombinant HSV-1 strains *in1316* or *in1360*, expressing either EYFP-tagged or wt pp71, respectively, were used to infect human fibroblasts. This virus has mutations that inactivate HSV-1 proteins VP16, ICP0 and ICP4, which allow it to infect cells without detectable HSV-1 protein synthesis or cytopathology. Secondly, pp71 was expressed alone by transfecting an EYFP-pp71 encoding plasmid vector. And thirdly, a cell line expressing pp71 constitutively was used. These assays demonstrated that in cells where pp71 was expressed in low amounts and localised to ND10, ATRX was dispersed and hDaxx remained associated with pp71 foci, suggesting the potential significance of pp71-mediated dispersal of ATRX.

Having demonstrated the pp71-dependent dispersal of ATRX *via* transfection and HSV-1 recombinant infection assays, the experiments were performed to investigate whether a similar effect on ATRX displacement from ND10 results from wt HCMV infection. For this purpose, HCMV strain AD169 was used (see Chapter 2, Section 2.1.7). ATRX displacement from ND10 occurred in cells infected with AD169 as early as 1 hour post

adsorption of the virus, before any effects on hDaxx were observed. The increase in the number of cells with dispersed ATRX distribution was dependent on the amount of virus used, suggesting multiplicity dependence of this effect. Infection with pp71-null mutant HCMV did not result in dispersal of ATRX, and instead ATRX remained associated with ND10, confirming the pp71-mediated dispersal of ATRX in wt HCMV infection. No detectable changes at the early time points post HCMV infection in the expression levels of either hDaxx or ATRX were seen in western blot analyses, and therefore ATRX dispersal could not be attributed to changes in protein expression levels. Overall the results described in the current section provide evidence that ATRX is displaced from ND10 at the very early stages of HCMV infection by pp71, and not by other viral tegument components.

#### **4.2.2 ATRX is not required for pp71 localisation to ND10**

It has previously been shown that hDaxx is required for pp71 targeting to ND10 (Ishov et al, 2002). Since pp71 displaces ATRX from ND10, as described above (see Lukashchuk et al, 2008), and given the fact that ATRX and hDaxx are present at ND10 as a complex (Tang et al, 2004), it was hypothesized that ATRX may also be required for pp71 localisation to ND10 and possibly for its interaction with hDaxx. To investigate this possibility, ATRX-depleted fibroblasts (named HF-ShATR<sub>X</sub>; see Figure 3.5), were infected with HSV-1 recombinant *in1316* that expresses EYFPpp71 and processed for analysis by immunofluorescence at 4 hours post infection. As evident from Figure 4.1 (panels A and B), in HF-ShATR<sub>X</sub> cells, EYFPpp71 co-localised with PML, as in control HF-ShLuci cells. Depletion of ATRX did not affect co-localisation between EYFPpp71 and hDaxx in cells expressing low amounts of the pp71 fusion protein and at this time point (Figure 4.1, panels C and D), demonstrating that ATRX is not required for the interaction between the two proteins. Staining for ATRX in EYFPpp71 expressing cells confirmed that ATRX was dispersed (Figure 4.1, panels E and F), consistent with the observations described in the previous section, underlying the importance of pp71-mediated dispersal of ATRX. Overall, the experiment has provided evidence that ATRX is not required for pp71 localisation and interaction with hDaxx at ND10.

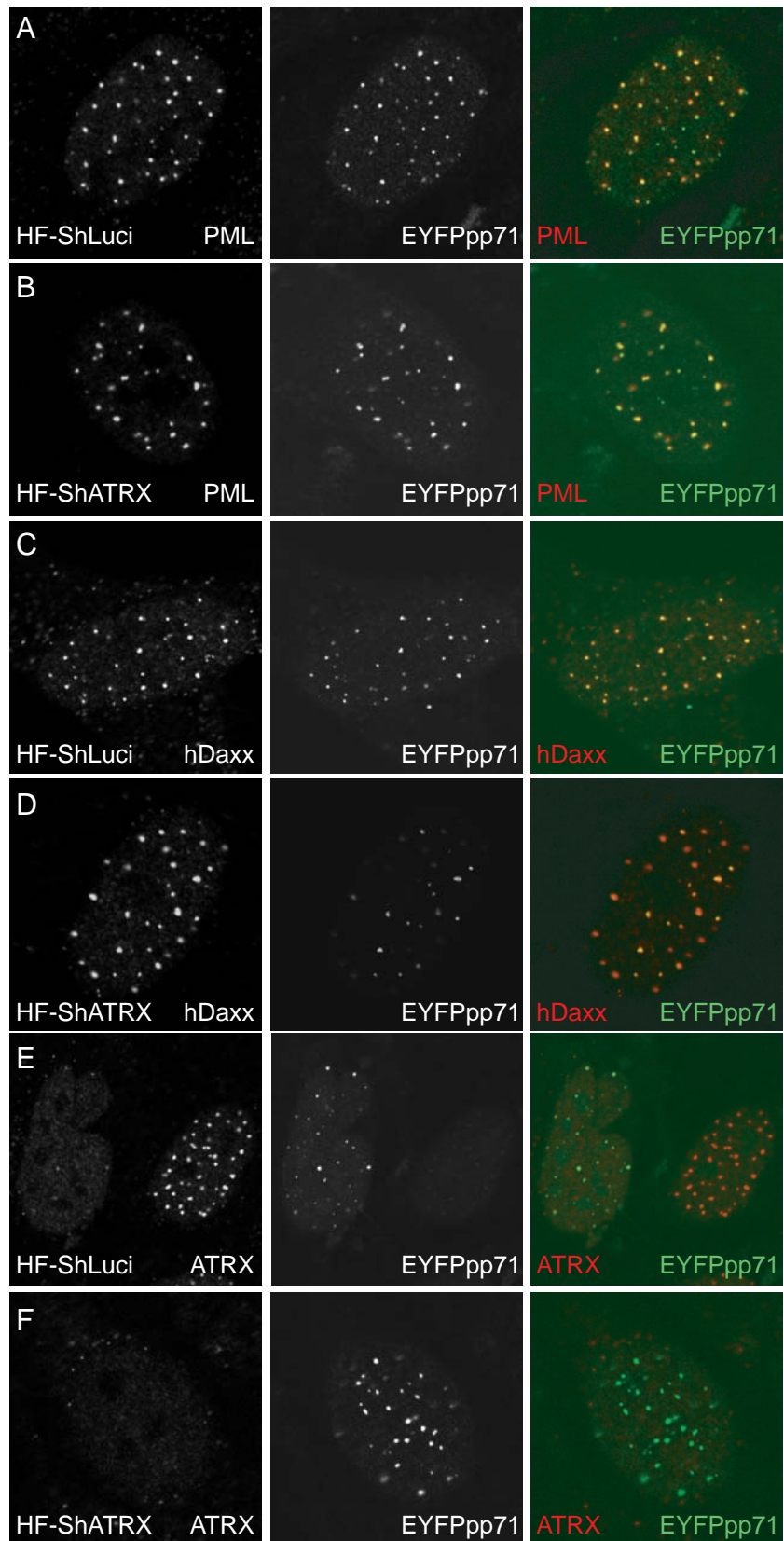


**Figure 4.1 ATRX depletion does not affect pp71 localisation**

Control or ATRX-depleted HF seeded onto coverslips were infected with *in1316* at MOI 0.3 pfu/cell and fixed for immunofluorescence analysis at 4 hours post infection. For protein detection, cells were stained with anti-PML (r8; panels A and B), anti-hDaxx (r1866, panels C and D) and anti-ATRAX (H300; panels E and F) antibodies. Secondary antibody was Cy3-conjugated anti-rabbit IgG. The EYFPpp71 signal resulted from autofluorescence of the expressed fusion protein.

### **4.2.3 ATRX contributes to the repression of HCMV IE protein synthesis in the absence of pp71**

Section 4.2.1 of this Chapter has shown pp71-mediated removal of ATRX from ND10 at the very early times after the initiation of wt HCMV infection. If such displacement of ATRX was functionally important for the efficiency of HCMV IE gene expression, then by analogy with the experiments on hDaxx (Cantrell & Bresnahan, 2006; Preston & Nicholl, 2006; Saffert & Kalejta, 2006; Woodhall et al, 2006), depletion of ATRX should support increased IE protein synthesis by pp71-null mutant HCMV. To investigate whether this was the case, the efficiency of IE protein synthesis of pp71-null mutant HCMV was analysed in ATRX-depleted HF cells (Figure 4.2). HF-ShLuci and HF-ShATRAX cells were seeded and infected the following day with the indicated HCMV strains (Figure 4.2, A and B). Samples were harvested for a western blot analysis at 18 or 2 hours post infection as specified within the Figure 4.2. Replication of the pp71-null mutant HCMV strain ADSubUL82 is severely reduced in HF cells due to its inability to express IE proteins efficiently, and therefore, as expected, infection of HF-ShLuci cells resulted in barely detectable levels of IE1 production (Figure 4.2 A, lane 3). However, ATRX-depletion resulted in a substantial increase of IE1 expression compared to that in HF-ShLuci cells, suggesting the requirement of ATRX for fully efficient repression of pp71-null HCMV genomes (Figure 4.2 A, lane 4). This increase in IE1 expression levels in ATRX-depleted cells was consistent amongst several individual experiments, however variation in the extent of such increase depending on the efficiency of ATRX-depletion was noted.

For additional controls, cells were co-infected with ADSubUL82 and AD169UV. AD169UV is the wild-type HCMV strain inactivated by UV-radiation and therefore was unable to replicate but provided functional pp71, therefore co-infection with the two viruses served as a measure of a maximum potential of ADSubUL82 strain to produce IE1. AD169 is a common laboratory wt HCMV strain. In cells infected with either AD169 (at MOI 0.3) or co-infected with ADSubUL82/AD169UV, IE1 levels of expression were essentially equivalent in HF-ShLuci and HF-ShATRAX90 cells, suggesting that ATRX depletion does not affect the ability of pp71 to transactivate IE gene expression. Infection with AD169UV alone was conducted in order to ensure that the virus was unable to replicate in either of the two cell lines (Figure 4.2 A, lanes 7 and 8). To confirm the efficiency of ATRX depletion in the experiment presented on Figure 4.2 A, the membrane was blotted for ATRX, indicating efficient reduction in ATRX levels. Because of the known relationships between hDaxx and pp71, hDaxx expression was also analysed in

these infected cells. In cells infected with ADSubUL82, hDaxx expression levels were equal to those seen in mock-infected cells, consistent with previous observations (Saffert & Kalejta, 2006; Tavalai et al, 2008). In the infections including AD169UV, a marginal reduction in hDaxx expression was observed (compare lanes 5-8 with 1-4 in Figure 4.2A), which partly correlates with the reports on pp71-dependent degradation of hDaxx (Hwang & Kalejta, 2007; Saffert & Kalejta, 2006; Tavalai et al, 2008). Infection with AD169 strain resulted in a further decrease of hDaxx intensity band when compared to AD169UV alone or during co-infection with AD169SubUL82/AD169UV (compare lanes 9 and 10 with 5-8 in Figure 4.2A).

Inconsistency in the levels of hDaxx degradation was observed throughout a number of repeated experiments (and in published papers), and the levels of degradation using the indicated MOI of AD169 were never as efficient as in previously published work (Hwang & Kalejta, 2007; Saffert & Kalejta, 2006). Figure 4.2 B demonstrates an independent experiment where viruses from the same stocks were used at the same MOIs. The membrane was blotted for IE protein levels, confirming the data presented in Figure 4.2 A, and for hDaxx levels (Figure 4.2 B). Degradation levels of hDaxx seen in lanes 3-5 and 8-10 were consistent with previously published data (Hwang & Kalejta, 2007; Saffert & Kalejta, 2006).

In order to confirm that both control and ATRX-depleted cells received an equivalent amount of viral load during the infection with ADSubUL82, separate wells of cells were seeded and infected using the same amounts of the indicated viruses in Figure 4.2A, lanes 3, 4, 5 and 6. Samples were prepared for analysis at 2 hours post infection and tested for the presence of pp65, an abundant tegument protein that is normally expressed at late times and therefore at early times can be used as a measure of the quantity of input virus particles. Equal levels of pp65 were present in HF-ShLuci and HF-ShATRX cells infected with ADSubUL82 only, and accordingly, when co-infected with ADSubUL82/AD169UV, the levels of pp65 were higher due to double infection.

In summary, ATRX contributes to the repression mechanism of the HCMV IE transcription, which occurs in the absence of pp71.

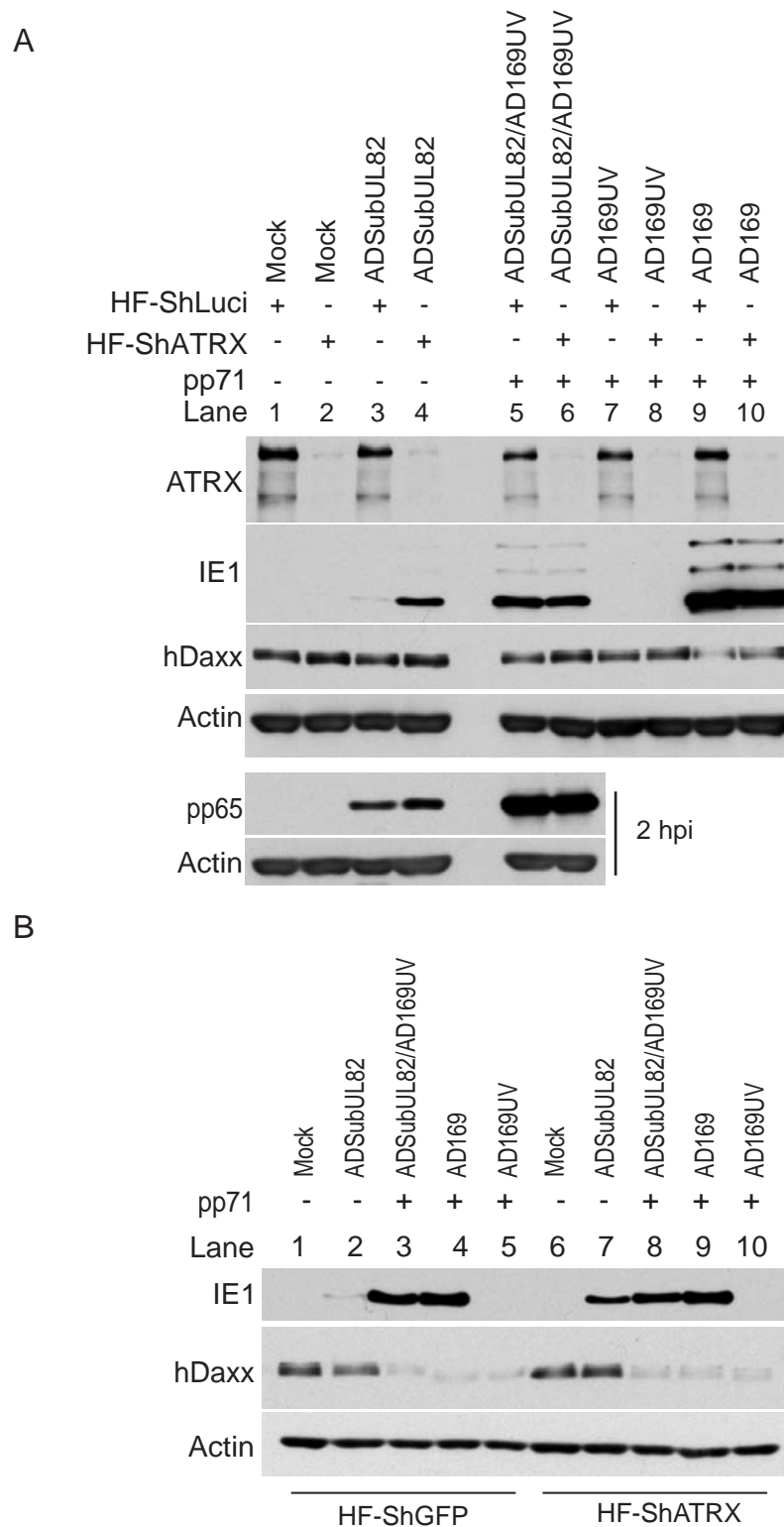


**Figure 4.2 ATRX depletion increases Immediate Early gene expression in cells infected with pp71-null mutant HCMV**

Control (HF-ShLuci or HF-ShGFP) and ATRX-depleted (HF-ShATRAX) cells were mock infected or infected with ADsubUL82 (0.2 infectious units per cell), AD169 (MOI 0.3), AD169UV alone (MOI 3, based on the original titer), or co-infected with AD169UV and ADSubUL82, and harvested for western blot analysis. A: Analysis of IE protein synthesis after infection of ATRX-depleted cultures with ADSubUL82. Samples were harvested at 18 (top) or 2 hours post infection (as indicated). The membranes were probed with anti-ATRAX 39F, anti-HCMV IE E13 and anti-hDaxx D7810 antibodies, or anti-pp65 ab2595 as indicated. B: An additional analysis of hDaxx degradation was performed on an independent experiment. The membrane was probed with anti-hDaxx D7810 and anti-HCMV IE E13 antibodies. Actin (AC-40) was a loading control in panels A and B.

#### **4.2.4 ATRX depletion results in the increased IE gene expression per cell infected with pp71-null mutant HCMV**

The above data demonstrate the increase in the total IE1 protein expression levels of pp71-null HCMV when ATRX expression was severely suppressed. In order to quantify the differences in IE1 expression between control and ATRX-depleted cells, the numbers of cells infected with pp71-null mutant HCMV and expressing IE1 were assessed and compared in control and ATRX depleted cells. This was achieved by infecting HF-ShLuci and HF-ShATRX cells on coverslips with 0.2 infectious units per cell of ADSubUL82 and processing for immunofluorescence with anti-IE1 and anti-ATRX antibodies at 12 hours post infection. This time point after infection was chosen to be the optimal for scoring and assessing the observed differences in IE1 expression between the two cell lines.

Based on the findings obtained by western blot analysis, it was expected that the numbers of cell nuclei positive for IE protein expression would be much higher in ATRX-depleted cells than those in control HFs. Surprisingly, it was found that the numbers of IE1 positive nuclei did not differ much between control and ATRX-depleted cells (9.1% and 14.8% of the total cell numbers, respectively; Table 4.1). However, it was the amount of IE1 protein expressed per cell that differed significantly. In HF-ShLuci cells the majority of the nuclei positive for IE1 demonstrated weak punctate IE1 distribution (Figure 4.3, panel A), suggesting lack of pp71 still allowed low levels of IE gene expression, consistent with data shown in Figure 4.2. In contrast, in ATRX-depleted cells the majority of IE1-positive nuclei showed nuclear dispersed localisation, and the protein was expressed at very high levels (Figure 4.3, panel B). The percentage of HF-ShLuci infected cells with bright dispersed IE1 signal was 0.6% of the total cell numbers, and that of HF-ShATRX infected cells was 10% (see Table 4.1). Panels C and D of the Figure 4.3 depict close-up images of typical IE1-positive nuclei of HF-ShLuci and HF-ShATRX cells, respectively. Co-infection of the two cell lines with ADSubUL82 and AD169UV, or infection with AD169 strain and analysis of the cells at 12 hours post infection for IE1 expression revealed that the majority of cell population expressed high levels of the IE proteins, independently of the presence or absence of ATRX. Table 4.1 summarises and compares the numbers obtained from scoring these nuclei in two independent experiments, scoring approximately 300 cells for each experiment from random fields of view. In control HF-ShLuci cells, those with punctate IE expression during ADSubUL82 infection correlated with the retention of ATRX foci at ND10, but when pp71 was added by co-infecting with AD169UV or infecting with AD169, ND10 were disrupted. This was consistent with the

findings presented on Figure 4.2, and in addition confirms that pp71 allows increased expression of IE proteins in the infected cell nucleus thereby causing disruption of ND10.

**Table 4.1 IE protein expression in ATRX-depleted cells<sup>1</sup>**

<i>Cells</i>	<i>Virus</i>	<i>Number of cells<sup>2</sup></i>			
		<i>High IE</i>	<i>Low IE</i>	<i>Total</i>	<i>IE positive (%)</i>
HF-ShLuci	Sub82	5	66	779	9.1
HF-ShATRX	Sub82	78	36	766	14.8
HF-ShLuci	Sub82+AD169UV	94	6	383	26.1
HF-ShATRX	Sub82+AD169UV	113	9	439	27.8
HF-ShLuci	AD169	69	6	158	47.5
HF-ShATRX	AD169	54	6	169	35.5

<sup>1</sup> HF-ShLuci or HF-ShATRX cultures were infected with ADSubUL82 (Sub82; 0.2 infectious units/cell), co-infected with ADSubUL82 plus uv-irradiated HCMV (AD169UV; MOI 0.3, based on original titer), or with wild type HCMV (AD169; MOI 0.3). At 12 h post infection, coverslips were fixed and processed for analysis by immunofluorescence with antibodies specific for HCMV IE proteins and ATRX.

<sup>2</sup> IE positive cells were classified as present in low (punctate localisation pattern) or high (dispersed localisation pattern) amounts, as shown in Figure 4.3.

According to the results presented on Figures 4.2 and 4.3 and those described in section 4.2.1, it was concluded that pp71-mediated removal of ATRX from ND10 is required for efficient initiation of IE gene expression. It has to be noted however, that careful immunofluorescence analysis of the normal HFs expressing endogenous levels of ATRX infected with wild-type HCMV revealed that some cells positive for IE1 retained ATRX at ND10, suggesting that removal of ATRX is important but not essential for the initiation of IE gene expression (Lukashchuk et al, 2008). In summary, this and the previous sections have demonstrated that the expression of IE proteins is substantially increased during pp71-null HCMV infection of ATRX-depleted cells. Hence, it is concluded that ATRX contributes to the efficient repression of pp71-null mutant HCMV IE gene expression.

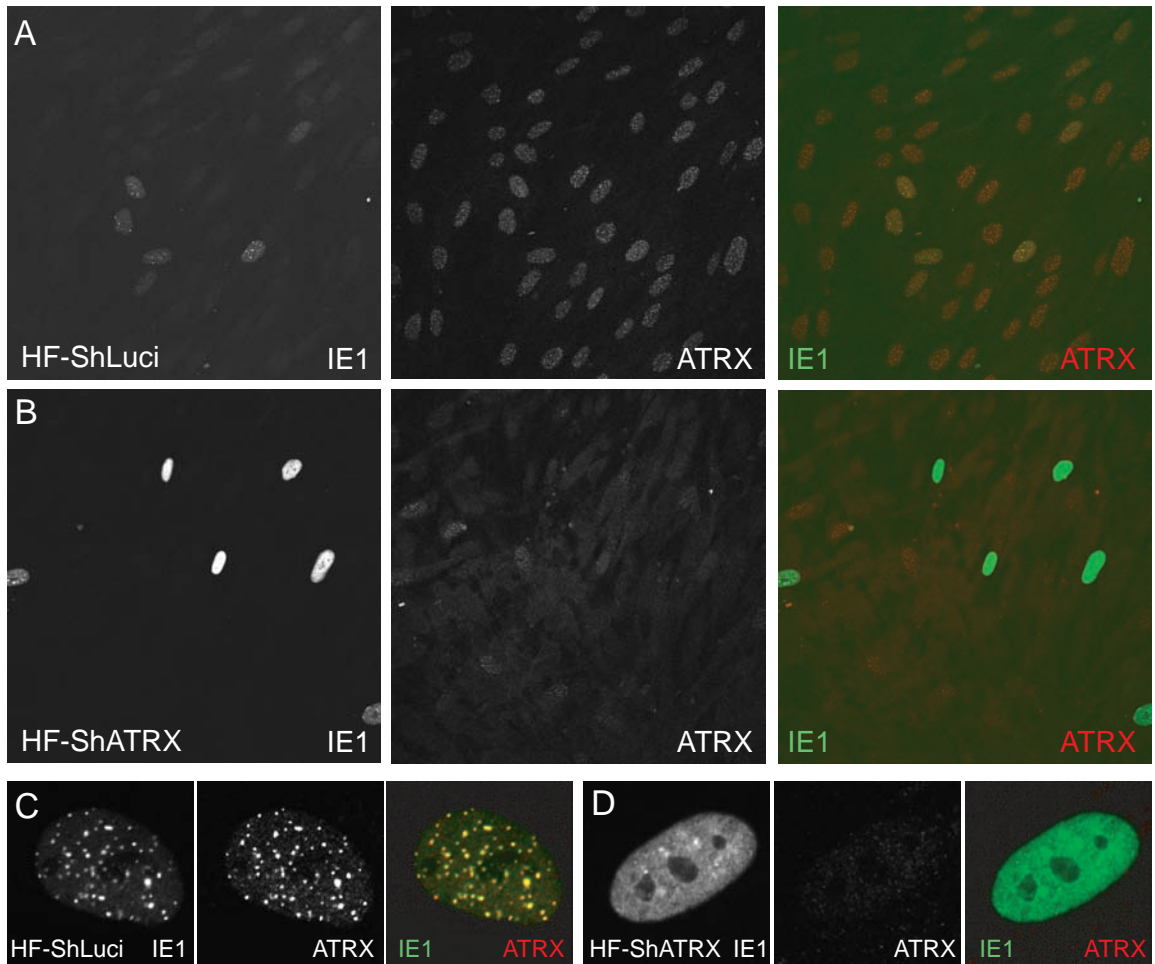


**Figure 4.3 ATRX depletion increases IE protein synthesis of the individual cells infected with pp71-null mutant HCMV**

Cells were infected with 0.2 infectious units of ADSubUL82 per cell and fixed for analysis by immunofluorescence at 12 hours post infection. HF-ShLuci (A and C) and HF-ShATR X (B and D) were stained with anti-IE1 ab2595 and anti-ATR X H300 antibodies. Secondary antibodies were anti-mouse FITC-conjugated and anti-rabbit Cy3-conjugated. Image capture settings in 488 channel (FITC) for HF-ShATR X cells were adjusted so that no over-exposure occurred in cells expressing high levels of IE proteins.

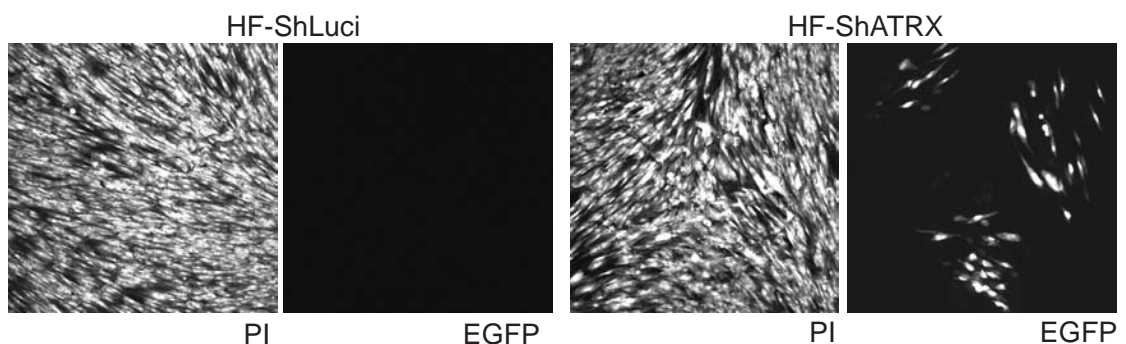


**Figure 4.4 ATRX depletion increases replication of pp71-null mutant HCMV**

HF-ShLuci and HF-ShATR X cells on coverslips were infected with ADSubUL82 (0.2 infectious units per cell) and incubated at 37 °C for 11 days. Replicating virus was detected by the expression of enhanced green fluorescent protein (EGFP), encoded by a *EGFP* gene inserted into the UL82 coding region. Cells were also stained with propidium iodide (PI) to detect all the cells in the sample.

#### **4.2.5 ATRX depletion supports increased replication of pp71-null mutant HCMV**

In the results presented above, the role of ATRX in the repression of pp71-null HCMV infection was demonstrated from the aspect of initiation of IE gene expression (Figures 4.2 and 4.3). In normally restrictive HFs, HCMV fails to establish efficient productive infection in the absence of its transactivator pp71. Therefore, the next question asked was whether the increase in IE gene expression of ADSubUL82 in ATRX-depleted cells was sufficient to trigger plaque formation and production of infectious viral progeny. HF-ShLuci and HF-ShATRAX cells on coverslips were infected with ADSubUL82 at a multiplicity of 0.2 infectious units per cell and incubated at 37 °C for up to 11 days. Because of an EGFP insertion within the deleted UL82 gene in ADSubUL82, the plaques could be detected by fluorescence microscopy. As expected, no plaques were detected on HF-ShLuci cells that express endogenous ATRX levels. In HF-ShATRAX cells however, the numbers of green fluorescent plaques was substantially increased (Figure 4.4) and averaged about 20 per coverslip. Viral yields were measured by infecting permissive HFFF cells using cell-released virus and determining the numbers of IE1 positive cells after a 24-hour infection (work performed by Chris Preston). Viral yields obtained on HF-ShATRAX cultures were between 140 and 560 infectious units per culture, whereas those from HF-ShLuci cultures between 0 and 5 infectious units (both sets of numbers were based on 5 determinations). Therefore, the increase in IE gene expression that was determined at the earlier stages of infection (Figure 4.2) is sufficient for initiation of productive infection by pp71-null mutant HCMV in the absence of ATRX. These data implied that ATRX depletion relieves the repression mechanism occurring on pp71-null mutant HCMV infection, allowing the virus to replicate in culture more efficiently.

### 4.3 Conclusions and discussion

Understanding of the events associated with the regulation of the early stages of lytic HCMV infection is important for identification of the factors that may contribute to repression of viral genomes. The investigation reported in the present chapter has identified the chromatin-remodelling enzyme ATRX as the novel component that contributes to the intrinsic repression mechanism in HCMV infection, which takes place at the early stages of IE transcription and during productive infection. The virus counteracts this intrinsic mechanism by displacing ATRX from ND10 at the very early time points after the infection, or immediately after the HCMV genomes and tegument components are released into the cell nucleus. The specific viral component that induces ATRX removal from ND10 before any effects on other ND10 proteins can be discerned is HCMV tegument protein pp71. The proof that it was indeed due to the action of pp71 came from a number of different assays, which were aimed to assess the effect of the HCMV tegument protein pp71 only, without the interference of other viral components (see Lukashchuk et al, 2008; attached). The relief of cell-mediated repression of pp71-null mutant HCMV IE gene expression and replication was achieved by producing an HF cell line in which ATRX expression was severely downregulated by shRNA. Moreover, increased IE gene expression in ATRX-depleted cells was sufficient for initiation of productive infection by pp71-null HCMV, which is incapable of plaque formation in normal fibroblasts. These data suggest the functional importance of pp71-mediated ATRX displacement from ND10, which allows successful gene expression and replication of HCMV in culture. The findings reported above have therefore provided the first evidence on the role of ATRX in intrinsic cellular defence against viral infection.

The concept of intrinsic resistance to HCMV infection has emerged from a number of independent studies, showing the importance of ND10 proteins such as hDaxx and PML in this process (reviewed in Tavalai & Stamminger, 2008). Based on results presented in the manuscript by Tavalai and colleagues it was concluded that the PML-dependent and hDaxx-dependent intrinsic resistance mechanisms preferentially follow different pathways, since one is counteracted by IE1 and the other by pp71, respectively (Tavalai et al, 2008). Whether ATRX acts independently or in a complex with additional co-factors is still to be understood in the context of HCMV infection. However, based on its protein-protein interaction properties, the latter option is the more likely. The possibility of its cooperation with hDaxx in an anti-viral defence mechanism is discussed further. Whether ATRX acts alone or as a subunit of a repressor complex is a subject of discussion in Chapter 6.

The fact that ATRX and hDaxx constitute a complex with chromatin remodelling activity (Ishov et al, 2004; Tang et al, 2004; Xue et al, 2003) suggests that the two proteins may act together to promote the assembly of a repressed chromatin structure on the incoming HCMV genomes. Since ATRX is capable of nucleosome remodelling *in vitro* (Xue et al, 2003), ATRX may function as the chromatin-remodelling subunit of the complex, thereby contributing to the repression of HCMV genomes immediately after the association of the ATRX/hDaxx complex with the incoming viral genomes in the absence of pp71. Inability of ATRX to localise to ND10, as a result of various mutations, leads to inefficient chromatin remodelling in ATR-X patients (Berube et al, 2008). In Chapter 3 it has been shown that hDaxx depletion results in ATRX dispersal, and it was discussed that in these cell lines regulation of chromatin remodelling by ATRX may therefore be ineffective. It is therefore feasible that the increase in HCMV IE gene expression in hDaxx-depleted cells reported previously can be partially attributed to dispersed localisation of ATRX.

Displacement of ATRX from ND10 by pp71 before any of the effects are seen on hDaxx localisation suggests that ATRX is one of the first targets of pp71, which thereby promotes disruption of ATRX/hDaxx complex during wt HCMV infection. Therefore the actions of pp71 can follow two slightly different paths. One model would state that pp71 first binds hDaxx, as previously shown in independent studies (Hofmann et al, 2002; Ishov et al, 2002; Saffert & Kalejta, 2006), and therefore alters the conformation of the ATRX/hDaxx complex, which results in subsequent ATRX displacement from ND10. Despite having shown to be specific using yeast two hybrid and CoIP assays (Hofmann et al, 2002), direct interaction between pp71 and hDaxx has not been shown definitively and there is a possibility of an intermediate co-factor responsible for the interaction between the two proteins. On the other hand, a different model could suggest competitive binding between pp71 and ATRX to hDaxx, where either pp71 transiently binds ATRX first, displaces it from ND10 and gains access for hDaxx interaction, or more likely competitive binding by ATRX and pp71 for the same region of hDaxx. In order for the latter model to be true, hDaxx interaction regions for ATRX and pp71 would overlap and span the PAH1 domain, which is known to be required for the hDaxx/ATRX interaction. The data investigating the pp71-interaction region of hDaxx, however, are controversial. According to Ishov et al (2002) the region lies between amino acids 142 and 290, whereas based on a report by Hofmann et al. 2002 the two regions responsible for pp71 interaction are those between amino acids 43-197 and 439-50 (Hofmann et al, 2002; Ishov et al, 2002). Based on the results of Hofmann et al, the involvement of hDaxx PAH1 domain in pp71 binding, which

is also required for interaction with ATRX, is likely. Preliminary experiments to investigate a possible interaction between pp71 and ATRX by CoIP methods in HCMV infected HF cells have been conducted, but no interaction between pp71 and ATRX was detected (Steven McFarlane, personal communication). This finding however still does not rule out the possibility of a very transient interaction between the two proteins.

The functional importance of pp71-mediated displacement of ATRX from ND10 resulted from an observation that IE gene expression of pp71-null mutant HCMV is substantially increased in ATRX-depleted cells, which implies that endogenous ATRX in normal cells contributes to the repression of pp71-null mutant virus. In contrast to analogous hDaxx-depletion experiments, in which an increase in the numbers of IE1-positive cells was seen after wt HCMV infection using strain AD169 (Tavalai et al, 2008), no significant differences were detected in IE gene expression in ATRX-depleted cells during wt infection, suggesting that ATRX was not required for the ability of pp71 to transactivate efficient gene expression. This finding correlates with the results presented on Figure 4.1 using immunofluorescence, demonstrating that ATRX was not required for pp71 interaction with hDaxx and hence its full transcriptional activation potential. In the absence of pp71, HCMV replicates very inefficiently in culture due to its substantially reduced capacity to initiate IE gene expression (Baldick et al, 1997; Bresnahan et al, 2000; Bresnahan & Shenk, 2000). Removal of ATRX significantly enhanced the ability of pp71-null mutant HCMV to replicate and produce infectious viral progeny, suggesting that the increase in IE1 expression was sufficient to initiate productive infection.

The strong evidence for the role of hDaxx in HCMV repression has also come from the observation that its overexpression reduces the infection efficiency of wt HCMV (Cantrell & Bresnahan, 2006; Tavalai et al, 2008; Woodhall et al, 2006). If the same were true in the case of ATRX, then by analogy, overexpression of ATRX would result in a similar extent of reduction of HCMV gene expression and plaque formation. Due to the size of ATRX, it is difficult to design a system in which ATRX could be stably overexpressed. Interestingly however, preliminary research from Chris Preston's group has shown that transfection of ATRX into U2OS cells, which do not normally express ATRX (Figure 3.1), resulted a decreased number of IE1-positive cells, after being infected with wt or pp71-null mutant HCMV for 24 hours (Steven McFarlane, personal communication). Hence, this observation provides more evidence for ATRX-mediated repression of HCMV gene expression and supports the data presented above for the role of ATRX in pp71-null HCMV infection.

The clue suggesting that the pathways of ATRX and hDaxx-mediated repression may be different results from analysing IE1 positive cells infected with pp71-null HCMV. Previous reports have demonstrated that in hDaxx-depleted HF, the numbers of IE1 positive wt or pp71-null mutant HCMV infected nuclei is substantially increased (Tavalai et al, 2008). In ATRX-depleted cells the situation was different. Whereas the numbers of cells expressing IE1 did not differ significantly between control or ATRX-depleted cells infected with pp71-null virus (see Table 4.1), the amount of IE protein expressed per cell was substantially higher in ATRX-depleted cells (see Table 4.1 and Figure 4.3). These observations imply that ATRX can block progression of IE transcription in the absence of pp71, despite a small amount of IE proteins still being produced (HF-ShLuci cells, Figure 4.3). Therefore, removal of ATRX by RNAi contributes to relief of this repression mechanism within the infected cells. It is however unclear whether ATRX targets HCMV genomes directly, particularly during pp71-null mutant HCMV infection. Downregulation of hDaxx by siRNA results in loss of a repressive chromatin structure around the HCMV MIEP (Woodhall et al, 2006), implying that hDaxx constitutes a part of a chromatin repressor complex, which forms around HCMV genomes. It remains to be investigated whether a similar mechanism applies in ATRX-depleted cells, although it is likely that many more chromatin-associated proteins are involved in this repression. Previous work suggests that the repression around HCMV genomes involves the action of HDACs (Murphy et al, 2002). The evidence concerning histone deacetylation as mechanism of repression in the context of both HCMV and HSV-1 will be discussed in Chapter 6.

In conclusion, ATRX contributes to cellular intrinsic resistance to HCMV infection, perhaps less potently than hDaxx. Whether the two proteins are acting as components of a complex or independently in order to induce chromatin assembly on the incoming HCMV genomes in the absence of pp71 is an issue yet to be investigated.

## **5 Regulation of HSV-1 Infection by ATRX and hDaxx**

### **5.1 Introduction to cellular intrinsic defence against HSV-1 infection**

The processes of HSV-1 latency establishment, maintenance and reactivation have been subjected to extensive research, but the cellular mechanisms involved remain incompletely understood. HSV-1 IE protein ICP0 is a strong transcriptional activator of viral gene expression that is required for both efficient lytic infection (reviewed in Everett, 2000; Hagglund & Roizman, 2004) and productive reactivation from latency (Everett, 2000; Halford & Schaffer, 2001; Harris et al, 1989; Russell et al, 1987; Thompson & Sawtell, 2006). HSV-1 mutants that fail to express ICP0 are highly sensitive to cell mediated repression, especially during low multiplicity infections of restrictive cell lines, such as human fibroblasts or hepatocytes. Consequently, these mutant viruses can establish quiescent infection that in some respects resembles latency (reviewed in Efstathiou & Preston, 2005). Since ICP0 is a non-essential gene, ICP0-null mutants are capable of replicating in cell culture when high MOIs are used. However, one has to take into the account the probability of initiating productive infection by ICP0-null mutant viruses when interpreting ICP0-null mutant HSV-1 phenotype (see Chapter 1, Section 1.6.3.5; reviewed in Everett, 2006).

As previously mentioned on several occasions, anti-HSV-1 intrinsic resistance is conferred by number of pre-existing cellular proteins, and analogous mechanisms are thought to operate during the early stages of HCMV infection (Chapter 4, Section 4.1; and reviewed in Saffert & Kalejta, 2008; Tavalai & Stamminger, 2008). ICP0 performs an essential function of counteracting cellular intrinsic antiviral resistance, which allows wt HSV-1 establishing a successful productive infection. However, the mechanisms which are utilized by cellular proteins to allow this process are incompletely understood and in some cases controversial. Therefore further studies on the proteins that are involved in intrinsic cellular defences against HSV-1 infection are required.

ND10 integrity is disrupted at early times after wt HSV-1 infection (Everett & Maul, 1994; Everett & Zafirooulos, 2004; Maul et al, 1993) due to the degradation of the SUMO-modified forms of Sp100 and PML, which is mediated by E3 ubiquitin ligase activity of ICP0 (Boutell et al, 2003; Boutell et al, 2002; Chelbi-Alix & de The, 1999; Everett et al, 1998a; Everett et al, 1998b). These reports provided evidence on the importance of both

PML and Sp100 in cellular anti-HSV-1 defence, which is antagonised by ICP0. During wt HSV-1 infection, PML and Sp100, as well as other ND10 proteins, are re-distributed to the sites closely associated with the incoming viral genomes, however this re-distribution is very transient and difficult to detect due to the activities of ICP0. In the absence of ICP0, these proteins are not degraded but instead are rapidly recruited to sites that are closely associated with parental viral genomes and early replication compartments (Everett & Murray, 2005), suggesting the potential role of ND10 proteins in the repression of ICP0-null mutant viral genomes that occurs at low multiplicities of infection. Consistent with this hypothesis, the recruitment is extremely rapid, and there is a close correlation between the abilities of mutant forms of ICP0 to inhibit this process and to stimulate lytic infection (Everett et al, 2007; Everett et al, 2009). This hypothesis was supported by the findings that in PML or Sp100 depleted cells ICP0-null mutant HSV-1 gene expression and plaque forming efficiencies were significantly increased (Everett et al, 2008; Everett et al, 2006).

In order to identify additional ND10 proteins than may be involved in this repression mechanism, the current part of the study has concentrated on the roles of ATRX and hDaxx in the context of HSV-1 infection. As previously discussed (Chapter 4), during HCMV infection, the viral tegument protein pp71 interacts with hDaxx and promotes its degradation, a process which is important for the initiation of efficient HCMV gene expression (Cantrell & Bresnahan, 2005; Cantrell & Bresnahan, 2006; Hofmann et al, 2002; Hwang & Kalejta, 2007; Ishov et al, 2002; Preston & Nicholl, 2006; Saffert & Kalejta, 2006; Saffert & Kalejta, 2007). ATRX, on the other hand, is displaced from ND10 by pp71, which is functionally significant for the ability of pp71 to stimulate gene expression since removal of ATRX supports substantially increased replication of pp71-null mutant HCMV (Lukashchuk et al, 2008). Therefore, ATRX and hDaxx have been confirmed as components of a cell-mediated intrinsic defence against HCMV infection, which is counteracted by pp71 (see Chapter 4). It is therefore possible that similar mechanisms apply in HSV-1 infection, assuming that ICP0 acts as a viral countermeasure in the cellular defences. This hypothesis has become the basis of the current chapter.

Since intrinsic cellular defences are efficiently overcome by ICP0, ICP0-null mutant HSV-1 has been utilised in the next set of the experiments in order to determine whether ATRX and hDaxx contribute to the cellular repression mechanism that occurs in the absence of ICP0. As described in previous chapter, RNA interference approach was used to generate ATRX- and hDaxx-depleted cell lines. The results provide the novel evidence for the role

of ATRX and hDaxx in cell-mediated anti-HSV response and suggest that the two components act as a complex during this process.

## **5.2 Results**

A general hypothesis underlying the research described in this thesis is that the recruitment of the ND10 components (and other proteins) to the sites closely associated with the incoming HSV-1 genomes and sites of IE transcription represents a cellular response to virus infection that may lead to viral genome repression. The function of ICP0 in counteracting the cellular repression mechanism correlates with this recruitment being very transient during the wild-type HSV-1 infection. In the absence of ICP0 however this recruitment is much more long-lived and can be visualised easily in cells at the edge of developing ICP0-null mutant HSV-1 plaques (Everett & Murray, 2005). The more stable recruitment in the plaque edge cells, where individual cells are infected at very high multiplicities, is not representative of ND10-mediated repression of the viral genomes in those cells, since intrinsic defence mechanisms have been saturated. What this phenomenon does represent is that at low MOIs of ICP0-null mutant HSV-1 infections association of the viral genomes and ND10 components subsequently results in silencing of the viral genomes and establishment of quiescence. Based on the general assumption that viral incoming DNA is repressed in the infected cells, the hypothesis that this may be performed, in part, by the chromatin-remodelling complexes such as ATRX and hDaxx forms the basis of the present chapter.

### **5.2.1 Analysis of ATRX and hDaxx redistribution in HSV-1 infected cells**

#### ***5.2.1.1 ATRX and hDaxx are recruited to the sites associated with incoming HSV-1 genomes***

In order to investigate the distribution of ATRX and hDaxx in HSV-1 infected cells, HF or HepaRG cells were infected with wt or ICP0-null mutant HSV-1 and the cells were fixed the following day for immunofluorescence analysis.

It was demonstrated earlier that both hDaxx and ATRX co-localise at ND10 with the major ND10 component PML (Figure 3.2). During wild-type HSV-1 infection both ATRX and hDaxx become rapidly dispersed in the great majority of the infected cells in which ICP4 is

expressed at readily detectable levels (Figure 5.1, panels A-B). As in previous studies (Everett & Murray, 2005; Everett et al, 2008; Everett et al, 2006), IE protein ICP4 is used here as a marker of the initiation of IE transcription and localization of HSV-1 genomes through its strong interaction with viral DNA (Pizer et al, 1991). However, in rare cells at the edges of developing wt HSV-1 plaques it was possible to detect re-distribution of ATRX and hDaxx to asymmetric foci in the apparent absence of ICP4 expression or where only very low ICP4 levels were detected (Figure 5.1, panels C-D). Based on the data presented in these four panels (Figure 5.1), recruitment of hDaxx and ATRX in these cells, before ICP4 has accumulated to detectable levels, emphasises the rapidity of the cellular response to the invasion of foreign viral DNA, followed by a viral counteracting response mediated by ICP0. In the absence of ICP0, both ATRX and hDaxx re-localise in a far more stable manner to the novel sites associated with viral genomes and early replication compartments (Figure 5.1, panels E and F).

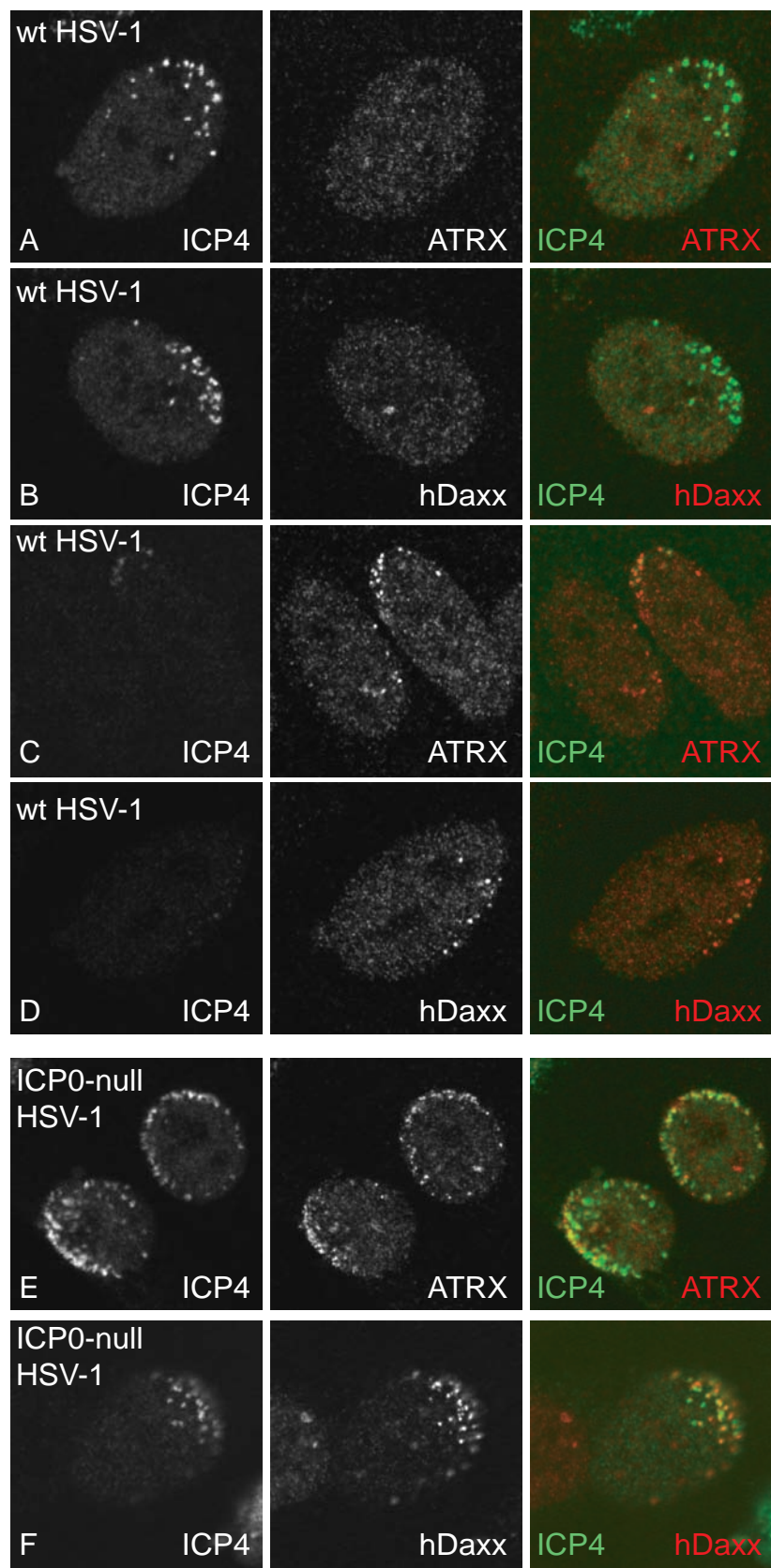


**Figure 5.1 ATRX and hDaxx are recruited to the sites of incoming HSV-1 genomes in HepaRG cells**

Immunofluorescence images of HepaRG cells infected with wt HSV-1 (MOI 0.001; panels A-D) and ICP0-null mutant HSV-1 (MOI 0.5; panels E-F) at the edge of a developing plaque. Cells were processed for immunofluorescence analysis 24 hours post infection and co-stained for ICP4 (58S) and ATRX (39F; panels A and C), or ICP4 and hDaxx (07-471, panels B and D). In panel F, hDaxx was detected with anti-rabbit r1866 serum. Secondary antibodies were anti-mouse FITC-conjugated (green, panels A-H), anti-rabbit AlexaFluor-conjugated 555 (red, panels A-D) or anti-rabbit Cy3-conjugated (red, E-F).

### *5.2.1.2 Analysis of hDaxx dynamics at the sites of ICP0-null HSV-1 genomes in comparison to normal ND10*

Previous studies established the highly dynamic nature of hDaxx at ND10 in cells expressing EYFP-hDaxx using a baculovirus vector (Everett & Murray, 2005). If ATRX and hDaxx are more stably present at sites associated with ICP0-null mutant viral genomes rather than normal cellular ND10, and if the ATRX/hDaxx complex were to act as a repressor during the ICP0-null mutant infection, according to the data presented in Figure 5.1 (panels E and F), it would be expected that the mobility of the two proteins would be reduced at the sites associated with the ICP0-null mutant viral genomes in comparison to that at ND10 sites of uninfected cells. Construction of the cell line expressing fluorescent EYFP-tagged hDaxx, namely HD-ED, in which the protein has been re-introduced into hDaxx-depleted cells (see Figure 3.11) allowed measuring the dynamics of hDaxx foci at the sites of the incoming viral genomes and comparing with those at ND10 in mock-infected cells using FRAP (Figure 5.2). HD-ED cells were infected with *dl1403* strain at MOI 1.2, infection was allowed to proceed overnight and the cells were processed for FRAP analysis, as described in Materials and Methods (Chapter 2, Section 2.5.2.5). Three or four dots per cell were chosen for photobleaching, as shown on Figure 5.2 A. Figure 5.2 B represents the mean values obtained from measuring fluorescence recovery times of a total of 43 hDaxx foci taken over the two independent experiments. Since the overall purpose of the experiment was to show a general trend and comparison of the recovery times, for simplicity error bars were omitted.

The overall decrease of about 20% in the fluorescence recovery values at the end of a scan after bleaching each dot was observed in HD-ED cells at the plaque edge compared to that in ND10 in uninfected cells. Although hDaxx foci at the sites associated with the incoming *dl1403* genomes appeared to be highly dynamic, this result supports the hypothesis that hDaxx dynamics is reduced at the sites of the incoming ICP0-null mutant viral genomes compared to that at ND10 of the uninfected cells, thereby allowing its accumulation at these sites in preference to pre-existing ND10.

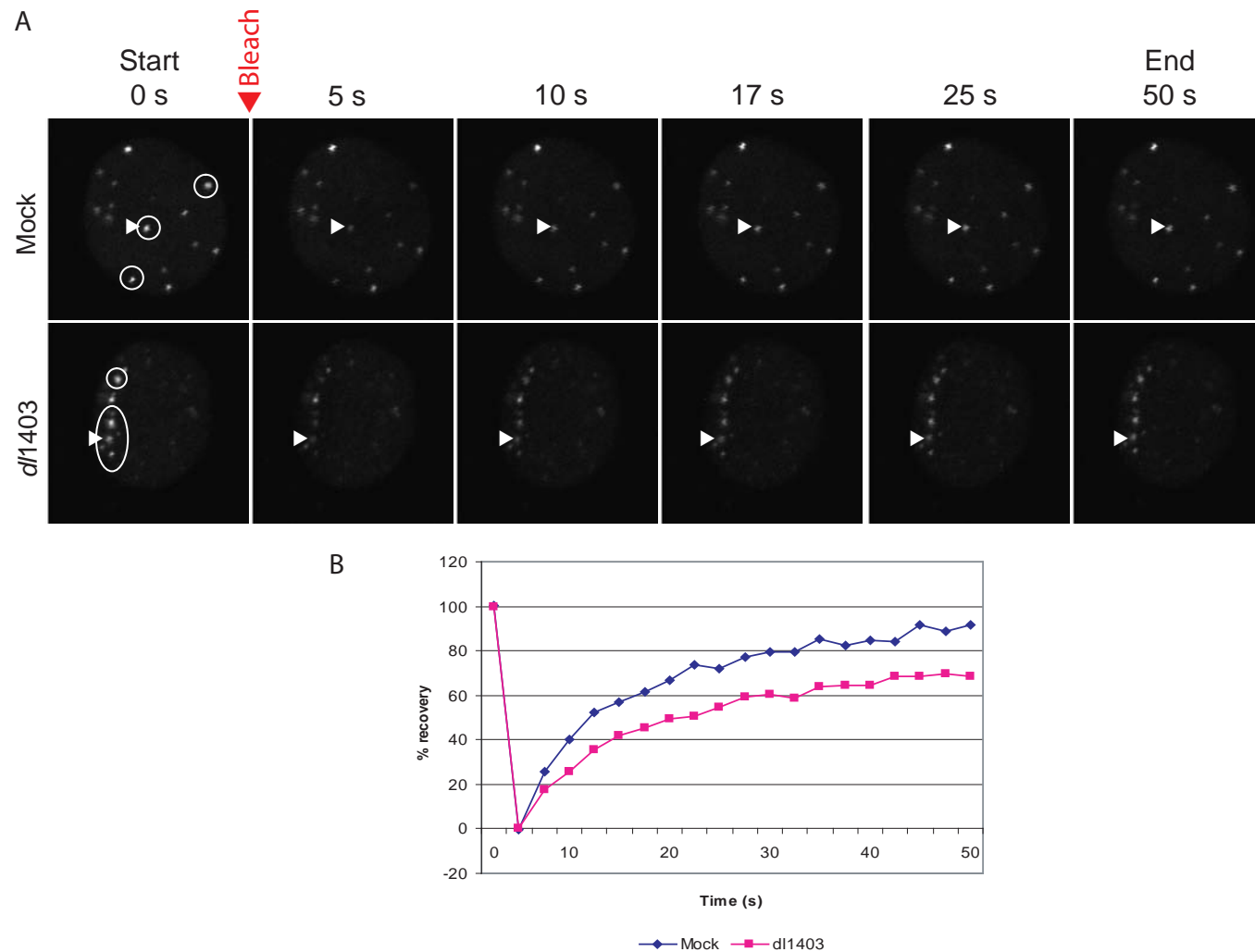


**Figure 5.2 Dynamics of EYFP-hDaxx foci at ND10 of the mock-infected cells and sites associated with ICP0-null mutant HSV-1 genomes**

For fluorescence recovery after photobleaching (FRAP) analysis, cells were seeded into a 35 mm tissue culture dish with a coverslip fixed over a hole into its centre and infected with *dl1403* at MOI 1.2. A: Detection of the cells at the edge of the developing plaque was achieved by visual scanning of the cells with asymmetric redistributions of EYFP-hDaxx foci. Representative cells are shown at various time points after photobleaching. Time 0 and 50 represent the start and the end of the image scan, respectively. The representative bleached dots are indicated by an arrow. Note, 3 dots in the mock-infected cells and 4 dots in the *dl1403* infected cells were bleached (circled). B: The graph shows the mean values of percent recovery of the fluorescence, obtained from a total of approximately 40 foci over the 2 independent experiments.

### ***5.2.1.3 ATRX recruitment to the sites associated with the incoming HSV-1 genomes is not dependent on PML***

PML, being the major ND10 component, is required for ND10 localisation of Sp100 and hDaxx, as previously demonstrated (Everett et al, 2006). However, the recruitment of both Sp100 and hDaxx to the sites of the incoming viral genomes in the absence of ICP0 occurs independently of PML (Everett et al, 2006), suggesting a different mechanism targeting these proteins to HSV-1 genomes. By analogy with these observations, ATRX localisation in uninfected or *dl1403*-infected PML-depleted fibroblasts was analysed. The HF-ShPML cells for this experiment were generated by Anne Orr (MRC Virology Unit). As expected, in uninfected or mock-infected HF-ShPML cells ATRX was dispersed (Figure 5.3, panels A and B), confirming the role of PML in the integrity of ND10 structures. In cells infected with the wt virus and analysed at 2 hpi, when IE gene expression had just been initiated, ATRX first re-localised to ICP0-associated foci in cells expressing very low levels of the viral protein (Figure 5.3, panel C), followed by its displacement from these newly formed foci and accumulation of ICP0 at the novel punctate structures (Figure 5.3, panel D). Whether this displacement occurs as a result of ICP0-mediated PML degradation or through a more direct effect on ATRX causing its displacement from the newly formed foci is unclear from this experiment, but this issue is considered later in this chapter. In the absence of ICP0 in the infected HF-ShPML cells at the edge of the developing plaque, ATRX was recruited to the sites associated with *dl1403* genomes and co-localised with ICP4 in an asymmetric manner (Figure 5.3, panel E) consistent with data shown in Figure 5.1, and demonstrating that PML is not required for ATRX recruitment to HSV-1 genome associated foci. Taking these data together with previous work (Everett et al, 2006), it is concluded that the recruitment of the ATRX/hDaxx complex to the sites associated with the incoming HSV-1 genomes is PML-independent.

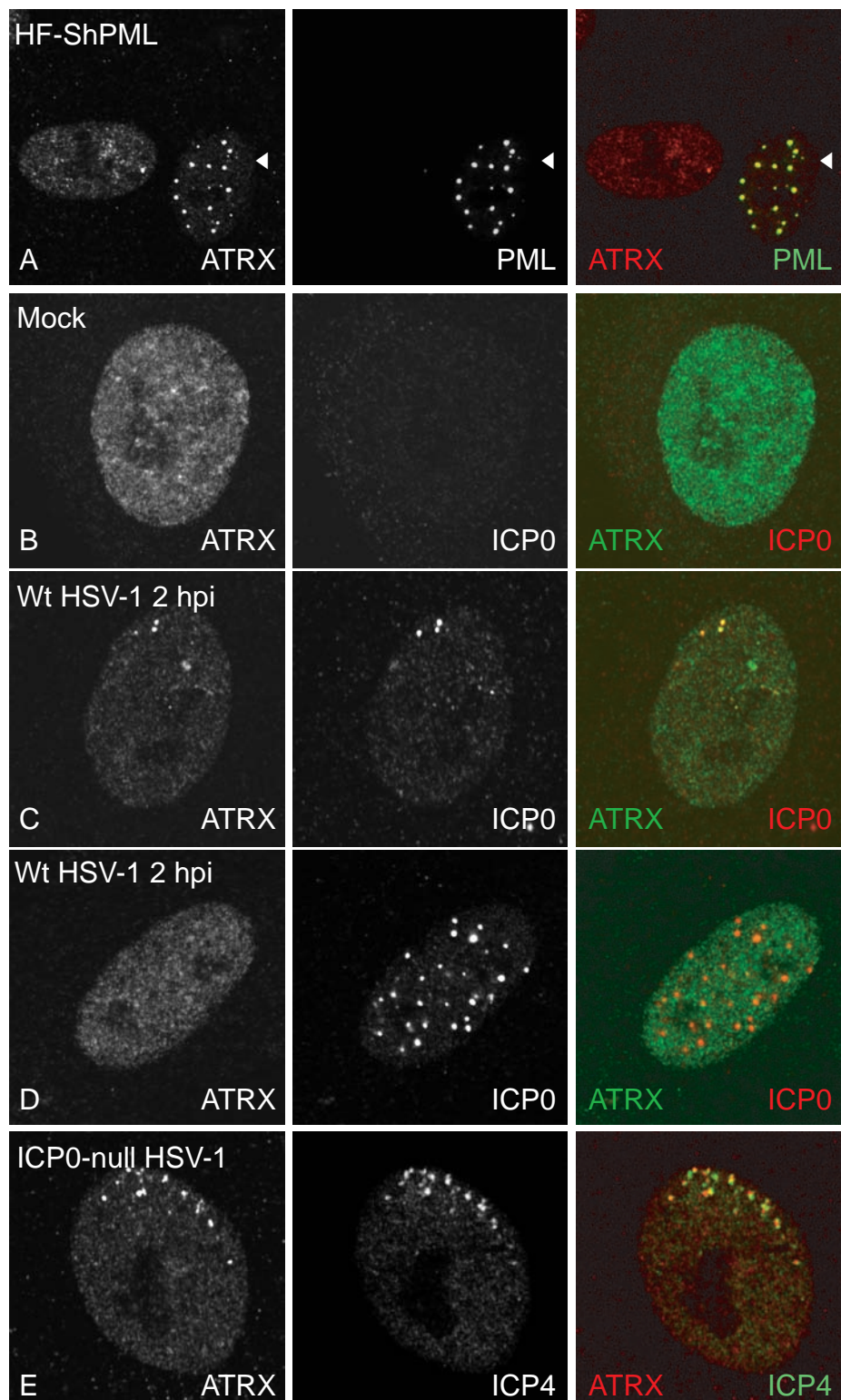


**Figure 5.3 PML is not required for ATRX recruitment to HSV-1 genome foci at the early stages of infection**

HF-ShPML cells were seeded onto coverslips and either left untreated (A), mock-infected (B), infected with 17+ at MOI 2.0 and fixed at 2 h (C-D), or with *dll1403* at MOI 0.5 and fixed the following day for the analysis. A: Uninfected cells were co-stained with anti-ATRX H300 and anti-PML 5E10 antibodies. A PML-positive cell, where ATRX localises to ND10 is indicated by an arrowhead, in comparison to a PML-depleted cell, where ATRX is dispersed. B-D: Wt HSV-1-infected cells were co-stained for ATRX and ICP0 (11060). E: ICP0-null HSV-1-infected cells were co-stained for ATRX and ICP4 (58S). The secondary antibody mix contained either anti-mouse FITC-conjugated and anti-rabbit Cy3-conjugated antibodies (panels A and E), or anti-mouse Cy3-conjugated and anti-rabbit AlexaFluor-conjugated 488 antibodies (panels B-D).

#### ***5.2.1.4 ATRX recruitment to viral genome foci requires its interaction with hDaxx***

The requirement of hDaxx in ATRX targeting to ND10 has been demonstrated in the current and previous studies (Ishov et al, 2004; Lukashchuk et al, 2008; Tang et al, 2004 and Figures 3.8 and 3.9). Hence, it was of interest to analyse the requirement of hDaxx in ATRX recruitment to ICP0 null mutant HSV-1 genomes during the early stages of infection, as a step towards investigating the role of the complex formed between the two proteins in HSV-1 infection. In order to do this, hDaxx-depleted HALD2 cells (see Figure 3.9) along with control HALL cells were infected with ICP0-null mutant HSV-1, and the cells at the edge of developing plaques were analysed by immunofluorescence (Figure 5.4). In uninfected hDaxx-depleted cells, ATRX fails to localise to ND10 and shows a dispersed distribution (Figure 3.9). Surprisingly, in ICP0-null mutant HSV-1 infected hDaxx-depleted cells, ATRX was no longer recruited to ICP4 foci in the absence of hDaxx (Figure 5.4, panel B) and showed dispersed distribution as in uninfected HALD2 cells, whereas PML was recruited normally (Figure 5.4, panel D). These results imply that if the recruitment of ATRX to sites associated with viral genomes has functional significance, then hDaxx may be an important factor in regulating the functions of ATRX and may serve as the essential factor that targets ATRX to viral genomes. This hypothesis was therefore investigated in more detail.

Chapter 3 has described the use of a system in which hDaxx is re-introduced at close to endogenous levels and is easily detectable by the N-terminal EYFP tag (Figures 3.10 and 3.11). This system therefore allowed the study of the role of hDaxx in more detail by introducing mutations that may affect its function. Using lentiviral vectors expressing the wt EYFP-hDaxx fusion protein and a derivative with the deletion of the PAH1 responsible for its interaction with ATRX, cell lines reconstituted with wt and mutant hDaxx proteins were produced and characterised as described in Chapter 3 (Figures 3.12 and 3.13). In summary of the data shown earlier, fusion protein EYFP-hDaxx targets ATRX back to ND10 but ATRX-interaction deficient mutant EYFP-hDaxx $\Delta$ PAH1 does not, although the mutant hDaxx protein still localises to ND10. Disruption of the interaction between ATRX and hDaxx has been confirmed by CoIP assays (Figure 3.12, C). The current section investigates the effect of re-introducing wt EYFP-hDaxx or mutant EYFP-hDaxx $\Delta$ PAH1 on ATRX recruitment to the sites associated with the incoming HSV-1 genomes in the absence of ICP0.

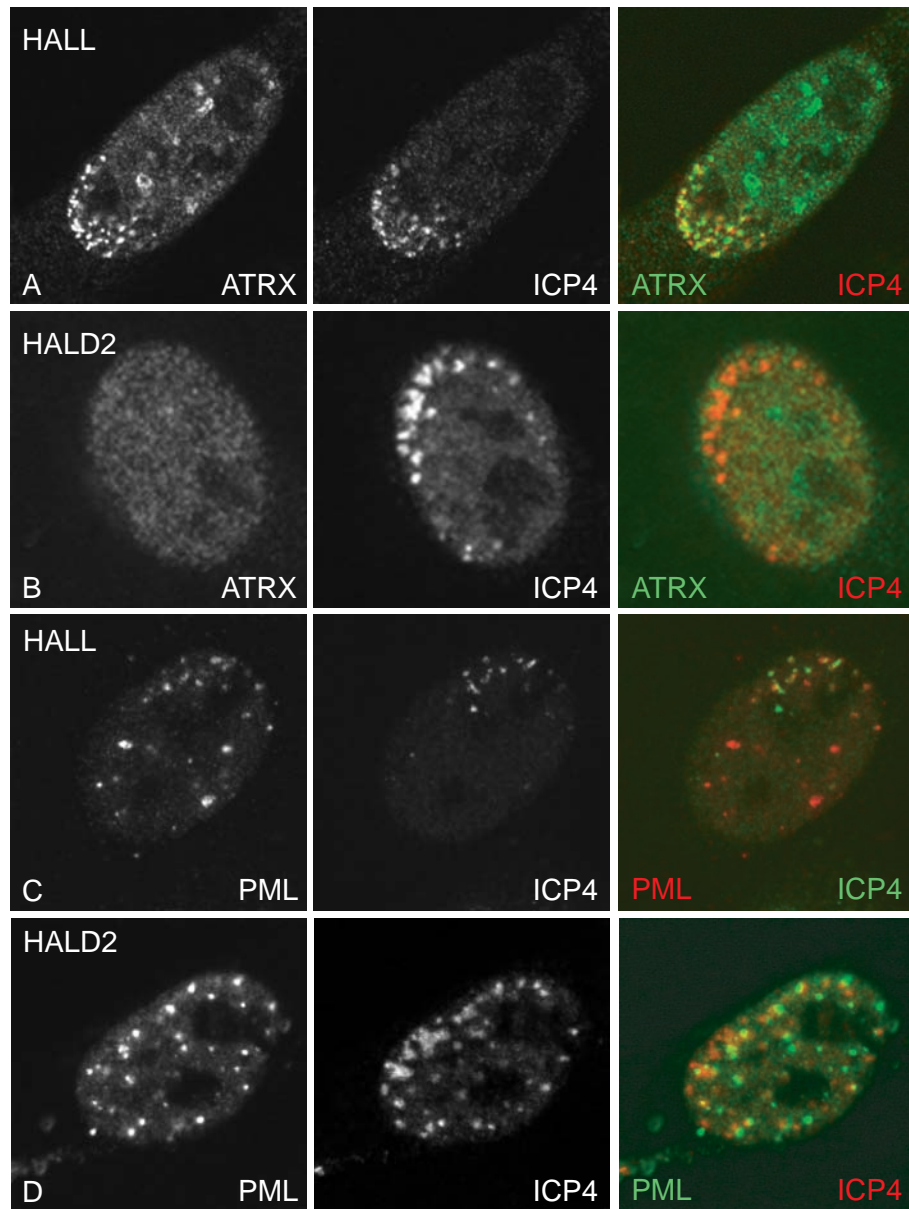


**Figure 5.4 ATRX is not recruited to the sites associated with ICP0-null mutant HSV-1 genomes in hDaxx-depleted HepaRG cells**

Immunofluorescence analysis of ATRX localisation in cells at the edge of ICP0-null mutant HSV-1 plaques in HALL (A and C) and HALD2 (B and D) cells. Cells were infected at MOI 0.5 (HALL) or 0.1 (HALD2) PFU/cell and co-stained the following day with anti-ATRX H300 and anti-ICP4 58S antibodies (A and B), or anti-PML 5E10 and anti-ICP4 58S antibodies (C and D). Secondary antibodies were anti-rabbit AlexaFluor-conjugated 488 and anti-mouse Cy3-conjugated (A, B and D) or anti-rabbit AlexaFluor-conjugated 555 and anti-mouse FITC-conjugated (C).

HD-ED (Figure 5.5) or HD. $\Delta$ PAH (Figure 5.6) cells, along with control cell lines HepaRG and hDaxx-depleted HD-E, were infected with *dll1403* at MOI 1 or 0.2, respectively, and stained the following day for ND10 and ICP4 protein analysis. The reason for the lower MOI used for infection of HD. $\Delta$ PAH cells will be evident in later sections of this chapter. In the absence of hDaxx, using the hDaxx-depleted cell line HD-E that expressed EYFP, ATRX remained dispersed within cells at the periphery of the *dll1403* plaques, when ICP4 foci were readily detectable (Figure 5.5 panel B). This was consistent with the results obtained with HALD2 cells, suggesting EYFP expression did not have an effect on this recruitment. HD-E will later be used as a control cell line in a number of assays. Upon re-introduction of EYFP-hDaxx, ATRX was recruited back into the sites of the incoming viral genomes (Figure 5.5, panel C), in the same way as in non-transduced HepaRG cells (panel A), supporting the evidence for the importance of hDaxx for ATRX recruitment to the viral genome foci. EYFP expression in hDaxx-depleted cells HD-E or re-introduction of EYFP-hDaxx in HD-ED cells did not have any detectable effect on the recruitment of PML (panels D-E). Notably, PML recruitment in EYFP-hDaxx expressing cells occurred rapidly, even before ICP4 expression could be detected (panel E). Infected HD-ED cells were also analysed with an anti-Daxx antibody, showing precise co-localisation with EYFP-hDaxx signal (Figure 5.5, panel F).

Consistent with its PAH1 dependent localisation to ND10 in uninfected cells (see Figure 3.13), ATRX remained dispersed in HD. $\Delta$ PAH cells at the edge of a developing ICP0-null mutant HSV-1 plaque, even though the mutant hDaxx protein was efficiently recruited to sites associated with viral genomes (Figure 5.6, panel A). Recruitment of PML and EYFP-hDaxx $\Delta$ PAH1 itself occurred normally in HD. $\Delta$ PAH cells (panels B and C). These results confirm that the interaction between ATRX and hDaxx is required for ATRX recruitment to the viral genome associated sites, and identify the hDaxx ATRX-interaction domain PAH1 as being important for this process. Therefore, the possibility that ATRX and hDaxx may act as a complex in HSV-1 infection was investigated further.

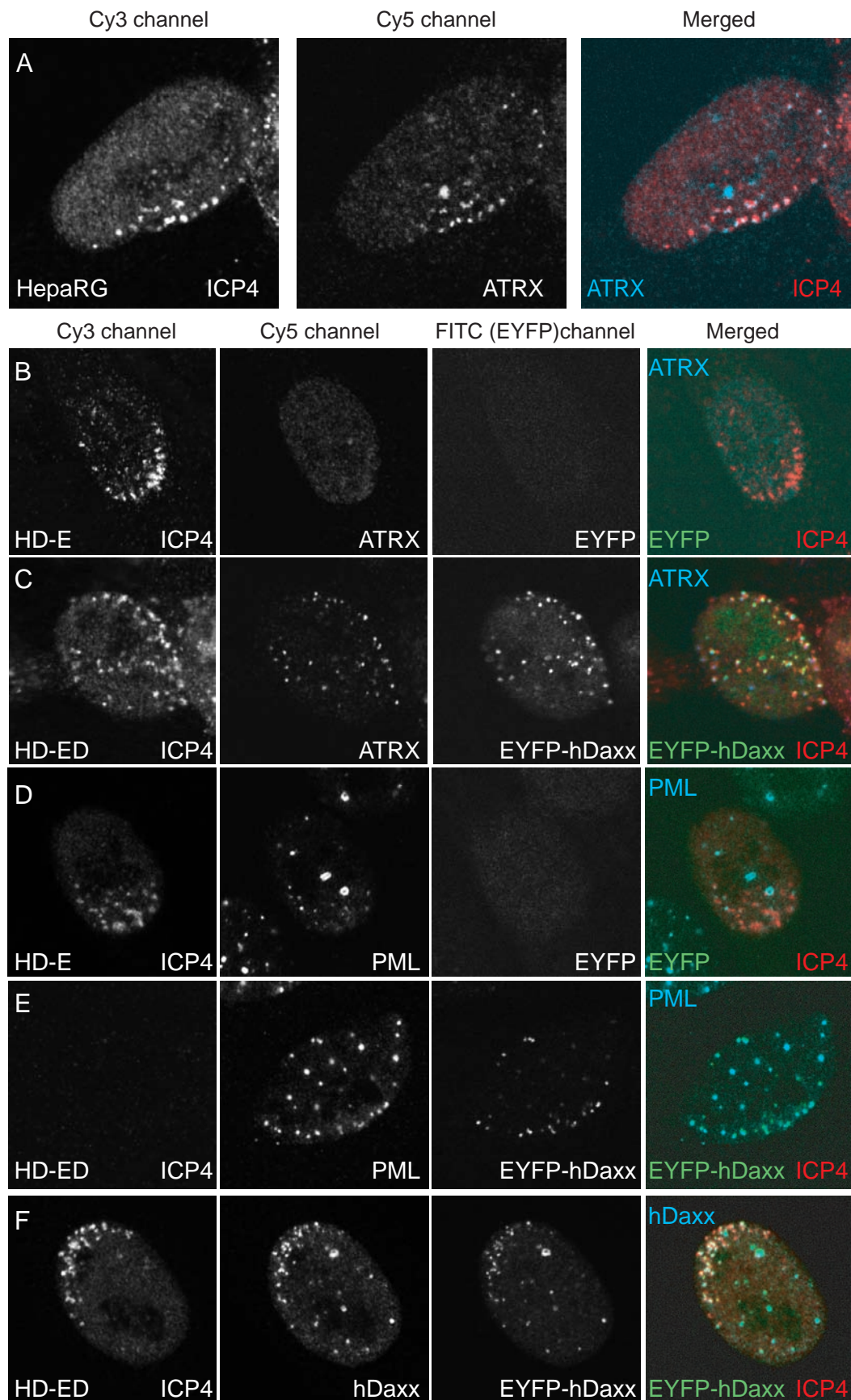


**Figure 5.5 EYFP-hDaxx targets ATRX back into foci associated with incoming viral genomes during ICP0-null mutant HSV-1 infection**

HepaRG, HD-E and HD-ED cells were infected with *dl1403* and cells processed for immunofluorescence the following day by co-staining for ICP4 (58S; panels A-F) and ATRX (H300; panels A-C), PML (r8; panels D-E) or hDaxx (07-471; panel F). Secondary antibodies were anti-mouse AlexaFluor 555-conjugated and anti-rabbit Cy5-conjugated. EYFP signal (green) resulted from autofluorescence of EYFP alone or EYFP-hDaxx, as indicated.

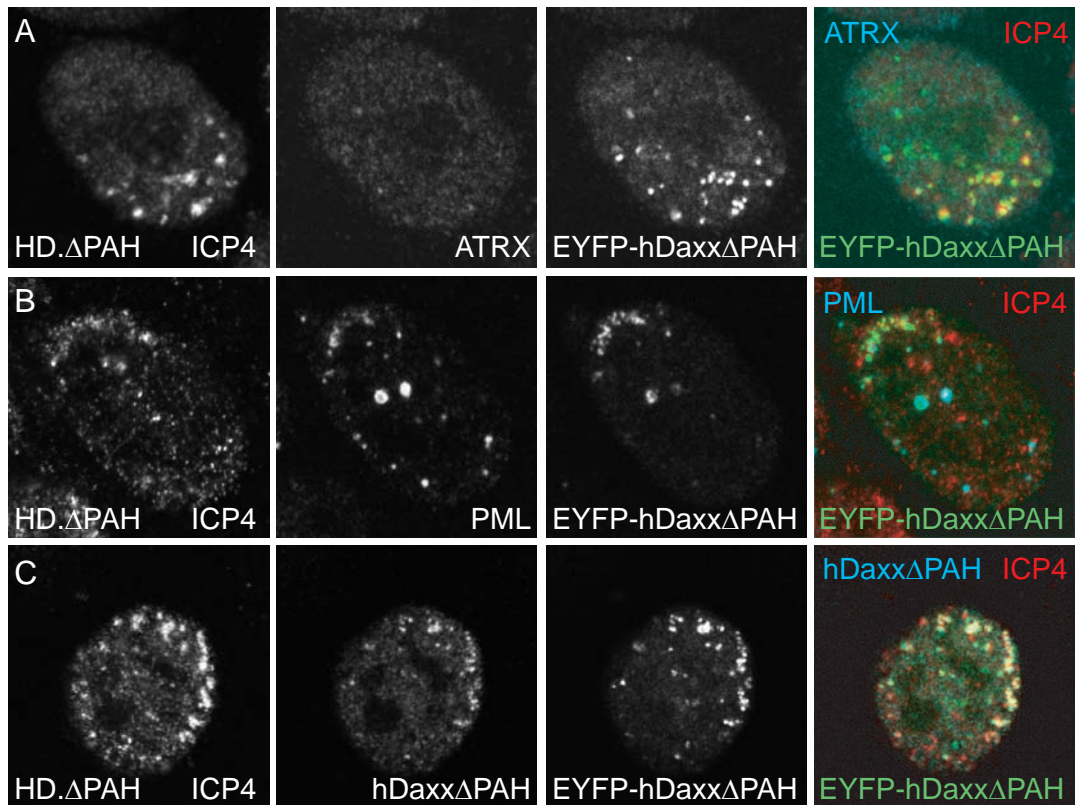


**Figure 5.6 Interaction between hDaxx and ATRX is required for ATRX recruitment to incoming viral genomes at the edge of ICP0-null mutant HSV-1 plaque**

HD.ΔPAH cells were infected with *dl1403* and processed for immunofluorescence the following day by co-staining for ICP4 (58S; panels A-C) and ATRX (H300; panels A), PML (r8; panel B) or hDaxx (07-471; panel C). Secondary antibodies were anti-mouse AlexaFluor 555-conjugated and anti-rabbit Cy5-conjugated. EYFP signal (green) resulted from autofluorescence.

## **5.2.2 The role of ATRX/hDaxx complex in the repression of HSV-1 infection in the absence of ICP0**

Previous reports have demonstrated that depletion of either PML or Sp100 improves the efficiency of ICP0-null mutant HSV-1 infection, and simultaneous depletion of both improves infection yet further. Both PML and Sp100 are recruited to sites closely associated with ICP0-null mutant HSV-1 genomes at the early stages of infection, so this phenomenon correlates well with their role in restricting ICP0-null mutant virus gene expression (Everett et al, 2008; Everett et al, 2006). In summary of the data demonstrated above, both ATRX and hDaxx are recruited to the sites associated with the HSV-1 incoming genomes in the absence of ICP0, and recruitment of ATRX requires its interaction with hDaxx. By analogy with previously published work (Everett et al, 2008; Everett et al, 2006), the hypothesis that recruitment of ATRX and hDaxx may also contribute to cell mediated repression of ICP0-null HSV-1 gene expression, particularly since ATRX and hDaxx constitute a chromatin-associated complex with repressive properties (Tang et al, 2004; Xue et al, 2003), underlies the remainder of the current chapter. The data presented below demonstrate the effect of ATRX or hDaxx depletion in the efficiency of wt and ICP0-null mutant HSV-1 infection from the perspective of viral gene expression and plaque forming efficiencies.

### ***5.2.2.1 Depletion of ATRX supports increased efficiency of ICP0-null mutant HSV-1 infection***

For the analysis of the effect of ATRX depletion on viral infection, both HF and HepaRG cells depleted of ATRX were utilized (described in Chapter 3, Figures 3.5-3.9). In order to assess the effect of ATRX on HSV-1 IE and Early gene expression, the control cells expressing shGFP or shLuci and ATRX-depleted cells were infected at MOI of 2 PFU/cell and expression of typical IE and Early proteins (ICP4 and UL42, respectively) was analysed by western blot at various time points over the course of an 8 hour infection (Figure 5.7 A-D). Both ICP4 and UL42 proteins are essential for HSV-1 replication. Due to the ability of ICP0 to counteract intrinsic cellular defences, depletion of ATRX in different cell types did not affect the expression of ICP4 or UL42 during wt HSV-1 infection (Figure 5.7, A and B), consistent with previously published work (Everett et al, 2008; Everett et al, 2006). When cells were infected with ICP0-null mutant HSV-1, however, ATRX depletion resulted in a slight but reproducible increase in UL42

expression (Figure 5.7, C and D). No differences in ICP4 expression were detected. These results suggest that ATRX contributes to the normally efficient repression of ICP0-null mutant HSV-1 gene expression.

These observations were extended to analyse the efficiency of plaque formation of both wt and ICP0-null mutant HSV-1 in both cell types. To achieve this, recombinant HSV-1 strains with the insertion of a *lacZ* marker in place of the *tk* gene were used. This insertion allows expression of  $\beta$ -galactosidase in the infected cells, hence providing a convenient way of determining plaque numbers at 24 hours post infection. Control and ATRX-depleted cells were infected using sequential dilutions of wt and mutant viruses and relative plaque forming efficiencies were determined following three independent experiments for each set of cells (Figure 5.7, E-H). No significant differences in the plaque numbers between wild-type HSV-1-infected control or ATRX-depleted cells were seen (Figure 5.7, panels E and F). During the infection with ICP0-null mutant virus, however, averages of a 4-fold increase in HF-ShATRAX cells and a 6-fold increase in HAA cells in plaque forming efficiencies were observed when compared to control HF-ShGFP or HALL cells, respectively (Figure 5.7, G and H). The greater increase observed in HAA cells is probably a result of more stable depletion of ATRX in HepaRG cell lines, and could not be attributed to control cell lines expressing different shRNAs (shGFP vs shLuci). This data provides additional support for the repressive activities of ATRX in ICP0-null mutant HSV-1 replication.

---

**Figure 5.7 The effects of ATRX depletion on the infection with wt and ICP0-null mutant HSV-1.** A-D: Analysis of viral gene expression. HF or HepaRG cells depleted of ATRX, and control cell lines expressing shGFP or shLuci, respectively, were infected with wt HSV-1 17+ (wt; A and B) or *dl1403* (ICP0-null; C and D) at MOI 2 and samples were harvested for analysis by western blot at 0, 4, 6 and 8 hours post infection (hpi). Membranes were probed for ICP4 (58S), UL42 (Z1F11) and actin (AL-40; loading control). E-F: Analysis of the plaque forming efficiency. ATRX-depleted HF (E and G) or HepaRG (F and H) and respective control cell lines were infected with *in1863* (E and F) or *dl1403/CMVlacZ* (G and H) at sequential dilutions. Cells were stained for  $\beta$ -galactosidase expression at approximately 24 hours post infection. Relative plaque numbers were determined against the numbers obtained on control infected cells. The plots represent mean values obtained from three independent experiments. Error bars are standard error values.

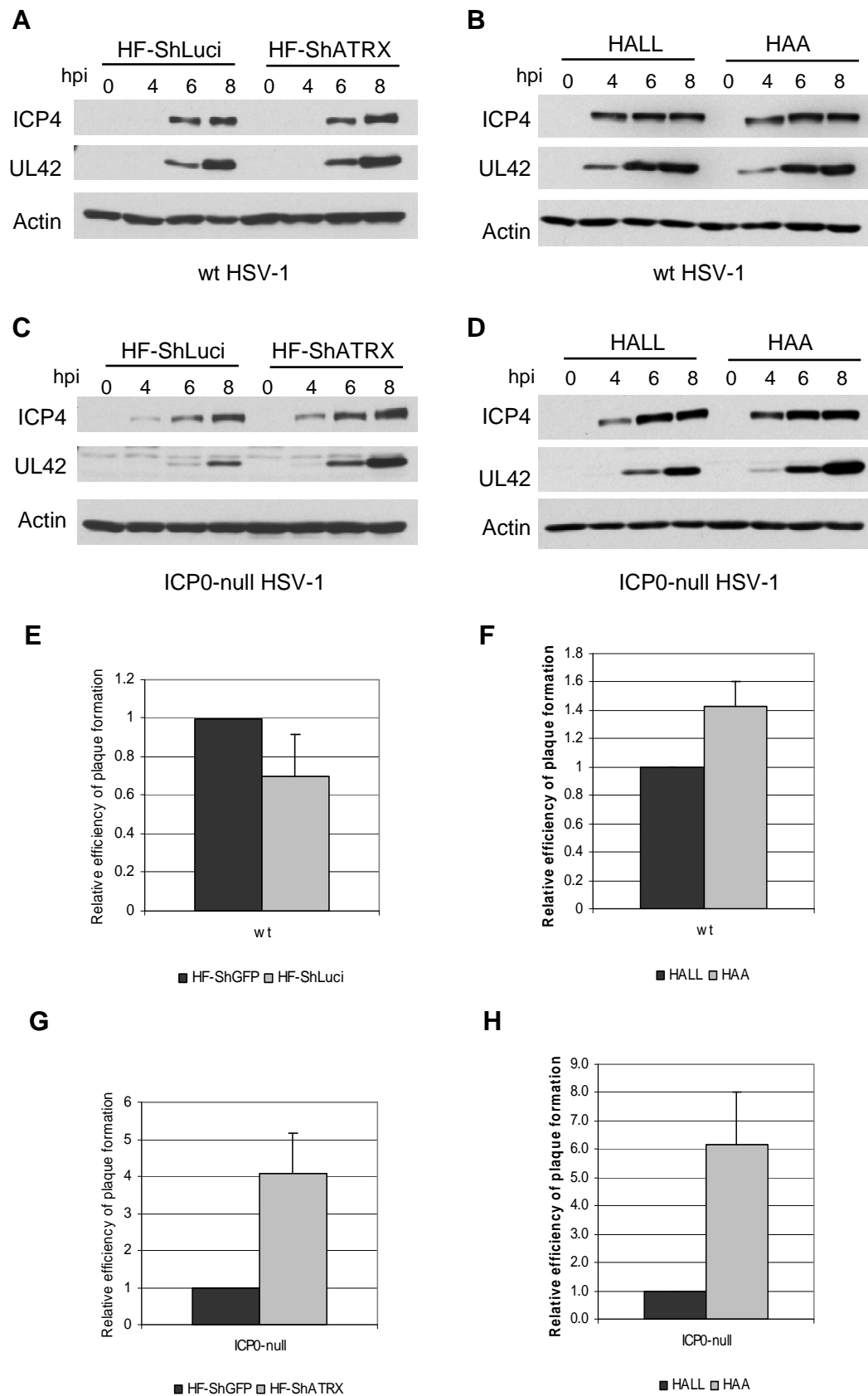


**Figure 5.7** The effects of ATRX depletion on the infection with wt and ICP0-null mutant HSV-1

Legend on the previous page.

#### ***5.2.2.2 hDaxx contributes to the repression of ICP0-null mutant HSV-1 infection***

Preliminary work indicated that hDaxx also contributes to the repression of ICP0-null mutant genomes in both HF-ShDaxx and HALD2 cells, using the same experimental approach as that described in Figure 5.7, A-D (Roger Everett and Anne Orr, personal communication). In order to test the optimal MOI for experiments in hDaxx-depleted cells, cells were infected with ICP0-null mutant HSV-1 strain *dl1403* at decreasing MOIs and samples were analysed for the levels of viral gene expression at 8 hours post infection (Figure 5.8, A). This analysis revealed that the most obvious differences in UL42 expression between HALD2 cells and HepaRG or HALL cells at this time of infection were at MOI of 2 PFU/cell. This increase in UL42 was more significant than that observed in ATRX-depleted cells. In addition, a slight increase in ICP4 expression in the absence of hDaxx was also detected in this assay, although this was variable between experiments. Based on these data (Figure 5.8, A) an MOI of 2 was chosen as the optimal virus amount to be used for further experiments (see below), consistent with the assays performed on ATRX-depleted cells (Figure 5.7 B and D).

Immunofluorescence analysis demonstrated that re-introduced EYFP-hDaxx targets ATRX back to the sites of the incoming *dl1403* genomes in the infected HD-ED cells (Figure 5.5). Hence, the use of HD-ED cells allowed investigation of whether re-introduction of hDaxx reverses the effect of hDaxx depletion in viral infection assays. Infection of HD-ED cells along with hDaxx-depleted HD-E and control cell lines which express endogenous hDaxx confirmed that this indeed was the case (Figure 5.8 B-C). Again, no differences in the levels of ICP4 and UL42 expression were detected during wt HSV-1 infection. In the absence of ICP0, however, there was a significant increase in UL42 production in HD-E cells, particularly when compared to transduced control HALL cells. These levels were reduced upon re-introduction of wt EYFP-hDaxx. The hDaxx blot provides confirmation of hDaxx depletion or re-introduction at the time of the experiment.

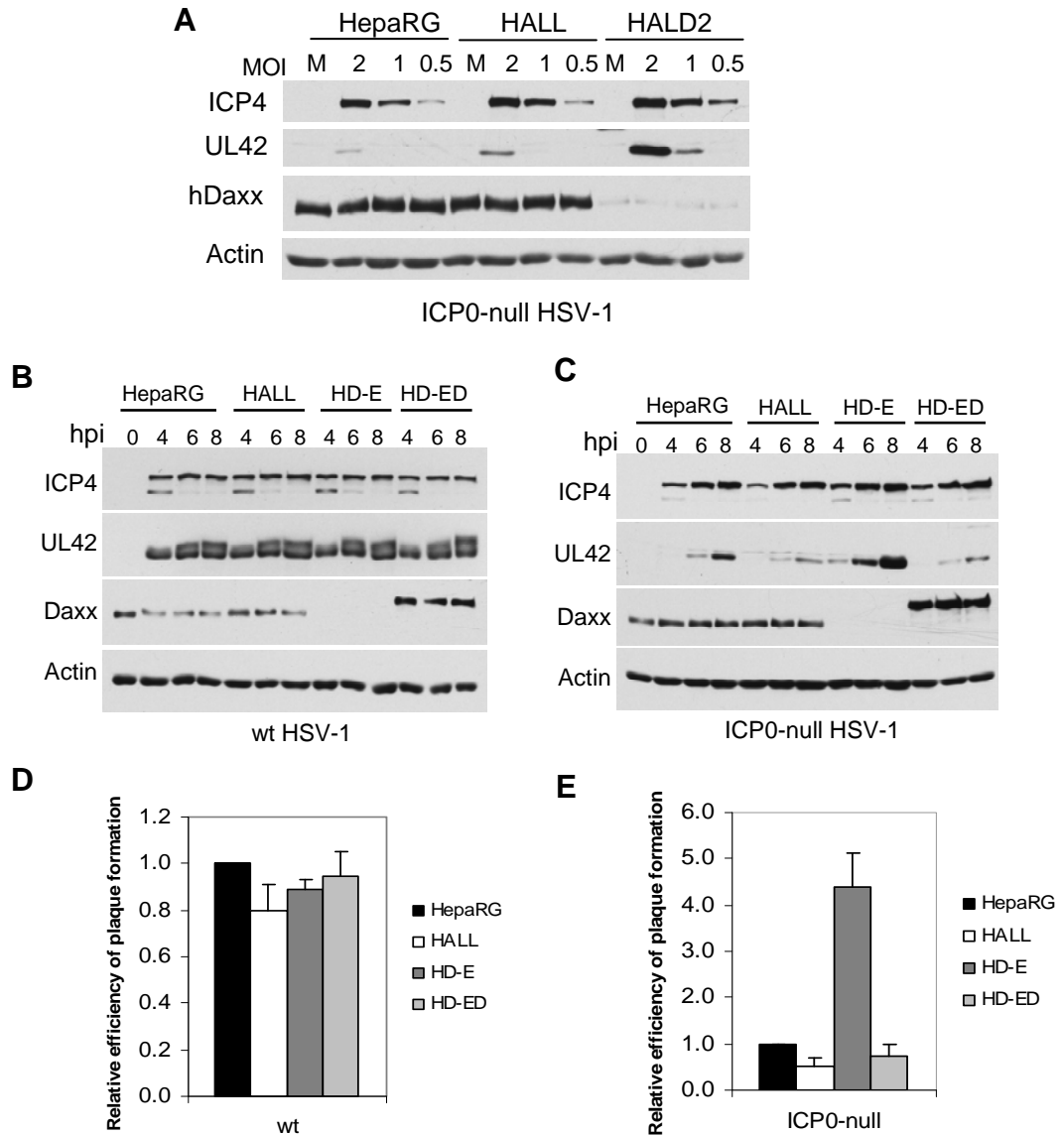


**Figure 5.8 hDaxx contributes to the efficient repression of ICP0-null mutant HSV-1**

A: Analysis of ICP0-null HSV-1 protein synthesis in hDaxx-depleted cells at different MOIs. HepaRG, HALL and HALD2 cells were mock-infected or infected with *dl1403* at MOI 2, 1 or 0.5 PFU/cell and samples were harvested for western blot analysis at 8 hpi. B and C: Kinetics of ICP4 and UL42 synthesis in hDaxx-depleted and hDaxx-reconstituted cells. HepaRG, HALL, HD-E and HD-ED cells were infected with 17+ (B) or *dl1403* (C) at MOI 2 and samples were harvested for western blot analysis at 0, 4, 6 and 8 hours post infection (hpi). In panels A-C membranes were probed for ICP4, UL42 and hDaxx using antibodies 58S, Z1F11 and D7810, respectively. Actin was a loading control. D and E: Efficiency of plaque formation of HSV-1 in hDaxx-depleted and hDaxx-reconstituted cells. Cells seeded into 24-well plates were infected with wt HSV-1 strain *in1863* (C) or ICP0-null HSV-1 *dl1403/CMVlacZ* (D) at sequential dilutions and stained for  $\beta$ -galactosidase expression 24 hours later. The plaque numbers are expressed as fold increase/decrease against control cells HepaRG. The plots represent mean values of plaque numbers relative to those in HepaRG cells, obtained from 4 independent experiments. Error bars represent standard error values.

Next, the effect of depletion or re-introduction of hDaxx on HSV-1 plaque formation was determined, using the same approach as above for ATRX-depleted cells. Similar to previous data, wt HSV-1 plaque formation was equally efficient in this set of cells (Figure 5.8 D), whereas that of ICP0-null mutant virus was increased approximately 5-fold in hDaxx-depleted HD-E cells when compared to naïve HepaRG cells. This equated to around a 10-fold increase when compared to control transduced HALL cells (Figure 5.8 E). Consistent with the viral protein expression analyses, re-introduction of EYFP-hDaxx reversed the effect of hDaxx depletion on plaque formation efficiency of ICP0-null mutant HSV-1 (Figure 5.8 E). Similar results to those in HD-E cells were obtained using HALD2 cells that express shDaxx2 only (data not shown), implying that EYFP expression in HD-E cells did not interfere with the assay. Taking all the data together, it is concluded that hDaxx contributes to the repression of HSV-1 infection in the absence of ICP0 to a higher extent than ATRX. Therefore, hDaxx recruitment to the sites of the incoming ICP0-null HSV-1 genomes is likely to be functionally significant for its repressive properties at these sites.

### ***5.2.2.3 The ATRX interaction region of hDaxx is required for fully efficient repression of ICP0-null mutant HSV-1 infection and gene expression***

The indication that the ATRX/hDaxx complex was responsible for targeting ATRX to the sites of the incoming viral genomes came from the observations that ATRX-interaction domain of hDaxx is required for ATRX recruitment into these foci. EYFP-hDaxx $\Delta$ PAH1, however, was still recruited to the sites of viral IE replication (see Figure 5.6). Hence, the next logical question to ask was whether the specific interaction between ATRX and hDaxx is required for the repressive properties of the ATRX/hDaxx complex during ICP0-null mutant HSV-1 infection.

Consistent with the data obtained with other cell lines during the wt HSV-1 infection, there were no differences in the efficiency of the wt virus gene expression or plaque formation between the control cell line HALL and HD-E, HD-ED or HD. $\Delta$ PAH cells (Figure 5.9, A and C). In the cells infected with ICP0-null mutant HSV-1, deletion of the hDaxx ATRX interaction domain resulted in an increase in ICP4 and UL42 production, which was comparable to that observed in hDaxx depleted cells (Figure 5.9, B). Moreover, the increase in ICP0-null mutant gene expression in HD-E and HD. $\Delta$ PAH cells was reflected in plaque formation efficiency assays. Whereas the plaque forming efficiency of wt HSV-1 was not significantly different in these cells (Figure 5.9, C), the increase in ICP0-null

mutant plaque formation in hDaxx-depleted HD-E cells could be reversed by reintroduction of wt hDaxx in HD-ED cells, but not by introduction of the ATRX-binding deficient hDaxx in HD. $\Delta$ PAH cells (Figure 5.9, D). It is therefore concluded that a functional ATRX/hDaxx complex is required for their role in the repression of ICP0-null mutant HSV-1 infection. This requirement is likely to be related to the chromatin-associated functions of the ATRX/hDaxx complex and identifies ATRX/hDaxx complex as a novel component in the regulation of ICP0-null mutant HSV-1 infection during the lytic cycle.

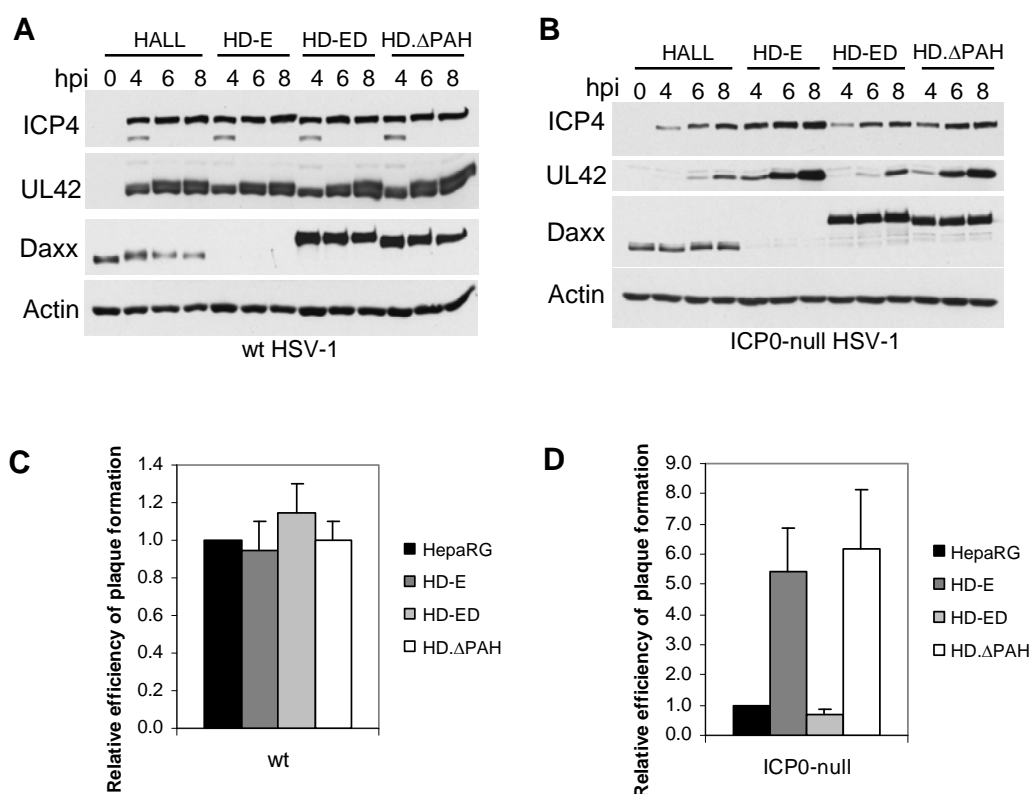


**Figure 5.9 The ATRX interaction region of hDaxx is required for fully efficient repression of ICP0-null mutant HSV-1 gene expression and plaque formation**

A and B: Cells were infected with the indicated viruses at MOI 2.0 PFU/cell and samples were harvested at the 0, 4, 6 and 8 hours post infection (hpi). Samples were resolved on a 7.5 % polyacrylamide gel. Membranes were probed for the expression of ICP4, UL42 and hDaxx using antibodies 58S, Z1F11 and D7810, respectively. Actin (AC-40) was a loading control. C and D: Cells seeded into 24-well plates were infected with wt HSV-1 strain *in1863* (C) or ICP0-null HSV-1 *dl1403/CMVlacZ* (D) at sequential dilutions and stained for  $\beta$ -galactosidase activity the following day to reveal the plaques. The plots represent mean values of plaque numbers relative to those in HepaRG cells, obtained from 3 independent experiments. Error bars represent standard error values.

### 5.2.3 The role of the ATRX/hDaxx complex in the establishment of HSV-1 quiescence

A number of reports have demonstrated the importance of ICP0 for reactivation of HSV-1 genomes in cultured cell models of quiescent infection (Harris et al, 1989; Preston, 2007; Preston & Nicholl, 1997; Samaniego et al, 1998; Terry-Allison et al, 2007), hence in the absence of ICP0 the virus has a higher probability of establishing a quiescent infection. Having demonstrated in the previous section of this manuscript the role of ATRX and hDaxx in the repression of ICP0-null HSV-1 infection as a complex, the potential of this complex in the repression of viral gene expression during the modelled establishment of quiescent viral genomes was also investigated.

In order to achieve this, the indicated cell cultures (Figure 5.10) were either mock-infected or infected with virus strain *in1374*, an ICP0-null mutant HSV-1 with a temperature sensitive mutation within ICP4 and a mutation within VP16 that eliminates its ability to form the complex that stimulates IE gene transcription. After infection was allowed to proceed at 38.5 °C for 18 hours, cells were processed for the analysis of  $\beta$ -galactosidase expression. Failure to establish quiescence by *in1374* was determined by the appearance of blue cells, expressing  $\beta$ -galactosidase. Figure 5.10A shows representative images of blue cell distributions in different cell cultures infected with *in1374* alone, mock-infected or co-infected with *in1374* plus strain *tsK*. HSV-1 strain *tsK* only bears a temperature sensitive mutation within ICP4, expresses ICP0 and stimulates the expression of the marker  $\beta$ -galactosidase gene in all *in1374* infected cells (Preston & Nicholl, 2005). Co-infection with *tsK* provided the measure of the maximal number of *in1374* infected cells. Figure 5.10A bottom right panel shows the representative image of  $\beta$ -galactosidase positive cells resulting from such co-infection (here HepaRG cells), and indicates that the majority of cells in these populations had been infected with *in1374*. There were no differences between the different cell lines used for this experiment in the proportion of blue cell numbers obtained from such co-infections. The representative image of the mock-infected sample (Figure 5.10 A, bottom left) indicates there was no background staining during the processing of the samples.

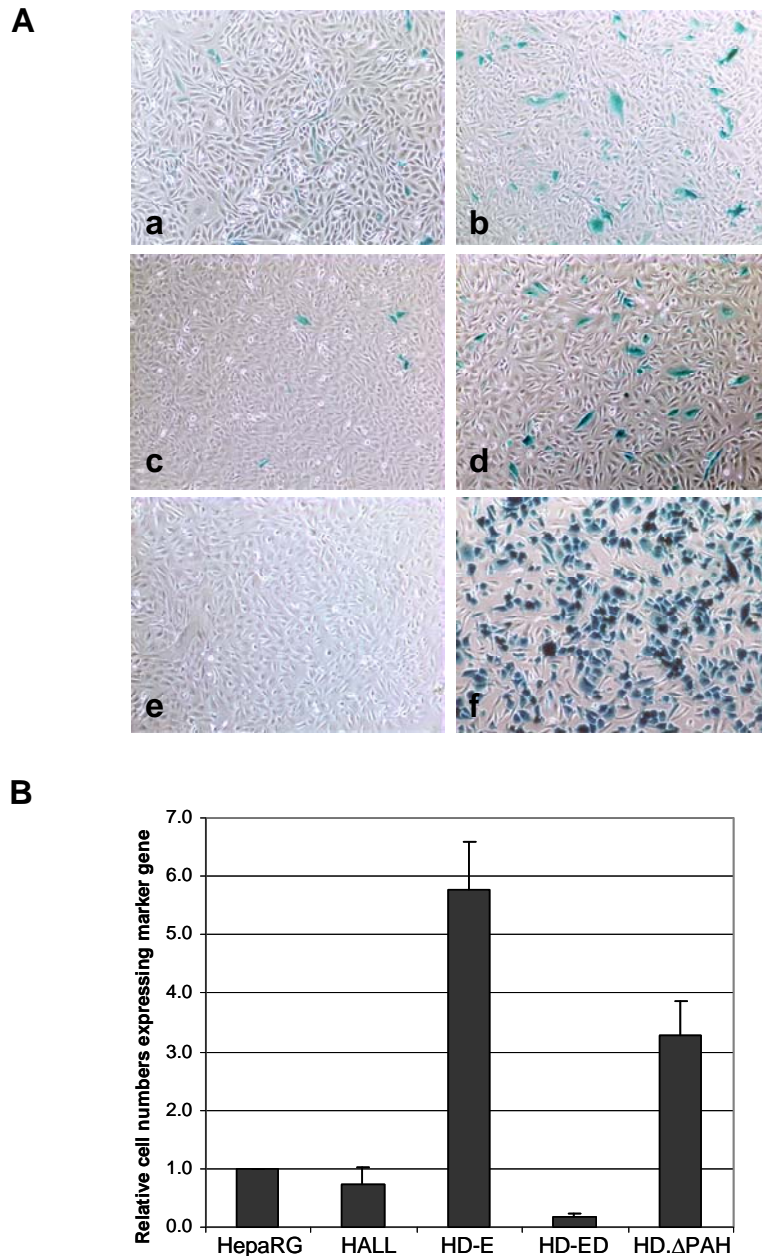


**Figure 5.10 Interaction between ATRX and hDaxx is required for the efficient establishment of quiescent infections in cultured cells**

Cells were mock-infected, infected with HSV-1 strain *in1374* at MOI 5 or co-infected with *in1374* (MOI 5) and *tsK* (MOI 1). Infected cells were incubated at restrictive temperature of 38.5 °C overnight and processed for b-galactosidase staining the following day. A: Images of HALL (a), HD-E (b), HD-ED (c) and HD.ΔPAH (d) cells at 24 h after infection with *in1374*, or HepaRG mock-infected (e) or co-infected with *in1374* and *tsK* (f). B: Relative cell numbers of β-galactosidase expressing cells in the above cell types compared to those obtained in parallel *in1374*- infected HepaRG cells. The plots represent mean values obtained from 3 independent experiments. Error bars are standard error values.

Results were quantified by comparing the blue cell numbers amongst this set of cell lines (Figure 5.10B). Positive cells were scored firstly in the HepaRG infected samples, and relative numbers of cells expressing the marker gene were obtained for each individual cell line in each set of independent experiments. Depletion of hDaxx resulted in a substantially increased number of  $\beta$ -galactosidase positive cells compared to the cells expressing endogenous levels of hDaxx. Re-introduction of the wt EYFP-tagged hDaxx fusion protein reversed the increase in the number of cells escaping the establishment of quiescence. However, in the cells expressing the EYFP-hDaxx. $\Delta$ PAH1 mutant protein, the number of  $\beta$ -galactosidase positive cells was significantly higher than that in HALL or HD-ED cells. These results indicate that the disrupted interaction between ATRX and hDaxx leads to a reduced capacity of the cells to repress *in1374* gene expression. This suggests that the ATRX/hDaxx complex may have a role in the efficiency of establishment of a quiescent HSV-1 infection in a cultured cell model.

#### **5.2.4 The role of hDaxx SUMO-interaction motif in regulating ICP0-null mutant HSV-1 infection**

In Chapter 3 the requirement of the hDaxx SIM in the ND10 localisation of itself and its interaction partner ATRX was demonstrated (Figure 3.14). Based on these findings and previous reports (Jang et al, 2002; Lin et al, 2006), it was concluded that the interaction between hDaxx and PML *via* the hDaxx SIM is essential for hDaxx localisation to ND10. The SIM of hDaxx is important for its interaction with other transcriptional repressors and hence its abilities to elicit its repressive activities (Holmstrom et al, 2008; Kuo et al, 2005; Lin et al, 2006; Meinecke et al, 2007; Shih et al, 2007; Zhong et al, 2000a). This section investigates whether the hDaxx SIM is required for recruitment of hDaxx to sites associated with HSV-1 genomes and whether it has a role in regulating the efficiency of viral gene expression and replication, using the same approaches as described above for other cell lines.

Examination of HD.MSIM cells at the edge of a developing *d11403* plaque revealed that EYFP-hDaxxMSIM failed to be recruited to the sites associated with ICP0-null HSV-1 genomes (Figure 5.11) and remained dispersed, as in non-infected cells (see Figure 3.14 in Chapter 3). In addition, dispersed hDaxxMSIM failed to target ATRX to the sites of the viral genomes (Figure 5.11, panel A). PML recruitment was not affected by the expression of EYFP-hDaxxMSIM. These data suggest that the hDaxx SIM is required for the recruitment of itself and therefore also ATRX to the sites associated with viral genomes.

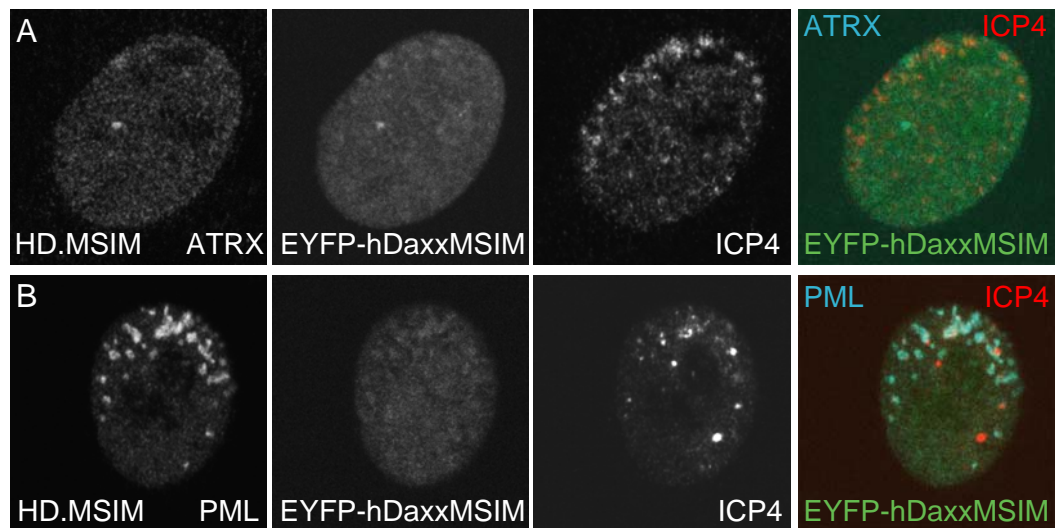


**Figure 5.11 hDaxx SUMO-interaction motif is required for hDaxx and ATRX recruitment to the sites associated with the incoming ICP0-null mutant HSV-1 genomes**

HD.MSIM cells were infected with *dl1403* at MOI 0.2 and processed for analysis by immunofluorescence the following day. Cells on coverslips were stained with anti-ATRAX H300, anti-PML r8 and anti-ICP4 58S antibodies. Secondary antibodies were anti-mouse AlexaFluor 555-conjugated and anti-rabbit Cy5-conjugated. EYFP-hDaxxMSIM is autofluorescent and appears in EYFP channel.

If neither ATRX nor hDaxx are recruited to the viral-induced foci, it is expected that they would not be able to repress ICP0-null viral gene expression and plaque formation efficiently. Indeed, when HD.MSIM cells and respective control cell lines were infected with ICP0-null HSV-1 virus (*dl1403* or *dl1403/CMVlacZ*; Figure 5.12, B and D respectively), the increases in ICP4 and UL42 production as well as in plaque formation were comparable to those obtained observed in hDaxx-depleted HD-E cells. The efficiency of wt HSV-1 infection remained unchanged, as in previous experiments (Figure 5.12, A and C). The ability of ATRX and hDaxxMSIM to interact was not tested, but it was expected that the complex between the two would not be disrupted since the N-terminal portion of hDaxx was sufficient for interaction with ATRX in CoIP assays in other studies (Tang et al, 2004). This suggests that interaction between ATRX and hDaxx is important for the repressive activities of the complex during ICP0-null mutant HSV-1 infection, but it also requires the interaction between hDaxx and SUMO and its SUMO-modified targets.

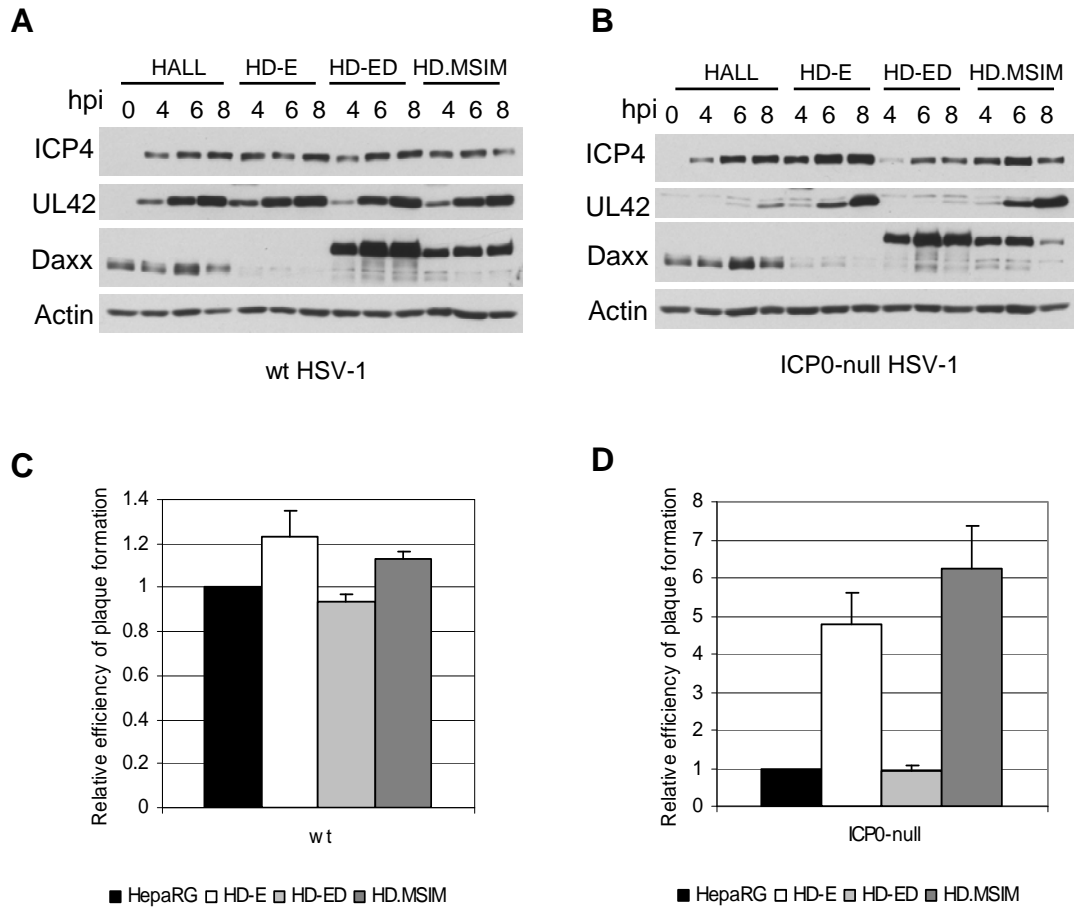


**Figure 5.12 The SUMO-interaction motif of hDaxx is required for fully efficient repression of ICP0-null mutant HSV-1 infection.**

A and B: Cells were infected with the indicated viruses at MOI 2.0 PFU/cell and samples were harvested at the 0, 4, 6 and 8 hours post infection (hpi). After resolving the samples on a 7.5 % polyacrylamide gel, membranes were probed for the expression of ICP4, UL42 and hDaxx using antibodies 58S, Z1F11 and D7810, respectively. Actin (AC-40) was a loading control. C and D: Cells were infected with wt HSV-1 strain *in1863* (C) or ICP0-null HSV-1 *dl1403/CMVlacZ* (D) at sequential dilutions and stained for  $\beta$ -galactosidase activity the following day to reveal the plaques. The plots represent mean values of plaque numbers relative to those in HepaRG cells, obtained from 3 independent experiments. Error bars represent standard error values.

## 5.2.5 Analysis of ATRX and hDaxx modification during HSV-1 infection

Previously published work has demonstrated that ICP0 stimulates the degradation of both PML and SUMO modified forms of Sp100 (Boutell et al, 2003; Boutell et al, 2002; Chelbi-Alix & de The, 1999; Everett et al, 1998b), an activity that correlates with its functions in counteracting the host intrinsic anti-viral response. The next set of results addresses the question whether ATRX and hDaxx expression is affected during HSV-1 infection. The aim of these analyses was to investigate whether ATRX and hDaxx were indeed displaced from the sites associated with viral genomes at the early stages of infection with wt HSV-1, rather than being targeted for degradation.

### 5.2.5.1 ATRX is not degraded during wt HSV-1 infection

As one of the preliminary steps in these studies, the levels of ATRX expression during the course of the infection were examined in infected fibroblasts. HFJs were infected with wt or ICP0-null mutant HSV-1 at the high MOI of 10 and samples were harvested for analysis every two hours during the course of 8 hours post infection (Figure 5.13). No significant changes in the expression of major ATRX isoforms were detected following the infection. Slight reduction in the levels of truncated ATRX isoform were noticed in ICP0-null mutant infection, although this observation was not subjected to any further investigation. It was therefore concluded that dispersal of ATRX, which is observed very soon after the entry of wt HSV-1 genomes into the nucleus, was not associated with its degradation.

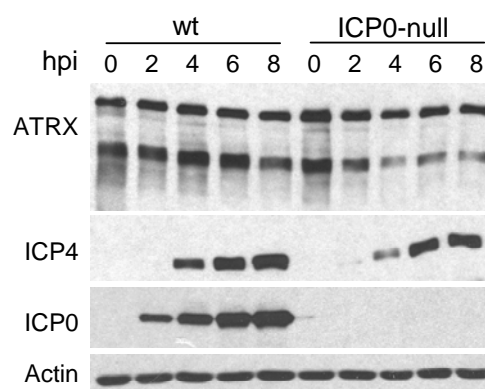


**Figure 5.13 Analysis of ATRX expression during infection with HSV-1**

HFJs were infected with either wt 17+ strain or ICP0-null *dl1403* strain of HSV-1 at MOI 10 and samples were harvested for analysis at indicated hours post infection (hpi). ATRX and ICP4 were resolved on a 6% polyacrylamide gel, and ICP0 and actin were resolved on a 7.5% gel. Antibodies used for western blotting were anti-ATRX 39F, anti-ICP4 58S, anti-ICP0 11060 and anti-actin AC-40.

#### ***5.2.5.2 The ATRX/hDaxx complex is neither disrupted during HSV-1 infection nor interacts with ICP0***

Previous evidence suggested that ICP0 associates with HDACs as well as with the chromatin repressor complex REST/CoREST/HDAC1 (Gu et al, 2005; Lomonte et al, 2004). Moreover, ICP0 disrupts the REST/CoREST/HDAC1 complex (Gu et al, 2005). Therefore, by analogy with these findings, the next experiment rests on the possibility that the dispersal of ATRX and hDaxx during the early stages of wt infection may be either a direct or an indirect consequence of ICP0-mediated disruption of the ATRX/hDaxx complex. CoIP assays were performed using HepaRG cells infected with wt HSV-1 at MOI 5, and the samples were harvested for analysis at 4 hours post infection. The reason for the chosen time point was the already observed changes in hDaxx gel mobility which seem to occur in ICP0-dependent manner at MOI of 2 Pfu/cell (Figure 5.8). In addition, if there was an effect of ICP0 on the integrity of the hDaxx/ATRX complex, it might be observed very early after infection (based on the earlier analysis of recruitment of the proteins to sites associated with viral genomes, Figure 5.1).

Figure 5.14 demonstrates the results of CoIP assays in which essentially the same buffer conditions were used as described in Figure 3.12C. Immunoprecipitation was carried out using anti-ICP0, anti-ATRX and anti-hDaxx antibodies (Figure 5.14; lanes 2 and 8; 3 and 9; 4 and 10, respectively). Controls with no added antibody (lanes 5 and 11) and an anti-USP7 antibody (lanes 6 and 12) were used as a negative control and a positive control for the interaction between USP7 and ICP0 (Everett et al, 1997). The input lane represents 2.5% of the cell extract used in each IP reaction. Evidently, there were no differences in the efficiency of CoIP of the ATRX/hDaxx complex with both anti-ATRX and anti-hDaxx antibodies in the mock-infected and wt HSV-1 infected cell extracts (Figure 5.14), suggesting unmodified integrity of the complex in the infected cells. IP using the anti-hDaxx antibody was more efficient in pulling down ATRX in the current assay than that presented in Figure 3.12 C, suggesting a certain level of variation in the assay efficiencies between the experiments. More importantly, ICP0 was not detected in the immune precipitates with either anti-ATRX or anti-hDaxx antibodies (lanes 9 and 10). The weak bands in anti-ICP0 blot are indicative of background since the same sized band is present in the negative control lane 11. Likewise, neither ATRX nor hDaxx specific bands were detected in the immune precipitates with anti-ICP0 antibody (lane 8), although ICP0 was clearly detected in the immune precipitates of infected cell extracts. Interaction between ICP0 and USP7, on the other hand, was successfully detected in the wt HSV-1 infected cells (lane 12) but not in mock-infected cells (lane 6). Based on these data, it is concluded

that HSV-1 ICP0 neither interacts with the components of ATRX/hDaxx complex, nor disrupts the ATRX/hDaxx complex.

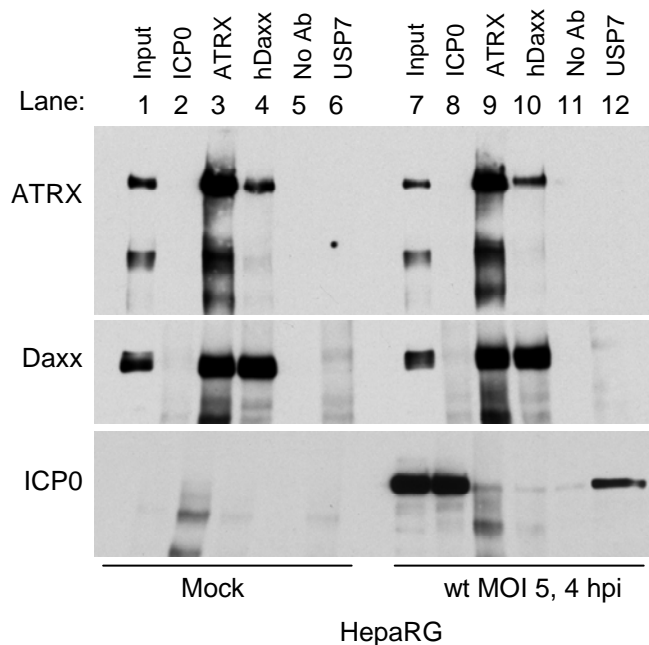


**Figure 5.14 ICP0 neither interacts with nor disrupts the ATRX/hDaxx complex**

HepaRG cells were either mock-infected or infected with wt HSV-1 at MOI 5 and cells were harvested in IP lysis buffer at 4 h post infection. Immunoprecipitation was carried out using no antibody or anti-ICP0 190, anti-ATRX H300, anti-Daxx 07-471 and anti-USP7 210 antibodies, as indicated. Input lanes contained 2.5% of the sample used for immunoprecipitation. Western blot analysis was performed using mouse anti-ATRX 39F, anti-Daxx D7810 and anti-ICP0 11060 antibodies.

### 5.2.5.3 hDaxx phosphorylation levels are increased during wild-type HSV-1 infection

In the course of earlier experiments shown in the current chapter it had been noted that hDaxx is subject to modification during wt but not ICP0-null mutant HSV-1 infection of HepaRG-based cells (Figure 5.8). Based on previously published work (Ecsedy et al, 2003), such a pattern of modification is reminiscent of increased phosphorylation of hDaxx. This hypothesis was investigated more thoroughly by analysing the expression pattern of endogenous hDaxx in naïve infected HepaRG cells over 10 hours of infection with wt or ICP0-null mutant viruses at MOI 5 (Figure 5.15). As the wt virus infection progressed, the lower band of the hDaxx doublet decreased in mobility and merged with the higher band isoforms (Figure 5.15, A). This shift did not occur in the parallel ICP0-null mutant virus infection, even at late times in this experiment when UL42 expression was abundant (Figure 5.15, B). During the course of replicate experiments, it was noted that the detail of

the hDaxx isoforms varied between gels, implying that the slight mobility shifts observed could be affected by minor variations in electrophoresis conditions.

A similar pattern of Daxx migration was observed in previous studies when kinase HIPK1, which is responsible for Daxx phosphorylation in mouse cells, was over-expressed (Ecsedy et al, 2003). Therefore, it was possible that the hDaxx band shift during wt virus infection could be a result of increased phosphorylation levels of hDaxx. To test this hypothesis, cells were infected with wt and ICP0-null mutant HSV-1 at MOIs of 5 and 10 and the infected samples were harvested in IP lysis buffer without EDTA (which is inhibitory to  $\lambda$ -phosphatase according to manufacturer's manual) at 4 and 7 hours post infection. These time points were picked based on the data presented in Figure 5.15 A and B. Samples were either left untreated or treated with phosphatase for 1 hour at 30 °C and analysed on 6% and 7.5% gels (Figure 5.15, C-D). As shown in this and previous chapters, hDaxx migrates as a double band, which is likely to result from varying mobility of phosphorylated and non-phosphorylated hDaxx forms. Phosphatase treatment of mock (M) infected samples resulted in the loss of the lower mobility bands and an increase in intensity of the highest mobility form, indicating that hDaxx phosphorylation was abolished in these cells (Figure 5.15 C-D). Analysis of the wt HSV-1 infected samples at MOI 5.0 and 10, harvested at 4 and 7 hours post infection indicated that the infection specific band shift was also due to phosphorylation (Figure 5.15) since phosphatase treatment of the infected samples caused loss of the lower mobility forms and the appearance of a single, more intense band of higher mobility (Figure 5.15, C). The faint appearance of hDaxx bands in untreated, wt HSV-1 infected samples was due to the slower migration of different multiply-phosphorylated hDaxx forms, rather than degradation, since the intensities of phosphatase treated bands were indistinguishable between non-infected and wt HSV-1 infected samples. In the cell extracts obtained from ICP0-null mutant infected samples interpretation of the results was not as straightforward as in the wt HSV-1 infection. Untreated samples from the ICP0-null mutant HSV-1 cells infected at MOI of 5 showed no evidence of increased phosphorylation at the same time points and were indistinguishable from the mock infected samples. At the MOI of 10, however, hDaxx migration pattern produced similar results to those observed with wt HSV-1 infection at MOIs 5 and 10 at the same time points. Phosphatase treatment of the ICP0-null mutant infected samples, particularly those infected at MOI of 10, resulted in disappearance of the higher mobility hDaxx bands (Figure 5.15 D), as in the wt infected samples. These observations indicate that the hDaxx phosphorylation events that occur during wt HSV-1 infection are not a direct effect of ICP0 itself (as might be concluded from the results of infections of MOI 5) but instead are

a consequence of high viral load. Despite the phosphorylation of hDaxx in *dl1403* infection at MOI 10, the process occurs far more readily in wt than ICP0-null mutant infections at lower multiplicities. It therefore remains possible that phosphorylation of hDaxx in some way reflects the role of ICP0 in overcoming hDaxx mediated repression.

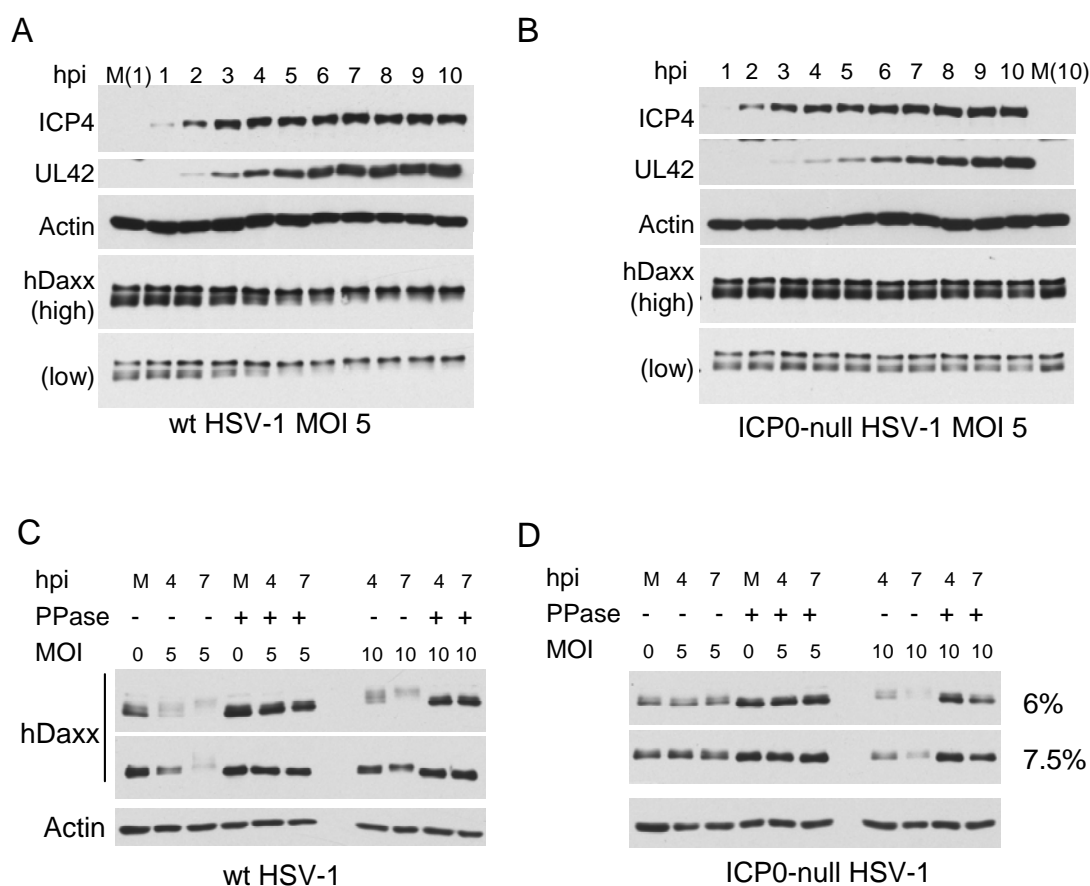


### Figure 5.15 Phosphorylation of hDaxx during wild-type HSV-1 infection

A-B: HepaRG cells were seeded into a 24-well plate at a density of  $1 \times 10^5$  cells per well and infected with wt (A and C) or ICP0-null HSV-1 (B and D) at the indicated MOIs. Samples were harvested at indicated time points (A-B) and resolved on 7.5% gels for ICP4, UL42 and actin, and on 6% gels for hDaxx. 'High' and 'low' marks in hDaxx blots indicate different exposure times. In panels C and D, samples were harvested in IP lysis buffer (without EDTA) and mock-treated or treated with  $\lambda$ -phosphatase. M, mock; wt, wild-type; MOI, multiplicity of infection.

## **5.3 Conclusions and discussion**

Previous work identified two major ND10 components, PML and Sp100, as factors contributing to intrinsic cellular defence against HSV-1 (Everett et al, 2008; Everett et al, 2006). In accordance with the ongoing investigation into the roles of additional ND10 components in HSV-1 infection, the results presented in the current chapter provide novel evidence for the role of ND10 chromatin-remodelling proteins ATRX and hDaxx in the regulation of ICP0-null mutant HSV-1 infection. In summary, it has been demonstrated that: (a) hDaxx targets ATRX to the sites associated with the incoming HSV-1 genomes; and (b) the interaction between ATRX and hDaxx is required for fully efficient repression of ICP0-null mutant viral genomes during the lytic cycle of infection and for the efficient establishment of quiescence in cell culture. The effect of viral genome repression by the ATRX/hDaxx complex is only evident in the context of ICP0-null mutant HSV-1 infection, due to the strong counteracting function of ICP0 in wt HSV-1 infection. The mechanisms underlying the chromatin-remodelling functions of ATRX and hDaxx in the infected cells and how ICP0 antagonises these mechanisms remains a complex issue. These issues are discussed further with regard to the events associated with HSV-1.

### **5.3.1 Fully efficient repression of the mutant HSV-1 genomes requires the ATRX/hDaxx complex**

During ICP0-null mutant HSV-1 infection both ATRX and hDaxx are recruited to and retained in association with viral genomes, whereas this recruitment is efficiently inhibited by the actions of ICP0 in wt HSV-1 infected cells (Figure 5.1). Hence the question posed next was whether the more stable recruitment of the two proteins to the sites of ICP0-null mutant genomes functionally correlates with the repression by ATRX/hDaxx complex. A number of observations have supported this hypothesis.

Firstly, FRAP analysis of the ICP0-null mutant HSV-1 infected cells expressing EYFP-tagged hDaxx has demonstrated that the mobility of hDaxx foci associated with viral genomes was reduced, in comparison to the dynamics of those at normal ND10 of the mock-infected cells (Figure 5.2). Although these cells are infected at very high MOI of ICP0-null mutant virus, this observation is another way to represent the requirement of ND10 proteins, for example hDaxx, in the repression mechanisms that occur at low MOIs of ICP0-null mutant HSV-1. The downsides of this approach however were the general difficulties in identifying cells at the edges of plaques, based only on re-distribution pattern

and the highly dynamic nature of hDaxx foci. The loss of focus during measurements of the fluorescence recovery times was also a problem, and might have contributed to inaccuracies. The former issue can be resolved by using the ICP0-null HSV-1 strain where ICP4 is tagged with the ECFP fluorescent protein (Sourvinos & Everett, 2002). Nevertheless, this evidence is consistent with the general hypothesis that the recruitment of ND10 proteins to the sites of the incoming ICP0-null mutant viral genomes correlates with their repressive properties. It is important to bear in mind, however, that the individual cells infected at the edge of a developing plaque in ICP0-null mutant infections contain a high load of viral genomes that saturate cellular intrinsic defences, and therefore these cells are productively infected.

Secondly, if stable recruitment of ATRX and hDaxx to ICP0-null mutant genomes at high MOIs correlates with the repression of ICP0-null mutant HSV-1 infections that occurs at low MOIs, then by analogy with previous findings on PML and Sp100 (Everett et al, 2008; Everett et al, 2006) removal of ATRX or hDaxx should support increased levels of gene expression and replication of ICP0-null mutant HSV-1. Indeed, in the ICP0-null mutant infected cells, depletion of either ATRX or hDaxx contributed to the more efficient infectivity by ICP0-null virus (Figures 5.7-5.8). Earlier work however, has demonstrated that depletion of PML or Sp100 contributed to a more pronounced increase of ICP0-null viral gene expression, which was clearly detected on the levels of both IE and Early protein synthesis (Everett et al, 2008; Everett et al, 2006). In contrast to those findings, whereas hDaxx depletion in the present study resulted in only a minor increase in ICP4 production (Figure 5.8), in ATRX depleted cells infected with ICP0-null mutant HSV-1 there were no detectable changes in ICP4 production at all (Figure 5.7). This may reflect the fact that ICP0-null mutant HSV-1 levels of ICP4 expression are higher than might be expected on the basis of the plaque forming defect of this virus (Cai & Schaffer, 1992; Everett et al, 2004). In spite of this, these increases in gene expression were sufficient for the detectable increases in plaque numbers of ICP0-null mutant virus in the absence of ATRX or hDaxx, when compared to cells expressing endogenous levels of both proteins. These data have provided evidence for the individual roles of the two proteins in regulation of ICP0-null mutant HSV-1 infection.

Thirdly and most importantly, a critical indication that ATRX and hDaxx act as a complex in the repression of ICP0-null mutant infection has come from the analysis of infected cells expressing ATRX-interaction deficient mutant hDaxx. In these cells the ATRX/hDaxx complex has been disrupted, but the mutant hDaxx $\Delta$ PAH protein was still capable of being

recruited to the sites associated with ICP0-null mutant HSV-1 genomes. The efficiency of ICP0-null mutant HSV-1 replication, however, was comparable to that observed in hDaxx-depleted cell lines (Figure 5.9). Therefore, targeting of hDaxx alone in the absence of ATRX to the sites associated with the viral genomes was insufficient for its full repressive potential. In addition, the data suggest that the increase in replication and plaque forming efficiency of ICP0-null mutant virus in the absence of hDaxx as seen on Figure 5.8 is also likely to be in part a result of the inability of ATRX to associate with the viral genome foci.

Additional supporting data for the role of the ATRX/hDaxx complex in the repression of viral genomes has been obtained in the model of quiescent infection using mutant virus *in1374* (Figure 5.10). The extent of increases in the relief of repression following removal of hDaxx or disruption of ATRX/hDaxx complex in this model correlated with that seen in ICP0-null mutant infections using the same cell lines. These data therefore suggest that similar repressive activities of ATRX and hDaxx may be responsible for both repression of ICP0-null mutant virus at low MOIs and establishment of quiescence by the mutant HSV-1. Having demonstrated the requirement of ATRX/hDaxx complex for fully efficient repression of mutant HSV-1 genomes, the precise mechanism of action of the ATRX/hDaxx complex on HSV-1 genomes still remains to be elucidated. However a number of models explaining the counteracting function of ICP0 can be proposed. These are addressed in the next paragraphs.

### **5.3.2 Phosphorylation of hDaxx as an ICP0-mediated response to antiviral cellular intrinsic defence**

Both ATRX and hDaxx are rapidly released from ND10 during wt HSV-1 infection. Unlike PML (Boutell et al, 2003; Boutell et al, 2002; Everett et al, 1998a), neither ATRX nor hDaxx are degraded during wt HSV-1 infection (Figures 5.13 and 5.15). Furthermore, ICP0 does not interfere with the integrity of the ATRX/hDaxx complex after infection with the wt HSV-1 (Figure 5.14). Hence, displacement of this complex away from the replicating viral genomes must occur *via* a different mechanism.

Whereas ATRX does not seem to undergo evident modification in HSV-1 infected cells, the band shift pattern of hDaxx during wt infection was suggestive of increased phosphorylation. Since hDaxx is not a direct substrate of ICP0 (Figure 5.14), the effects observed on hDaxx modification must be an indirect consequence of ICP0 expression. The hypothesis that HSV-1 induces phosphorylation of certain nuclear proteins during infection

is consistent with analogous observations on protein modifications in collaborative work from different groups (Antrobus et al, 2009; Kyle Grant, personal communication). Antrobus et al. have demonstrated a similar modification pattern, in an ICP0 RING-finger dependent fashion, of two chromatin associated proteins, HP1- $\gamma$  and minichromosome maintenance protein 4 (MCM4), as well as accumulating levels of phosphorylated histone H2AX ( $\gamma$ H2AX) during the time course of HSV-1 infection.

Interestingly, phosphatase assays conducted in the present study revealed that hDaxx becomes hyperphosphorylated during wt HSV-1 infection at MOI of 5 in an ICP0-dependent manner (Figure 5.15). The appearance of the smeared slow-migrating hDaxx bands is indicative of multiple phosphorylation events. At very high MOIs of ICP0-null mutant virus, ICP0 was not required for this phosphorylation. Although the sites of these hDaxx phosphorylation events during HSV-1 infection remain to be determined, previous work suggests some potential consequences of this activity. Phosphorylation of hDaxx at S178 allows binding of the prolyl isomerase Pin1 resulting in subsequent degradation of hDaxx (Ryo et al, 2007). In that hDaxx degradation does not seem to occur in the phosphatase assays (compare the bands of phosphatase treated samples in mock-infected and infected cells, Figure 5.15), it is unlikely that this mechanism is in operation during HSV-1 infection, but may provide some evidence for the regulation of hDaxx protein stability. It is interesting that mouse Daxx is a direct substrate for phosphorylation by HIPK1 (Ecsedy et al, 2003). Moreover, overexpression of HIPK1 results in Daxx being displaced from ND10 which leads to a reduction in its repressive potential (Ecsedy et al, 2003). Consistent with this finding, overexpression of HIPK2 in human cells results in hDaxx phosphorylation and delocalisation from ND10 (Hofmann et al, 2003). Therefore, in the context of HSV-1 infection, it is possible that wt HSV-1 acts to promote hyperphosphorylation of hDaxx in order to (a) decrease its functions in transcriptional repression on viral genomes and (b) displace it from virally induced ND10-like foci that form in close association with viral genomes. Based on these data and the results presented in Figure 5.15, it is possible that HSV-1 induces phosphorylation of certain proteins in order to counteract cellular intrinsic defence mechanism in an ICP0-dependent manner.

### 5.3.3 SUMO-dependent targeting of hDaxx to the sites of the viral genomes

Another mechanism by which the ATRX/hDaxx complex may be targeted and removed from the sites of early viral replication during wt HSV-1 infection may relate to the ability of hDaxx to interact with SUMO and SUMO-modified substrates (Li et al, 2000; Lin et al, 2006). SUMO-modification of hDaxx target proteins is known to be significant in hDaxx-mediated transcriptional repression (reviewed in Shih et al, 2007). This property correlates with the observations that the hDaxx SIM is required for the fully efficient repression of ICP0-null mutant HSV-1 genomes during the active replication phase of infection (Figure 5.12). Consistent with these findings, in cells expressing an hDaxx mutant deficient for the interaction with SUMO (hDaxxMSIM), hDaxx fails to get recruited to the sites associated with the viral genomes and remains dispersed in the nucleus (Figure 5.11). Dispersal of hDaxxMSIM in infected cells and the inability of mutant hDaxx to fully perform its normal repressive functions during ICP0-null mutant infection indicate the importance of SUMO-mediated regulation of HSV-1 infection. The mechanism of this regulation, however, can only be a subject of speculation, based on the available evidence, as discussed further.

Mutations within the hDaxx SIM do not affect PML recruitment to viral genomes, and it is attractive to suggest that PML targets hDaxx to the sites of the viral genomes *via* the SUMO/SIM association. However, this proposal is not supported by the evidence that both hDaxx and ATRX are recruited to the virus-induced foci in the absence of PML (Everett et al, 2006; Figure 5.3). Nevertheless, the possibility that the dispersal of both components during wt HSV-1 infection can be a result of ICP0-mediated degradation of PML should not be excluded due to the ability of ICP0 to preferentially target SUMO-modified PML isoforms for degradation and its overall effect on disintegration of ND10 (Boutell et al, 2003; Boutell et al, 2002; Chelbi-Alix & de The, 1999; Everett et al, 1998a).

If the ATRX/hDaxx-mediated pathway of the antiviral intrinsic defence mechanism were to be SUMO-dependent, then ICP0 would target SUMO-modified substrates to induce removal of hDaxx from the sites of the HSV-1 genomes by disrupting the SUMO/SIM<sup>hDaxx</sup> interactions. A number of observations support this hypothesis. Earlier evidence has demonstrated that exogenously expressed ICP0 induces removal of SUMO-1 from ND10-associated foci (Bailey & O'Hare, 2002). This correlates with the ability of ICP0 to target SUMO-modified proteins for degradation (Everett et al, 1998a; Muller & Dejean, 1999; Boutell et al. unpublished observations). Similarly, in ICP0-null HSV-1 infection SUMO-modified proteins are recruited to the viral genome foci in a PML-independent manner (Boutell et al, unpublished observations). Based on these findings and the data presented in

Figure 5.11, the following model can be proposed: hDaxx removal from the sites of incoming viral genomes during wt infection results from ICP0-mediated global degradation of SUMO-modified substrates; whereas in ICP0-null mutant infection an interaction between hDaxx SIM and SUMO-1 provides a mechanism of retention of the ATRX/hDaxx complex at the sites of the viral genomes, thereby contributing to repression of viral gene expression.

The investigation presented in the current chapter explored the role of the ATRX/hDaxx complex in the intrinsic resistance to HSV-1 infection. In summary, the data suggest that ATRX and hDaxx act as a complex in order to contribute to the repression of the incoming ICP0-null mutant HSV-1 genomes as well as to the efficient establishment of quiescent genomes. This repression is efficiently counteracted by the functions of ICP0. Currently proposed models of ICP0 actions include: (i) hyperphosphorylation of hDaxx that results indirectly from ICP0 expression and leads to ATRX/hDaxx complex displacement from the sites of the genomes; (ii) ICP0-mediated degradation of SUMO-modified proteins associated with the early viral genome foci leading to disruption of SUMO/SIM<sup>hDaxx</sup> interactions. The precise mechanisms underlying both models remain to be clarified. The evidence that exists so far may provide important clues in understanding the mode of action of ICP0 during the lytic cycle of HSV-1 infection and reactivation.

## 6 Summary, Discussion and Future Prospects

Members of the virus family *Herpesviridae*, HSV-1 and HCMV, are important human pathogens that actively replicate during lytic stage of the life cycle and persist in the host during latency. Ongoing aims of HSV-1 and HCMV research are to identify the processes of the cell-virus interactions that are responsible for successful lytic replication, latency establishment and maintenance, and reactivation. In Chapter 1, three classes of host immunity to the infection have been outlined: innate, adaptive and intrinsic. The recently emerged concept of anti-viral intrinsic immunity, or intrinsic defence rests on the fact that cells constitutively express a number of proteins that in addition to their functions in cellular pathways have properties that inhibit virus infection (reviewed in Bieniasz, 2004). The rapid changes in cellular dynamics associated with the intrinsic defence mechanisms are therefore observed immediately after the virus invades the subcellular environment. Identification of the underlying molecular events and how the virus counteracts them in order to achieve successful replication will provide a better understanding of viral life cycle and promote the identification of the potential anti-viral drug targets.

### 6.1 Summary of the data

One aspect of anti-viral intrinsic resistance against both HSV-1 and HCMV is associated with components of the intranuclear dynamic sites known as ND10 (reviewed in Maul, 1998; Tavalai & Stamminger, 2008). The current study was aimed to explore the relationships between ND10, viral genomes and chromatin modifying enzymes, and focus on the roles of the two chromatin-associated ND10 proteins ATRX and hDaxx in the regulation of HSV-1 and HCMV infection. The key results presented in the previous chapters can be summarised as follows:

- (i) During HCMV infection, viral tegument protein pp71 displaces ATRX from ND10. This allows efficient stimulation of HCMV IE transcription by pp71, since repression of pp71-null mutant virus is relieved to a substantial extent in the absence of ATRX.
- (ii) In ICP0-null mutant HSV-1 infected cells, the complex formed between ATRX and hDaxx contributes to the repression of viral gene expression that occurs in the absence of ICP0. ICP0 counteracts this repression by promoting displacement of ATRX/hDaxx complex from the incoming viral genomes.

These sets of evidence have led to a conclusion that ATRX and hDaxx are components of cell-mediated intrinsic immunity against HSV-1 and HCMV. Moreover, in the case of

HSV-1, this intrinsic immunity requires the sequences of hDaxx that are responsible for its interaction with ATRX. This may indicate that ATRX and hDaxx act as a complex in pp71-null mutant HCMV infection as well. Putting these data together with previously published work (Cantrell & Bresnahan, 2005; Cantrell & Bresnahan, 2006; Everett et al, 2008; Everett et al, 2006; Hwang & Kalejta, 2007; Ishov et al, 2002; Preston & Nicholl, 2006; Saffert & Kalejta, 2006; Tavalai et al, 2006; Tavalai et al, 2008; Woodhall et al, 2006), it can be concluded that the effects of PML, Sp100, ATRX and hDaxx in anti-viral defence mechanisms are cumulative and complementary to each other. This fits into the general definition of intrinsic cellular anti-viral defence, as noted above, which suggests a collective set of cellular activities that act to repress viral gene expression. It can be predicted that simultaneous depletion of more than one ND10 protein should further improve the efficiency of viral infection. This implies that the proteins are likely to act in unison to accelerate the assembly of repressive chromatin-like structures on viral genomes.

## **6.2 Evidence for ATRX and hDaxx as the components of a multisubunit repressor complex during viral infection**

The aspects of chromatin remodelling have been partially covered in Chapter 1. In brief, chromatin repression is associated with the assembly of DNA into compact heterochromatin structure, which is generally marked by core nucleosomal histone methylation and DNA methylation at CpG islands. Histone H4 methylated at lysine position 9 can attract HP1 proteins for establishing a more stably repressed nucleosomal structures, while protein MeCP2 can bind CpG islands on DNA to bring about transcriptional repression. A specialised class of enzymes DNMTs is involved in directly methylating cytosine residues, which serves as a binding site for MeCP2 (Nan et al, 1997; Siedlecki & Zielenkiewicz, 2006), as well as in HP1 and Suv39H1 (HMT) binding (Fuks et al, 2003). A densely packed heterochromatin structure is proposed to result from the tight association of the proteins residing at the sites of methylated DNA and methylated histones of the adjacent nucleosomes, according to the model reviewed elsewhere (Brenner & Fuks, 2007). Analysis of the conserved domains and protein-protein interaction properties within different transcriptional co-repressors suggests that formation of such repressed chromatin structures can also be induced by recruitment of additional repressor factors and complexes. ATRX and hDaxx are both candidates for being components of these complexes, and this hypothesis can be supported by a number of observations.

Firstly, ATRX interacts with both MeCP2 (Nan et al, 2007) and HP1 (Le Douarin et al, 1996; Lechner et al, 2005), which indicates a bridging function of ATRX in chromatin repression, in a similar model as proposed above. Interestingly, the interaction between ATRX and MeCP2 is abolished in patients with ATR-X syndrome, suggesting an important role in transcriptional regulation mediated by the MeCP2/ATRX complex (Nan et al, 2007). The same group also demonstrated that MeCP2 is a component of multi-subunit complex that contains Class 1 HDACs and a transcriptional repressor mSin3a (Nan et al, 1998). mSin3a contains a PAH1 domain, related to that in hDaxx required for interaction with ATRX (Tang et al, 2004). Therefore, it is possible that mSin3a recruits ATRX to this repressor complex *via* competitive binding with hDaxx, or that ATRX is dynamically exchanged between the two co-repressors, depending on the target gene.

Secondly, hDaxx has been shown to interact with HDAC1 and -2 (Hollenbach et al, 2002; Li et al, 2000), which suggests that the ATRX/hDaxx complex itself can interact with HDACs. Repression mediated by hDaxx is dependent on this interaction, as suggested by experiments using TSA treatment (Li et al, 2000). In a different system using cells undergoing meiosis, TSA treatment results in disruption ATRX interaction with meiotic centromeres, which indicates of HDAC-dependent regulation of ATRX functions (De La Fuente et al, 2004). Since the ATRX- and HDAC-interacting regions of hDaxx (the PAH1 domain and the S/P/T region, respectively; see Figure 1.8) do not overlap, it is possible that the interaction between hDaxx and HDACs recruits ATRX to target promoters. On the other hand, the PHD-like finger domain of ATRX itself may be involved in an interaction with HDAC1 (Figure 1.7) (Gibbons et al, 2000; Zhang et al, 1999). Although the presence of HDAC within the ATRX/hDaxx-containing complex is speculative, it can explain the mechanism of regulation of transcriptional repression by ATRX and hDaxx.

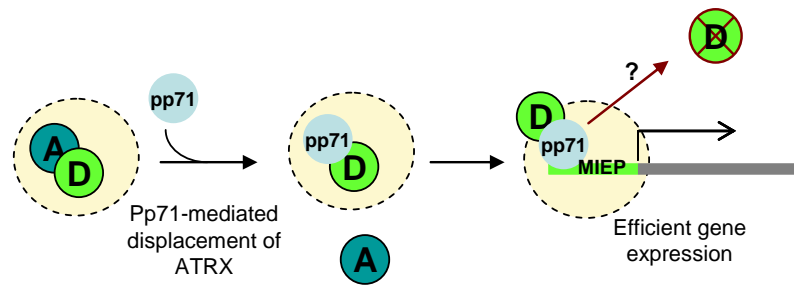
A third possibility of ATRX and hDaxx being a part of a multisubunit transcriptional repressor complex is based on their ability to interact with HDACs, which themselves are in a complex consisting of REST, CoREST and HDACs. REST (repressor element-1-silencing transcription factor) and its co-factor Co-repressor of REST (CoREST) play an important role in transcriptional regulation of neuronal gene expression. Both REST and CoREST can independently bind additional transcription co-repressors (reviewed in Lakowski et al, 2006). The ability of ATRX/hDaxx complex to associate with HDACs, at least *via* hDaxx, makes feasible their presence in this multi-protein repressor complex. Based on the substantial evidence that implicates the role of HDACs in the regulation of

chromatin state of HSV-1 and HCMV genomes, the issue of whether ATRX and hDaxx are components of this repression mechanism is addressed further below.

### **6.3 The mechanisms of repression by ATRX/hDaxx complex during HCMV and HSV-1 infection**

Despite the facts that HSV-1 and HCMV represent viruses of the same virus family, and that ND10 proteins such as PML and ATRX are involved in repression of gene expression of both viruses (Everett et al, 2006; Tavalai et al, 2006; Figures 4.2 and 5.7 C-D), the mechanisms of their action on viral genomes and the ways viruses counteract them appear to differ substantially (Figure 6.1). This is true in the context of the role of ATRX/hDaxx complex in HSV-1 and HCMV infectivity, based on the results of the Chapters 4 and 5 of this thesis. Chapter 4 discusses the possible mechanisms which may be utilised by pp71 to counteract repression by ATRX and hDaxx: pp71-induced displacement of ATRX from ND10 followed by interaction with hDaxx and its subsequent degradation. Similarly, results presented in Chapter 5 suggest at least two mechanisms of how ICP0 may counteract ATRX/hDaxx-mediated gene expression, which are not exclusive of each other: one suggests increased phosphorylation of hDaxx followed by the removal of the ATRX/hDaxx complex from the sites associated with the viral foci; the other indicates on ICP0-mediated degradation of SUMO-modified ND10 components, the presence of which is required for ATRX/hDaxx targeting to the viral incoming genomes *via* the hDaxx SUMO-interaction motif. The models of ICP0 and pp71 actions on the ATRX/hDaxx complex are depicted on Figure 6.1. These results however neither provide evidence for the mechanism of action of the ATRX/hDaxx complex, nor suggest that the ATRX/hDaxx complex may be directly involved in the assembly of repressed chromatin structures on viral genomes. The next two subsections discuss some evidence that may provide clues to: (a) whether the pathways of HSV-1 and HCMV gene repression are related; and (b) to the mode of action of ATRX and hDaxx as a complex on HSV-1 and HCMV genomes.

## I. HCMV



## II. HSV-1

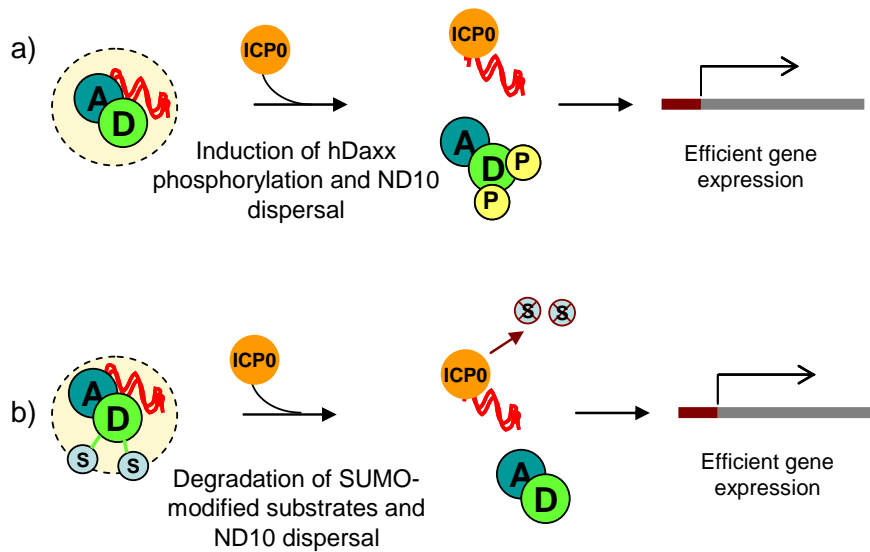


**Figure 6.1 Models of HCMV pp71 and HSV-1 ICP0 counteracting functions on ATRX/hDaxx complex during the initial stages of lytic infection**

I. HCMV pp71 counteracts the repressive functions of ATRX/hDaxx (designated as A and D) complex by displacing ATRX from ND10, interacting with hDaxx and inducing efficient gene expression. hDaxx may be subsequently degraded (crossed circle), although the data is controversial. II. (a) ICP0 expressed by HSV-1 can indirectly induce phosphorylation (P) of hDaxx. Because hDaxx is the targeting component of the ATRX/hDaxx complex, this causes displacement of the entire complex away from the viral genomes (marked in red) and relieves cellular repressive mechanism. (b) hDaxx is targeted to the sites associated with the incoming HSV-1 genomes *via* interaction with SUMO-modified proteins. ICP0 targets SUMO-modified substrates for degradation, thereby causing displacement of ATRX/hDaxx complex.

### **6.3.1 Evidence that the pathways of ATRX/hDaxx-mediated repression of HSV-1 and HCMV infection are distinct**

Pp71 can substitute to some extent for the lack of ICP0 (Preston and Nicholl, 2005), suggesting they may be functional analogues. Identification of ATRX and hDaxx in related pathways of repression that occurs in the absence of pp71 or ICP0 in HCMV and HSV-1 infected cells, respectively, may indicate similarities between ATRX/hDaxx-mediated processes associated with this repression. But is this really the case?

During HCMV infection the ATRX/hDaxx complex is likely to be efficiently disrupted by the action of pp71, since ATRX is displaced from ND10 prior to any effects on hDaxx are observed, and indeed before detectable IE gene expression (Lukashchuk et al, 2008). Therefore any repression mechanism operating during the very early stages of wt HCMV infection may not rely on the function of the actual complex, but rather on ATRX and hDaxx acting independently. Furthermore, hDaxx is subsequently degraded by pp71 according to some reports (Hwang & Kalejta, 2007; Saffert & Kalejta, 2006). Localisation of pp71 to ND10 is required for efficient stimulation of IE gene expression and is dependent on hDaxx (Ishov et al, 2002), but not ATRX (Figure 4.1). Hence, disruption of the ATRX/hDaxx complex by pp71 may be required for pp71 to access hDaxx and stimulate induction of the immediate early transcript environment (Ishov et al, 2002). In the case of HSV-1 infection, however, the ATRX/hDaxx complex remains intact and neither of the components interacts with nor are they degraded by ICP0 (using the assay presented in Figure 5.13). These results suggest that in HSV-1 and HCMV infection components of ND10 are differentially targeted by viral regulators during the initiation of viral gene expression, and indicate of the differences in progression of viral replication between the viruses of the same family.

HCMV is a slow-replicating virus and cellular intrinsic defences may be easier to detect during infection with this virus. On the other hand, HSV-1 replicates rapidly in cell culture, once the genomes have been released, indicating that cellular intrinsic responses have been saturated or are overcome very efficiently. This links with the observations that initial repression of HCMV genomes during lytic infection is associated with nucleosome assembly (Nitzsche et al, 2008), whereas some reports suggest this is not the case for HSV-1 (Herrera & Triezenberg, 2004; Leinbach & Summers, 1980). The role for histone association with HSV-1 genomes, however, remains controversial. Although HSV-1 DNA is associated with histones and particularly with active transcription histone markers at early times post infection (Cliffe & Knipe, 2008; Herrera & Triezenberg, 2004; Huang et al,

2006; Kent et al, 2004), nucleosomes are underrepresented on IE promoters, and the histone load is further reduced as infection progresses (Herrera & Triezenberg, 2004; Oh & Fraser, 2008). Association of latent and quiescent HSV-1 DNA with nucleosomes appears to be more likely, according to several reports (Deshmane & Fraser, 1989; Ferenczy & DeLuca, 2009).

How does this evidence correlate with ATRX- and hDaxx-driven repression of HSV-1 and HCMV genomes? If ATRX and hDaxx associate with additional repressive chromatin markers such as MeCP2, HP1 and HDACs (see above in Section 6.2), it is attractive to suggest that they enhance assembly of heterochromatin on viral genomes. It appears that these mechanisms differ in efficiency during infection with wt and pp71-null mutant HCMV, based on the ability of pp71 to disrupt the ATRX/hDaxx complex. Assuming that heterochromatin assembly during HSV-1 infection is more likely to occur during latency and quiescence, it is possible that in ICP0-null mutant infections at low MOIs, and in quiescent infection models using viral strains such as *in1374* and *d109* that are unable to initiate IE gene expression (Preston & Nicholl, 2005; Samaniego et al, 1998), related pathways operate whereby ATRX and hDaxx are involved in inducing the formation of repressed chromatin on viral genomes. This would therefore correlate with the data presented in Chapter 5, which demonstrate that depletion of either ATRX or hDaxx increases the proportion of cells that escape repression and do not enter quiescence.

Another mechanism of regulation may rely on the proposed role of ATRX in histone deposition. Interestingly, novel evidence suggests incorporation of histone variants H3.1 and H3.3 on HSV-1 promoters during the early hours post infection (Placek et al, 2009). Incorporation of H3.3 is associated with active transcription, although deposition of H3.3 at heterochromatic sites also occurs (reviewed in Elsaesser et al, 2010). This is intriguing since ATRX has been recently shown to interact with H3.3 (Goldberg et al, 2010; Wong et al, 2010), which correlates with its previously published function in histone H3 binding (Otani et al, 2009). This evidence may therefore indicate additional pathways of ATRX-mediated regulation of chromatin assembly and modification during viral infection. In summary, it can be concluded that ATRX and hDaxx may assist in the assembly of repressed chromatin at different stages of the viral life cycle. The subsequent section therefore presents a more detailed discussion regarding repressed chromatin markers, with the focus on the role of HDACs in HCMV and HSV-1 infection.

### 6.3.2 Regulation of the chromatin state of HSV-1 and HCMV genomes: the role of histone deacetylases

Since hDaxx interacts with HDAC1 and is known to repress transcription in some assays through this activity (Hollenbach et al, 2002; Li et al, 2000), it is attractive to suggest that hDaxx influences the efficiency of transcription from parental viral genomes *via* HDAC-dependent chromatin remodelling. Whether that is the case during HSV-1 and HCMV infection in both latency and lytic cycle is therefore an issue that has been subjected to extensive investigation.

With regard to HSV-1 infection, a lot of research has primarily concentrated on the role of viral transcriptional activators in counteracting chromatin assembly on viral genomes. One group has shown that ICP0 interacts with the REST/CoREST/HDAC complex, and causes HDAC1 dissociation from the complex (Gu et al, 2005; Gu & Roizman, 2007). These data correlated with the findings that TSA treatment of certain cell lines partially compensates for the lack of ICP0 during ICP0-null mutant replication. Based on these data, it was concluded that ICP0 acts to inhibit the action of HDACs (Poon et al, 2006; Poon et al, 2003). A number of other observations, however, contradict this conclusion. Firstly, despite an independent report showing the interaction between ICP0 and class II HDACs, ICP0 expression does not increase levels of acetylated histone H4, unlike TSA (Lomonte et al, 2004). Furthermore, in many restrictive cells lines, TSA treatment does not increase the plaque forming efficiency of ICP0-null HSV-1 (Everett et al, 2008). Secondly, ICP0 interaction with the CoREST complex is not essential for ICP0 function in HSV-1 lytic and de-repression assays, and depletion of CoREST does not improve ICP0-null mutant replication, assessed by gene expression and virus yield assays (Everett, 2010; Everett et al, 2009). Therefore these latter observations are inconsistent with the hypothesis that the interaction of ICP0 with the REST/CoREST/HDAC is a core requirement for ICP0 function. Since ICP0 does not co-immunoprecipitate with either hDaxx or ATRX according to the findings of this investigation (Figure 5.14), the overall evidence is not strong enough to speculate that ICP0 directly causes disruption of the ATRX/hDaxx chromatin-repressor activity assembled around incoming HSV-1 genomes during the early stages of the lytic phase of infection. It is plausible however that ICP0 does so indirectly by recruiting additional factors or *via* its E3 ligase activity on other protein components.

If one excludes HDAC-dependent repression mechanisms being essential for repression of HSV-1 genomes (based on the results of HDAC inhibition cited above), histone deposition on HSV-1 promoters reported elsewhere (Cliffe & Knipe, 2008; Herrera & Triezenberg,

2004; Huang et al, 2006; Kent et al, 2004; Oh & Fraser, 2008) may therefore represent the earliest cellular responses to the intrusion of foreign viral DNA. This is also true of the cells infected with high MOIs of ICP0-null mutant virus at the edge of a developing plaque, where cells show more stable recruitment of both ATRX and hDaxx to the sites associated with the incoming viral genomes. In these cells repression does not occur because of the multiplicity dependence of the ICP0-mutant virus phenotype, which reflects saturation of the intrinsic resistance due to high genome numbers. It is assumed that the more stable recruitment at high MOI is indicative of similar events, which occur at low MOI and reflect the repression mechanisms that act on ICP0-null mutant virus. Although limited histone assembly on viral genomes occurs during high MOI infections, these genomes are unlikely to be repressed by nucleosomes and heterochromatin formation due to the saturation of cellular intrinsic defences.

A different scenario can be proposed for HCMV infection. The means by which the virus successfully achieves initiation of lytic infection, allowing the expression of its IE proteins, involves the functions of the tegument protein pp71 and IE product IE1. These aspects of HCMV infection have been addressed in Chapters 1 and 4. The model suggested by the findings presented in this study illustrates that HCMV tegument protein pp71 displaces ATRX from ND10 (see Chapter 4 and (Lukashchuk et al, 2008), and interacts with and subsequently leads to degradation of hDaxx (Cantrell & Bresnahan, 2005; Hwang & Kalejta, 2007; Saffert & Kalejta, 2006). Removal of either ATRX or hDaxx contributes to a substantially increased efficiency of infectivity of pp71-null mutant virus (Preston & Nicholl, 2006; Saffert & Kalejta, 2006; Tavalai et al, 2008); Figures 4.2 and 4.3). It is therefore possible that ATRX and hDaxx act through mechanisms that involve assembly of heterochromatin in HCMV infected cells. A few reports have directly implicated hDaxx in this aspect: (a) downregulation of hDaxx increases the load of acetylated nucleosomal histone markers on HCMV promoters (Woodhall et al, 2006); and (b) TSA treatment together with stabilization of hDaxx allows increased IE1 production (Saffert & Kalejta, 2006). The observation that HCMV DNA is associated with nucleosomes (Nitzsche et al, 2008) is consistent with a role for both ATRX- and hDaxx-mediated repression mechanisms, according to the potential models that involve multi-protein chromatin modification repressor complexes as discussed above. Whether ATRX performs an HDAC-dependent role in this repression mechanism, by analogy with hDaxx, is currently unclear, however one can assume that interactions of the ATRX/hDaxx complex with additional co-repressors may contribute to heterochromatin assembly on HCMV genomes.

Based on the role of hDaxx in ATRX targeting to ND10 and viral nucleoprotein complexes, it is possible that hDaxx may be required for ATRX functions at HCMV genome promoters. This hypothesis would therefore correlate with the fact that depletion of hDaxx affects not only gene expression of pp71-null mutant virus but also that of wt virus (Tavalai et al, 2008). Whereas the role of the interaction between ATRX and hDaxx has been subject to a detailed investigation in the context of HSV-1 infection in the present study, further investigations could address the same issues in HCMV infection. This evidence provides further support that the chromatin repression mechanisms during the early lytic phase of HSV-1 and HCMV infection are distinct.

Mechanisms regulating the latent and quiescent states of HSV-1 and HCMV genomes may be more related than during lytic infection. Thus, it appears that in models of both HSV-1 (Figure 5.10) and HCMV (Saffert & Kalejta, 2007) quiescent infection hDaxx contributes to the normally efficient repression of the viral genomes. Whether this reflects the requirement of hDaxx in biological latency, however, is an issue of further complexity and controversy. In HCMV-based studies, hDaxx has been shown to be important for maintenance of repression of HCMV genomes in latent systems, using undifferentiated quiescently HCMV-infected cells (Saffert & Kalejta, 2007). Consistent with the situation in lytic infection, hDaxx appears to function through the activity of HDACs, since (a) TSA treatment of normally non-permissive to HCMV cells reverses the cell phenotype to permissive, followed by association with the increase in acetylated histone levels; and (b) overexpression of HDAC3 reduced permissiveness to HCMV infection in differentiated cells (Murphy et al, 2002). In the situation when pp71-null mutant genomes are repressed (as presented in Chapter 4, 4.2), it is possible that the mechanisms operating during this repression are related to some extent to the latency systems demonstrated in these reports. This therefore would explain the increased gene expression of pp71-null mutant virus once hDaxx or ATRX are removed. Taking into account the role of HDACs in maintaining nucleosome structure by catalysing removal of acetyl groups on histones, this indicates a role for nucleosome assembly during repression in HCMV infected cells. Hence, this discussion links HDAC-dependent heterochromatin formation on viral genomes to the functions of hDaxx and ATRX.

When analysing data concerning the mechanisms of chromatin-regulated latency and reactivation in HSV-1 infected cells, consideration of the different systems must be taken into account. According to several reports reactivation from quiescence in infected neuronal cell cultures can occur *via* supplying ICP0, VP16, ICP4, as well as by treating

with TSA and other HDAC inhibitors or inducing stress (Arthur et al, 2001; Danaher et al, 2005; Halford et al, 2001; Miller et al, 2006; Terry-Allison et al, 2007). These data indicate that the functions of viral transcriptional activators can be compensated by the inhibition of HDAC activities. In non-neuronal restrictive cell cultures however such as fibroblasts, establishment of quiescently infected cell lines corresponds to the formation of very tight repression mechanisms that are reactivated by ICP0 and not by TSA (Everett et al, 2008; Preston & Nicholl, 2005; Terry-Allison et al, 2007). These studies therefore indicate either HDAC-independent repression mechanisms or much more densely arranged heterochromatin-like structures than those observed in quiescently infected cell lines of neuronal origin. An exception is in Vero cells in which the defect in ICP0-null plaque formation is significantly lower than in fibroblasts, and TSA treatment result in some level of derepression of quiescent HSV-1 genomes (Terry-Allison et al, 2007). Taking into account the differences in experimental systems used in these studies, the importance of a cell type when interpreting the involvement of heterochromatin-mediated repression mechanisms occurring on viral genomes cannot be underestimated.

#### **6.4 Future directions in anti-viral cellular intrinsic immunity**

In the present investigation, ATRX and hDaxx have been identified as components of cellular anti-viral intrinsic resistance mechanisms. Although the analysis of the precise mechanisms of their action is beyond the scope of the present investigation, evidence suggests that chromatin has a large part to play. In the summary of the results presented in this thesis, and the evidence discussed above, it is proposed that ATRX and hDaxx constitute components of multi-subunit chromatin repressor complexes that assemble on viral DNA and that recruit additional co-factors involved in histone modification and repression. Further investigation into the roles of histone and nucleosome association on viral promoters may reveal the cellular response mechanisms of the early stages of infection as well as the mode of chromatin-mediated regulation of quiescent herpesvirus genomes. So far, the evidence that both HCMV and HSV-1 latent DNA is associated with nucleosomes (Deshmane & Fraser, 1989; Ferenczy & DeLuca, 2009; Nitzsche et al, 2008) suggests that the ATRX/hDaxx complex may contribute to the maintenance of repression of viral genomes by assisting in heterochromatin formation *via* interacting with the co-repressor complexes. The existing evidence, however, is not conclusive enough to suggest that the mechanisms of heterochromatin assembly acting on viral genomes reflect those that assemble on densely packed cellular heterochromatin. One of the hypotheses driving the current line of research states that the factors implicated in repressed chromatin

assembly and maintenance of the cellular heterochromatin may also be involved to some extent in repressed chromatin assembly on viral genomes.

Evidently, the precise molecular mechanisms that are involved in formation of DNA repressor complexes would need to be further clarified. Therefore, one of the aspects for future work should be aimed at identifying novel components involved in the formation of such chromatin complexes. The primary candidates for studies should undoubtedly be those proteins that are involved in direct histone and DNA interactions and maintenance of repressed chromatin structures. These have been mentioned throughout and include such proteins such as HP1 and MeCP2. These proteins have previously been observed to localise to ND10 (Luciani et al, 2006; Nan et al, 2007). Despite the fact that HDACs do not reside at ND10 (Li et al, 2000), PML interacts with HDAC1 to induce transcriptional repression (Wu et al, 2001). These properties make HP1, MeCP2 and HDACs obvious candidates to study ND10-mediated anti-viral intrinsic resistance. Evidently, in EBV infection, transcriptional repression regulated by MeCP2/HDAC-dependent mechanisms of certain genes and induced by the expression of EBV latent membrane protein 1 correlates with the increased invasive potential of EBV-transformed tumourigenic cells (Tsai et al, 2006). Although gamma-herpesviruses differ substantially in their life cycles from alpha- and beta-herpesviruses, this evidence may indicate that these cellular factors may play similar roles in transcriptional repression during HSV-1 and HCMV infection. In addition, other candidate proteins for analysis that are involved in regulation of repressed or active chromatin structures may include a histone chaperone HIRA and centromeric proteins (CENPs) that are recruited to pericentromeric heterochromatin. CENP-A, -B and -C have all been demonstrated to be degraded by HSV-1 ICP0 (Everett et al, 1999a; Lomonte & Morency, 2007; Lomonte et al, 2001). CENP-A is a histone H3 variant (Black & Bassett, 2008), and its ICP0-mediated degradation may provide the link between the counteracting function of ICP0 and the low histone occupancy on replicating viral genomes. HIRA, which also localises to ND10 (Zhang et al, 2005), functions as the H3.3 chaperone and is required for H3.3 enrichment at active and repressed chromatin sites (Goldberg et al, 2010). Downregulation of HIRA results in reduction in H3.3 incorporation in HSV-1 infected cells (Placek et al, 2009), indicating a role for HIRA in the regulation of histone deposition on lytic viral promoters. Further research should focus on how this regulation correlates with viral infectivity and the ability to establish and maintain latency.

The reported interaction between PML and several HDACs (Wu et al, 2001) and between Sp100 and HP1 (Seeler et al, 1998), may provide a link between PML-, Sp100- and

ATRX/hDaxx-mediated repression during viral infection. Indeed, residence of the heterochromatin-associated proteins at ND10 (Luciani et al, 2006) can yield useful clues to the assembly of ND10 chromatin repressor complexes on the incoming viral DNA. Investigating the requirement for the interactions within these complexes may unravel the complexities that underlie assembly of the chromatin repressor complexes on cellular and viral genomes.

Although ATRX and hDaxx still remain largely uncharacterised in various aspects of their transcriptional regulation, their potential in chromatin assembly appears to be significant but requires further understanding. The work presented in this thesis suggests novel clues to the regulation of HSV-1 and HCMV infection by heterochromatin. Expanding these issues into the context of other herpesviruses and deeper understanding of the mechanisms involved in the regulation of repressed viral genomes can potentially contribute to the development of the new approaches aimed to prevent reactivation and transmission of these viruses.

## Reference List

- Ace CI, Dalrymple MA, Ramsay FH, Preston VG, Preston CM (1988) Mutational analysis of the herpes simplex virus type 1 trans-inducing factor Vmw65. *J Gen Virol* **69** ( Pt 10): 2595-2605
- Ace CI, McKee TA, Ryan JM, Cameron JM, Preston CM (1989) Construction and characterization of a herpes simplex virus type 1 mutant unable to transinduce immediate-early gene expression. *J Virol* **63**: 2260-2269
- Adamson AL, Kenney S (2001) Epstein-barr virus immediate-early protein BZLF1 is SUMO-1 modified and disrupts promyelocytic leukemia bodies. *J Virol* **75**: 2388-2399
- Ahn JH, Brignole EJ, 3rd, Hayward GS (1998) Disruption of PML subnuclear domains by the acidic IE1 protein of human cytomegalovirus is mediated through interaction with PML and may modulate a RING finger-dependent cryptic transactivator function of PML. *Mol Cell Biol* **18**: 4899-4913
- Ahn JH, Hayward GS (1997) The major immediate-early proteins IE1 and IE2 of human cytomegalovirus colocalize with and disrupt PML-associated nuclear bodies at very early times in infected permissive cells. *J Virol* **71**: 4599-4613
- Ahn JH, Hayward GS (2000) Disruption of PML-associated nuclear bodies by IE1 correlates with efficient early stages of viral gene expression and DNA replication in human cytomegalovirus infection. *Virology* **274**: 39-55
- Alexeev A, Mazin A, Kowalczykowski SC (2003) Rad54 protein possesses chromatin-remodeling activity stimulated by the Rad51-ssDNA nucleoprotein filament. *Nat Struct Biol* **10**: 182-186
- Amin HM, Saeed S, Alkan S (2001) Histone deacetylase inhibitors induce caspase-dependent apoptosis and downregulation of daxx in acute promyelocytic leukaemia with t(15;17). *Br J Haematol* **115**: 287-297
- Anders DG, Kerry JA, Pari, GS, "CMV DNA synthesis and late viral gene expression" In: Arvin, AM, Mocarski, ES, Moore, P, et al., Editors. Human Herpesviruses: Biology, Therapy and Immunoprophylaxis. Cambridge: Cambridge Press; 2007: 295–311
- Antrobus R, Grant K, Gangadharan B, Chittenden D, Everett RD, Zitzmann N, Boutell C (2009) Proteomic analysis of cells in the early stages of herpes simplex virus type-1 infection reveals widespread changes in the host cell proteome. *Proteomics* **9**: 3913-3927
- Argentaro A, Yang JC, Chapman L, Kowalczyk MS, Gibbons RJ, Higgs DR, Neuhaus D, Rhodes D (2007) Structural consequences of disease-causing mutations in the ATRX-DNMT3-DNMT3L (ADD) domain of the chromatin-associated protein ATRX. *Proc Natl Acad Sci U S A* **104**: 11939-11944
- Arthur JL, Scarpini CG, Connor V, Lachmann RH, Tolkovsky AM, Efstathiou S (2001) Herpes simplex virus type 1 promoter activity during latency establishment, maintenance, and reactivation in primary dorsal root neurons in vitro. *J Virol* **75**: 3885-3895

- Ascoli CA, Maul GG (1991) Identification of a novel nuclear domain. *J Cell Biol* **112**: 785-795
- Bailey D, O'Hare P (2002) Herpes simplex virus 1 ICP0 co-localizes with a SUMO-specific protease. *J Gen Virol* **83**: 2951-2964
- Baldick CJ, Jr., Marchini A, Patterson CE, Shenk T (1997) Human cytomegalovirus tegument protein pp71 (ppUL82) enhances the infectivity of viral DNA and accelerates the infectious cycle. *J Virol* **71**: 4400-4408
- Bannister AJ, Zegerman P, Partridge JF, Miska EA, Thomas JO, Allshire RC, Kouzarides T (2001) Selective recognition of methylated lysine 9 on histone H3 by the HP1 chromo domain. *Nature* **410**: 120-124
- Barlow PN, Luisi B, Milner A, Elliott M, Everett R (1994) Structure of the C3HC4 domain by 1H-nuclear magnetic resonance spectroscopy. A new structural class of zinc-finger. *J Mol Biol* **237**: 201-211
- Baumann C, Schmidtman A, Muegge K, De La Fuente R (2008) Association of ATRX with pericentric heterochromatin and the Y chromosome of neonatal mouse spermatogonia. *BMC Mol Biol* **9**: 29
- Bego M, Maciejewski J, Khaiboullina S, Pari G, St Jeor S (2005) Characterization of an antisense transcript spanning the UL81-82 locus of human cytomegalovirus. *J Virol* **79**: 11022-11034
- Bell P, Lieberman PM, Maul GG (2000) Lytic but not latent replication of epstein-barr virus is associated with PML and induces sequential release of nuclear domain 10 proteins. *J Virol* **74**: 11800-11810
- Berube NG, Healy J, Medina CF, Wu S, Hodgson T, Jagla M, Picketts DJ (2008) Patient mutations alter ATRX targeting to PML nuclear bodies. *Eur J Hum Genet* **16**: 192-201
- Berube NG, Mangelsdorf M, Jagla M, Vanderluit J, Garrick D, Gibbons RJ, Higgs DR, Slack RS, Picketts DJ (2005) The chromatin-remodeling protein ATRX is critical for neuronal survival during corticogenesis. *The Journal of clinical investigation* **115**: 258-267
- Berube NG, Smeenk CA, Picketts DJ (2000) Cell cycle-dependent phosphorylation of the ATRX protein correlates with changes in nuclear matrix and chromatin association. *Hum Mol Genet* **9**: 539-547
- Bieniasz PD (2004) Intrinsic immunity: a front-line defense against viral attack. *Nature immunology* **5**: 1109-1115
- Bienz M (2006) The PHD finger, a nuclear protein-interaction domain. *Trends in biochemical sciences* **31**: 35-40
- Biron CA, Nguyen KB, Pien GC, Cousens LP, Salazar-Mather TP (1999) Natural killer cells in antiviral defense: function and regulation by innate cytokines. *Annual review of immunology* **17**: 189-220
- Bischof O, Kim SH, Irving J, Beresten S, Ellis NA, Campisi J (2001) Regulation and localization of the Bloom syndrome protein in response to DNA damage. *J Cell Biol* **153**: 367-380

- Black BE, Bassett EA (2008) The histone variant CENP-A and centromere specification. *Current opinion in cell biology* **20**: 91-100
- Boddy MN, Howe K, Etkin LD, Solomon E, Freemont PS (1996) PIC 1, a novel ubiquitin-like protein which interacts with the PML component of a multiprotein complex that is disrupted in acute promyelocytic leukaemia. *Oncogene* **13**: 971-982
- Boutell C, Orr A, Everett RD (2003) PML residue lysine 160 is required for the degradation of PML induced by herpes simplex virus type 1 regulatory protein ICP0. *J Virol* **77**: 8686-8694
- Boutell C, Sadis S, Everett RD (2002) Herpes simplex virus type 1 immediate-early protein ICP0 and its isolated RING finger domain act as ubiquitin E3 ligases in vitro. *J Virol* **76**: 841-850
- Brenner C, Fuks F (2007) A methylation rendezvous: reader meets writers. *Developmental cell* **12**: 843-844
- Bresnahan WA, Hultman GE, Shenk T (2000) Replication of wild-type and mutant human cytomegalovirus in life-extended human diploid fibroblasts. *J Virol* **74**: 10816-10818
- Bresnahan WA, Shenk TE (2000) UL82 virion protein activates expression of immediate early viral genes in human cytomegalovirus-infected cells. *Proc Natl Acad Sci U S A* **97**: 14506-14511
- Bringhurst RM, Schaffer PA (2006) Cellular stress rather than stage of the cell cycle enhances the replication and plating efficiencies of herpes simplex virus type 1 ICP0-viruses. *J Virol* **80**: 4528-4537
- Brown SM, Ritchie DA, Subak-Sharpe JH (1973) Genetic studies with herpes simplex virus type 1. The isolation of temperature-sensitive mutants, their arrangement into complementation groups and recombination analysis leading to a linkage map. *J Gen Virol* **18**: 329-346
- Butcher SJ, Aitken J, Mitchell J, Gowen B, Dargan DJ (1998) Structure of the human cytomegalovirus B capsid by electron cryomicroscopy and image reconstruction. *Journal of structural biology* **124**: 70-76
- Cai W, Schaffer PA (1992) Herpes simplex virus type 1 ICP0 regulates expression of immediate-early, early, and late genes in productively infected cells. *J Virol* **66**: 2904-2915
- Cai WZ, Schaffer PA (1989) Herpes simplex virus type 1 ICP0 plays a critical role in the de novo synthesis of infectious virus following transfection of viral DNA. *J Virol* **63**: 4579-4589
- Campadelli-Fiume G, Menotti L, "Entry of alphaherpesviruses into the cell" in: Arvin, AM, Mocarski, ES, Moore, P, et al., Editors. *Human Herpesviruses: Biology, Therapy and Immunoprophylaxis*. Cambridge: Cambridge Press; 2007: pp. 93-111
- Canning M, Boutell C, Parkinson J, Everett RD (2004) A RING finger ubiquitin ligase is protected from autocatalyzed ubiquitination and degradation by binding to ubiquitin-specific protease USP7. *J Biol Chem* **279**: 38160-38168

- Cantrell SR, Bresnahan WA (2005) Interaction between the human cytomegalovirus UL82 gene product (pp71) and hDaxx regulates immediate-early gene expression and viral replication. *J Virol* **79**: 7792-7802
- Cantrell SR, Bresnahan WA (2006) Human cytomegalovirus (HCMV) UL82 gene product (pp71) relieves hDaxx-mediated repression of HCMV replication. *J Virol* **80**: 6188-6191
- Carvalho T, Seeler JS, Ohman K, Jordan P, Pettersson U, Akusjarvi G, Carmo-Fonseca M, Dejean A (1995) Targeting of adenovirus E1A and E4-ORF3 proteins to nuclear matrix-associated PML bodies. *J Cell Biol* **131**: 45-56
- Castillo JP, Kowalik TF (2002) Human cytomegalovirus immediate early proteins and cell growth control. *Gene* **290**: 19-34
- Chang CC, Lin DY, Fang HI, Chen RH, Shih HM (2005) Daxx mediates the small ubiquitin-like modifier-dependent transcriptional repression of Smad4. *J Biol Chem* **280**: 10164-10173
- Chang HY, Nishitoh H, Yang X, Ichijo H, Baltimore D (1998) Activation of apoptosis signal-regulating kinase 1 (ASK1) by the adapter protein Daxx. *Science* **281**: 1860-1863
- Chang JT, Schmid MF, Rixon FJ, Chiu W (2007) Electron cryotomography reveals the portal in the herpesvirus capsid. *J Virol* **81**: 2065-2068
- Chelbi-Alix MK, de The H (1999) Herpes virus induced proteasome-dependent degradation of the nuclear bodies-associated PML and Sp100 proteins. *Oncogene* **18**: 935-941
- Chelbi-Alix MK, Pelicano L, Quignon F, Koken MH, Venturini L, Stadler M, Pavlovic J, Degos L, de The H (1995) Induction of the PML protein by interferons in normal and APL cells. *Leukemia* **9**: 2027-2033
- Chelbi-Alix MK, Quignon F, Pelicano L, Koken MH, de The H (1998) Resistance to virus infection conferred by the interferon-induced promyelocytic leukemia protein. *J Virol* **72**: 1043-1051
- Chen J, Silverstein S (1992) Herpes simplex viruses with mutations in the gene encoding ICP0 are defective in gene expression. *J Virol* **66**: 2916-2927
- Chen SF, Zhu CM, Wan YP (2009) Progress on the subcellular localization of Daxx. *Chinese journal of cancer* **28**: 1333-1336
- Cherrington JM, Khoury EL, Mocarski ES (1991) Human cytomegalovirus ie2 negatively regulates alpha gene expression via a short target sequence near the transcription start site. *J Virol* **65**: 887-896
- Cherrington JM, Mocarski ES (1989) Human cytomegalovirus ie1 transactivates the alpha promoter-enhancer via an 18-base-pair repeat element. *J Virol* **63**: 1435-1440
- Cliffe AR, Knipe DM (2008) Herpes simplex virus ICP0 promotes both histone removal and acetylation on viral DNA during lytic infection. *J Virol* **82**: 12030-12038

- Cohen JI (2000) Epstein-Barr virus infection. *The New England journal of medicine* **343**: 481-492
- Coleman HM, Connor V, Cheng ZS, Grey F, Preston CM, Efstathiou S (2008) Histone modifications associated with herpes simplex virus type 1 genomes during quiescence and following ICP0-mediated de-repression. *J Gen Virol* **89**: 68-77
- Condemine W, Takahashi Y, Zhu J, Puvion-Dutilleul F, Guegan S, Janin A, de The H (2006) Characterization of endogenous human promyelocytic leukemia isoforms. *Cancer Res* **66**: 6192-6198
- Cook ML, Bastone VB, Stevens JG (1974) Evidence that neurons harbor latent herpes simplex virus. *Infect Immun* **9**: 946-951
- Cunningham AL, Diefenbach RJ, Miranda-Saksena M, Bosnjak L, Kim M, Jones C, Douglas MW (2006) The cycle of human herpes simplex virus infection: virus transport and immune control. *J Infect Dis* **194 Suppl 1**: S11-18
- Danaher RJ, Jacob RJ, Steiner MR, Allen WR, Hill JM, Miller CS (2005) Histone deacetylase inhibitors induce reactivation of herpes simplex virus type 1 in a latency-associated transcript-independent manner in neuronal cells. *Journal of neurovirology* **11**: 306-317
- Daniel MT, Koken M, Romagne O, Barbey S, Bazarbachi A, Stadler M, Guillemin MC, Degos L, Chomienne C, de The H (1993) PML protein expression in hematopoietic and acute promyelocytic leukemia cells. *Blood* **82**: 1858-1867
- Davison A, Bhella D "Comparative betaherpesvirus genome and virion structure" in: Arvin, AM, Mocarski, ES, Moore, P, et al., Editors. *Human Herpesviruses: Biology, Therapy and Immunoprophylaxis*. Cambridge: Cambridge Press; 2007 pp. 177-203
- Davison A "Comparative analysis of the genomes" in: Arvin, AM, Mocarski, ES, Moore, P, et al., Editors. *Human Herpesviruses: Biology, Therapy and Immunoprophylaxis*. Cambridge: Cambridge Press; 2007 pp. 10-26
- Davison AJ, Eberle R, Ehlers B, Hayward GS, McGeoch DJ, Minson AC, Pellett PE, Roizman B, Studdert MJ, Thiry E (2009) The order Herpesvirales. *Archives of virology* **154**: 171-177
- De La Fuente R, Viveiros MM, Wigglesworth K, Eppig JJ (2004) ATRX, a member of the SNF2 family of helicase/ATPases, is required for chromosome alignment and meiotic spindle organization in metaphase II stage mouse oocytes. *Dev Biol* **272**: 1-14
- de Ruijter AJ, van Gennip AH, Caron HN, Kemp S, van Kuilenburg AB (2003) Histone deacetylases (HDACs): characterization of the classical HDAC family. *The Biochemical journal* **370**: 737-749
- Delboy MG, Siekavizza-Robles CR, Nicola AV (2010) Herpes simplex virus tegument ICP0 is capsid associated, and its E3 ubiquitin ligase domain is important for incorporation into virions. *J Virol* **84**: 1637-1640
- Deshmane SL, Fraser NW (1989) During latency, herpes simplex virus type 1 DNA is associated with nucleosomes in a chromatin structure. *J Virol* **63**: 943-947

- Deshpande SP, Kumaraguru U, Rouse BT (2000) Dual role of B cells in mediating innate and acquired immunity to herpes simplex virus infections. *Cellular immunology* **202**: 79-87
- Dohner K, Wolfstein A, Prank U, Echeverri C, Dujardin D, Vallee R, Sodeik B (2002) Function of dynein and dynactin in herpes simplex virus capsid transport. *Molecular biology of the cell* **13**: 2795-2809
- Dolan A, Cunningham C, Hector RD, Hassan-Walker AF, Lee L, Addison C, Dargan DJ, McGeoch DJ, Gatherer D, Emery VC, Griffiths PD, Sinzger C, McSharry BP, Wilkinson GW, Davison AJ (2004) Genetic content of wild-type human cytomegalovirus. *J Gen Virol* **85**: 1301-1312
- Doniger J, Muralidhar S, Rosenthal LJ (1999) Human cytomegalovirus and human herpesvirus 6 genes that transform and transactivate. *Clinical microbiology reviews* **12**: 367-382
- Doucas V, Ishov AM, Romo A, Juguilon H, Weitzman MD, Evans RM, Maul GG (1996) Adenovirus replication is coupled with the dynamic properties of the PML nuclear structure. *Genes & development* **10**: 196-207
- Douglas MW, Diefenbach RJ, Homa FL, Miranda-Saksena M, Rixon FJ, Vittone V, Byth K, Cunningham AL (2004) Herpes simplex virus type 1 capsid protein VP26 interacts with dynein light chains RP3 and Tctex1 and plays a role in retrograde cellular transport. *J Biol Chem* **279**: 28522-28530
- Duffy C, Lavail JH, Tauscher AN, Wills EG, Blaho JA, Baines JD (2006) Characterization of a UL49-null mutant: VP22 of herpes simplex virus type 1 facilitates viral spread in cultured cells and the mouse cornea. *J Virol* **80**: 8664-8675
- Ecsedy JA, Michaelson JS, Leder P (2003) Homeodomain-interacting protein kinase 1 modulates Daxx localization, phosphorylation, and transcriptional activity. *Mol Cell Biol* **23**: 950-960
- Efstathiou S, Preston CM (2005) Towards an understanding of the molecular basis of herpes simplex virus latency. *Virus Res* **111**: 108-119
- Elgadi MM, Hayes CE, Smiley JR (1999) The herpes simplex virus vhs protein induces endoribonucleolytic cleavage of target RNAs in cell extracts. *J Virol* **73**: 7153-7164
- Elsaesser SJ, Goldberg AD, Allis CD (2010) New functions for an old variant: no substitute for histone H3.3. *Current opinion in genetics & development* **20**: 1-8
- Everett R, O'Hare P, O'Rourke D, Barlow P, Orr A (1995) Point mutations in the herpes simplex virus type 1 Vmw110 RING finger helix affect activation of gene expression, viral growth, and interaction with PML-containing nuclear structures. *J Virol* **69**: 7339-7344
- Everett RD (1984) Trans activation of transcription by herpes virus products: requirement for two HSV-1 immediate-early polypeptides for maximum activity. *Embo J* **3**: 3135-3141
- Everett RD (1987) A detailed mutational analysis of Vmw110, a trans-acting transcriptional activator encoded by herpes simplex virus type 1. *Embo J* **6**: 2069-2076

Everett RD (1988) Analysis of the functional domains of herpes simplex virus type 1 immediate-early polypeptide Vmw110. *J Mol Biol* **202**: 87-96

Everett RD (2000) ICP0, a regulator of herpes simplex virus during lytic and latent infection. *Bioessays* **22**: 761-770

Everett RD (2001) DNA viruses and viral proteins that interact with PML nuclear bodies. *Oncogene* **20**: 7266-7273

Everett RD (2006) Interactions between DNA viruses, ND10 and the DNA damage response. *Cellular microbiology* **8**: 365-374

Everett RD "The roles of ICP0 during HSV-1 infection". In: Alpha Herpesviruses - Molecular and Cellular Biology. R. M. Sandri-Goldin, Editors. Wymondham, Caister Academic Press 2006: pp. 39-64

Everett RD (2010) Depletion of CoREST Does Not Improve the Replication of ICP0 Null Mutant Herpes Simplex Virus Type 1. *J Virol* **84**: 3695-3698

Everett RD, Barlow P, Milner A, Luisi B, Orr A, Hope G, Lyon D (1993a) A novel arrangement of zinc-binding residues and secondary structure in the C3HC4 motif of an alpha herpes virus protein family. *J Mol Biol* **234**: 1038-1047

Everett RD, Boutell C, Orr A (2004) Phenotype of a herpes simplex virus type 1 mutant that fails to express immediate-early regulatory protein ICP0. *J Virol* **78**: 1763-1774

Everett RD, Chelbi-Alix MK (2007) PML and PML nuclear bodies: implications in antiviral defence. *Biochimie* **89**: 819-830

Everett RD, Cross A, Orr A (1993b) A truncated form of herpes simplex virus type 1 immediate-early protein Vmw110 is expressed in a cell type dependent manner. *Virology* **197**: 751-756

Everett RD, Earnshaw WC, Findlay J, Lomonte P (1999a) Specific destruction of kinetochore protein CENP-C and disruption of cell division by herpes simplex virus immediate-early protein Vmw110. *Embo J* **18**: 1526-1538

Everett RD, Earnshaw WC, Pluta AF, Sternsdorf T, Ainsztein AM, Carmena M, Ruchaud S, Hsu WL, Orr A (1999b) A dynamic connection between centromeres and ND10 proteins. *J Cell Sci* **112** ( Pt 20): 3443-3454

Everett RD, Freemont P, Saitoh H, Dasso M, Orr A, Kathoria M, Parkinson J (1998a) The disruption of ND10 during herpes simplex virus infection correlates with the Vmw110- and proteasome-dependent loss of several PML isoforms. *J Virol* **72**: 6581-6591

Everett RD, Maul GG (1994) HSV-1 IE protein Vmw110 causes redistribution of PML. *Embo J* **13**: 5062-5069

Everett RD, Meredith M, Orr A (1999c) The ability of herpes simplex virus type 1 immediate-early protein Vmw110 to bind to a ubiquitin-specific protease contributes to its roles in the activation of gene expression and stimulation of virus replication. *J Virol* **73**: 417-426

- Everett RD, Meredith M, Orr A, Cross A, Kathoria M, Parkinson J (1997) A novel ubiquitin-specific protease is dynamically associated with the PML nuclear domain and binds to a herpesvirus regulatory protein. *Embo J* **16**: 1519-1530
- Everett RD, Murray J (2005) ND10 components relocate to sites associated with herpes simplex virus type 1 nucleoprotein complexes during virus infection. *J Virol* **79**: 5078-5089
- Everett RD, Murray J, Orr A, Preston CM (2007) Herpes simplex virus type 1 genomes are associated with ND10 nuclear substructures in quiescently infected human fibroblasts. *J Virol* **81**: 10991-11004
- Everett RD, Orr A, Preston CM (1998b) A viral activator of gene expression functions via the ubiquitin-proteasome pathway. *Embo J* **17**: 7161-7169
- Everett RD, Parada C, Gripon P, Sirma H, Orr A (2008) Replication of ICP0-null mutant herpes simplex virus type 1 is restricted by both PML and Sp100. *J Virol* **82**: 2661-2672
- Everett RD, Parsy ML, Orr A (2009) Analysis of the functions of herpes simplex virus type 1 regulatory protein ICP0 that are critical for lytic infection and derepression of quiescent viral genomes. *J Virol* **83**: 4963-4977
- Everett RD, Rechter S, Papior P, Tavalai N, Stamminger T, Orr A (2006) PML contributes to a cellular mechanism of repression of herpes simplex virus type 1 infection that is inactivated by ICP0. *J Virol* **80**: 7995-8005
- Everett RD, Zafiropoulos A (2004) Visualization by live-cell microscopy of disruption of ND10 during herpes simplex virus type 1 infection. *J Virol* **78**: 11411-11415
- Everly DN, Jr., Feng P, Mian IS, Read GS (2002) mRNA degradation by the virion host shutoff (Vhs) protein of herpes simplex virus: genetic and biochemical evidence that Vhs is a nuclease. *J Virol* **76**: 8560-8571
- Farrell MJ, Dobson AT, Feldman LT (1991) Herpes simplex virus latency-associated transcript is a stable intron. *Proc Natl Acad Sci U S A* **88**: 790-794
- Ferenczy MW, DeLuca NA (2009) Epigenetic modulation of gene expression from quiescent herpes simplex virus genomes. *J Virol* **83**: 8514-8524
- Fishman JA, Emery V, Freeman R, Pascual M, Rostaing L, Schlitt HJ, Sgarabotto D, Torre-Cisneros J, Uknis ME (2007) Cytomegalovirus in transplantation - challenging the status quo. *Clinical transplantation* **21**: 149-158
- Flint J, Shenk T (1997) Viral transactivating proteins. *Annual review of genetics* **31**: 177-212
- Fuks F, Hurd PJ, Deplus R, Kouzarides T (2003) The DNA methyltransferases associate with HP1 and the SUV39H1 histone methyltransferase. *Nucleic Acids Res* **31**: 2305-2312
- Fusconi M, Cassani F, Govoni M, Caselli A, Farabegoli F, Lenzi M, Ballardini G, Zauli D, Bianchi FB (1991) Anti-nuclear antibodies of primary biliary cirrhosis recognize 78-92-kD and 96-100-kD proteins of nuclear bodies. *Clinical and experimental immunology* **83**: 291-297

- Ganem D “Kaposi's Sarcoma-associated Herpesvirus” in Fields' Virology 5th Edition. D.M. Knipe, P. Howley, D.E. Griffin, R.A. Lamb, M.A. Martin, B. Roizman, and S.E. Straus, Editors. Lippincott-Williams and Wilkins, New York, N.Y. 2007: p 2848-2888
- Garrick D, Samara V, McDowell TL, Smith AJ, Dobbie L, Higgs DR, Gibbons RJ (2004) A conserved truncated isoform of the ATR-X syndrome protein lacking the SWI/SNF-homology domain. *Gene* **326**: 23-34
- Gibbons R (2006) Alpha thalassaemia-mental retardation, X linked. *Orphanet J Rare Dis* **1**: 15
- Gibbons RJ, Bachoo S, Picketts DJ, Aftimos S, Asenbauer B, Bergoffen J, Berry SA, Dahl N, Fryer A, Keppler K, Kurosawa K, Levin ML, Masuno M, Neri G, Pierpont ME, Slaney SF, Higgs DR (1997) Mutations in transcriptional regulator ATRX establish the functional significance of a PHD-like domain. *Nature genetics* **17**: 146-148
- Gibbons RJ, McDowell TL, Raman S, O'Rourke DM, Garrick D, Ayyub H, Higgs DR (2000) Mutations in ATRX, encoding a SWI/SNF-like protein, cause diverse changes in the pattern of DNA methylation. *Nature genetics* **24**: 368-371
- Gibbons RJ, Picketts DJ, Villard L, Higgs DR (1995) Mutations in a putative global transcriptional regulator cause X-linked mental retardation with alpha-thalassemia (ATR-X syndrome). *Cell* **80**: 837-845
- Gilden DH, Mahalingam R, Cohrs RJ, Tyler KL (2007) Herpesvirus infections of the nervous system. *Nature clinical practice* **3**: 82-94
- Goldberg AD, Banaszynski LA, Noh KM, Lewis PW, Elsaesser SJ, Stadler S, Dewell S, Law M, Guo X, Li X, Wen D, Chapgier A, Dekelver RC, Miller JC, Lee YL, Boydston EA, Holmes MC, Gregory PD, Grealley JM, Rafii S, Yang C, Scambler PJ, Garrick D, Gibbons RJ, Higgs DR, Cristea IM, Urnov FD, Zheng D, Allis CD (2010) Distinct Factors Control Histone Variant H3.3 Localization at Specific Genomic Regions. *Cell* **140**: 678-691
- Goldsmith K, Chen W, Johnson DC, Hendricks RL (1998) Infected cell protein (ICP)47 enhances herpes simplex virus neurovirulence by blocking the CD8+ T cell response. *The Journal of experimental medicine* **187**: 341-348
- Goodrum F, Reeves M, Sinclair J, High K, Shenk T (2007) Human cytomegalovirus sequences expressed in latently infected individuals promote a latent infection in vitro. *Blood* **110**: 937-945
- Grant PA (2001) A tale of histone modifications. *Genome Biol* **2**: REVIEWS0003
- Greaves RF, O'Hare P (1990) Structural requirements in the herpes simplex virus type 1 transactivator Vmw65 for interaction with the cellular octamer-binding protein and target TAATGARAT sequences. *J Virol* **64**: 2716-2724
- Gripon P, Rumin S, Urban S, Le Seyec J, Glaise D, Cannie I, Guyomard C, Lucas J, Trepo C, Guguen-Guillouzo C (2002) Infection of a human hepatoma cell line by hepatitis B virus. *Proc Natl Acad Sci U S A* **99**: 15655-15660

- Groves IJ, Sinclair JH (2007) Knockdown of hDaxx in normally non-permissive undifferentiated cells does not permit human cytomegalovirus immediate-early gene expression. *J Gen Virol* **88**: 2935-2940
- Grunewald K, Desai P, Winkler DC, Heymann JB, Belnap DM, Baumeister W, Steven AC (2003) Three-dimensional structure of herpes simplex virus from cryo-electron tomography. *Science* **302**: 1396-1398
- Grunstein M (1997) Histone acetylation in chromatin structure and transcription. *Nature* **389**: 349-352
- Gu B, Kuddus R, DeLuca NA (1995) Repression of activator-mediated transcription by herpes simplex virus ICP4 via a mechanism involving interactions with the basal transcription factors TATA-binding protein and TFIIB. *Mol Cell Biol* **15**: 3618-3626
- Gu H, Liang Y, Mandel G, Roizman B (2005) Components of the REST/CoREST/histone deacetylase repressor complex are disrupted, modified, and translocated in HSV-1-infected cells. *Proc Natl Acad Sci U S A* **102**: 7571-7576
- Gu H, Roizman B (2007) Herpes simplex virus-infected cell protein 0 blocks the silencing of viral DNA by dissociating histone deacetylases from the CoREST-REST complex. *Proc Natl Acad Sci U S A* **104**: 17134-17139
- Guldner HH, Szostecki C, Schroder P, Matschl U, Jensen K, Luders C, Will H, Sternsdorf T (1999) Splice variants of the nuclear dot-associated Sp100 protein contain homologies to HMG-1 and a human nuclear phosphoprotein-box motif. *J Cell Sci* **112** ( Pt 5): 733-747
- Hagglund R, Roizman B (2004) Role of ICP0 in the strategy of conquest of the host cell by herpes simplex virus 1. *J Virol* **78**: 2169-2178
- Halford WP, Kemp CD, Isler JA, Davido DJ, Schaffer PA (2001) ICP0, ICP4, or VP16 expressed from adenovirus vectors induces reactivation of latent herpes simplex virus type 1 in primary cultures of latently infected trigeminal ganglion cells. *J Virol* **75**: 6143-6153
- Halford WP, Schaffer PA (2001) ICP0 is required for efficient reactivation of herpes simplex virus type 1 from neuronal latency. *J Virol* **75**: 3240-3249
- Hardwicke MA, Sandri-Goldin RM (1994) The herpes simplex virus regulatory protein ICP27 contributes to the decrease in cellular mRNA levels during infection. *J Virol* **68**: 4797-4810
- Harris RA, Everett RD, Zhu XX, Silverstein S, Preston CM (1989) Herpes simplex virus type 1 immediate-early protein Vmw110 reactivates latent herpes simplex virus type 2 in an in vitro latency system. *J Virol* **63**: 3513-3515
- Hay RT (2005) SUMO: a history of modification. *Mol Cell* **18**: 1-12
- Hayes JJ, Hansen JC (2001) Nucleosomes and the chromatin fiber. *Current opinion in genetics & development* **11**: 124-129
- Heckman KL, Pease LR (2007) Gene splicing and mutagenesis by PCR-driven overlap extension. *Nat Protoc* **2**: 924-932

- Hermiston TW, Malone CL, Stinski MF (1990) Human cytomegalovirus immediate-early two protein region involved in negative regulation of the major immediate-early promoter. *J Virol* **64**: 3532-3536
- Herrera FJ, Triezenberg SJ (2004) VP16-dependent association of chromatin-modifying coactivators and underrepresentation of histones at immediate-early gene promoters during herpes simplex virus infection. *J Virol* **78**: 9689-9696
- Hershko A, Ciechanover A (1998) The ubiquitin system. *Annual review of biochemistry* **67**: 425-479
- Heuser M, van der Kuip H, Falini B, Peschel C, Huber C, Fischer T (1998) Induction of the pro-myelocytic leukaemia gene by type I and type II interferons. *Mediators of inflammation* **7**: 319-325
- Hofmann H, Sindre H, Stamminger T (2002) Functional interaction between the pp71 protein of human cytomegalovirus and the PML-interacting protein human Daxx. *J Virol* **76**: 5769-5783
- Hofmann TG, Stollberg N, Schmitz ML, Will H (2003) HIPK2 regulates transforming growth factor-beta-induced c-Jun NH(2)-terminal kinase activation and apoptosis in human hepatoma cells. *Cancer Res* **63**: 8271-8277
- Hollenbach AD, McPherson CJ, Mientjes EJ, Iyengar R, Grosveld G (2002) Daxx and histone deacetylase II associate with chromatin through an interaction with core histones and the chromatin-associated protein Dek. *J Cell Sci* **115**: 3319-3330
- Holmstrom SR, Chupreta S, So AY, Iniguez-Lluhi JA (2008) SUMO-mediated inhibition of glucocorticoid receptor synergistic activity depends on stable assembly at the promoter but not on DAXX. *Mol Endocrinol* **22**: 2061-2075
- Homer EG, Rinaldi A, Nicholl MJ, Preston CM (1999) Activation of herpesvirus gene expression by the human cytomegalovirus protein pp71. *J Virol* **73**: 8512-8518
- Honess RW, Roizman B (1974) Regulation of herpesvirus macromolecular synthesis. I. Cascade regulation of the synthesis of three groups of viral proteins. *J Virol* **14**: 8-19
- Huang J, Kent JR, Placek B, Whelan KA, Hollow CM, Zeng PY, Fraser NW, Berger SL (2006) Trimethylation of histone H3 lysine 4 by Set1 in the lytic infection of human herpes simplex virus 1. *J Virol* **80**: 5740-5746
- Huh YH, Kim YE, Kim ET, Park JJ, Song MJ, Zhu H, Hayward GS, Ahn JH (2008) Binding STAT2 by the acidic domain of human cytomegalovirus IE1 promotes viral growth and is negatively regulated by SUMO. *J Virol* **82**: 10444-10454
- Huthoff H, Towers GJ (2008) Restriction of retroviral replication by APOBEC3G/F and TRIM5alpha. *Trends Microbiol* **16**: 612-619
- Hwang J, Kalejta RF (2007) Proteasome-dependent, ubiquitin-independent degradation of Daxx by the viral pp71 protein in human cytomegalovirus-infected cells. *Virology* **367**: 334-338
- Ishov AM, Sotnikov AG, Negorev D, Vladimirova OV, Neff N, Kamitani T, Yeh ET, Strauss JF, 3rd, Maul GG (1999) PML is critical for ND10 formation and recruits the

- PML-interacting protein daxx to this nuclear structure when modified by SUMO-1. *J Cell Biol* **147**: 221-234
- Ishov AM, Stenberg RM, Maul GG (1997) Human cytomegalovirus immediate early interaction with host nuclear structures: definition of an immediate transcript environment. *J Cell Biol* **138**: 5-16
- Ishov AM, Vladimirova OV, Maul GG (2002) Daxx-mediated accumulation of human cytomegalovirus tegument protein pp71 at ND10 facilitates initiation of viral infection at these nuclear domains. *J Virol* **76**: 7705-7712
- Ishov AM, Vladimirova OV, Maul GG (2004) Heterochromatin and ND10 are cell-cycle regulated and phosphorylation-dependent alternate nuclear sites of the transcription repressor Daxx and SWI/SNF protein ATRX. *J Cell Sci* **117**: 3807-3820
- Jang MS, Ryu SW, Kim E (2002) Modification of Daxx by small ubiquitin-related modifier-1. *Biochem Biophys Res Commun* **295**: 495-500
- Jarvis MA, Nelson JA, "HCMV: Molecular basis of persistence and latency" in: Arvin, AM, Mocarski, ES, Moore, P, et al., Editors. Human Herpesviruses: Biology, Therapy and Immunoprophylaxis. Cambridge: Cambridge Press; 2007: 765-779
- Joazeiro CA, Weissman AM (2000) RING finger proteins: mediators of ubiquitin ligase activity. *Cell* **102**: 549-552
- Johnson ES (2004) Protein modification by SUMO. *Annual review of biochemistry* **73**: 355-382
- Kalejta RF (2008a) Functions of human cytomegalovirus tegument proteins prior to immediate early gene expression. *Current topics in microbiology and immunology* **325**: 101-115
- Kalejta RF (2008b) Tegument proteins of human cytomegalovirus. *Microbiol Mol Biol Rev* **72**: 249-265, table of contents
- Kalejta RF, Bechtel JT, Shenk T (2003) Human cytomegalovirus pp71 stimulates cell cycle progression by inducing the proteasome-dependent degradation of the retinoblastoma family of tumor suppressors. *Mol Cell Biol* **23**: 1885-1895
- Kalejta RF, Shenk T (2003) Proteasome-dependent, ubiquitin-independent degradation of the Rb family of tumor suppressors by the human cytomegalovirus pp71 protein. *Proc Natl Acad Sci U S A* **100**: 3263-3268
- Kaye S, Choudhary A (2006) Herpes simplex keratitis. *Progress in retinal and eye research* **25**: 355-380
- Kelly BJ, Fraefel C, Cunningham AL, Diefenbach RJ (2009) Functional roles of the tegument proteins of herpes simplex virus type 1. *Virus Res* **145**: 173-186
- Kelly C, Van Driel R, Wilkinson GW (1995) Disruption of PML-associated nuclear bodies during human cytomegalovirus infection. *J Gen Virol* **76 ( Pt 11)**: 2887-2893

- Kent JR, Zeng PY, Atanasiu D, Gardner J, Fraser NW, Berger SL (2004) During lytic infection herpes simplex virus type 1 is associated with histones bearing modifications that correlate with active transcription. *J Virol* **78**: 10178-10186
- Kieff E.D., Rickison A.B., "Epstein-Barr virus and its replication" in Fields' Virology 5th Edition. D.M. Knipe, P. Howley, D.E. Griffin, R.A. Lamb, M.A. Martin, B. Roizman, and S.E. Straus, Editors. Lippincott-Williams and Wilkins, New York, N.Y. 2007: pp. 2604-2654
- Knipe DM, Cliffe A (2008) Chromatin control of herpes simplex virus lytic and latent infection. *Nat Rev Microbiol* **6**: 211-221
- Korioth F, Maul GG, Plachter B, Stamminger T, Frey J (1996) The nuclear domain 10 (ND10) is disrupted by the human cytomegalovirus gene product IE1. *Experimental cell research* **229**: 155-158
- Kubat NJ, Amelio AL, Giordani NV, Bloom DC (2004a) The herpes simplex virus type 1 latency-associated transcript (LAT) enhancer/rcr is hyperacetylated during latency independently of LAT transcription. *J Virol* **78**: 12508-12518
- Kubat NJ, Tran RK, McAnany P, Bloom DC (2004b) Specific histone tail modification and not DNA methylation is a determinant of herpes simplex virus type 1 latent gene expression. *J Virol* **78**: 1139-1149
- Kuddus RH, DeLuca NA (2007) DNA-dependent oligomerization of herpes simplex virus type 1 regulatory protein ICP4. *J Virol* **81**: 9230-9237
- Kuo HY, Chang CC, Jeng JC, Hu HM, Lin DY, Maul GG, Kwok RP, Shih HM (2005) SUMO modification negatively modulates the transcriptional activity of CREB-binding protein via the recruitment of Daxx. *Proc Natl Acad Sci U S A* **102**: 16973-16978
- Kuo MH, Allis CD (1998) Roles of histone acetyltransferases and deacetylases in gene regulation. *Bioessays* **20**: 615-626
- Kutluay SB, Triezenberg SJ (2009a) Regulation of histone deposition on the herpes simplex virus type 1 genome during lytic infection. *J Virol* **83**: 5835-5845
- Kutluay SB, Triezenberg SJ (2009b) Role of chromatin during herpesvirus infections. *Biochim Biophys Acta* **1790**: 456-466
- Kyratsous CA, Silverstein SJ (2009) Components of nuclear domain 10 bodies regulate varicella-zoster virus replication. *J Virol* **83**: 4262-4274
- La Boissiere S, Hughes T, O'Hare P (1999) HCF-dependent nuclear import of VP16. *Embo J* **18**: 480-489
- Laemmli UK (1970) Cleavage of structural proteins during the assembly of the head of bacteriophage T4. *Nature* **227**: 680-685
- Lakowski B, Roelens I, Jacob S (2006) CoREST-like complexes regulate chromatin modification and neuronal gene expression. *J Mol Neurosci* **29**: 227-239

- Lalioti VS, Vergarajauregui S, Pulido D, Sandoval IV (2002) The insulin-sensitive glucose transporter, GLUT4, interacts physically with Daxx. Two proteins with capacity to bind Ubc9 and conjugated to SUMO1. *J Biol Chem* **277**: 19783-19791
- Lamond AI, Sleeman JE (2003) Nuclear substructure and dynamics. *Curr Biol* **13**: R825-828
- LaMorte VJ, Dyck JA, Ochs RL, Evans RM (1998) Localization of nascent RNA and CREB binding protein with the PML-containing nuclear body. *Proc Natl Acad Sci U S A* **95**: 4991-4996
- Le Douarin B, Nielsen AL, Garnier JM, Ichinose H, Jeanmougin F, Losson R, Chambon P (1996) A possible involvement of TIF1 alpha and TIF1 beta in the epigenetic control of transcription by nuclear receptors. *The EMBO journal* **15**: 6701-6715
- Lechner MS, Schultz DC, Negorev D, Maul GG, Rauscher FJ, 3rd (2005) The mammalian heterochromatin protein 1 binds diverse nuclear proteins through a common motif that targets the chromoshadow domain. *Biochem Biophys Res Commun* **331**: 929-937
- Lee HR, Kim DJ, Lee JM, Choi CY, Ahn BY, Hayward GS, Ahn JH (2004) Ability of the human cytomegalovirus IE1 protein to modulate sumoylation of PML correlates with its functional activities in transcriptional regulation and infectivity in cultured fibroblast cells. *J Virol* **78**: 6527-6542
- Lehman IR, Boehmer PE (1999) Replication of herpes simplex virus DNA. *J Biol Chem* **274**: 28059-28062
- Leinbach SS, Summers WC (1980) The structure of herpes simplex virus type 1 DNA as probed by micrococcal nuclease digestion. *J Gen Virol* **51**: 45-59
- Leone P (2005) Reducing the risk of transmitting genital herpes: advances in understanding and therapy. *Current medical research and opinion* **21**: 1577-1582
- Li H, Leo C, Zhu J, Wu X, O'Neil J, Park EJ, Chen JD (2000) Sequestration and inhibition of Daxx-mediated transcriptional repression by PML. *Mol Cell Biol* **20**: 1784-1796
- Lilley CE, Chaurushiya MS, Boutell C, Landry S, Suh J, Panier S, Everett RD, Stewart GS, Durocher D, Weitzman MD (2009) A viral E3 ligase targets RNF8 and RNF168 to control histone ubiquitination and DNA damage responses. *Embo J* **29**: 943-955
- Lin DY, Fang HI, Ma AH, Huang YS, Pu YS, Jenster G, Kung HJ, Shih HM (2004) Negative modulation of androgen receptor transcriptional activity by Daxx. *Mol Cell Biol* **24**: 10529-10541
- Lin DY, Huang YS, Jeng JC, Kuo HY, Chang CC, Chao TT, Ho CC, Chen YC, Lin TP, Fang HI, Hung CC, Suen CS, Hwang MJ, Chang KS, Maul GG, Shih HM (2006) Role of SUMO-interacting motif in Daxx SUMO modification, subnuclear localization, and repression of sumoylated transcription factors. *Mol Cell* **24**: 341-354
- Liu B, Stinski MF (1992) Human cytomegalovirus contains a tegument protein that enhances transcription from promoters with upstream ATF and AP-1 cis-acting elements. *J Virol* **66**: 4434-4444

- Liu F, Zhou ZH, “Comparative virion structures of human herpesviruses” in: Arvin, AM, Mocarski, ES, Moore, P, et al., Editors. *Human Herpesviruses: Biology, Therapy and Immunoprophylaxis*. Cambridge: Cambridge Press; 2007: pp 27-43
- Lomonte P, Morency E (2007) Centromeric protein CENP-B proteasomal degradation induced by the viral protein ICP0. *FEBS Lett* **581**: 658-662
- Lomonte P, Sullivan KF, Everett RD (2001) Degradation of nucleosome-associated centromeric histone H3-like protein CENP-A induced by herpes simplex virus type 1 protein ICP0. *J Biol Chem* **276**: 5829-5835
- Lomonte P, Thomas J, Texier P, Caron C, Khochbin S, Epstein AL (2004) Functional interaction between class II histone deacetylases and ICP0 of herpes simplex virus type 1. *J Virol* **78**: 6744-6757
- Long MC, Leong V, Schaffer PA, Spencer CA, Rice SA (1999) ICP22 and the UL13 protein kinase are both required for herpes simplex virus-induced modification of the large subunit of RNA polymerase II. *J Virol* **73**: 5593-5604
- Lu X, Triezenberg SJ (2009) Chromatin assembly on herpes simplex virus genomes during lytic infection. *Biochim Biophys Acta*
- Luciani JJ, Depetris D, Usson Y, Metzler-Guillemain C, Mignon-Ravix C, Mitchell MJ, Megarbane A, Sarda P, Sirma H, Moncla A, Feunteun J, Mattei MG (2006) PML nuclear bodies are highly organised DNA-protein structures with a function in heterochromatin remodelling at the G2 phase. *J Cell Sci* **119**: 2518-2531
- Lukashchuk V, McFarlane S, Everett RD, Preston CM (2008) Human cytomegalovirus protein pp71 displaces the chromatin-associated factor ATRX from nuclear domain 10 at early stages of infection. *J Virol* **82**: 12543-12554
- Maillet S, Naas T, Crepin S, Roque-Afonso AM, Lafay F, Efstathiou S, Labetoulle M (2006) Herpes simplex virus type 1 latently infected neurons differentially express latency-associated and ICP0 transcripts. *J Virol* **80**: 9310-9321
- Malm G, Engman ML (2007) Congenital cytomegalovirus infections. *Seminars in fetal & neonatal medicine* **12**: 154-159
- Marks PA, Richon VM, Rifkind RA (2000) Histone deacetylase inhibitors: inducers of differentiation or apoptosis of transformed cells. *Journal of the National Cancer Institute* **92**: 1210-1216
- Marsden HS, Crombie IK, Subak-Sharpe JH (1976) Control of protein synthesis in herpesvirus-infected cells: analysis of the polypeptides induced by wild type and sixteen temperature-sensitive mutants of HSV strain 17. *J Gen Virol* **31**: 347-372
- Marshall KR, Rowley KV, Rinaldi A, Nicholson IP, Ishov AM, Maul GG, Preston CM (2002) Activity and intracellular localization of the human cytomegalovirus protein pp71. *J Gen Virol* **83**: 1601-1612
- Maul GG (1998) Nuclear domain 10, the site of DNA virus transcription and replication. *Bioessays* **20**: 660-667

- Maul GG, Everett RD (1994) The nuclear location of PML, a cellular member of the C3HC4 zinc-binding domain protein family, is rearranged during herpes simplex virus infection by the C3HC4 viral protein ICP0. *J Gen Virol* **75** ( Pt 6): 1223-1233
- Maul GG, Guldner HH, Spivack JG (1993) Modification of discrete nuclear domains induced by herpes simplex virus type 1 immediate early gene 1 product (ICP0). *J Gen Virol* **74** ( Pt 12): 2679-2690
- Maul GG, Ishov AM, Everett RD (1996) Nuclear domain 10 as preexisting potential replication start sites of herpes simplex virus type-1. *Virology* **217**: 67-75
- McGeoch DJ, Dalrymple MA, Davison AJ, Dolan A, Frame MC, McNab D, Perry LJ, Scott JE, Taylor P (1988) The complete DNA sequence of the long unique region in the genome of herpes simplex virus type 1. *J Gen Virol* **69** ( Pt 7): 1531-1574
- McManus MT, Sharp PA (2002) Gene silencing in mammals by small interfering RNAs. *Nat Rev Genet* **3**: 737-747
- McVoy MA, Adler SP (1994) Human cytomegalovirus DNA replicates after early circularization by concatemer formation, and inversion occurs within the concatemer. *J Virol* **68**: 1040-1051
- Meinecke I, Cinski A, Baier A, Peters MA, Dankbar B, Wille A, Drynda A, Mendoza H, Gay RE, Hay RT, Ink B, Gay S, Pap T (2007) Modification of nuclear PML protein by SUMO-1 regulates Fas-induced apoptosis in rheumatoid arthritis synovial fibroblasts. *Proc Natl Acad Sci U S A* **104**: 5073-5078
- Meister G, Tuschl T (2004) Mechanisms of gene silencing by double-stranded RNA. *Nature* **431**: 343-349
- Memedula S, Belmont AS (2003) Sequential recruitment of HAT and SWI/SNF components to condensed chromatin by VP16. *Curr Biol* **13**: 241-246
- Mettenleiter TC (2002) Herpesvirus assembly and egress. *J Virol* **76**: 1537-1547
- Mettenleiter TC, Klupp BG, Granzow H (2009) Herpesvirus assembly: an update. *Virus Res* **143**: 222-234
- Michaelson JS, Bader D, Kuo F, Kozak C, Leder P (1999) Loss of Daxx, a promiscuously interacting protein, results in extensive apoptosis in early mouse development. *Genes & development* **13**: 1918-1923
- Michaelson JS, Leder P (2003) RNAi reveals anti-apoptotic and transcriptionally repressive activities of DAXX. *J Cell Sci* **116**: 345-352
- Miller CS, Danaher RJ, Jacob RJ (2006) ICP0 is not required for efficient stress-induced reactivation of herpes simplex virus type 1 from cultured quiescently infected neuronal cells. *J Virol* **80**: 3360-3368
- Mocarski E.S., Jr, Shenk T., Pass R.F. Cytomegaloviruses in Fields' Virology 5th Edition. D.M. Knipe, P. Howley, D.E. Griffin, R.A. Lamb, M.A. Martin, B. Roizman, and S.E. Straus, Editors. Lippincott-Williams and Wilkins, New York, N.Y. 2007: pp. 2703-2772

- Mocarski ES., Jr “Comparative analysis of herpesvirus-common proteins” in: Arvin, AM, Mocarski, ES, Moore, P, et al., Editors. *Human Herpesviruses: Biology, Therapy and Immunoprophylaxis*. Cambridge: Cambridge Press; 2007: pp. 44-60
- Morozov VM, Massoll NA, Vladimirova OV, Maul GG, Ishov AM (2008) Regulation of c-met expression by transcription repressor Daxx. *Oncogene* **27**: 2177-2186
- Muchardt C, Yaniv M (1999) ATP-dependent chromatin remodelling: SWI/SNF and Co. are on the job. *J Mol Biol* **293**: 187-198
- Muller S, Dejean A (1999) Viral immediate-early proteins abrogate the modification by SUMO-1 of PML and Sp100 proteins, correlating with nuclear body disruption. *J Virol* **73**: 5137-5143
- Murphy JC, Fischle W, Verdin E, Sinclair JH (2002) Control of cytomegalovirus lytic gene expression by histone acetylation. *Embo J* **21**: 1112-1120
- Nan X, Campoy FJ, Bird A (1997) MeCP2 is a transcriptional repressor with abundant binding sites in genomic chromatin. *Cell* **88**: 471-481
- Nan X, Hou J, Maclean A, Nasir J, Lafuente MJ, Shu X, Kriaucionis S, Bird A (2007) Interaction between chromatin proteins MECP2 and ATRX is disrupted by mutations that cause inherited mental retardation. *Proc Natl Acad Sci U S A* **104**: 2709-2714
- Nan X, Ng HH, Johnson CA, Laherty CD, Turner BM, Eisenman RN, Bird A (1998) Transcriptional repression by the methyl-CpG-binding protein MeCP2 involves a histone deacetylase complex. *Nature* **393**: 386-389
- Nandakumar S, Woolard SN, Yuan D, Rouse BT, Kumaraguru U (2008) Natural killer cells as novel helpers in anti-herpes simplex virus immune response. *J Virol* **82**: 10820-10831
- Negorev D, Maul GG (2001) Cellular proteins localized at and interacting within ND10/PML nuclear bodies/PODs suggest functions of a nuclear depot. *Oncogene* **20**: 7234-7242
- Negorev DG, Vladimirova OV, Ivanov A, Rauscher F, 3rd, Maul GG (2006) Differential role of Sp100 isoforms in interferon-mediated repression of herpes simplex virus type 1 immediate-early protein expression. *J Virol* **80**: 8019-8029
- Negorev DG, Vladimirova OV, Maul GG (2009) Differential functions of interferon-upregulated Sp100 isoforms: herpes simplex virus type 1 promoter-based immediate-early gene suppression and PML protection from ICP0-mediated degradation. *J Virol* **83**: 5168-5180
- Newcomb WW, Juhas RM, Thomsen DR, Homa FL, Burch AD, Weller SK, Brown JC (2001) The UL6 gene product forms the portal for entry of DNA into the herpes simplex virus capsid. *J Virol* **75**: 10923-10932
- Nisole S, Stoye JP, Saib A (2005) TRIM family proteins: retroviral restriction and antiviral defence. *Nat Rev Microbiol* **3**: 799-808
- Nitzsche A, Paulus C, Nevels M (2008) Temporal dynamics of cytomegalovirus chromatin assembly in productively infected human cells. *J Virol* **82**: 11167-11180

- Oh J, Fraser NW (2008) Temporal association of the herpes simplex virus genome with histone proteins during a lytic infection. *J Virol* **82**: 3530-3537
- Ooi SK, Qiu C, Bernstein E, Li K, Jia D, Yang Z, Erdjument-Bromage H, Tempst P, Lin SP, Allis CD, Cheng X, Bestor TH (2007) DNMT3L connects unmethylated lysine 4 of histone H3 to de novo methylation of DNA. *Nature* **448**: 714-717
- Otani J, Nankumo T, Arita K, Inamoto S, Ariyoshi M, Shirakawa M (2009) Structural basis for recognition of H3K4 methylation status by the DNA methyltransferase 3A ATRX-DNMT3-DNMT3L domain. *EMBO reports* **10**: 1235-1241
- Parkinson J, Everett RD (2000) Alphaherpesvirus proteins related to herpes simplex virus type 1 ICP0 affect cellular structures and proteins. *J Virol* **74**: 10006-10017
- Pellet, P.E. and Roizman, B. (2007). The Family Herpesviridae: A brief introduction. Fields' Virology 5th Edition. D.M. Knipe, P. Howley, D.E. Griffin, R.A. Lamb, M.A. Martin, B. Roizman, and S.E. Straus, Editors. Lippincott-Williams and Wilkins, New York, N.Y. 2007: pp. 2479-2499.
- Pereira L, Maidji E, Fisher SJ, McDonagh S, Tabata T, "HCMV persistence in the population: potential transplacental transmission" in: Arvin, AM, Mocarski, ES, Moore, P, et al., Editors. Human Herpesviruses: Biology, Therapy and Immunoprophylaxis. Cambridge: Cambridge Press; 2007: pp 814-830
- Perry LJ, Rixon FJ, Everett RD, Frame MC, McGeoch DJ (1986) Characterization of the IE110 gene of herpes simplex virus type 1. *J Gen Virol* **67** ( Pt 11): 2365-2380
- Picketts DJ, Higgs DR, Bachoo S, Blake DJ, Quarrell OW, Gibbons RJ (1996) ATRX encodes a novel member of the SNF2 family of proteins: mutations point to a common mechanism underlying the ATR-X syndrome. *Hum Mol Genet* **5**: 1899-1907
- Picketts DJ, Tastan AO, Higgs DR, Gibbons RJ (1998) Comparison of the human and murine ATRX gene identifies highly conserved, functionally important domains. *Mamm Genome* **9**: 400-403
- Pizer LI, Everett RD, Tedder DG, Elliott M, Litman B (1991) Nucleotides within both proximal and distal parts of the consensus sequence are important for specific DNA recognition by the herpes simplex virus regulatory protein ICP4. *Nucleic Acids Res* **19**: 477-483
- Placek BJ, Huang J, Kent JR, Dorsey J, Rice L, Fraser NW, Berger SL (2009) The histone variant H3.3 regulates gene expression during lytic infection with herpes simplex virus type 1. *J Virol* **83**: 1416-1421
- Pluta AF, Earnshaw WC, Goldberg IG (1998) Interphase-specific association of intrinsic centromere protein CENP-C with HDaxx, a death domain-binding protein implicated in Fas-mediated cell death. *J Cell Sci* **111** ( Pt 14): 2029-2041
- Poma EE, Kowalik TF, Zhu L, Sinclair JH, Huang ES (1996) The human cytomegalovirus IE1-72 protein interacts with the cellular p107 protein and relieves p107-mediated transcriptional repression of an E2F-responsive promoter. *J Virol* **70**: 7867-7877

- Poon AP, Gu H, Roizman B (2006) ICP0 and the US3 protein kinase of herpes simplex virus 1 independently block histone deacetylation to enable gene expression. *Proc Natl Acad Sci U S A* **103**: 9993-9998
- Poon AP, Liang Y, Roizman B (2003) Herpes simplex virus 1 gene expression is accelerated by inhibitors of histone deacetylases in rabbit skin cells infected with a mutant carrying a cDNA copy of the infected-cell protein no. 0. *J Virol* **77**: 12671-12678
- Preston CM (1979) Control of herpes simplex virus type 1 mRNA synthesis in cells infected with wild-type virus or the temperature-sensitive mutant tsK. *J Virol* **29**: 275-284
- Preston CM (2000) Repression of viral transcription during herpes simplex virus latency. *J Gen Virol* **81**: 1-19
- Preston CM (2007) Reactivation of expression from quiescent herpes simplex virus type 1 genomes in the absence of immediate-early protein ICP0. *J Virol* **81**: 11781-11789
- Preston CM, Nicholl MJ (1997) Repression of gene expression upon infection of cells with herpes simplex virus type 1 mutants impaired for immediate-early protein synthesis. *J Virol* **71**: 7807-7813
- Preston CM, Nicholl MJ (2005) Human cytomegalovirus tegument protein pp71 directs long-term gene expression from quiescent herpes simplex virus genomes. *J Virol* **79**: 525-535
- Preston CM, Nicholl MJ (2006) Role of the cellular protein hDaxx in human cytomegalovirus immediate-early gene expression. *J Gen Virol* **87**: 1113-1121
- Preston CM, Nicholl MJ (2008) Induction of cellular stress overcomes the requirement of herpes simplex virus type 1 for immediate-early protein ICP0 and reactivates expression from quiescent viral genomes. *J Virol* **82**: 11775-11783
- Reeves M, Sinclair J (2008) Aspects of human cytomegalovirus latency and reactivation. *Current topics in microbiology and immunology* **325**: 297-313
- Reeves MB, MacAry PA, Lehner PJ, Sissons JG, Sinclair JH (2005) Latency, chromatin remodeling, and reactivation of human cytomegalovirus in the dendritic cells of healthy carriers. *Proc Natl Acad Sci U S A* **102**: 4140-4145
- Regad T, Chelbi-Alix MK (2001) Role and fate of PML nuclear bodies in response to interferon and viral infections. *Oncogene* **20**: 7274-7286
- Revello MG, Gerna G (2010) Human cytomegalovirus tropism for endothelial/epithelial cells: scientific background and clinical implications. *Reviews in medical virology*
- Rice SA, Long MC, Lam V, Schaffer PA, Spencer CA (1995) Herpes simplex virus immediate-early protein ICP22 is required for viral modification of host RNA polymerase II and establishment of the normal viral transcription program. *J Virol* **69**: 5550-5559
- Ritchie K, Seah C, Moulin J, Isaac C, Dick F, Berube NG (2008) Loss of ATRX leads to chromosome cohesion and congression defects. *J Cell Biol* **180**: 315-324
- Rodriguez MS, Dargemont C, Hay RT (2001) SUMO-1 conjugation in vivo requires both a consensus modification motif and nuclear targeting. *J Biol Chem* **276**: 12654-12659

Roizman B, Knipe DM, Whitley RJ, "Herpes Simplex Viruses" in Fields' Virology 5th Edition. D.M. Knipe, P. Howley, D.E. Griffin, R.A. Lamb, M.A. Martin, B. Roizman, and S.E. Straus, Editors. Lippincott-Williams and Wilkins, New York, N.Y. 2007: pp 2503-2600

Ruger B, Klages S, Walla B, Albrecht J, Fleckenstein B, Tomlinson P, Barrell B (1987) Primary structure and transcription of the genes coding for the two virion phosphoproteins pp65 and pp71 of human cytomegalovirus. *J Virol* **61**: 446-453

Russell J, Stow ND, Stow EC, Preston CM (1987) Herpes simplex virus genes involved in latency in vitro. *J Gen Virol* **68** ( Pt 12): 3009-3018

Ryo A, Hirai A, Nishi M, Liou YC, Perrem K, Lin SC, Hirano H, Lee SW, Aoki I (2007) A suppressive role of the prolyl isomerase Pin1 in cellular apoptosis mediated by the death-associated protein Daxx. *J Biol Chem* **282**: 36671-36681

Ryu SW, Chae SK, Kim E (2000) Interaction of Daxx, a Fas binding protein, with sentrin and Ubc9. *Biochem Biophys Res Commun* **279**: 6-10

Sacks WR, Schaffer PA (1987) Deletion mutants in the gene encoding the herpes simplex virus type 1 immediate-early protein ICP0 exhibit impaired growth in cell culture. *J Virol* **61**: 829-839

Saffert RT, Kalejta RF (2006) Inactivating a cellular intrinsic immune defense mediated by Daxx is the mechanism through which the human cytomegalovirus pp71 protein stimulates viral immediate-early gene expression. *J Virol* **80**: 3863-3871

Saffert RT, Kalejta RF (2007) Human cytomegalovirus gene expression is silenced by Daxx-mediated intrinsic immune defense in model latent infections established in vitro. *J Virol* **81**: 9109-9120

Saffert RT, Kalejta RF (2008) Promyelocytic leukemia-nuclear body proteins: herpesvirus enemies, accomplices, or both? *Future virology* **3**: 265-277

Salomoni P, Khelifi AF (2006) Daxx: death or survival protein? *Trends Cell Biol* **16**: 97-104

Salomoni P, Pandolfi PP (2002) The role of PML in tumor suppression. *Cell* **108**: 165-170

Samaniego LA, Neiderhiser L, DeLuca NA (1998) Persistence and expression of the herpes simplex virus genome in the absence of immediate-early proteins. *J Virol* **72**: 3307-3320

Sampath P, Deluca NA (2008) Binding of ICP4, TATA-binding protein, and RNA polymerase II to herpes simplex virus type 1 immediate-early, early, and late promoters in virus-infected cells. *J Virol* **82**: 2339-2349

Schenk P, Pietschmann S, Gelderblom H, Pauli G, Ludwig H (1988) Monoclonal antibodies against herpes simplex virus type 1-infected nuclei defining and localizing the ICP8 protein, 65K DNA-binding protein and polypeptides of the ICP35 family. *J Gen Virol* **69** ( Pt 1): 99-111

Schrag JD, Prasad BV, Rixon FJ, Chiu W (1989) Three-dimensional structure of the HSV1 nucleocapsid. *Cell* **56**: 651-660

- Seeler JS, Marchio A, Sitterlin D, Transy C, Dejean A (1998) Interaction of SP100 with HP1 proteins: a link between the promyelocytic leukemia-associated nuclear bodies and the chromatin compartment. *Proc Natl Acad Sci U S A* **95**: 7316-7321
- Sengupta N, Seto E (2004) Regulation of histone deacetylase activities. *J Cell Biochem* **93**: 57-67
- Shanda SK, Wilson DW (2008) UL36p is required for efficient transport of membrane-associated herpes simplex virus type 1 along microtubules. *J Virol* **82**: 7388-7394
- Shih HM, Chang CC, Kuo HY, Lin DY (2007) Daxx mediates SUMO-dependent transcriptional control and subnuclear compartmentalization. *Biochem Soc Trans* **35**: 1397-1400
- Shinkai Y (2007) Regulation and function of H3K9 methylation. *Sub-cellular biochemistry* **41**: 337-350
- Showalter SD, Zweig M, Hampar B (1981) Monoclonal antibodies to herpes simplex virus type 1 proteins, including the immediate-early protein ICP 4. *Infect Immun* **34**: 684-692
- Siedlecki P, Zielenkiewicz P (2006) Mammalian DNA methyltransferases. *Acta biochimica Polonica* **53**: 245-256
- Sinclair J (2008) Human cytomegalovirus: Latency and reactivation in the myeloid lineage. *J Clin Virol* **41**: 180-185
- Sinclair J (2009) Chromatin structure regulates human cytomegalovirus gene expression during latency, reactivation and lytic infection. *Biochim Biophys Acta*
- Sinclair J, Sissons P (2006) Latency and reactivation of human cytomegalovirus. *J Gen Virol* **87**: 1763-1779
- Smibert CA, Johnson DC, Smiley JR (1992) Identification and characterization of the virion-induced host shutoff product of herpes simplex virus gene UL41. *J Gen Virol* **73** ( Pt 2): 467-470
- Smiley JR (2004) Herpes simplex virus virion host shutoff protein: immune evasion mediated by a viral RNase? *J Virol* **78**: 1063-1068
- Smith CA, Bates P, Rivera-Gonzalez R, Gu B, DeLuca NA (1993) ICP4, the major transcriptional regulatory protein of herpes simplex virus type 1, forms a tripartite complex with TATA-binding protein and TFIIB. *J Virol* **67**: 4676-4687
- Smith JS, Robinson NJ (2002) Age-specific prevalence of infection with herpes simplex virus types 2 and 1: a global review. *J Infect Dis* **186 Suppl 1**: S3-28
- Smith RW, Malik P, Clements JB (2005) The herpes simplex virus ICP27 protein: a multifunctional post-transcriptional regulator of gene expression. *Biochem Soc Trans* **33**: 499-501
- Sokolskaja E, Berthoux L, Luban J (2006) Cyclophilin A and TRIM5alpha independently regulate human immunodeficiency virus type 1 infectivity in human cells. *J Virol* **80**: 2855-2862

- Soliman TM, Sandri-Goldin RM, Silverstein SJ (1997) Shuttling of the herpes simplex virus type 1 regulatory protein ICP27 between the nucleus and cytoplasm mediates the expression of late proteins. *J Virol* **71**: 9188-9197
- Song J, Durrin LK, Wilkinson TA, Krontiris TG, Chen Y (2004) Identification of a SUMO-binding motif that recognizes SUMO-modified proteins. *Proc Natl Acad Sci U S A* **101**: 14373-14378
- Song JJ, Lee YJ (2004) Tryptophan 621 and serine 667 residues of Daxx regulate its nuclear export during glucose deprivation. *J Biol Chem* **279**: 30573-30578
- Sourvinos G, Everett RD (2002) Visualization of parental HSV-1 genomes and replication compartments in association with ND10 in live infected cells. *Embo J* **21**: 4989-4997
- Spear PG, Eisenberg RJ, Cohen GH (2000) Three classes of cell surface receptors for alphaherpesvirus entry. *Virology* **275**: 1-8
- Speck PG, Simmons A (1991) Divergent molecular pathways of productive and latent infection with a virulent strain of herpes simplex virus type 1. *J Virol* **65**: 4001-4005
- Spector DL (2001) Nuclear domains. *J Cell Sci* **114**: 2891-2893
- Stayton CL, Dabovic B, Gulisano M, Gecz J, Broccoli V, Giovanazzi S, Bossolasco M, Monaco L, Rastan S, Boncinelli E, et al. (1994) Cloning and characterization of a new human Xq13 gene, encoding a putative helicase. *Hum Mol Genet* **3**: 1957-1964
- Steininger C (2007) Clinical relevance of cytomegalovirus infection in patients with disorders of the immune system. *Clin Microbiol Infect* **13**: 953-963
- Stern-Ginossar N, Saleh N, Goldberg MD, Prichard M, Wolf DG, Mandelboim O (2009) Analysis of human cytomegalovirus-encoded microRNA activity during infection. *J Virol* **83**: 10684-10693
- Sternsdorf T, Guldner HH, Szostecki C, Grotzinger T, Will H (1995) Two nuclear dot-associated proteins, PML and Sp100, are often co-autoimmunogenic in patients with primary biliary cirrhosis. *Scandinavian journal of immunology* **42**: 257-268
- Sternsdorf T, Jensen K, Reich B, Will H (1999) The nuclear dot protein sp100, characterization of domains necessary for dimerization, subcellular localization, and modification by small ubiquitin-like modifiers. *J Biol Chem* **274**: 12555-12566
- Sternsdorf T, Jensen K, Will H (1997) Evidence for covalent modification of the nuclear dot-associated proteins PML and Sp100 by PIC1/SUMO-1. *J Cell Biol* **139**: 1621-1634
- Stevens JG, Cook ML (1971) Latent herpes simplex virus in spinal ganglia of mice. *Science* **173**: 843-845
- Stinski MF, Isomura H (2008) Role of the cytomegalovirus major immediate early enhancer in acute infection and reactivation from latency. *Medical microbiology and immunology* **197**: 223-231
- Stow EC, Stow ND (1989) Complementation of a herpes simplex virus type 1 Vmw110 deletion mutant by human cytomegalovirus. *J Gen Virol* **70** ( Pt 3): 695-704

- Stow ND, Stow EC (1986) Isolation and characterization of a herpes simplex virus type 1 mutant containing a deletion within the gene encoding the immediate early polypeptide Vmw110. *J Gen Virol* **67** ( Pt 12): 2571-2585
- Strang BL, Stow ND (2005) Circularization of the herpes simplex virus type 1 genome upon lytic infection. *J Virol* **79**: 12487-12494
- Stremlau M, Owens CM, Perron MJ, Kiessling M, Autissier P, Sodroski J (2004) The cytoplasmic body component TRIM5 $\alpha$  restricts HIV-1 infection in Old World monkeys. *Nature* **427**: 848-853
- Stuurman N, de Graaf A, Floore A, Josso A, Humbel B, de Jong L, van Driel R (1992) A monoclonal antibody recognizing nuclear matrix-associated nuclear bodies. *J Cell Sci* **101** ( Pt 4): 773-784
- Sudarsanam P, Winston F (2000) The Swi/Snf family nucleosome-remodeling complexes and transcriptional control. *Trends Genet* **16**: 345-351
- Tang J, Qu LK, Zhang J, Wang W, Michaelson JS, Degenhardt YY, El-Deiry WS, Yang X (2006) Critical role for Daxx in regulating Mdm2. *Nat Cell Biol* **8**: 855-862
- Tang J, Wu S, Liu H, Stratt R, Barak OG, Shiekhattar R, Picketts DJ, Yang X (2004) A novel transcription regulatory complex containing death domain-associated protein and the ATR-X syndrome protein. *J Biol Chem* **279**: 20369-20377
- Tang S, Bertke AS, Patel A, Wang K, Cohen JI, Krause PR (2008) An acutely and latently expressed herpes simplex virus 2 viral microRNA inhibits expression of ICP34.5, a viral neurovirulence factor. *Proc Natl Acad Sci U S A* **105**: 10931-10936
- Tang S, Patel A, Krause PR (2009) Novel less-abundant viral microRNAs encoded by herpes simplex virus 2 latency-associated transcript and their roles in regulating ICP34.5 and ICP0 mRNAs. *J Virol* **83**: 1433-1442
- Tatham MH, Geoffroy MC, Shen L, Plechanovova A, Hattersley N, Jaffray EG, Palvimo JJ, Hay RT (2008) RNF4 is a poly-SUMO-specific E3 ubiquitin ligase required for arsenic-induced PML degradation. *Nat Cell Biol* **10**: 538-546
- Tavalai N, Papior P, Rechter S, Leis M, Stamminger T (2006) Evidence for a role of the cellular ND10 protein PML in mediating intrinsic immunity against human cytomegalovirus infections. *J Virol* **80**: 8006-8018
- Tavalai N, Papior P, Rechter S, Stamminger T (2008) Nuclear domain 10 components promyelocytic leukemia protein and hDaxx independently contribute to an intrinsic antiviral defense against human cytomegalovirus infection. *J Virol* **82**: 126-137
- Tavalai N, Stamminger T (2008) New insights into the role of the subnuclear structure ND10 for viral infection. *Biochim Biophys Acta* **1783**: 2207-2221
- Taylor-Wiedeman J, Sissons P, Sinclair J (1994) Induction of endogenous human cytomegalovirus gene expression after differentiation of monocytes from healthy carriers. *J Virol* **68**: 1597-1604

- Terry-Allison T, Smith CA, DeLuca NA (2007) Relaxed repression of herpes simplex virus type 1 genomes in Murine trigeminal neurons. *J Virol* **81**: 12394-12405
- Thompson RL, Sawtell NM (2006) Evidence that the herpes simplex virus type 1 ICP0 protein does not initiate reactivation from latency in vivo. *J Virol* **80**: 10919-10930
- Torii S, Egan DA, Evans RA, Reed JC (1999) Human Daxx regulates Fas-induced apoptosis from nuclear PML oncogenic domains (PODs). *Embo J* **18**: 6037-6049
- Towbin H, Staehelin T, Gordon J (1979) Electrophoretic transfer of proteins from polyacrylamide gels to nitrocellulose sheets: procedure and some applications. *Proc Natl Acad Sci U S A* **76**: 4350-4354
- Tsai CL, Li HP, Lu YJ, Hsueh C, Liang Y, Chen CL, Tsao SW, Tse KP, Yu JS, Chang YS (2006) Activation of DNA methyltransferase 1 by EBV LMP1 Involves c-Jun NH(2)-terminal kinase signaling. *Cancer Res* **66**: 11668-11676
- Tyler KL (2004) Herpes simplex virus infections of the central nervous system: encephalitis and meningitis, including Mollaret's. *Herpes* **11 Suppl 2**: 57A-64A
- Ullman AJ, Hearing P (2008) Cellular proteins PML and Daxx mediate an innate antiviral defense antagonized by the adenovirus E4 ORF3 protein. *J Virol* **82**: 7325-7335
- Umbach JL, Kramer MF, Jurak I, Karnowski HW, Coen DM, Cullen BR (2008) MicroRNAs expressed by herpes simplex virus 1 during latent infection regulate viral mRNAs. *Nature* **454**: 780-783
- Wagner EK, Bloom DC (1997) Experimental investigation of herpes simplex virus latency. *Clinical microbiology reviews* **10**: 419-443
- Wang QY, Zhou C, Johnson KE, Colgrove RC, Coen DM, Knipe DM (2005) Herpesviral latency-associated transcript gene promotes assembly of heterochromatin on viral lytic-gene promoters in latent infection. *Proc Natl Acad Sci U S A* **102**: 16055-16059
- Watson RJ, Clements JB (1980) A herpes simplex virus type 1 function continuously required for early and late virus RNA synthesis. *Nature* **285**: 329-330
- Weir JP (2001) Regulation of herpes simplex virus gene expression. *Gene* **271**: 117-130
- Wethkamp N, Klempnauer KH (2009) Daxx is a transcriptional repressor of CCAAT/enhancer-binding protein beta. *J Biol Chem* **284**: 28783-28794
- Whitley RJ, Kimberlin DW, Roizman B (1998) Herpes simplex viruses. *Clin Infect Dis* **26**: 541-553; quiz 554-545
- Whitley RJ, Roizman B (2001) Herpes simplex virus infections. *Lancet* **357**: 1513-1518
- Whitton JL, Slifka MK, Liu F, Nussbaum AK, Whitmire JK (2004) The regulation and maturation of antiviral immune responses. *Advances in virus research* **63**: 181-238
- Wilcox CL, Smith RL, Everett RD, Mysofski D (1997) The herpes simplex virus type 1 immediate-early protein ICP0 is necessary for the efficient establishment of latent infection. *J Virol* **71**: 6777-6785

- Wilkinson DE, Weller SK (2003) The role of DNA recombination in herpes simplex virus DNA replication. *IUBMB life* **55**: 451-458
- Wilkinson GW, Kelly C, Sinclair JH, Rickards C (1998) Disruption of PML-associated nuclear bodies mediated by the human cytomegalovirus major immediate early gene product. *J Gen Virol* **79** ( Pt 5): 1233-1245
- Wong LH, McGhie JD, Sim M, Anderson MA, Ahn S, Hannan RD, George AJ, Morgan KA, Mann JR, Choo KH (2010) ATRX interacts with H3.3 in maintaining telomere structural integrity in pluripotent embryonic stem cells. *Genome research* **20**: 351-360
- Woodhall DL, Groves IJ, Reeves MB, Wilkinson G, Sinclair JH (2006) Human Daxx-mediated repression of human cytomegalovirus gene expression correlates with a repressive chromatin structure around the major immediate early promoter. *J Biol Chem* **281**: 37652-37660
- Wu WS, Vallian S, Seto E, Yang WM, Edmondson D, Roth S, Chang KS (2001) The growth suppressor PML represses transcription by functionally and physically interacting with histone deacetylases. *Mol Cell Biol* **21**: 2259-2268
- Wysocka J, Herr W (2003) The herpes simplex virus VP16-induced complex: the makings of a regulatory switch. *Trends in biochemical sciences* **28**: 294-304
- Xue Y, Gibbons R, Yan Z, Yang D, McDowell TL, Sechi S, Qin J, Zhou S, Higgs D, Wang W (2003) The ATRX syndrome protein forms a chromatin-remodeling complex with Daxx and localizes in promyelocytic leukemia nuclear bodies. *Proc Natl Acad Sci U S A* **100**: 10635-10640
- Xue Y, Wong J, Moreno GT, Young MK, Cote J, Wang W (1998) NURD, a novel complex with both ATP-dependent chromatin-remodeling and histone deacetylase activities. *Mol Cell* **2**: 851-861
- Yang X, Khosravi-Far R, Chang HY, Baltimore D (1997) Daxx, a novel Fas-binding protein that activates JNK and apoptosis. *Cell* **89**: 1067-1076
- Yao F, Courtney RJ (1992) Association of ICP0 but not ICP27 with purified virions of herpes simplex virus type 1. *J Virol* **66**: 2709-2716
- Yao F, Schaffer PA (1995) An activity specified by the osteosarcoma line U2OS can substitute functionally for ICP0, a major regulatory protein of herpes simplex virus type 1. *J Virol* **69**: 6249-6258
- Yeung PL, Chen LY, Tsai SC, Zhang A, Chen JD (2008) Daxx contains two nuclear localization signals and interacts with importin alpha3. *J Cell Biochem* **103**: 456-470
- Yondola MA, Hearing P (2007) The adenovirus E4 ORF3 protein binds and reorganizes the TRIM family member transcriptional intermediary factor 1 alpha. *J Virol* **81**: 4264-4271
- Zhang R, Poustovoitov MV, Ye X, Santos HA, Chen W, Daganzo SM, Erzberger JP, Serebriiskii IG, Canutescu AA, Dunbrack RL, Pehrson JR, Berger JM, Kaufman PD, Adams PD (2005) Formation of MacroH2A-containing senescence-associated heterochromatin foci and senescence driven by ASF1a and HIRA. *Developmental cell* **8**: 19-30

Zhang Y, LeRoy G, Seelig HP, Lane WS, Reinberg D (1998) The dermatomyositis-specific autoantigen Mi2 is a component of a complex containing histone deacetylase and nucleosome remodeling activities. *Cell* **95**: 279-289

Zhang Y, Ng HH, Erdjument-Bromage H, Tempst P, Bird A, Reinberg D (1999) Analysis of the NuRD subunits reveals a histone deacetylase core complex and a connection with DNA methylation. *Genes & development* **13**: 1924-1935

Zhong S, Muller S, Ronchetti S, Freemont PS, Dejean A, Pandolfi PP (2000a) Role of SUMO-1-modified PML in nuclear body formation. *Blood* **95**: 2748-2752

Zhong S, Salomoni P, Pandolfi PP (2000b) The transcriptional role of PML and the nuclear body. *Nat Cell Biol* **2**: E85-90

Zhou ZH, Dougherty M, Jakana J, He J, Rixon FJ, Chiu W (2000) Seeing the herpesvirus capsid at 8.5 Å. *Science* **288**: 877-880